# Bioprocessing of Mammalian Cells for Tissue Engineering and Cell Therapies

A thesis submitted for the degree of
Doctor of Engineering
in
Biochemical Engineering

by
Barnaby James Henry Zoro
MA MEng MSc

The Advanced Centre for Biochemical Engineering
Department of Biochemical Engineering
University College London

August 2005





ProQuest LLC
789 East Eisenhower Parkway
P.O. Box 1346
Ann Arbor, MI 48106-1346

Abstract

It is envisaged that in order to achieve the stringent quality requirements of future human cell and tissue manufacturing processes, implementation of automated processing systems will be required. As automated systems are capable of operating at high speeds, throughput is likely to be constrained by sensitivity of cellular materials to mechanical stress. The effect of laminar capillary shear stress (pipe flow) on rat aortic smooth muscle cells was investigated. Initial studies showed that repeated exposure to high shear stress (>100 Pa) causes substantial cell damage, with surviving cells able to grow normally. A flow cytometry assay for cell membrane integrity was developed and exhibited high assay resolution, precision and speed. Further shear studies indicated minimal cell damage or loss in the shear stress range 5-25 Pa, with some evidence of cell damage at high shear stresses (35-75 Pa). Cell loss at very low shear stress (< 2 Pa) was attributed to surface adhesion.

Manufacture of cell based therapeutics requires the generation and processing of concentrated cell suspensions. Volume mean cell diameter for rat aortic smooth muscle cells was measured to be 22.4 μm and enabled conversion between cell concentration and cell volume fraction in suspensions. Concentrated cell suspensions (cell volume fraction ≤ 0.34) behaved as 'power law' (shear thinning) fluids and showed similarity with reported rheology of concentrated yeast and plant cell suspensions. Predictions based on literature values for oxygen uptake rate of mammalian cells indicated that oxygen depletion is likely to occur during processing of cell pellets and concentrates.

Two semi-automated cell concentration protocols (centrifuge-resuspend) were developed and compared. Both protocols achieved cell volume fraction of around 0.3-0.4 (wet pellet) and the superior protocol exhibited intact cell yield of ~75%. Apparent loss of cells was mainly attributed to formation of large aggregates during concentration.

A 'windows of operation' analysis was constructed to examine process feasibility in the context of experimental results. Three different processing scenarios were predicted to be feasible and it was shown that processing yield is a critical factor in determining overall process feasibility and manufacturing costs.

Acknowledgements

Heartfelt thanks to my supervisor Mike for his ongoing support, advice and vision and to all my family, friends, colleagues and others who have helped me to stay focused along the way. Special thanks go to Matt for giving me inspiration, determination and the ability to keep life in perspective, Julia for giving me confidence that we could make it work, Beth for riding shotgun and also to Roberto, Mark, Anna and Celi for providing welcome distraction while I wasn't hard at it. Grateful thanks to Rosemary, Steve, Neil, Richard and all the others at The Automation Partnership for lending me their experience and enthusiasm and of course to the EPSRC and The Automation Partnership for keeping me in bread and water all these years.

Table of contents

List of figures

List of tables

# Chapter 1: Introduction

## 1.0. Organisation of the thesis

The introduction, chapter 1, provides a brief overview of tissue engineering and cell therapy, including materials used, various processing operations and key processing issues. In addition, principles, considerations and tools for the design of automated processes and processing systems are discussed, followed by a summary of the aims, scope and framework for investigations. Descriptions of experimental techniques and various calculations are provided in chapter 2. Experimental results are presented in chapters 3 and 4 along with associated discussion. Chapter 5 comprises discussion of more general issues, including a process feasibility study based on results gained, a roundup of process design issues and also a brief consideration of process costs and process validation issues. Final conclusions and recommendations for further work are incorporated at the end of chapter 5. Supplementary material for reference is included in appendices.

## 1.1. Tissue engineering and regenerative medicine

Tissue and organ failure is a major health problem, accounting for around half of the total annual healthcare expenditure in the US [Persidis A, 1999]. While many such medical conditions not amenable to treatment with (bio-)pharmaceuticals can now be treated by direct transplantation of donated cells, tissues or organs, the demand for suitable transplants generally far exceeds supply. In recent years the field of tissue engineering has emerged, offering real potential to create off-the-shelf or patient-specific replacement cells, tissues, organs or other cell-based devices for a wide range of conditions. While some tissue regeneration techniques rely on matrices alone, and others rely on cells alone (cell therapies), most investigators in tissue engineering use cells combined with matrices [Vacanti and Langer, 1999] to provide both complex cellular and structural functions when applied. The goal of tissue engineering is to design, develop and manufacture tissue products which are able to impart, induce or assist regeneration of normal physiological tissue function, significantly improving patient outcomes. Significant challenges exist in establishing the range of technologies required to develop suitable biomaterials, control cell/tissue growth and function, develop robust manufacturing processes and process systems, and achieve quality control and regulatory approval. The field is thus widely interdisciplinary, requiring

skills and knowledge drawn from areas such as developmental and cell biology, biochemistry, medicine, polymer and materials science and process and systems engineering.

### 1.1.1. Previous approaches to tissue engineering

Due to the complexity of tissue products, with such a wide range of enabling technologies requiring research and development, to date the field has been largely research-oriented and has brought few products to clinical trial or large-scale manufacture; by the end of 2002 only 20 products had entered clinical trials in the US, with only four having received Food and Drug Administration (F.D.A.) approval [Lysaght and Hazelhurst, 2004]. Major areas of technology development include cell sourcing, characterisation, expansion and control (e.g. of differentiation), biomolecular and polymer design of biomaterials and associated scaffold manufacture techniques, and development of product-specific bioreactors. Approaches to tissue engineering have largely focussed on invention and development of novel technologies [Pangarkar and Hutmacher, 2003] typically utilising small-scale methods to achieve proof-of-principle for a specific process technology and/or product. Consequently, the level of understanding and control over individual process operations has not widely been developed to the level required for highly reproducible scaleable product manufacture. In order to facilitate rapid transition from proof of principle processes to full-scale manufacture for a wide range of products, it is useful to examine generic process design issues and engineering fundamentals (e.g. behaviour and response of cellular materials in the process environment) and processing operations (e.g. culture and formulation of cells). A clear understanding of mechanisms controlling performance of various processing operations should enable creation of suitable design bases assisting rapid development of scaleable processes with optimal productivity.

### 1.1.2. Example therapies under development

Major tissue engineered product areas under investigation include skin, cardiovascular, musculoskeletal and cartilage repair, neurological and nerve regeneration, bladder replacement [Oberpenning et al., 1999], organ-assist devices such as the 'bioartificial liver' and a variety of cell therapies. Skin constructs have attracted much attention, with many different approaches investigated [Wilkins et al., 1994; Rochon et al., 2001; Boyce, 2004]. Cardiovascular disease offers many therapeutic targets for tissue

engineering, including cellular heart valves [Breuer et al., 1996], replacement blood vessels [Weinberg and Bell, 1986; L'Heureux et al., 1998; Nicklason et al, 1999] (usually matured in pulsatile flow bioreactors), and intramyocardial injection of myoblasts (muscle cells) for the repair of damaged cardiac tissue [Pouzet et al., 2000; Menasche P et al., 2003]. Musculoskeletal repair includes regeneration of bone [Kose et al., 2004; Hokugo et al., 2004], and other connective tissues such as ligaments [Cartmell and Dunn, 2004]. Examples in cartilage repair include implantation of cultured autologous chondrocytes (cartilage cells) [Mayhew et al., 1998] and cellular constructs [Hauselmann et al., 1996], including constructs cultivated in bioreactors providing mechanical stimulation [Temenoff and Mikos, 2000]. Neurological regeneration involves cellular therapies such as intracerebral injection of cells for treatment of Parkinson's disease [Bellamkonda and Aebischer, 1994], with nerve repair including synthetic [Sundback et al., 2003] and biological [Meek et al., 2004] nerve-regeneration guides. Extracorporeal liver support devices typically utilise hollow-fibre blood perfusion cartridges pre-loaded with hepatocytes [Kamlot et al., 1996; Zeilinger et al., 2004]. Substantial work is also ongoing in a wide variety of cell therapies such as bone marrow transplantation and activated immune cell therapies [du Moulin et al., 1994], transplantation of pancreatic islet cells [Rabkin et al., 1999] for diabetes and implantation of encapsulated cells genetically engineered to produce therapeutic biomolecules (e.g. endostatin for tumour suppression) [Bergers and Hanahan, 2001].

### 1.1.3. Industrial perspective

In 2002, of the four F.D.A. approved products, three were living skin equivalents for diabetic or venous ulcers (Apligraf, Organogenesis; Dermagraft, Advanced Tissue Sciences) or burns (OrCel, Ortec), and one autologous cell cartilage repair treatment (Carticell, Genzyme Biosurgery). Between 2000 and 2002 there was a substantial shift within industry from structural applications towards cellular therapies, largely driven by the collapse of large firms in living skin equivalents (Organogenesis, Advanced Tissue Sciences) and a growth in small stem cell-based firms [Lysaght and Hazlehurst, 2004]. The demise of these pioneering firms was reported in the media as being due to a variety of reasons, including high product price, poor sales due to slow product uptake, high costs associated with delays achieving regulatory and reimbursement approval, a generalised collapse of private sector funding [Stone A, 2003], a lack of process automation and scalability and poor manufacturing efficiency resulting in high

production costs and small profit margins [Moore SK, 2002]. These developments in the tissue engineering industry have underlined the need for a shift in approach to product development, making a realistic appraisal during early research and development of issues such as product functional requirement, scaleable manufacture, clarifying and meeting regulatory requirements, and ensuring cost-effectiveness, reimbursement and commercial viability of a product and the manufacturing process.

## 1.2. Materials used in regenerative medicine

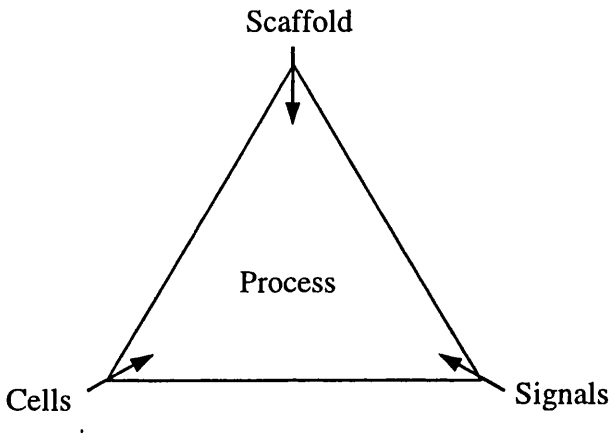


Figure 1-1. 'The tissue engineering triad'

Two major process feedstocks used within tissue formation are the scaffold for growth and the cells for seeding onto, or encapsulation within, the scaffold (figure 1-1). In addition, various signals may be required to direct cell differentiation, extracellular matrix secretion and tissue development, with media as required to support tissue growth. While many of the signals used involve biochemicals such as hormones, vitamins and growth factors, other cues such as mechanical stimuli (stretch, compression) can be important for tissue development.

### 1.2.1. Cells

One of the major issues in cellular applications is achieving the necessary cell mass; various cell types and sources are available for investigation, each with various advantages and disadvantages. Major issues relating to cell type and source include immunogenicity, number available, accessibility, growth potential, functionality, tumourigenicity, differentiated state and plasticity of differentiation. The three main sources are autologous (patient's own), allogeneic (from another human) and xenogeneic (from another species). Within each of these categories there exist stem

cells (adult or embryonic) and mature differentiated cells within specific tissues [Naughton, 2002]. Autologous cells are typically viewed as non-immunogenic, being recognised by the patients own immune system, but may be in short supply and have problems with growth potential [Ruiz-Torres et al., 1999] and functionality (e.g. in old diseased patients). Variability of cells between patients may also complicate development of robust manufacturing processes. Both allogeneic and xenogeneic cells typically present immune rejection problems [Babensee et al., 1998], but may be available in larger numbers and offer potential for cell line generation and detailed characterisation; once a cell line is established, it may provide feedstock material for many product batches. A major problem in the use of xenogeneic cells is the potential for inter-species transfer of diseases, such as porcine endogenous retrovirus (PERV); due to the risk of bringing new pathogens into the human population, the prospect of using xenogeneic cells remains controversial [Griffith and Naughton, 2002].

Generally the cells used are matched directly to the application, as required to achieve the appropriate physiological, pharmacological and secretory properties, e.g. articular chondrocytes for cartilage applications [Mayhew et al., 1998], a combination of smooth muscle, endothelial and fibroblast cells for vascular constructs [L'Heureux et al., 1998], fibroblasts and keratinocytes for skin formation [Wilkins et al., 1994]. Some approaches use mixed cell populations, while others rely on separation or enrichment of specific cell types. In certain instances where the appropriate mature cell type is unavailable for biopsy and cannot be otherwise cultured (e.g. from stem cells), other types may be substituted in the hope of therapeutic benefit (e.g. autologous myoblasts substituted for cardiac myocytes in cardiac repair [Pouzet et al., 2000]), including unrelated cell types which may be have genetically engineered to perform a specific function (e.g. fibroblasts or muscle cells engineered to secrete L-dopa or tyrosine hydroxylase [Bellamkonda and Aebischer, 1994]).

Within the area of stem cells, therapeutic cloning offers the possibility of generating embryonic stem cells genetically identical to the patient, thus avoiding immune rejection. Adult stem cells have been discovered in many mature tissues, and in some cases they may be differentiated into a diverse range of cell types [Zuk et al., 2001; Lysaght and Hazlehurst, 2003]. While embryonic stem (ES) cells ultimately offer the potential for generation of any cell type in the body, there are ethical issues relating to use of embryos, limitations on the availability of oocytes (human egg cells) for embryo creation and substantial technical hurdles to be overcome in the control of development

and differentiation of many cell types and generating sufficient cell mass from embryos [Petit-Zeman, 2001]. One class of adult stem cells which has recently drawn much interest are mesenchymal stem cells (MSC), isolated from the bone marrow or peripheral blood [Naughton GK, 2002]. MSC are relatively accessible with current bone marrow aspiration or mobilisation and apheresis techniques and have been shown to be capable of differentiating into multiple cell types including skin, bone, cartilage, fat, tendon, muscle, marrow stroma [Pittenger et al., 1999], hepatocytes (liver cells), cardiac muscle cells and lung tissue [Griffith and Naughton, 2002]. Cells should be well characterised coming into the process and be monitored to ensure maintenance of sterility, identity, phenotype and function. Sterility must be assured with rigorous screening to ensure pathogens such as mycoplasma and viruses are not transferred to the patient or allowed to contaminate the manufacturing facility [Omstead et al., 1998].

### 1.2.2. Cell growth media

Expansion of cells in culture flasks and tissue constructs requires supply of essential nutrients, including glucose, amino acids and vitamins. In addition primary mammalian cell culture media are typically supplemented with 5-10% bovine serum to provide complex growth factors and other biomolecules required for growth of mammalian cells in culture, and antibiotics to prevent contamination of cultures. In addition other growth factors may be required for the maintenance or control of differentiation of certain cell types, e.g. stem cells. Specific growth factor supplements may be very costly, particularly for cell types where multiple growth factors are required. In addition other supplements may be used, e.g. ascorbic acid, which induces abundant synthesis (secretion) of extracellular matrix proteins in mesenchymal cells, including smooth muscle cells and fibroblasts [L'Heureux et al., 1998].

### 1.2.3. Biomaterials

Tissue engineering scaffolds or encapsulation matrices consist of natural or synthetic materials, or combinations thereof. Natural materials used include a variety of substances (depending on application) such as hydroxyapatite, marine polysaccharides (e.g. alginate), and proteins [Vacanti and Langer, 1999] (e.g. collagen, fibrin, fibrinogen, fibronectin) or other extracellular matrix components (e.g. hyaluronic acid, glycosaminoglycan). The most widely used synthetic polymers are polylactic acid (PLA), polyglycolic acid (PGA) and associated mixtures or copolymers (e.g. PLGA);

these materials are approved for clinical use, can degrade completely to $CO_2$ and water *in vivo* and have proved successful in many applications [Naughton, 2002].

General requirements for tissue engineering biomaterials include processability (e.g. melt point, solubility), biocompatibility (no inflammatory or toxicological response), strength and compliance, good bio-resorption or degradation profiles, good mass-transfer properties (where appropriate, e.g. encapsulation hydrogels), well-defined and reproducible characteristics (problematic with natural materials), and appropriate surface properties [Christenson et al., 1997]. Surface properties control biomaterial interaction with cells, affecting adhesion, motility, proliferation, ingrowth and even differentiation and molecular uptake or secretion. Cells may also be influenced by factors such as surface wetting, chemistry, texture, patterning and porosity; these behaviours are generally controlled by ligand-induced receptor-mediated cell signalling and regulation processes [Christenson et al., 1997]. The discovery of the amino acid adhesion sequence 'RGD' has enabled the design of synthetic materials modulating cell adhesion, with design principles emerging for the 'normal' presentation of other proteins and/or growth factors as a part of the extracellular matrix, rather than simply releasing them into the growth medium [Griffith and Naughton, 2002].

## 1.3. Processing operations in regenerative medicine

Typically in the process industries, manufacturing processes are considered as being made up of separate operations, known as unit operations. Each unit operation is usually quite different in terms of function, apparatus and methods employed, with the performance and design of different unit operations being controlled by different physical principles in each case. It is useful to classify separate unit operations in order to identify commonality between different manufacturing processes and to facilitate focusing of design efforts towards the key issues and controlling mechanisms in common unit operations. A generalised process flow diagram for tissue engineering and cell therapy manufacturing processes is presented in figure 1-2.

### 1.3.1. Biopsy harvest and cell isolation

Within autologous processes the initial steps are to source the cellular material by a surgical biopsy or blood collection procedure and subsequently isolate the desired cells from the collected material. Allogeneic processes involving use of established cell lines

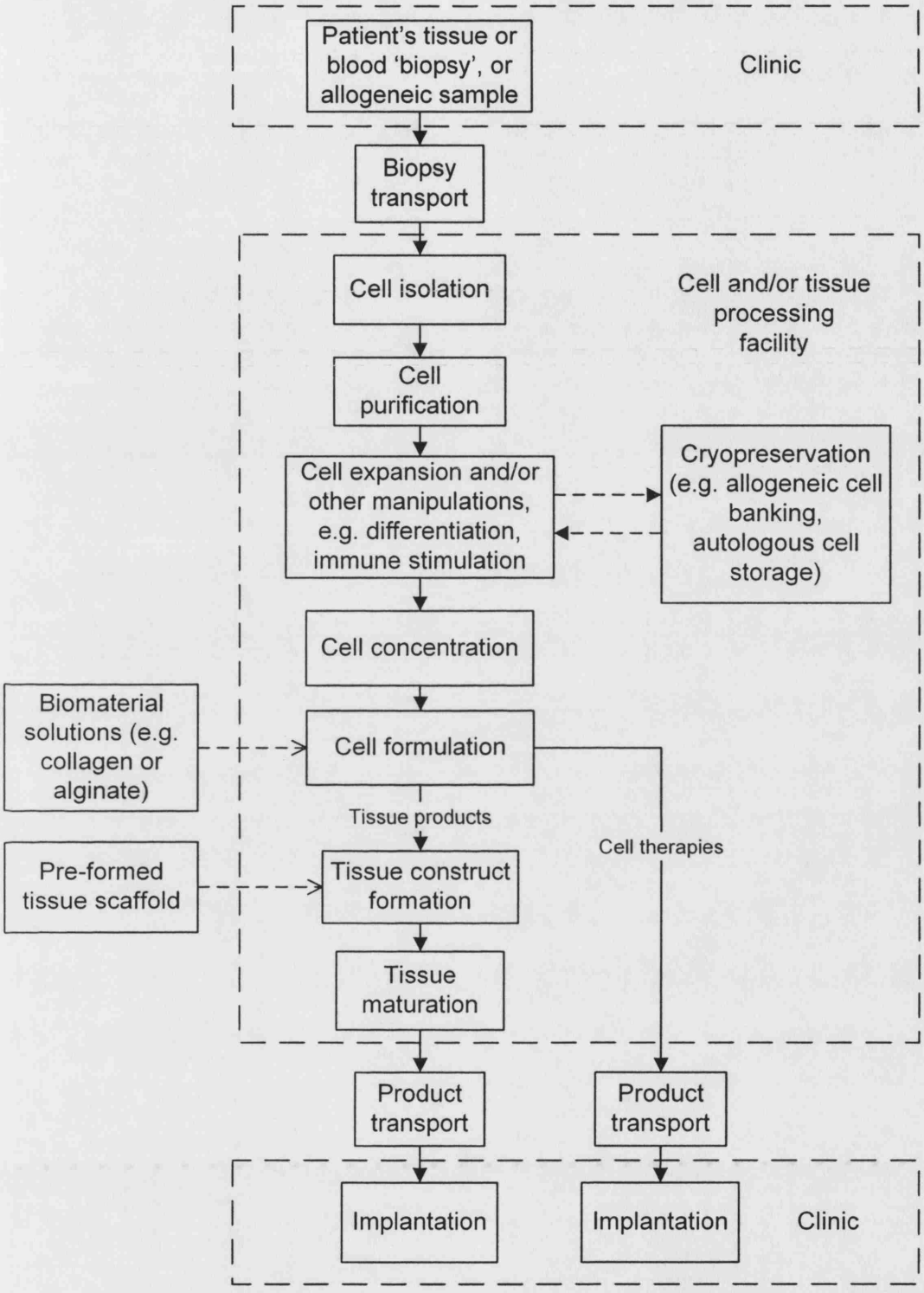


Figure 1-2. Generalised process flow diagram for regenerative medicine processes. This flow diagram provides an overview of the major unit operations common throughout many tissue engineering and cell therapy processes. In some processes one or more operations may be combined (e.g. cell isolation and purification) or not required. (— —) Likely process locations. (– –) Various process alternatives. NB solid arrow heads (➔) represent transfer of cellular materials between unit operations; these transfers are themselves significant process operations and are likely to involve a wide variety of processing demands and conditions.

may require material collection and cell isolation only in the initial process development stage (i.e. cell bank generation), or periodically throughout the lifetime of the manufacturing process. It is necessary to establish procedures for the procurement and separation of cells designed to ensure the function and integrity of the cells are maintained and to prevent the transmission of communicable disease agents [F.D.A. 21 CFR Part 1271, 2001].

The nature of biopsy and cell isolation procedures vary widely depending on the cell type and location in the body. Standardisation of biopsy collection procedures is essential to provide a sufficiently reproducible feedstock material for subsequent processing. Surgical biopsy collection procedures must currently be performed manually and are considered to be outside the scope of this work. Briefly, typical examples of human materials used include peripheral vein for blood vessel constructs [Button et al., 2002; Shin'oka et al., 2001], articular cartilage for cartilage repair [Temenoff and Mikos, 2000], neonatal foreskin [Halberstadt et al., 1994] or adult skin [Rochon et al., 2001; Boyce, 2004] for skin substitutes, muscle tissue providing myoblasts for cardiac repair [Menasche et al., 2003], bone marrow for mesenchymal stem cells [Reyes M et al., 2002] and adipose (fat) tissue for multipotent cells [Zuk et al., 2001].

The difficulty of cell isolation from biopsy material varies depending on the geometry and composition of the biopsy and the number of different cell types required from the same sample. Some therapeutic cell sources, such as umbilical cord blood, bone marrow aspirates and apheresis products are cell suspensions as collected. Various cell types can be isolated from blood or apheresis products by density gradient centrifugation, such as dendritic cells [Tuyaerts et al., 2002] and blood mononuclear cells [Luhm et al., 2002, Berger at al., 2002]. Cartilage cells (chondrocytes) may be isolated by dicing of cartilage tissue and collagenase/trypsin digestion [Gooch et al., 2001; Shortkroff and Spector, 1999]. Isolation of the multiple cell types from more structurally complex tissues, such as vein biopsies, are typically performed manually, e.g. by scraping of the endothelial cell lining followed by microdissection to separate out smooth muscle cell and fibroblast tissue layers [L'Heureux et al., 2001; Grenier et al., 2003]. Micro-dissected tissue may be plated in culture, allowing cells to migrate from tissue sections (explant method); migration of smooth muscle cells from vascular tissue sections may take from a week [Villaschi et al., 1994; Caleb et al., 1996] to a month [Button et al., 2002], to yield sufficient cells for expansion by normal culture. Alternatively, tissue

may be dissected or minced and digested enzymatically, yielding either a single or mixed cell suspension, depending on the tissue type and biopsy procedure. Enzymatic digestion of micro-dissected tissue takes from around 30min [Oakes and Batty, 1982; Devore-Carter et al., 1988] up to 4h-overnight [Shortkroff and Spector, 1999] depending on the tissue and conditions used.

### 1.3.2. Storage and transport

Transport of cellular material between unit operations forms an integral part of every process; this may be over very short distances and timescales within a manufacturing facility or over much larger distances and timescales between biopsy collection clinics, cell and tissue processing facilities and point of product use. The effect on cellular material of transport or storage conditions must be considered, such as buffer fluids used, temperature, oxygenation, other nutrient supply or waste product accumulation/removal and the timescales involved. Options available for transport and storage of cells, tissues or tissue constructs include immersing in a suitable buffer (e.g. serum-free DMEM with gentamycin [Tubo and Binette, 1999], ViaSpan organ preservation solution [Rabkin et al., 1999]), controlled temperature storage (e.g. 4°C) and cryopreservation. Cryopreservation (using liquid nitrogen) is the only available method for the long-term storage of cells and so is required for the preservation of cell banks in processes using established cell lines. The cryopreservation process typically causes significant injury and loss of function of cells and tissues; while many freeze-thaw protocols result in low recovery rates or entirely non-viable tissue [Karlsson and Toner, 1996], cryopreservation has been used for the storage of a cultured human skin substitute [Halberstadt et al., 1994]. Cryopreservation is likely to be required in processes where different cell types from the same biopsy are required at different stages of the manufacturing process, for example envisaged autologous blood vessel manufacturing processes where smooth muscle cells (SMC), fibroblasts (FB) and endothelial cells (EC) are initially isolated from the same biopsy, with SMC used immediately and FB, EC cryopreserved for later seeding stages.

### 1.3.3. Cell purification

In some cases mixed cell populations have been used for tissue seeding, such as blood vessel [Shum-Tim et al., 1999; Shin'oka et al., 2001]. However the approach used more widely is the purification of the cell type(s) specific to the tissue in question, such that

native tissue architecture may be recreated by design with cell types in appropriate locations. Certain therapies may require absolute purity due to the nature of the medical condition; autologous marrow replacement after ablative chemotherapy must not return cancer cells to the patient. It is also important to rapidly achieve a high yield of cells without adversely affecting their viability or function.

The most widely used techniques in the separation of primary cells for biochemical or functional studies are fluorescence-activated cell sorting (FACS) and immunomagnetic separation [Partington et al., 1999]. FACS separates cells according to surface markers [Lawry, 1998]; antibody-linked fluorescent tags associate with cell surface markers and cells are then automatically sorted individually according to their fluorescence. Immunomagnetic separation uses antibody-coated magnetic beads to bind or flocculate cells; magnetised cells or cell clumps may be sorted magnetically. Immunomagnetic separation is widely used [Safarik and Safaikova, 1999; Murphy et al 1992; Linge et al., 1989], with a variety of research and clinical separation systems available.

Other techniques include immunopanning [Linge et al., 1989], magnetic or centrifugal elutriation techniques [Bauer, 1999] or culturing with selective growth medium [Feng et al., 1999; L'Heureux et al., 1998]. Some cell types do not exhibit well characterised distinctive surface antigens (e.g. SMC), making positive selection by immunological methods problematic; however, it is possible to separate SMC from a known cell population (e.g. mixed EC and SMC) by negative depletion [Breuer et al., 1996].

After sorting, cells may require washing (e.g. buffer or media exchange) to remove any agents used during separation. Cells must be screened to ensure that their key characteristics fall within the allowable ranges for the process (e.g. growth rate, function) and also for the presence of infectious agents. Appropriate cell culture assays with indicator cell lines may be used to check for sterility (e.g. mycoplasma contamination). In the laboratory washing steps are normally carried out either on attached cell sheets within the culture vessel (e.g. T-flask) or by centrifuging a cell suspension and resuspending in the new fluid e.g. growth medium. Various devices are commercially available for performing immunological cell selection, cell washing and cell concentration in clinical applications such as bone marrow autotransplantation.

### 1.3.4. Cell expansion

Following cell isolation and any selection, it is usually necessary to expand the cell population many fold to provide sufficient cells for therapeutic application from a

relatively small biopsy. Many primary cell types are adherent, i.e. require a culture surface on which to attach and proliferate. Adherent cell culture is normally carried out either in large numbers of parallel (rectangular) T-flasks or (cylindrical) roller bottles, with incubation at 37°C under a humidified 5-10% $CO_2$ atmosphere; $CO_2$ is used in combination with bicarbonate-buffered culture medium to maintain pH in culture. Subculture operations are always carried out using aseptic technique within sterile laminar airflow hoods. A few systems have been developed with alternative geometries, including the Nunc Cell Factory ® and the Corning CellCube ®, Aastrom Replicell ® [Armstrong et al., 2001], which may incorporate circulation of medium and/or gas.

Cell (and tissue) culture is inherently variable, principally due to biological variability in cells (especially autologous cells), raw materials (e.g. serum) and humans (operator variability). Removing the possibility of variations in one or more areas will lead to a more consistent product. While an individual scientist can skilfully compensate for variations in cell culture by adjusting parameters 'on the fly', at the large scale, technicians are required to carry out repetitive operations very many times and the human factor causes variations to creep in due to fatigue or due to the tedium. Accumulation of variables at the larger scale can rapidly result in unacceptable inconsistencies [Edwards, 1998].

### 1.3.5. Cell formulation

Following expansion and harvest, cells are reformulated in preparation for use, either directly in cell therapies or for seeding to, or encapsulation within, tissue constructs or other devices such as hollow fibre bioartificial liver cartridges [Patzer, 2004]. It is likely that this is generally carried out by centrifugation of cells and resuspension to the desired cell concentration in the relevant fluid, e.g. culture medium [Yang et al., 2001] or gel-forming solution such as collagen [Weinberg and Bell, 1986], Matrigel® [Radisic et al., 2003] or alginate [Read et al., 2001] solutions; literature reports rarely describe the process used to prepare cell suspensions for tissue formation. Typical cell concentrations following adherent cell culture and harvest are of the order of $1x10^5$ cells/mL, while the desired cell concentrations for cell seeding may be as high as ~$1x10^8$ cells/mL [Radisic et al., 2003; Dar et al., 2002]. Centrifugation is probably the method employed due to the ease of use, availability of centrifuges within research laboratories and the high concentration factors and small final volumes which can be achieved with cell pellets. Membrane based techniques may also be employed; one

commercial apheresis system (Nexcell Cytomate) employs a spinning membrane filter for automated washing and concentration of cell suspension by diafiltration.

### 1.3.6. Scaffold fabrication techniques

Formation of polymers and other biomaterials into scaffolds for cell growth has been carried out using a wide variety of techniques. As pre-formed scaffold materials are essentially a feedstock material for the cell-processing aspects of tissue engineering, formation processes are considered to be outside the scope of this research. Briefly, techniques used for the formation of soft tissue scaffolds include fibre formation and tangling to form wool, fibre bonding producing mesh structures, electrospinning, fibre weaving and knitting to form sheets or tubes, three-dimensional printing (e.g. of dissolved polymer onto successive layers of base powder) [Marler et al., 1998], solvent casting, melt moulding, extrusion, gas foaming and freeze-drying [Thomson et al., 2000].

Scaffolds for cell seeding should be highly porous (>90%) for diffusion and cell migration, have a large surface area for cell attachment and must possess sufficient strength to maintain structural integrity. Unless the scaffold formation process is carried out under sterile conditions with sterile materials, the scaffold must subsequently be sterilised, typically by gamma-irradiation, steam, or exposure to $H_2O_2$ or ethylene oxide gas [Omstead et al., 1998]. Certain pre-formed scaffolds may require pre-coating with attachment factors to improve cell attachment [Kim et al., 1998]; this may involve wetting with serum supplemented culture medium, covalent bonding of suitable molecules to the matrix material [Rowley et al., 1999] and other methods.

### 1.3.7. Tissue construct assembly

In many instances it is desirable to achieve a high concentration of cells within a nascent tissue construct; a high number of initially seeded cells can improve structural stability and biochemical composition of engineered tissues from chondrocytes and cardiac muscle cells [Li et al., 2001]; reduced cell density within blood vessel tissue constructs has been associated with decreased contractility [L'Heureux et al., 2001].

A variety of cellular construct formation techniques have been reported, including seeding to fibrous meshes [Nicklason et al., 1999; Li et al., 2001; Wendt et al., 2003] or porous scaffolds [Yang et al., 2001; Dar et al., 2002], collagen or hydrogel

encapsulation [Weinberg and Bell, 1986; Lee and Mooney, 2001] and hybrid [Radisic et al., 2003] approaches.

Various methods have been applied when seeding cells to pre-formed scaffold, including immersion in static or stirred cell suspension [Kim et al., 1998], absorption [Dar et al., 2002], or perfusion [Wendt et al., 2003] of cell suspension. Further modifications include scaffold seeding assisted by centrifugal force [Yang et al., 2001] and absorption of cells suspended in a gel-forming extracellular matrix (Matrigel®) solution [Radisic et al., 2003]. Where reported, seeding protocols vary greatly in length, from 30min [Nicklason et al., 1999] to 20h [Kim et al., 1998] to 12days [$10^6$ cells/day, Breuer et al., 1996]. Cell seeding suspension concentrations employed range from around $10^5$ cells/mL [Li et al., 2001] up to typical *in vivo* cell densities of $0.5\text{-}1x10^8$ cells/mL for cardiac myocytes [Radisic et al., 2003] or higher; $3x10^8$ cells/mL [Dar et al., 2002]. Reported seeding efficiencies vary from <50% [Yang et al., 2001; Breuer et al., 1996] to 100% [Radisic et al., 2003], depending on the method and conditions employed.

Approaches not requiring a pre-formed scaffold include mould injection of cells suspended in gel-forming solutions such as collagen [Weinberg and Bell, 1986; Kobashi and Matsuda, 1999], macro-encapsulation of cells within a surrounding gel layer [Aebischer et al., 1991; Honiger et al., 2000], 3D co-printing of scaffold and cells [Griffith and Naughton, 2002] and direct construct formation from cell sheets [L'Heureux et al., 1998].

### 1.3.8. Tissue development; bioreactors

Following initial construct formation, there may follow a lengthy period of tissue maturation culture, during which cells are expected to proliferate and secrete extracellular matrix, generating the desired tissue strength, compliance and structural organisation. Timescales for tissue construct maturation vary depending on product and method: skin substitutes typically require 2-3 weeks [Wilkins et al., 1994; Halberstadt et al., 1994; Boyce, 2004] while blood vessels may require 8 weeks or more [Nicklason et al, 1999; L'Heureux et al., 1998]. It is widely reported that application of mechanical stimuli can promote extracellular matrix secretion and tissue self-organisation and development, e.g. intermittent mechanical or hydrostatic pressure applied to cartilage constructs [Carver and Heath, 1999; Temenoff and Mikos, 2000] and pulsatile luminal flow causing radial distension in blood vessel constructs [Nicklason et al., 1999; Solan

et al., 2003]. Tissue maturation bioreactors tend to be highly specialised depending on the application, with geometries and mechanical conditioning systems varying according to the specific tissue requirements. Common requirements are for media circulation or perfusion, gas and media exchange, temperature control and media sampling. With autologous processes, individual patient bioreactors must be isolated such that cross-contamination between patients cannot occur. For products based on allogeneic cell lines it may be possible to develop much larger reactors or reactor complexes supporting multiple product units.

### 1.3.9. Unit operations in the envisaged process

The model process considered in this work is the manufacture of a simplified autologous blood vessel construct consisting of smooth muscle cells encapsulated within an alginate hydrogel. Alginate hydrogels have previously been investigated for tissue engineering applications including cartilage [Hauselman et al., 1996] and urinary tract [Koh and Atala, 2004]. It is envisaged that the entire process from cell isolation to tissue maturation would be fully automated with no manual handling of cellular materials between surgical biopsy harvest and implantation of the manufactured blood vessel. Brief descriptions of established techniques (section 1.3.) which could be directly adapted for the various unit operations are given below.

Biopsies would be surgically harvested in a clinic either at or near the tissue processing facility or otherwise couriered under suitable storage conditions. Cell isolation could be performed by biopsy maceration and enzymatic digestion, yielding a mixed cell suspension of endothelial cells (EC), smooth muscle cells (SMC) and fibroblasts (FB). EC could be depleted or positively selected from the mixture using immunological methods; aliquots of the remaining mixed population could be cultured in selective media to yield SMC and FB populations. Small samples taken from the initial mixed cell population would be screened for pathogens, evaluating the risks of product (therapeutic) failure and facility contamination. Expansion of cells would be performed robotically, using a commercially available system such as SelecT (The Automation Partnership, Cambridge, UK). Cell concentration would be by centrifuge and resuspend, initially resuspending the cell pellet into a small volume of saline solution by orbital shaking. Formulation of cell-alginate suspension could involve initial dispersion of cell suspension through alginate solution (or vice versa) by automated dispensing of many small volumes at a series of coordinates. Mixing could then follow by methods such as

repeated aspirate-dispense, orbital shaking or flow through a static mixer. Cell-alginate suspension would then be formed into a tubular structure by rod coating and crosslinking with calcium chloride solution. Tissue maturation would take place under pulsatile flow (mimicking blood flow) in a blood vessel bioreactor similar in principle to previously established systems [Nicklason et al., 1999]. The tissue product would then be couriered to the point of use within a suitable tissue support device (probably the maturation bioreactor adapted for transport).

## 1.4. Key process issues

Central to many tissue engineering processes are the cells used; the cells are generally critical to the therapeutic and/or regenerative function of the final product. Functionality of the cells must be maintained throughout processing *in vitro*, despite the cells being subjected to a considerable range of abnormal environmental conditions, stresses and cues. It is important to consider the requirements for cell health and function, and also the main processing issues which have the potential for compromising cell health and thus product efficacy.

### 1.4.1. Maintaining cell function

Tissue engineered products rely on cells for tissue development and function; large numbers of cells are required during tissue maturation (extracellular matrix secretion) stages and also to provide physiological functions in the final tissue. 'Basic' cellular functions or attributes include cell membrane integrity, functional basic metabolism and the ability to grow or proliferate. 'Higher' functions are typically specific to individual cell types, e.g. metabolism of extracellular molecules and secretion of certain proteins (e.g. hepatocytes), contractile response to pharmacological or other stimuli (smooth muscle cells, cardiomyocytes), and many others. As the potency of tissue engineered products is heavily dependent on maintaining both basic and higher cellular functions, the manufacturing process must be developed such that these functions are not compromised.

A major problem associated with monolayer culture of cells *in vitro* is alteration or loss of cellular differentiation with alteration or loss of morphology and biochemical and 'higher' functional properties, as typically observed with chondrocytes [Sittinger et al., 1996] and smooth muscle cells [Halayko and Solway, 2001]. In some cases the normal phenotype and function may be restored by various means such as return to 3D culture

of cells (i.e. within a tissue construct) or application of mechanical strain, although this 're-differentiation' becomes more difficult as the length of time in culture increases [Sittinger et al., 1996]. Characterisation of cell types and differentiated states typically relies on techniques such as immunostaining of cell-type specific surface antigens or cytosolic or secreted proteins and morphological assessment. Current developments in gene array and proteomics profiling technologies may soon enable detailed and comprehensive quantitative analysis of differentiated states.

### 1.4.2. Shear stress

A major processing stress is hydrodynamic (flow) stress, which may alter suspension structure and rheology and also the health of suspended cell populations. It is important to understand the physical interactions between biological process materials (e.g. cell suspension) and processing (i.e. effects of shear stress) as this can form a basis for the design of processing equipment and the specification of process parameters (e.g. flowrate, pipe size). To date, the majority of studies of the effects of shear stress on mammalian cells have examined either culture systems with production cells (e.g. hybridomas) or parallel plate systems using defined forces in medical research [Kretzmer, 2000]. Shear stress is know to cause a wide variety of effects on cell populations, including cell death by lysis (i.e. gross mechanical damage), transmembrane ion leakage, physiological and metabolic changes (e.g. cell morphology, gene expression levels), apoptosis or necrosis [Chisti, 2001] and loss in cell number [Born et al., 1992]. Biochemical changes induced by shear are not immediately obvious; it takes a time scale of the order of a cell-generation time before such changes can be measured, whereas gross mechanical damage to cells is immediately detectable [Mardikar and Niranjan, 2000]. As a result shear damage studies typically use assays probing cell membrane integrity/permeability, such as trypan blue [Born et al., 1992], lactate dehydrogenase (LDH) release [McQueen et al., 1987] and flow cytometric assays [Al-Rubeai et al., 1995]. It should be noted that, in many studies where the cell characteristic analysed is 'membrane integrity/permeability', results are reported in terms of 'cell viability'; although membrane integrity is an indicator of cell viability (ability to recover function and grow), there may not be a direct correlation between the two parameters. In this work, classification of cells as 'viable/non-viable' is thus avoided in favour of classification as 'intact/permeable'.

Cell damage may occur under elongational or extensional flow (e.g. at a flow constriction such as capillary entry); cells experiencing deformation under elongational flow or stable laminar flow will rupture if elongational forces exceed the bursting tension of the cell membrane [Born et al., 1992; Chisti, 2001]. Under turbulent flow, damage is attributed to interaction between cells and small turbulent eddies of the order of cell size; if a micro-eddy collides with a cell and imparts energy greater than the membrane surface bursting energy, cell disruption will occur [Zhang et al., 1993]. In turbulent capillary flow, cell death can be correlated with power dissipation [Chisti, 2001] within the capillary. The principal cause of damage to suspended cells in sparged bioreactors has been identified as very high shear forces generated locally during bubble disengagement (burst) at the fluid surface [Chisti, 1999].

Animal cell disruption in turbulent capillary flow has previously been successfully modelled as an exponential decay process [Zhang et al., 1993]; whereas disruption under laminar shear stress has been shown to occur as a two-phase process [Born et al., 1992]. As turbulent hydrodynamic conditions are generally accepted as being more damaging than laminar conditions [Chisti, 2001], it is assumed that the optimum conditions for cell survival will be found in the laminar regime. Studies investigating sensitivity of animal cells to laminar shear stress have demonstrated shear-susceptibility in this flow regime, showing loss of cell number and membrane integrity [Born et al., 1992]. The shear stresses reported as causing damage vary considerably, from $2x10^{-2}$ to 100 Pa [Born et al., 1992]. One recent report has highlighted an effect where cell loss or damage at low shear (~1 Pa) and high shear (~100 Pa) is greater than at intermediate shear (~10 Pa) [Mardikar and Niranjan, 2000].

As automated processing systems are capable of operating at high speeds, throughput is likely to be constrained by sensitivity of biological materials to physical stress. Typical cell transfer steps such as aspirate, dispense (e.g. to/from pipettes) and pipe flow all involve exposure of cells to hydrodynamic shear stress (flow stress) in a capillary geometry. Such exposure of cells to flow stress typically occurs for a very short period of time (sub-second) but may be repeated many times during processing. As any cell losses or adverse effects on the functional characteristics of the cell population must be minimised, it is necessary to characterise the effects of capillary shear stress on a relevant adherent cell type over the appropriate range of flow conditions and timescales.

1.4.2.1. Hydrodynamic conditions in the experimental apparatus

Experimental studies in this work were designed to investigate shear damage to cells resulting from aspirate/dispense to/from standard disposable syringes fitted with capillaries. This apparatus setup was chosen as it represents a likely candidate for application to automated fluid handling operations with small volumes of cell concentrate: fluid flowrates and volumes may be tightly controlled using this type of positive displacement pumping system, and capillary dimensions may be specified according to fluid flowrates required and also the geometry of relevant process equipment (e.g. specify capillary length to reach the bottom of a centrifuge tube).

A schematic representation of likely hydrodynamic conditions in this apparatus geometry is presented in figure 1-3, including possible fluid rotation zones, regions of elongational flow (fluid acceleration), a turbulent region at the capillary inlet, a region of stable laminar flow in the capillary, and a region of unstable flow (with possible turbulence) where fluid is discharged from the capillary. 'No capillary control' experiments (figure 2-1b) were performed to separate out the impact of these various (uncharacterised) regions as far as possible, with a view to characterising the effect on cell membrane integrity due to capillary flow. However it should be noted that the studies were also intended to mimic a realistic capillary-based automated fluid handling apparatus: hence, as the end effects (elongational flow and possible turbulence near the capillary inlet, fluid deceleration and chaotic flow near capillary outlet) are likely to be present in the industrial apparatus, it is appropriate to include these effects when studying the overall effect of capillary flow on suspended cell membrane integrity.

Previous studies in the literature investigating shear damage effects (under laminar or turbulent flow conditions and in a wide variety of apparatus geometries) often use the fluid shear stress ($\tau$), or the capillary wall shear stress ($\tau_w$) as the quoted flow parameter for correlation of the magnitude of shear damage, and also for ease of reference and comparison with other literature studies. In order to ensure that data obtained in this work may be compared directly with literature reports, it is appropriate to represent the capillary flow conditions in terms of the characteristic fluid shear stress in this geometry, i.e. the capillary wall shear stress ($\tau_w$).

Figure 1-3. Schematic of hydrodynamic conditions in the experimental setup (dispense cycle). (*) Possible zone of fluid rotation. (†) Zone of elongational flow (fluid acceleration). (‡) Approximate region of unstable flow prior to development of a stable laminar flow profile in the capillary. (#) Approximate region of fully developed stable laminar flow. ($) Region of unstable poorly defined flow, including deceleration and possible rotation and turbulence. NB 'Skin friction' occurs at all fluid-surface interfaces; skin friction at the capillary wall is represented directly by the calculated capillary wall shear stress, $\tau_w$.

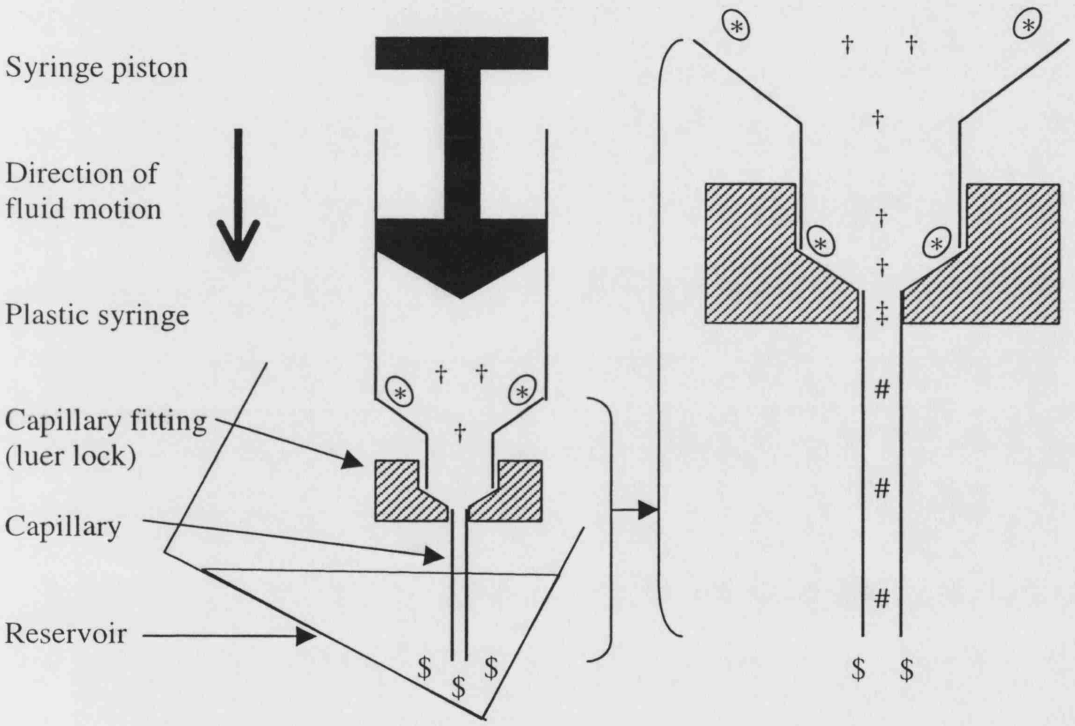

1.4.3. Biochemical stress

Mammalian cell metabolism is affected by a range of conditions such as temperature, pH, dissolved oxygen and nutrient and metabolite concentrations. Mammalian cells use glucose and glutamine for energy production and produce lactate and ammonia [Ozturk et al., 1997; Kretzmer, 2000] as metabolic by-products. Excessive accumulation of waste products such as lactate and ammonia must be avoided as these are known to be toxic metabolites [Kretzmer, 2000]. While high levels of lactate [>2g/L, Ozturk et al., 1997] and ammonia have been shown to inhibit growth of mammalian cells, some recent reports have suggested inhibition of growth may be largely attributed to changes in pH associated with accumulation of lactate [Patel et al., 2000] or ammonia [Kretzmer et al., 2000]. Medium osmolarity can significantly affect cell survival and metabolism; hybridoma cell growth rates are reported to be suppressed at increased osmolarity (relative to isotonic medium), with concomitant increases in cell size and metabolic and death rates [Ozturk and Palsson, 1991].

In the case of bioreactor culture of mammalian cells, glucose is generally the limiting nutrient supplied in the medium [Ozturk et al., 1997]. Oxygen is typically supplied via the gas phase and is the main limiting nutrient in high density cell cultures due to the relatively low oxygen solubility in cell culture media, with associated mass transfer limitations on oxygen supply. Without oxygen supply even a relatively dilute mammalian cell suspension culture ($10^6$ cell/mL) might consume all available oxygen in under an hour [Peng and Palsson, 1996]. Either too little or too much oxygen (hypoxia or hyperoxia) is harmful to cells, causing intracellular production of damaging reactive oxygen species and damaging oxidative stress [Pandian et al., 2003]. Too low a concentration is inhibitory to cell growth and too high a concentration can be cytotoxic, with optimal oxygen concentrations existing for cultures of cells such as bone marrow cells [Peng and Palsson, 1996]. Cell crowding effects have been reported for some cell types such as hepatocyes, where specific (per cell) oxygen uptake rate (OUR) is reduced at high (3D) cell density, possibly due to mass transfer limitations, Michaelis-Menten kinetics of oxygen uptake, or intrinsic reduction in biochemical stress or increase in neighbour-cell regulation within a 'more normal' high cell density environment [Patzer, 2004]. Such cell density effects are not observed with conventional production cell types, such as BHK, CHO, and murine hybridoma cells [Jorjani and Ozturk, 1999].

Oxygen supply is particularly problematic in high cell density tissue engineering applications; within soft tissues, cells further than approximately 200μm from a blood

vessel will suffer from hypoxia and limitation of other nutrients [Eiselt et al., 1998]. Due to the low oxygen solubility and potentially very high cell densities, hypoxia might also occur during cell processing, e.g. during cell concentration (cell pellet) or initial tissue formation or seeding stages prior to application of nutrient and oxygen supply. The temperature dependence of OUR of mammalian cells may be modelled using a simple Arrehnius rate equation, with OUR at 30°C being around half that observed at 37°C; as mammalian cells require temperatures of around 33-38°C for optimal growth, reducing the temperature within a cell culture could potentially enable maintenance of a higher cell density where oxygen transfer rate is limiting [Jorjani and Ozturk, 1999].

### 1.4.4. Regulatory, monitoring and control aspects

Achieving regulatory approval of products is hampered by difficulty of classifying many novel tissue-engineered products according to conventional product classes. In the US separate regulatory centres deal with the three major product classes: pharmaceuticals (i.e. small molecule drugs), biologics (i.e. biopharmaceuticals such as proteins, antibodies, gene therapies) and devices (i.e. non-biological synthetic implants and diagnostics). As tissue-engineered products may combine mechanisms of action from all three product classes (i.e. combination products), they can be very difficult for regulators to handle within existing frameworks; such combination products are handled via a 'lead centre', selected according to the product's primary mechanism of action. International harmonisation of regulation is at present difficult; for example the Apligraf living skin equivalent is classified as a class III device in the US, a medicinal drug in Europe, and a transplant product in Australia [Naughton, 2001]. Quality control and release testing of tissue products according to standard (bio)pharmaceutical attributes of identity, purity and potency may be problematic [Omstead et al., 1998]; sacrificial or invasive assessment methods may compromise product function and in many cases the complexity of a living tissue product renders thorough characterisation impracticable as a routine quality assurance procedure.

In situations where product characterization is limited (e.g. cell-based therapeutic products), process characterisation and control (i.e. process validation) takes on an even greater importance than usual as controlled and consistent processes should yield maximally consistent products. Rigorous implementation of both current good tissue practice (cGTP) and current good manufacturing practice (cGMP) reflect common goals of manufacturing safe and effective products via well-controlled processes and

providing comprehensive supporting documentation. Thorough process validation can also provide an essential bridge for product comparison (demonstration of equivalence) across changes (developments) in manufacturing processes and testing methods [Burger, 2003].

### 1.4.5. Other issues

The key bulk physical (handling) property of a suspension is viscosity, which is typically strongly dependent on suspended solids (cell) volume fraction, with particle shape and size distribution also being important parameters [Matijasic and Glasnovic 2002]. Previous work on concentrated suspension rheology has typically examined and/or modelled the behaviour of fine particle [Usui, 2001; Barthelmes, 2003; Matijasic and Glasnovic 2002], red blood cell [Snabre, 1999], plant cell [Curtis and Emery, 1993; Ballica and Ryu, 1993], microbial or yeast cell [Ward, 1989] suspensions. As different cell types may exhibit different size distributions and it may be helpful to relate cell suspension rheology results to the established literature, it is useful to evaluate cell size (distribution) and subsequently express suspension cell concentrations in terms of cell volume fraction.

Maintenance of a sterility throughout all stages of the process is crucial; in autologous processes bioreactors must be individual (per patient) to prevent cross-contamination, either between patients or to/from the manufacturing facility. To prevent this risk, current good manufacturing and tissue practices (GMPs and GTPs) must be implemented [Omstead et al., 1998], and robust patient-unit tracking and record-keeping systems must be employed throughout processing. Both US and EU cGMP guidelines stipulate a manufacturing area with clean room conditions of EUGMP class A [US standard class 100, ISO 14644-1 Class 5] for critical aseptic processing operations and manufacture of aseptic preparations [Omstead et al., 1998; Lowel, 2003]. For operations in which cells are exposed to the environment, Class 2 [ISO 14644-1] conditions are required to protect both the process and the operator [Timoney and Felder, 2002]. Procedures for sterilising the system need careful examination and validation; the ability to seal and flood the system with a sterilizing gas such as ethylene oxide or VHP (vaporised hydrogen peroxide) is desirable.

## 1.5. Principles and considerations for automated process design

It is envisaged that in order to achieve the stringent quality requirements of future human cell and tissue manufacturing processes, implementation of automated processing systems will be required. Automation has previously been applied to many individual processing operations, such as pancreatic islet cell isolation [Lakey et al., 1997], mammalian cell culture [Archer and Wood, 1992], mammalian cell sampling and sample management [Lutkemeyer et al., 2000], assessment of cell number and membrane integrity [Szabo, 2003], bone marrow cell concentration [Rodriguez et al., 1992], 3D freeform scaffold manufacture techniques [Sherwood et al., 2002; Sachlos et al., 2003; Cooke et al., 2003], cell encapsulation [Honiger et al., 2000], skin graft bioreactor control [Prenosil and Kino-oka, 1999] and intracranial implantation of cells [Bankiewicz et al., 2000]. While automation has been applied in such instances, extensive automation of tissue engineering processes has not yet been realised; it has been reported that a lack of effective process automation and process scalability was a factor in the commercial failure of tissue engineering products to date [Moore SK, 2002]. The development of manufacturing systems that cost-effectively enable *ex-vivo* cell (and tissue) therapy to be practised in a highly reproducible manner is a critical requirement for the implementation of new cell therapies [Armstrong et al., 1995].

### 1.5.1. Advantages and disadvantages of automated processing systems

Automated manufacturing systems offer advantages in terms of greater speed, precision and reproducibility than that which can be achieved by human operators. For example manual pipetting steps are typically variable in terms of pipette positioning and time taken for aspirate/dispense (i.e. flowrate) and other operations, whereas computer-controlled machine systems may be designed to perform such tasks with highly reproducible precision. The level of fine control associated with automation provides the potential to evaluate and optimise such process parameters (e.g. dispense height, flowrate), whereas under manual operation such procedures may be poorly controlled. Automated cell culture processing has been applied to a variety of cell-propagation process, including tissue product manufacture [Offin, 1999]; improvements in cell culture associated with process automation can provide increased yield and more consistent batch to batch output compared with a manual approach, such as higher cell 'viability' following trypsinisation of adherent cells [Archer and Wood, 1992]. Replacement of human operators with cleanroom robotics systems in laminar airflow

enclosures reduces the risk of transfer of infections agents, either to or from human operators and cellular process materials. Such enclosed robotic systems can also be routinely sterilised with gaseous agents such as formalin [Archer and Wood, 1992]. Robotic processing has been shown to reduce contamination rates (for large numbers of roller bottles) from around 5% to less than 0.01% [Offin, 1999].

A key benefit of automation is the ability to rapidly transfer an established (small-scale) process to large-scale manufacture. Conventional process scale-up involves re-development with different apparatus (e.g. large-scale bioreactors), which may involve costly and time-consuming design, commissioning and validation work and product equivalence studies. With automated systems a small-scale process can be scaled linearly by simply increasing the number of small batches, known as 'scale-out'. A scale-out approach is well-suited for many tissue engineering applications, particularly autologous processes where small, individual patient batches must always be handled separately and identically. The increased speed of scale-up (scale-out) with automated systems can result in a dramatic decrease in time to market for many products [Kempner and Felder, 2002]. Automated methods for identification and tracking of individual process units, such as barcodes, may be linked to a computerised database allowing rapid cross-matching and checking of batch identity with associated electronic record-keeping of process operations. Computerised database systems utilising barcodes for transfusion tracking and patient cross-matching (including autologous transfusion) are ideal for preventing errors associated with traditional hospital practices [Lau and Cheng, 2001].

A key practical limitation with robotic handling systems is their lack of intelligence or inability to respond to unusual circumstances, unless specifically programmed. For example robotic systems require precise knowledge of item location (e.g. culture flask) and may be unable to cope with variations (e.g. a misaligned culture flask) or other unexpected process events. Automated handling of flexible items (e.g. culture bags, tubing) may be problematic as shape and position of such items can vary unexpectedly and would typically require development of sophisticated sensor and intelligence systems.

1.5.2. Design concepts

Various design concepts exist within the manufacturing sector; four such concepts are introduced briefly here in terms of their relevance to the development of new tissue products, processes or processing systems.

Design for use: Products should be designed based on a clear specification of the user requirements. The 'user' may include anyone interacting with the product or process apparatus during its manufacture, transport or use. The patient requires certain functional attributes from a product, while the physician may have requirements in terms of ease of product use, conformance with established clinical practice and product storage or shelf-life. Process systems should be designed with the operator in mind to facilitate compliance with standard operating procedures (SOPs), and there may also be a requirement for easy access to product manufacturing information for the physician e.g. confirmation of autologous graft maturation progress to enable optimal scheduling of surgical use. Understanding operations and requirements of couriering services is advisable to ensure reliable, efficient product transport to point of use.

Design for validation: Delays in product approvals can have a severe impact on commercial viability of novel tissue products [Stone, 2003]. The Food and Drug Administration (F.D.A.) has proposed new regulations requiring manufacturers to follow current good tissue practice (cGTP) in the methods, facilities, controls, recordkeeping and quality programs used for the manufacture of human cellular and tissue-based products [F.D.A. 21 CFR Part 1271, 2001]. Due consideration should be given to the validation approach which will ultimately be employed and possible product or processing alternatives which may lead to a reduced validation burden, e.g. maximal use of pre-validated process feedstock materials and other consumables.

Design for manufacture: The principle of design for manufacture is to invest upfront in product/process design to reduce manufacture cost, generating product/process/ apparatus designs which are ultimately cheaper to produce. Generally, the larger the number of product units to be manufactured, the more it is worth investing in improving product/process design. This concept may be applied both to the product and to the production equipment; this may be a very important consideration for both tissue products and 'scale-out' automated process systems where large numbers of identical machines may be employed in manufacture.

Risk management: An approach based on systematic assessment, prioritisation and reduction of risks associated with a product or process. Risks are typically assessed as

the product of the chance (risk) of an adverse event and the severity of associated consequences (hazard). Consequences may include financial impact of lost product batches (financial risk), effect on the patient of a failed therapy (patient risk) and exposure of operators to dangerous materials (operator risk). During development of a product or manufacturing process, it is useful to examine all areas to be developed and make an assessment of their feasibility. For a processing step or product attribute where the technology to be used is unknown or unproved, there exists the possibility that a cost-effective solution cannot be found; these areas are high risk (development risk) and must be addressed as high priority to ensure successful process/product development.
The F.D.A. recently (2002) launched an initiative to reduce the burdens associated with validation and inspection of manufacturing processes "*Pharmaceutical cGMPs for the 21st Century: A Risk-Based Approach*" which encourages implementation of risk-based approaches to validation prioritising both industry and regulatory agency attention on high-risk processes. Within a cell or tissue production process key risks are contamination and excessive product variation leading to non-compliance and batch failure, or even release of contaminated product. Risks associated with a manufacturing systems could include machine or power failure, which might be mitigated by preventative maintenance or use of backup systems.

### 1.5.3. Cost factors

Along with increased safety and product quality (through machine precision and reproducibility), reduction in production cost is a major driver for development and implementation of automation in the process industries [Jerney TD, 1999]. If an automated solution is predicted to be cost-beneficial for both the user and the supplier, compared to a manual process, then development and application of the automated system is appropriate. While traditional batch processing techniques can be difficult to employ for an autologous process, making economies of scale problematic [Mayhew et al., 1998], cell culture automation has been shown to be economically favourable compared to manual processing for large-scale roller bottle biopharmaceutical production processes [Archer and Wood, 1992].
The complexity and hence cost of an automated processing system will reflect that of the process. It is appropriate to critically assess a process and simplify as far as possible before embarking on the design of automated systems. Lengthier process operations are more equipment intensive; minimisation of process times (e.g. trypsinisation,

centrifugation, aspirate, dispense) can reduce the total apparatus requirement and lower capital costs.

Maximising yields at each processing step increases overall process productivity and reduces costs. Minimising the number of material transfers and separate vessels used will reduce hold-up losses. Unit operations yield should be maximised both on a volume basis (i.e. minimise hold-up loss) and also by reducing deleterious effects on process materials (e.g. due to shear damage, nutrient deprivation).

While at the development stage consumables costs (e.g. media, culture flasks) may appear to be major process costs, it is important to keep consumables costs in perspective as they may be small in comparison to other costs such as packaging and delivery of tissue product in a controlled environment. The major direct costs for a cleanroom project are the facility itself, the process equipment, process support utilities and the final pre-production validation [Rogers, 1993]. The generalised turnkey cost of a GMP biopharmaceutical facility can be estimated at \$800 - \$1200 /ft$^2$ [Reisman, 1999]. Running costs associated with provision of facilities such as space, basic staffing, HVAC (heating ventilation air conditioning), utilities etc. within a cGMP manufacturing environment are considerable; basic light industrial facility running costs are around \$26 /ft$^2$ p.a. [Beggs M, The Automation Partnership, Cambridge, UK, personal communication], with additional running costs for general utilities required by GMP biopharmaceutical processes estimated at \$28 /ft$^2$ p.a. [Farid, 2002].

Development costs for specialist automated processing systems are high compared to the manufacture cost of an individual system. Development cost is often dominated by design, build and testing of the control software required. Development costs can be largely avoided if it is possible to utilise a platform which is already available; cost of modifications to existing systems is typically low compared to development of a new system. [Bargh N, The Automation Partnership, Cambridge, UK, personal communication].

Alternative process scheduling strategies exist for automated systems: implementation of just-in-time scheduling requires considerable investment in control infrastructure and process development; alternatively scheduling processes with allowable holding times (decoupling points) between operations is more straightforward, but may entail higher inventory costs and the deleterious effects of a holding interval on labile product.

### 1.5.4. Regulatory, monitoring and control aspects

An automated biological process requires validation of the biological integrity of the process, validation of (any) adaptation of the process to the machine and validation of the machine function [Jervis D, The Automation Partnership, Cambridge, UK, personal communication]. Adherence to regulatory guidelines and cGMP (current good manufacturing practice) is vital to achieve straightforward regulatory approval for a manufacturing process. To implement cGMP in a production facility, plant automation is an important tool [Dorresteijn et al., 1997]. Record-keeping is an important part of process validation and automated systems should comply with F.D.A. regulations on electronic records and signatures [F.D.A. 21 CFR part 11, 2003]. Autologous cell products are inherently variable and control systems will be required to monitor process performance and either notify operators of required intervention or follow pre-programmed procedures (e.g. increase culture time). Integrated on-line sampling may be required for process monitoring and control (e.g. automated calculation of dilutions, glucose and lactate monitoring) and could also be used for the prediction of [cell or] tissue harvest times [Naughton, 2002].

### 1.5.5. Tools for process documentation and visualisation

Various design tools are available which can assist the process development scientist and equipment design engineer to visualise the whole process in detail and to elucidate the key processes, parameters and design constraints within the process.

Process flow diagrams: The use of process flow diagrams (flowsheets) is well established in process engineering and the purpose and utility varies greatly depending on the type of diagram and application. Successively more detailed diagrams will be constructed as the process is developed. Typically, a whole process may be visualised using a simple high level diagram, describing the main process steps; an example of this type is shown in figure 1-2. At the next level of detail diagrams would include process requirement specifications, in terms of material flow volumes, cell concentrations, timescales and other parameters such as required temperature. Further diagrams would comprise specification of particular technologies or devices to be used for operations (e.g. centrifuge for concentration, shaker for resuspension) and precise parameters (e.g. centrifuge time, speed) as they are determined. At the lowest level the exact details of the process are established and described; process times, temperatures, data and material flows, control inputs/outputs and feedback are included. The lowest-level

diagram represents a precise functional specification for the process, equivalent to standard operating procedures, and represents the exact specifications to which (automated) processing systems must operate.
Construction and manipulation of process flow diagrams can have several important benefits in process and automated system design, such as facilitating identification and prioritisation of 'development risk' (section 1.5.2.), identifying key breaks in the process for the design of separate processing systems, clarifying material flows facilitating the design and scheduling of material transfer operations, and identifying process bottlenecks or operations where improvements are required.

Timing diagrams: A timing diagram (or process schedule) is effectively a Gantt chart for the process. Once a reasonably detailed process specification (process flow diagram) has been drawn up for a single process (e.g. one autologous batch), a timing diagram can be constructed for single and multiple parallel batches. Analysis of timing diagrams can help identify key time and timing constraints on the process, distinguishing between constrained (e.g. minimum) and flexible (e.g. maximum wait) processing times. By analysing the usage of various pieces of apparatus when multiple parallel batches are considered, processing bottlenecks can be identified and requirements for added processing flexibility or capacity clarified. Use of such diagrams can help optimise equipment usage. A solution whereby the required number of parallel process streams are interleaved successfully without resource conflicts represents an overall (manufacturing) schedule for the facility.

Design windows or 'windows of operation': A "window of operation" is defined as being the operational space determined by the system [chemical, physical and biological] and process [engineering] constraints and correlations governing a particular process or operation under consideration [Woodley and Titchener-Hooker, 1996]. This methodology is useful in elucidating the sensitivity of the overall process to changes in various process parameters, such as product specification or processing yields. Process visualisation tools utilising a 'windows of operation' approach have previously been constructed for biopharmaceutical manufacturing processes to aid in the evaluation of alternative processing schemes [Zhou and Titchener-Hooker, 1999; Woodley and Titchener-Hooker, 1996] on the basis of changes to process parameters such as

productivity. Development of manufacturing strategy in bioprocesses may also be aided by decisional tools based on manufacturing models, including costs [Farid et al., 2000].

## 1.6. Project aims, scope and strategy

### 1.6.1. Aims and scope

The primary aim of this work is to develop engineering design bases for systematic design of automated processing systems for application in cell and tissue product manufacture. Efforts will be focussed on processes (unit operations) common to many or all tissue engineering and cell therapy processes (see figure 1-2), with principal investigations relating to cell loss during cell suspension transfers and cell concentration. In order to apply a systematic approach to process characterisation and design it is appropriate to consider and/or examine handling properties and sensitivities of cellular process materials such as rheology, cell size, potential for nutrient limitation and effects of hydrodynamic (flow) damage on cell recovery. In addition it is desirable to elucidate any other important process factors which may influence automated processing strategy or design, such as potential problems with cell aggregation or process variability.

Cell culture has traditionally been thought to be non-amenable to automation but experience has shown that automation can improve productivity and reproducibility through tight control of processing parameters [Archer and Wood, 1992]. It is thought that a similar situation and potential for improvements may exist with other process operations such as cell concentration. It is anticipated that development and performance characterisation of semi-automated cell concentration procedures may demonstrate benefits associated with implementation of process automation.

In order to examine the practicality of applying currently available automated cell culture systems in autologous tissue manufacture, a study will be undertaken examining the feasibility of generating sufficient cells for a stipulated autologous product. Utilising a 'windows of operation' approach for a predicted manufacturing process will enable visualisation of predicted process feasibility and examination of the effect on feasibility of altering process parameters such as cell yield, thus demonstrating the utility of using such design tools early in tissue process development.

### 1.6.2. Framework for investigations

Given the direct relevance of process 'scale-out' to producing many small products batches to autologous therapies, an autologous tissue product was specified as the model process for investigations. Manufacture of living artery substitutes from a small vein biopsy was chosen due to the large clinical potential for such a technology and the large number of investigations which tissue engineered vascular grafts have attracted in recent years [Ratcliffe, 2000]. An alginate hydrogel encapsulation technology was selected for tissue formation due to the precedent for application of alginate hydrogels as extracellular matrix materials [Rowley et al., 1999], novelty of alginate encapsulation in vascular graft formation, and the high yields which can potentially be achieved during tissue formation using an encapsulation approach.

As the primary focus of the research was to develop process design approaches rather than a functional tissue product, the vascular graft construct considered in the model process was specified as a simplified construct consisting of only one cell type (smooth muscle cells). The cell type selected for experimental investigations was an immortalised rat aortic smooth muscle cell line (which had been previously screened for major pathogens); being a mammalian vascular cell smooth muscle cell type this cell line has direct relevance to the vascular engineering application considered. It was considered appropriate to use an immortalised cell line rather than primary cells in order to facilitate generation of a large cell bank and reliable production of large numbers of matching cells throughout the duration of the work, avoiding any requirements for costly, time consuming or unreliable cell sourcing procedures or complex or expensive growth media.

# Chapter 2: Materials and Methods

## 2.1. Cell culture

Table 2-1. Fluid volumes for cell culture and harvest reagents, per flask. 'Typical' values given were subject to variation of the order of ± 0.5mL, excepting T500 values for 'medium' and 'inoculum'. The 'inoculum' volume was varied to allow for cell concentration in the harvested cell suspension (to ensure cells were planted at 5000 ± 500 1/cm$^2$) and the 'medium' volume was adjusted accordingly to achieve a total (inoculum + medium) of 100 ± 1 mL per T500 flask. In experiments where smaller flasks were used (e.g. T25, T75), reagents volumes were proportional to area, as for T150 flasks.

| Flask type | Culture area | PBS rinse | Trypsin / EDTA | Trypsin quench | Typical harvest | Typical medium | Typical inoculum |
|---|---|---|---|---|---|---|---|
| - | cm$^2$ | mL | mL | mL | mL | mL | mL |
| T150 | 150 | 30 | 6 | 18 | 24 | 22 | 8 |
| T500 | 500 | 100 | 20 | 20 | 40 | 87 | 13.3 |

A cell bank of immortalised rat aortic smooth muscle cells (Crl-1444, ATCC) had previously been laid down. Cells were normally cultured either in T150 flasks (Corning Inc., NY, USA) or T500 flasks (Nalge Nunc Intl., NY, USA). In either case cells were passaged every three or four days alternately and incubated under 10% $CO_2$ at 37°C. The flask passage procedure comprised media removal, rinsing of the cell sheet with PBS (Biowhittaker, Walkersville, MD, USA), subsequent incubation with 0.25% Trypsin / 0.02% EDTA (Sigma, UK) for 5-10 mins, dislodging cells by tapping each flask five times and quenching of trypsin/EDTA with culture medium (for fluid volumes see table 2-1). The resulting harvested cell suspension was pooled, 0.5mL sample taken for a cell count and the appropriate volumes of cell culture medium and harvested cell suspension dispensed to fresh T-flasks. Culture medium was Dulbecco's Modified Eagles Medium (DMEM, Biowhittaker) supplemented to 10% fetal bovine serum (FBS, Biowhittaker), 1% (2 mM) l-glutamine (Biowhittaker) and 1%

penicillin/streptomycin (Biowhittaker). Cells cultured in T150 flasks were passaged using a 1:3 split ratio (three new flasks planted per flask harvested, cell seeding density not directly controlled). Cells cultured in T500 flasks were inoculated into fresh flasks at a seeding density of $5000 \pm 500$ cells/cm$^2$. Cells were used for experiments between passages 7 and 20; passage numbers were counted from the initial vial purchased, denoted 'passage 0'.

## 2.2. Analytical

### 2.2.1. Trypan blue assay

Standard cell counts were performed at least in triplicate, normally quadruplicate. Where necessary (e.g. when assaying cell concentrates) cell samples were diluted to ~$1 \times 10^5$ cells/mL with 0.2 μm sterile filtered 9g/L NaCl/$H_2O$. Normally over 100 cells were counted in total for each measurement to ensure statistical reliability; in a few specific experiments this number was not achievable due to the very dilute nature of the samples generated (e.g. number of cells remaining in the supernatant after cell concentration, section 4.3.2.).

100μL of sample was mixed with 100μL of 0.4% trypan blue dye (Biowhittaker) by brief vortex mixing (~1s) and 20.5μL was applied to a standard (improved Neubauer) haemocytometer slide (Camlab, Camridge, UK). Slides were then assayed immediately with an inverted phase contrast microscope at 100x magnification (IX70, Olympus, Southall, UK). Unstained cells (appearing bright white) were scored as intact, stained cells (appearing dark blue) were scored as permeable (i.e. not intact); cells with an intermediate degree of staining were assigned to either group according to the staining intensity. Cell fragments, 'ghost' cells or cell debris particles were not scored. Replicates within a count were averaged and the error quoted as the standard deviation on the replicates performed. The volumetric concentration of intact, permeable and total (intact + permeable) cells was calculated via the known volume within a haemocytometer slide. For comparison with the flow cytometry assay, trypan blue assay error was investigated by performing quintuplicate repeats on three intact cell samples ($2 \times 10^6$ cells/mL) and calculating the standard deviation on results for each sample.

2.2.2. Biochemical analysis

For experiments involving metabolite analysis, 1 mL samples were taken from T-flasks following cell inoculation and from spent media prior to cell harvest (where appropriate, spent media was pooled prior to sampling). All samples were stored at -70°C and later analysed in batches using a biochemical analyser (YSI Inc, Ohio, USA); each batch was analysed in duplicate, the results averaged and standard deviation calculated as a measure of error. Changes in glucose and lactate concentration and uptake (or production) rates were calculated from initial and final metabolite concentrations in culture.

2.2.3. Flow cytometry

The assay was adapted from the Fluorescein diacetate (FDA) and Propidium iodide (PI) staining protocol described by Darzynkiewicz et al. [1994], substituting 7-Aminoactinomycin D (7AAD) for PI and adding fluorospheres for determination of absolute cell numbers. The mechanism of action of 7AAD (see below) is similar to trypan blue and identical to PI. 7AAD exhibits far less spectral overlap (than PI) with dyes emitting in the same frequency band as FDA [Schmid at al., 1992], facilitating 2-colour assay setup. Incubation of cells in the presence of FDA labels intact cells green while incubation with 7AAD labels permeable cells deep red. FDA (non-fluorescent) crosses intact or permeable cell membranes and is cleaved by cytosolic esterase proteins to yield a charged Fluorescein molecule (fluorescent) which is retained within intact, but not permeable cells. 7AAD preferentially diffuses into permeable cells and binds to DNA; DNA-binding substantially increases 7AAD fluorescence.

Flow cytometry sample tubes were pre-loaded with 800μL of 0.2μm sterile filtered 9g/L $NaCl/H_2O$. 100μL of cell sample was added, followed by 20μL of 5mg/mL 7AAD solution (Beckman-Coulter, UK), 5μL of 1mg/mL Fluorescein diacetate (Sigma, UK) in acetone (Sigma, UK) and 100μL 'Flow-count' fluorospheres (Beckman-Coulter, UK). Samples were incubated at room temperature in the dark for 15 minutes and analysed immediately by Argon laser (488nm, 15mW) flow cytometry (EPICS XL4, Beckman-Coulter, UK). Data acquisition recorded FDA emission at 525nm, fluorospheres at 620nm and 7AAD emission at 675nm, all via bandpass filters; data acquisition was stopped at 5000 non-fluorosphere events (i.e. 5000 cells or other particles). The 'discriminator' threshold was set at forward scatter (FS) $\leq 5$ to exclude small debris

particles from data acquisition. Counting beads formed a distinct population and were gated in a plot of FDA intensity (525nm) vs. BEADS intensity (620nm), figure 3-6c. Intact and permeable cells formed distinct populations and were gated accordingly in a plot of FDA intensity (525nm) vs. 7AAD intensity (675nm), figure 3-6b. Intact and permeable cell concentrations were calculated within the flow cytometry software based on the known concentration of stock fluorospheres and a 1:1 mixture with cell sample; 'total cell concentration' (intact + permeable) and 'percentage integrity' (100% * intact / total) were calculated from these outputs. Accuracy of the assay was investigated by assaying a dilution curve, generated by serially diluting a suspension of intact cells (~$1x10^7$ cell/mL in 9g/L $NaCl/H_2O$), dilution factor 2.3. An intact/permeable stepped curve was generated by mixing aliquots of intact and permeabilised (heated 60°C 15min) cells at $2x10^6$ cell/mL. Standard curves were assayed first by flow cytometry and subsequently manually by trypan blue. Assay precision was investigated by performing quintuplicate repeats on three different intact cell samples ($2x10^6$ cell/mL) and calculating standard deviation on results for each sample. Expected flow cytometry assay error (coefficient of variation, cv) was also calculated based on counting and sampling errors: the [statistical] error in a cell count is approximated by the square root of the number of cells counted [Biowhittaker, 2003]; the sampling error was calculated based on the micro-pipette tolerances as quoted by the manufacturer.

### 2.2.4. Cell size distribution

Four samples of cell harvest suspension were collected from either T150 or T500 flasks, on days 3, 4 or 5 of culture. A few µL were applied to a standard glass slide with coverslip and cell diameters were measured (>100 cells per sample) by eye with a graticule on an inverted phase contrast microscope (IX70, Olympus, UK) at 600x magnification. At 600x magnification, the 100 graticule divisions corresponded to 1.7µm per graticule division. Any non-spherical cells were measured at 45° to an observed axis of symmetry.

### 2.2.5. Rheology

Concentrated cell suspensions were prepared by concentration protocol (A) (sections 2.3.4., 4.3.2.) and concentrate rheology was measured using a 0.5mL cone (cone angle 0.8°) and plate rheometer (LVDV-II+, Brookfield, MA, USA); no replicates were

performed due to practical limitations on generating sufficient cells for the highly concentrated samples. Rheometer and sample temperature were controlled at 25 ± 0.5 °C using a water bath and peristaltic recirculation pump. The rheometer calibration was checked against a low-viscosity (~5 mPa.s) silicone oil standard (RT5, Cannon instrument company, PA, US); measurement error was found to be less than 3%. For each sample several different shear rates spanning the measuring range of the apparatus were investigated (the magnitude of measurable shear rates was reduced with more viscous samples). The measured shear stress was allowed to stabilise at each shear rate and was then recorded. First the lowest shear rate was measured, stepping up to the highest shear rate and then stepping down to the lowest shear rate. Newtonian, Bingham plastic and Power law fluid parameters were determined by linear regression analysis of appropriate plots. For correlation of apparent viscosity with volume fraction it was necessary to either extrapolate or interpolate data to a standard shear rate; 200 $s^{-1}$ was chosen as this shear rate minimised the extrapolation required. Extrapolation was performed manually using best fits to full data sets (i.e. including data from both stepping up and stepping down of shear rate in the rheometer) on a plot of apparent viscosity vs. shear rate (figure 4-3).

Viscosity of cell suspensions in cell culture medium was determined as above (section 2.2.5.) except that different cone was fitted to the rheometer, allowing a sample volume of 1.0mL. Five samples were investigated, cell concentration being 0, 0.5 $x10^5$, 1.0 $x10^5$, 1.5 $x10^5$ and $3x10^5$ cells/mL. Fluids were observed to be approximately Newtonian and so viscosity was calculated with a best fit line through all data points (and forced through the origin) in a shear stress vs. shear rate plot. Viscosity did not change significantly in this concentration range and so viscosity of cell culture medium and dilute cell suspensions was taken as the average of the five samples (1.25 mPa.s).

### 2.2.6. Photography

Cell suspension (20μL) was applied to a standard haemocytometer slide and visualised with an inverted phase contrast microscope (Olympus, UK). Images were recorded with a digital camera (DB12, Olympus, UK). Magnification and sample staining varied by experiment, although the minimum magnification (100x) was usually used for photography due to the low image capture area of the camera.

## 2.3. Cell concentration

### 2.3.1. Predicted cell sedimentation time

Predictions were made for the sedimentation time in cell harvest suspension based on Stokes' law [Lentfer et al., 2003], modified for centrifugal application:

$$t = 6.\pi.r.\mu_o.h / ((\rho_o - \rho_f).V.(RCF).g) \qquad \text{(eq. 2-1)}$$

Where:

- $t$ = sedimentation time (s)
- $h$ = height of fall (m)
- $r$ = radius of particle, in this case a cell (m)
- $\mu_o$ = viscosity of suspending fluid (Pa.s)
- $\rho_o$ = density of particle, being cells in this case (kg/m$^3$)
- $\rho_f$ = density of suspending fluid (kg/m$^3$)
- $V$ = volume of particle (m$^3$) ; volume of a sphere = $4/3.\pi.r^3$
- RCF = relative centrifugal force (no units)
- $g$ = force of gravity (9.81 m/s$^2$ or N/kg)

The analysis considers the smallest cells (12.5μm (section 2.2.4., figure 4-2) cf volume mean cell diameter, 22.4μm) being sedimented from the fluid top surface (maximum height of fall) in a centrifuge tube. As smaller cells will sediment more slowly, and cells at the fluid top surface have the furthest distance to travel, the analysis predicts the maximum time taken to sediment *all* cells. The 'height of fall' used corresponds to the depth of fluid of 40mL of liquid in a standard 50mL centrifuge tube. The viscosity of the suspending fluid was assumed to be equal to cell culture medium, which had been previously measured as 1.25 mPa.s (section 2.2.5.). The density of mammalian cells was assumed to be 1050 kg/m$^3$ [Willoughby N, Lonza Biologics, Slough, UK, personal communication]. The density of suspending fluid was assumed to be equal to cell culture medium, measured to be 1008 kg/m$^3$: the mass of both cell culture medium and deionised water (both at 20 ± 0.1°C) required to fill a volumetric flask (500 ± 0.1mL at 20°C) was measured using a laboratory balance and the density of cell culture medium was calculated against the water as a standard (1000 kg/m$^3$). Relative centrifugal force (RCF), which is simply a multiplication factor applied to the gravitational force at the earths surface, g, is the variable in the analysis and was the standard input variable on the centrifuge used. It was assumed that the sedimentation force is constant throughout the depth of suspension, that the sedimentation force acts along the axis of the centrifuge tube and that wall effects (i.e. cell-wall collisions) are negligible.

2.3.2. Predicted oxygen depletion time

A simple calculation was performed for the time taken for mammalian cells in suspension to consume all the oxygen in the suspending fluid:

$$t = s \cdot (1 - \phi) \cdot (c \cdot OUR)^{-1} \quad ; \quad \phi = c \cdot v \qquad \text{(eq. 2-2)}$$

Where:

- $t$ = predicted time to oxygen depletion (h)
- $s$ = oxygen solubility in suspending fluid ($g.L^{-1}$)
- $\phi$ = volume fraction of cells (v/v)
- $c$ = cell concentration (cell/L)
- $v$ = cell volume (L/cell)
- $OUR$ = oxygen uptake rate ($g.cell^{-1}.h^{-1}$)

Initial assumptions: suspending fluid is initially saturated with oxygen; oxygen solubility = 7.3 $g.m^{-3}$ (for water at 37°C) [Doran, 1995]; oxygen uptake rate (OUR) of cells is constant; there is no mass transfer of oxygen to or from the system; OUR is not limited by mass transfer (kinetic) limitations; cell diameter = 22.4μm (section 4.1.2.). Values of OUR were adapted from reported literature values (table 4-3b.) to represent the order of magnitude range of OUR expected for primary cells (table 4-3a.). Three separate values were used to generate scenarios for 'Low', 'Moderate' and 'High' OUR.

2.3.3. Preliminary concentration protocol development

Initially cell concentration was carried out by a centrifuge/resuspend protocol using a pipette to perform manual pellet resuspension, denoted protocol (M). Subsequently protocols using either a vortex mixer or an orbital shaker for pellet resuspension were developed, denoted protocols (A) and (B) respectively. Descriptions of all three protocols are given below (section 2.3.4.). During development of protocol (B), two preliminary studies were carried out to determine appropriate centrifugation and resuspension conditions.

Preliminary centrifugation study (see also table 4-5a.): Rat aortic smooth muscle cells were harvested from T500 flasks, aliquoted into 50mL centrifuge tubes (50mL harvested cell suspension per tube) and centrifuged (swing bucket centrifuge) for either 100g 7min, 300g 3min, 500g 2min or 1000g 2min. The supernatant was aspirated, being careful not disturb cell pellets and cell pellets were subsequently resuspended by orbital

shaking (4.5 mm orbital throw, IKA, Staufen, Germany) with 0.5 mL of supernatant, at either 100, 300 or 500 RPM. Shaking was briefly interrupted and pellets examined after 30, 60, 120, 240 and 360 seconds; the fraction of cell pellet remaining (not resuspended) was estimated by eye.

Preliminary resuspension study (see also table 4-5b): Rat aortic smooth muscle cells were harvested from T500 flasks, aliquoted into 50mL centrifuge tubes (50mL harvested cell suspension per tube) and centrifuged (swing bucket centrifuge) at 300g for 3 minutes. The supernatant was aspirated, being careful not disturb cell pellets and cell pellets were subsequently resuspended by orbital shaking (4.5 mm orbital throw, IKA, Staufen, Germany) with 0.5 mL of supernatant, at either 400, 600 or 800 RPM. Shaking was briefly interrupted and pellets examined after 7.5, 15, 30, 60, 120 seconds; the fraction of cell pellet remaining (not resuspended) was estimated by eye.

2.3.4. Cell concentration protocols

Three different protocols were used to concentrate cells during the course of this work (table 4-4.). In all protocols, cell harvest suspension was dispensed into standard 50mL polypropylene centrifuge tubes (Corning, UK), loaded into a swing-bucket centrifuge (Eppendorf, Cambridge, UK) and centrifuged for a specified time at a specified force (quoted as relative centrifugal force, RCF). Supernatant was then aspirated from the centrifuge tube, resuspension fluid added and pellet resuspension carried out according to the specific protocol (see table 4-4.). The three protocols are now briefly described:

Protocol (M): Centrifugation was carried out for 7 minutes at 100g at room temperature. Following addition of resuspension fluid (9g/L saline solution), pellet resuspension was carried out by tapping the centrifuge tube against a hard surface to dislodge the cell pellet and subsequently resuspending the pellet by repeated aspirate-dispense cycles using either an electric pipettor fitted with either a 1mL or 2mL pipette, or using manual pipettes, fitted with either 100µL or 1mL pipette tips.

Protocol (A): Centrifugation was carried out for 7 minutes at 100g at room temperature. Excepting the last ~5mL, supernatant was aspirated rapidly; for the last ~5mL the centrifuge tube was angled at ~60° to the vertical and the supernatant aspirated very slowly (figure 4-8, 4-9). Following addition of resuspension fluid (9g/L saline solution), the centrifuge tube was manually held on a vortex mixer (7mm throw, Nickel-Electro Ltd, Somerset, UK) for 5 seconds.

Protocol (B): Harvested cell suspension (40 ± 2 mL) was dispensed to the centrifuge tube. The centrifuge had been pre-cooled to 20°C and centrifugation was carried out for 3 minutes at 300g. Excepting the last ~5mL, supernatant was aspirated rapidly; for the last ~5mL the centrifuge tube was angled at ~60° to the vertical and the supernatant aspirated very slowly (figure 4-8, 4-9). Following addition of resuspension solution (9g/L saline, 2.4 ± 0.1 mL), the centrifuge tube was placed in a rack fitted to an orbital shaker (4.5mm throw, IKA, Staufen, Germany) and shaken at 600 RPM for 60 seconds.

2.3.5. Cell concentration protocol performance

For protocols (A) and (B), volumes of initial harvest suspension dispensed to the centrifuge tube, added resuspension solution and final resuspended cell concentrate were measured by graduated pipette. In addition samples were taken from initial and final cell suspensions and analysed by trypan blue cell count. To investigate the location of cells following concentration, an experiment was performed in which samples were taken from initial cell harvest suspension, aspirated supernatant, final cell concentrate and 2mL of 0.2μm filtered 9g/L $NaCl/H_2O$ which had been used to rinse out the centrifuge tube following concentrate removal. The cell concentration in these samples was subsequently assayed either by manual trypan blue haemocytometer count or flow cytometry.

## 2.4. Shear studies

2.4.1. Calculation of capillary wall shear stress and Reynolds number

Considering the opposing forces on a cylindrical fluid element in pipe flow, it can be shown that the wall shear stress, $\tau_w$, in a cylindrical pipe (length L, diameter d) is theoretically given by :

$$\tau_w = \frac{d.\Delta P}{4L} \qquad \text{(eq. 2-3)}$$

The superficial (i.e. average) fluid velocity in a pipe, u, for a Newtonian fluid (viscosity μ) is theoretically related to the pressure drop, ΔP [Coulson and Richardson, 1996] by :

$$u = \frac{\Delta P.d^2}{32L.\mu} \qquad \text{(eq. 2-4)}$$

Combining (eq. 2-3) and (eq. 2-4), the wall shear stress in the capillary may be calculated as :

$$\tau_w = \frac{8.\mu.u}{d} \qquad \text{(eq. 2-5)}$$

Where:

u = superficial fluid velocity (m/s)

d = capillary internal diameter (m)

$\mu$ = fluid viscosity (N.s/m$^2$)

$\tau_w$ = wall shear stress (N/m$^2$ or Pa)

Viscosity of harvested cell suspension in cell culture medium between 0-3x10$^5$ cell/mL (n = 5) was found to be constant at 1.25 mPa.s (section 2.2.5.). Capillary internal diameter was quoted by the supplier and superficial fluid velocity was calculated from the know syringe pump flowrate:

(superficial velocity) = (flowrate) / (cross-section area)

The Reynolds number for a pipe (eq. 2-6) may be calculated using the standard formula [Coulson and Richardson, 1996] :

$$\mathrm{Re}_p = \frac{\rho u d}{\mu} \qquad \text{(eq. 2-6)}$$

Where:

$\mathrm{Re}_p$ = Reynolds number for pipe flow

$\rho$ = fluid density (kg/m$^3$)

u = superficial fluid velocity (m/s)

d = capillary internal diameter (m)

$\mu$ = fluid viscosity (N.s/m$^2$)

For the purposes of Reynolds number calculations, fluid density was assumed to be equal to water, i.e. 1000 kg/m$^3$.

2.4.2. Effect of 0-20 capillary passes (120 Pa wall stress) on cell number, membrane integrity, growth and metabolism

All steps were carried out under sterile conditions within a laminar flow biosafety cabinet. Harvested cell suspension (~10$^5$ cells/mL) from the normal passage protocol (section 2.1.) was divided into 15mL aliquots for shearing and a 'no flow reference sample' (figure 2-1a). The suspension was taken up into a disposable 25mL polypropylene syringe (Beckton-Dickinson, Oxford, UK) and the syringe was fitted

with a hypodermic needle (Microlance 0.45x23mm, Beckton-Dickinson, Oxford, UK). Air bubbles were expelled, the syringe was mounted onto a syringe pump (PHD2000, Harvard Apparatus, MA, USA) and the cell suspension was expelled at 50 mL/min into a 50mL sample tube. This procedure was repeated up to twenty times; the needle was removed prior to taking cell suspension up into the syringe. A 'no capillary control' (figure 2-1b) was carried out using five repeat passes without the capillary fitted to the syringe. At the end of the experiment standard trypan blue cell counts (section 2.2.1.) were performed all samples. Wall shear stress and Reynolds number were calculated for the specified flowrate (section 2.4.1.). Cells from each sheared sample were inoculated into four T25 flasks at a standardised intact cell density (5300 cells/cm$^2$). T25 flasks had been prepared as per standard culture protocol (i.e. pre-loaded with 3.7 mL of culture medium) and where intact cell concentration had fallen during shearing, larger volumes of cell suspension were inoculated into T-flasks to compensate. A dilution of remaining cell suspension with culture medium, equivalent to seeded T-flasks, was sampled (1mL) for analysis of initial metabolite concentrations. T25 flasks were incubated as normal and sacrificed on days 1, 2, 4 and 6, taking a spent media sample (1mL) for metabolite analysis and using the standard cell harvest protocol (section 2.1.) to perform a cell count for assessment of cell density on the culture surface.

Growth of attached cells in T25 culture flasks was considered as a first order process:

$$\frac{dn_c}{dt} = k_c n_c \qquad \text{(eq. 2-7)}$$

Where: $n_c$ = cell number density (cm$^{-2}$)

$t$ = time in culture (h)

$k_c$ = growth rate of cells (1/h)

Integration and then taking logarithms of (eq. 2-7) yields a linearised form which was used to calculate growth rate of cells during the exponential growth phase, $k_c$ (observed to be from day 1 to day 4, figure 3-2) and the initial number of cells able to grow, $n_{c0}$ :

$$\ln n_c = k_c t + \ln n_{c0} \qquad \text{(eq. 2-8)}$$

Where: $n_{c0}$ = initial growing cell number density (cm$^{-2}$)

2.4.3. Effect of 1-100 Pa wall shear stress (0-5 capillary passes) on cell number and membrane integrity

For each flowrate investigated harvested cell suspension from the normal passage protocol (24mL, ~1x10$^5$ cell/mL) was divided into 6mL aliquots for shearing and a 'no

flow reference sample' (figure 2-1a). The four samples were sheared for 0 (no flow reference sample), 1, 2, and 5 capillary passes and standard cell counts performed on each sample. For each shear pass the sample was taken up into a disposable polypropylene syringe (10mL, Beckton-Dickinson UK Ltd.) and expelled though a small bore hypodermic needle (0.45x23mm, Beckton-Dickinson UK Ltd.) into a 15 mL cryovial (Nalge Nunc, NY, USA) using a syringe pump (PhD2000, Harvard Apparatus Ltd, UK). The Reynolds number and wall shear stress were calculated for each flowrate (section 2.4.1.). Rheology of the cell suspension had been previously measured (section 2.2.5.). A calculation was performed to check that the syringe pump was able to generate sufficient force to achieve the maximum specified flowrate, according to the manufacturer's specification.

2.4.4. Effect of capillary shear on cell number assessed by flow cytometry

For each flowrate investigated in the range 0-11 mL/min (0-15 Pa wall stress), cell harvest suspension (~40mL) from one T500 flask was concentrated (to ~2.5mL) using protocol (B), section 2.3.4.. The sample was transferred by pipette into a reservoir (15 mL cryovial, Nalge Nunc Intl., NY, USA) with any visible aggregates dispensed to waste during the transfer operation. 100µL of suspension was taken as 'no flow reference sample' (figure 2-1a). The sample was manually aspirated into a disposable plastic syringe (2.5mL, Beckton-Dickinson UK Ltd.), a capillary was fitted and air expelled from the syringe and capillary. Capillaries used were custom 0.51x120mm (21 gauge) luer lock 304 stainless steel with polished entry and exit (Coopers Needleworks, Birmingham, UK). The syringe was mounted vertically onto a syringe pump (PhD2000, Harvard Apparatus Ltd, UK) with the capillary tip positioned at the bottom corner of the (slightly tilted) reservoir base. The entire sample was dispensed at the specified flowrate and 100µL sample taken from the reservoir. The syringe pump was then used to repeat the aspirate-dispense cycle via the capillary, at the specified flowrate, with further 100µL samples being taken from the reservoir following sample dispense. Samples were then assayed for intact and permeable cell number by using the flow cytometry method developed (section 2.2.3.). For all experiments the significant parameter is the change of cell concentration with respect to the initial value and the results are presented as flow cytometry cell counts normalised with respect to the 'no flow reference sample' (figure 2-1a).

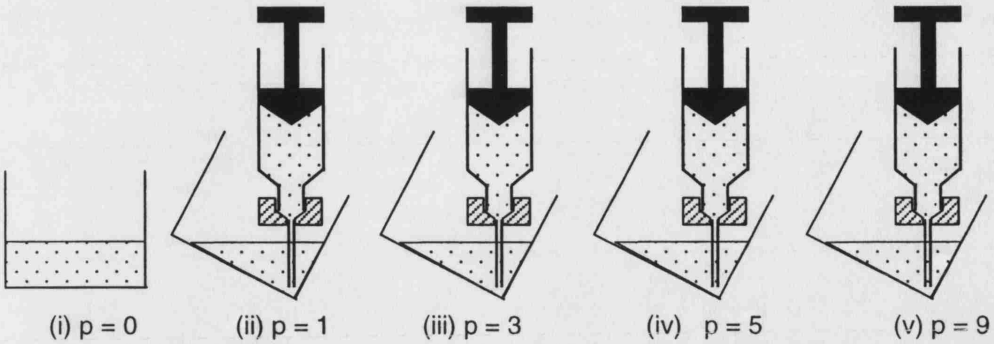


Figure 2-1a. 'No flow reference sample'. This example given is for capillary flow studies with cells in saline solution (sections 2.4.4. and 3.3.), and corresponds to experimental setup for each flowrate (shear stress) investigated. (i) The 'no flow reference sample' was not taken up into a syringe. (ii)-(v) Separate aliquots of concentrated cell suspension were taken up into a syringe, the capillary assembly was fitted and samples were sheared by either a single dispense (ii) or dispense-aspirate-dispense cycles for a total of 'p' capillary passes. Following shearing of all samples and cell concentration assay, data were expressed as 'fraction of cells remaining after shear', calculated with respect to the 'no flow reference sample' (i). NB this image illustrates the experiment part-way through aspirate or dispense. During an 'aspirate' cycle all of the sample was aspirated to the syringe, excepting a few μL to ensure bubbles were not drawn into the capillary.

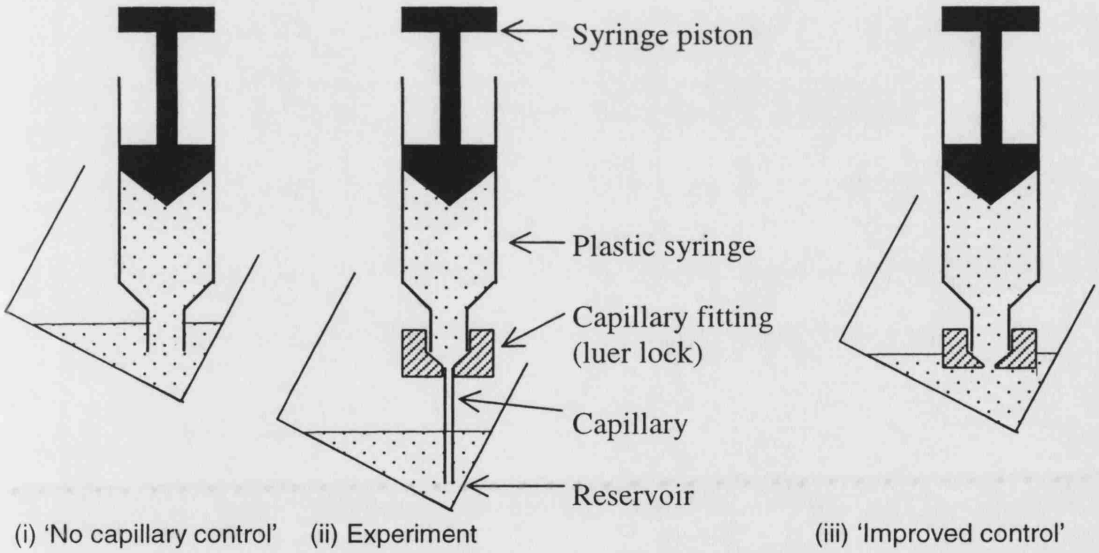


Figure 2-1b. 'No capillary control'. Normal capillary flow experiments were performed with a capillary (plus fitting) attached to the syringe (ii). To exclude any effects of the general procedure and any flow damage effects due to the syringe, a 'no capillary control' experiment (i), was performed for one or more experimental conditions (flowrates) in each study. 'No capillary control' experiments were otherwise performed as for the normal experimental protocol and included a 'no flow reference sample' (as above, figure 2-1a). Data for 'no capillary controls' are presented alongside normal experiment (ii) data at the same flowrate (shear stress), to compare the effect of the presence of the capillary assembly (capillary plus fitting). (iii) A suggested improved control to exclude effects of the capillary fitting (this 'improved control' experiment was not performed).

A second experiment was performed for higher flowrates, in the range 11-54 mL/min (15-75 Pa wall shear stress). In this experiment the protocol was identical, except that samples were resuspended in 5mL of 9g/L $NaCl/H_2O$ and sheared using a 20mL syringe; this larger syringe was required to achieve the higher flowrates under investigation.

In addition a control was carried out to quantify any cell loss in the reservoir over the maximum time on the experiment, sampling at time points equivalent to the lowest flowrate (i.e. slowest, longest) shearing run. On four occasions following shear experiments, the capillary was rinsed with 200μL of trypsin and a cell count performed to quantify any washed out cells which had adhered to the capillary.

## 2.5. Windows of operation

This analysis examines the ability of a robotic cell culture system to provide sufficient cells for tissue formation from a limited biopsy size; surgical and tissue maturation processing stages are excluded. A generalised process flowsheet for autologous tissue formation processes is presented in figure 1-2 and the stipulated autologous blood vessel process considered in this analysis is described in section 1.3.9.

### 2.5.1. Formulation of the analysis

As performance correlations are not widely available for novel tissue engineering unit operations a simplified approach was taken, using predicted process specifications and performance parameters and setting up windows diagrams on a case-by-case basis. Initial assumptions relating to the process and processing system considered are presented in tables 2-2a-b. Predicted process data used in the analysis are presented in tables 2-3a-c and estimated processing yields are given in table 5-1. The effect of changes in two major process parameters was examined: 'process yield' is unknown or uncertain for many novel tissue process operations and may have a major impact on process feasibility and economics; **'throughput'** (no. patient **units** produced, on a per cell culture robot per day basis) is examined as a design specification and is a representation, in core process terms, of processing capacity per capital investment (i.e. cost of automated cell culture systems per product unit (per patient)).

The analysis was formulated on a per-patient basis: one 'patient unit' is the discrete processing batch required to treat one patient, with each individual 'unit' requiring a multiple-passage cell culture train. A key variable in the analysis is the number of

passages in each culture train, with biopsy size dictated as that required to seed the first passage in the culture train.

The graphical output of the analysis was formulated in two parts ((1) and (2) below), each generating a 'stepped line' (essentially a histogram plot) in the final windows diagrams. These output lines are presented in the final 'windows of operation' diagrams as a function of initial biopsy size and number of passages in the cell culture train. (1) The number of cells which must be generated during cell culture (i.e. number of cells required for the downstream tissue formation process to operate) is a function of **'downstream process yield'** and is represented by the **'operating line'**. (2) The number of cell culture flasks which a culture robot can process (per patient) is a function of **'throughput'** and affects the maximum achievable cell culture area at the end of each cell culture train. Thus the maximum achievable final cell culture area (maximum no. cells which can be generated) at the specified **'throughput'** (design parameter), is represented by the **'design line'**.

2.5.2. Computational

Windows of operation were generated for individual case studies within a standard spreadsheet (Microsoft Excel, Microsoft, USA).

The 'operating line' was constructed on the basis of final cell culture area required, as calculated from predicted process parameters (table 2-3a) and yields (table 5-1):

$$A = \frac{c_t . V_t}{Y_d . c_f} \qquad \text{(eq. 2-9)}$$

Where:

- A = Equivalent cell culture area required at final passage ($cm^2$)
- $Y_d$ = **'Downstream process yield'** factor (all operations downstream of cell culture)
- $c_t$ = Cell density in formed tissue (cell/mL)
- $V_t$ = Volume of formed tissue (mL)
- $c_f$ = Cell density in culture flasks at harvest (cell/$cm^2$)

The number of cells (culture area) required at the final cell culture passage is only dependent on yield factors downstream of cell culture; thus the process yield factor applied in this analysis is 'downstream yield factor' (table 5-1). Passage trains were constructed 'backwards' from the equivalent final passage area required such that passages always provided sufficient cells to seed the next passage (see table 2-4).

The 'design line' (representing achievable cell number for a specified process throughput) was constructed on the basis of the maximum number of flasks which could be processed for each patient unit (individual cell culture trains), calculated according to the processing time available per unit (table 2-3b-c, figures 2-2a-b).

$$f_u = \frac{t_d.(1-(D_m + D_c))}{t_f.T} \qquad \text{(eq. 2-10)}$$

Where: $f_u$ = Max. number of culture flasks per patient unit (flask/unit)

$t_d$ = Total time per day (min)

$D_m$ = Robot downtime factor for maintenance

$D_c$ = Robot downtime factor for changeover and cleaning

$t_f$ = Processing time required per flask (min/flask)

T = **'throughput' (units)** [per robot per day basis], see below.

Basis: One robotic cell culture module, considering one day of production; on each day every robot completes the cell culture train (i.e. harvests all the flasks in the final passage) for 'T' [patient] **units**. The maximum number of flasks per [patient] **units** (culture train) was then translated into suitable cell culture trains (see table 2-4); the culture trains achieving the highest final passage area BUT NOT exceeding $f_u$ (flasks/unit) were used to construct the 'design line'. For both the operating and design lines, the required biopsy size was calculated according to the number of cells required to seed the first passage and the expected recovery of cells from a length of peripheral vein biopsy (table 2-3a, table 2-4).

2.5.3. Cell culture cost estimation

Required quantities of cell culture consumables (flasks, media etc.) were specified according to cell culture trains constructed for the 'operating line' (section 2.5.2.) with fluid volumes as for the standard experimental cell culture protocols (section 2.1.). Costs for flasks, media, FBS etc. were taken as the respective supplier's 2005 list price +VAT at 17.5% i.e. costs as per experimental studies in this work; NB costs for GMP supplies or complex media (e.g. for stem cells) could be significantly higher than values used here. Briefly, costs were: FBS £72.86 per 500 mL, DMEM £4.24 per 500mL, Trypsin/EDTA £25.90 per 500mL, PBS £7.83 per 1000mL, Penicillin/Streptomycin £28.23 per 500mL, L-glutamine £7.75 per 500mL. Once made up, complete medium cost was £22.81 per 500mL. T25 flasks £139.42 per case of 200, T175 flasks £159.56 per case of 50, T500 flasks £175.35 per case of 32.

Table 2-2a. Initial assumptions for the 'windows of operation' analysis. Values for estimated process parameters and automated cell culture system capacity are presented in tables 2-3 a-c.

| |
|---|
| The model process considers a simplified blood vessel construct comprising only one cell type (smooth muscle cells). |
| The analysis is based around an existing commercially available automated cell culture system (SelecT, The Automation Partnership, UK), capable of sub-culturing multiple cell types in parallel. The system essentially comprises a central robotic arm, a bank of automated incubators and various fluid handling systems. The central robot performs standard cell culture operations in a similar fashion to a human operator. Data for process times (i.e. machine capacity) are either adapted from data provided by the manufacturer or estimated based on manual processing times; data used are presented in table 2-3b, process flow sheet presented in figures 2-2a-b. |
| Within an automated cell culture system, the limiting factor on capacity is the time taken to process (passage) culture flasks. Flask incubators within the system would be sized according to the maximum capacity (throughput) of the central robot performing flask processing operations. |
| Cell culture is carried out using a combination of T25 ($25cm^2$), T175 ($175cm^2$) and T500 ($500cm^2$) culture flasks. The SelecT system currently uses T175 culture flasks. T500 (triple-deck) flasks have identical external dimensions to T175 flasks. T25 flasks are likely to be required where there are not enough cells available to seed the larger flasks, e.g. early passages in cell culture trains. The SelecT culture system could be easily adapted to process the additional flask sizes. |
| All three sizes of cell culture flask require the same time for processing. |
| Process wait times associated with trypsinisation (i.e. incubation with trypsin) may be ignored as the culture system could be set up to interleave harvesting operations for multiple flasks, i.e. the central robot would continue processing other flasks while waiting for trypsinisation (see figure 2-2a). |
| The growth rate of cells is constant, i.e. incubation time is the same for every passage, being an integer number of days. Typical incubation time for the cell line used in experimental studies was 3 or 4 days, although incubation time is not an important factor in this analysis (incubation time is independent of subculture processing time; incubation time only affects required incubator size, which is not considered in this analysis). |

| |
|---|
| Each passage provides a 3-fold expansion in the number of cells per flask, including yield losses during subculture operations. This was observed to be typical of smooth muscle cells used in experimental studies over a 3 or 4-day incubation. |
| Cell loss due to overproduction of cells in any passage is neglected. Any mismatch (excess) between the number of cells harvested from a passage and the number of cells required to seed the subsequent passage could be eliminated by optimisation of the passage train during specification of the final process. The analysis is constructed such that the number of cells harvested from each passage is always sufficient to seed the following passage (table 2-4). |
| Daily cell culture work schedules are identical, with the same (integer) number of patient units (i.e. culture trains) being started and completed each day; on each day the number of flasks harvested is equal to the number of flasks seeded. The result of this assumption is that, for a throughput of 1 patient unit per day, every day the robot will process the equivalent of all subculture operations within the entire culture train, with different passage numbers corresponding to different patient units. e.g. passage p1→p2 for patient (A), p2→p3 for patient (B), and so on. |
| Precise scheduling of culture operations on each day is not considered; it is assumed that scheduling clashes may be avoided, with final passage harvest being scheduled at a suitable time of day for further processing (i.e. tissue formation). |

Table 2-2 b. Additional process constraints for the 'windows of operation' analysis.

| |
|---|
| Biopsy size: The minimum possible biopsy size corresponds to the number of cells required to seed the smallest flask in use (T25), i.e. 1cm biopsy. Maximum biopsy size is arbitrarily specified at 10cm, being approximately one order of magnitude lower than the length of native autologous blood vessel used in standard coronary artery bypass grafting. |
| Maximum number of passages: Cell culture is limited to 5 passages to minimise phenotypic drift of cell cultures. This figure is typical of reported literature values for primary cells: cells used at passage 3-7 [L'Heureux et al., 1998], passage 5 or less [Breuer et al., 1996]. |

Table 2-3a. Estimated process parameters determining the number of cells required following cell culture. (*) Data as for windows of operation case (A), figure 5-1a.

| Parameter | Units | Value | Rationale |
|---|---|---|---|
| | | | |
| Tissue engineered blood vessel ID | (mm) | 4 | Unmet clinical need for small-diameter (<6mm) vascular replacements [Ratcliffe, 2000] |
| Vessel wall thickness | (mm) | 0.3 | Typical of native small-diameter vessel [Nicklason et al., 1999] |
| Vessel length | (cm) | 30 | As advised by a heart surgeon |
| No. vessels per patient unit | (-) | 5 | Four for quadruple bypass plus one for lot release testing; ~95% of operations require ≤ 4 grafts [Keogh and Kinsman, 2002]. |
| Total volume per patient unit | (mL) | 6.1 | Calculated |
| Cell density in formed vessel | ($x10^7$ cell/mL) | 1 | Typical value for alginate vessel constructs [Markusen, 2005]. Cubic 3D equivalent of 5000 cell/$cm^2$ 2D seeding density. |
| no. cells/unit | ($x10^7$) | 6.1 | Calculated |
| (*) **Downstream process yield** factor | (-) | 0.5 | Predicted based on observed experimental results (table 5-1) |
| (*) Equivalent no. cells required | ($x10^7$ cells) | 12.2 | Calculated |
| Cell density at flask harvest | ($x10^3$ cell/$cm^2$) | 18 | Adapted from cell culture data (figure 3-2) |
| (*) Culture area required | ($x10^3$ $cm^2$) | 6.8 | Calculated |
| Cells recovered from vein biopsy | ($x10^5$ cell/cm) | 1.5 | [Button et al., 2002] |
| Cell proliferation factor | (per passage) | 3 | Typical of experimental cell culture observations |

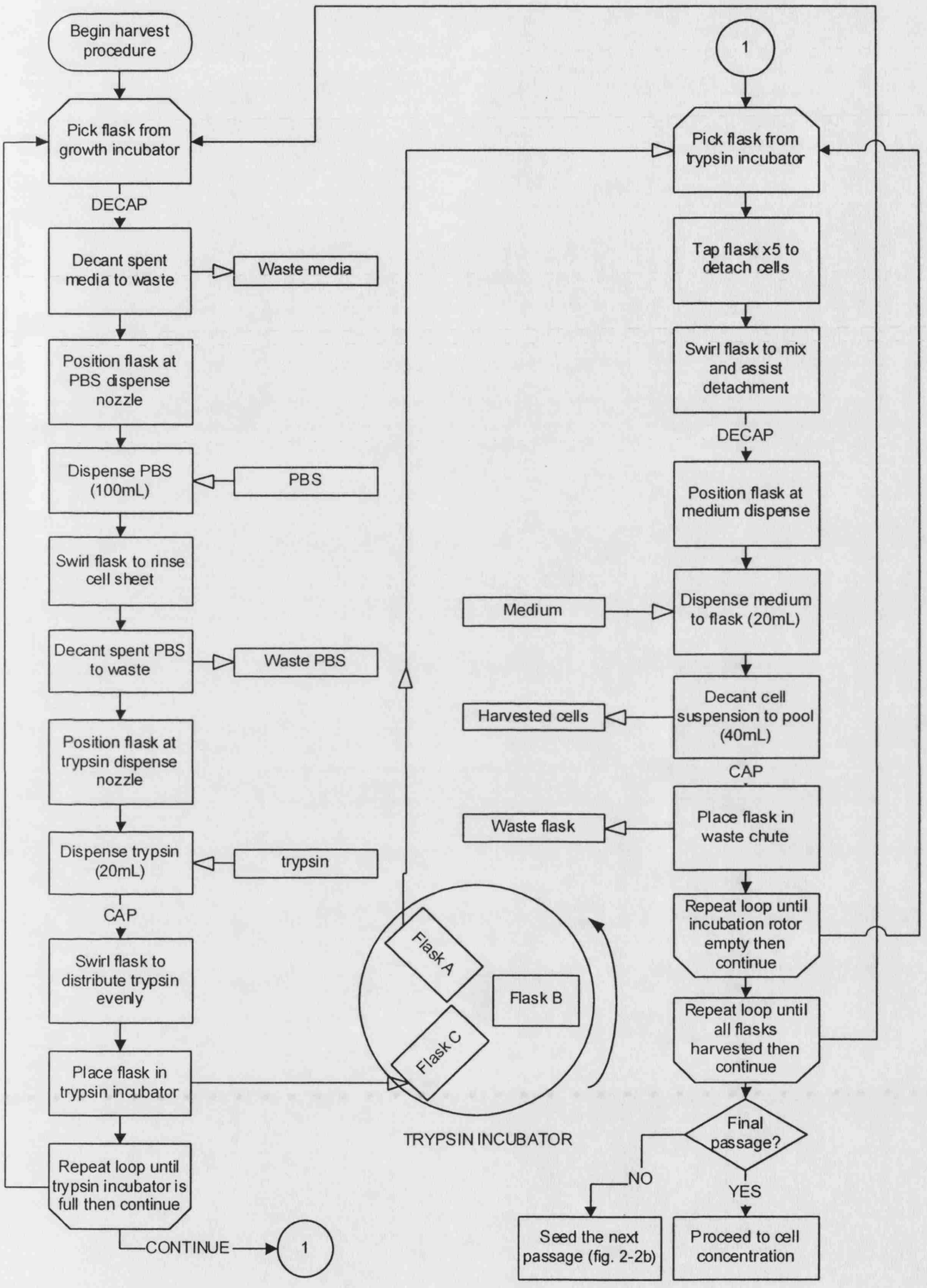


Figure 2-2a. Process flow diagram for cell culture flask harvest. This diagram represents a single patient unit i.e. all flasks for one passage. Solid arrow heads indicate process logic. Open arrow heads indicate material flows. Fluid volumes are for T500 flasks. Flask processing proceeds during trypsin incubation, so trypsin incubation time may be neglected (table 2-3b).

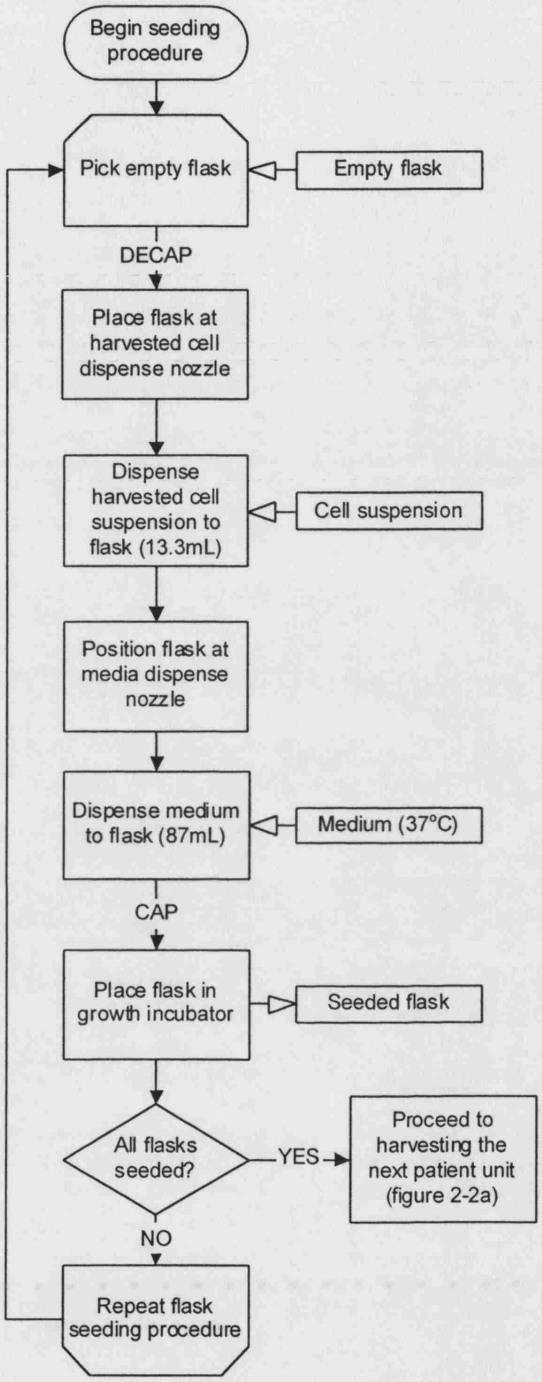


Figure 2-2b. Process flow diagram for cell culture flask seeding. This diagram represents a single patient unit i.e. all flasks for a single patient. Solid arrow heads indicate process logic. Open arrow heads indicate material flows. Fluid volumes are for T500 flasks.

Table 2-3b. Predicted automated cell culture flask processing (passaging) times.
Values are either adapted from data provided by the manufacturer of the SelecT robotic cell culture system, or estimated based on manual processing times (personal laboratory experience). Process times are for a single robotic cell culture module (SelecT). (*) It is assumed that trypsin incubation time can be neglected (see figures 2-2a-b).

| Flask harvest operation | time (s) | | Flask seeding operation | time (s) |
|---|---|---|---|---|
| Pick flask from incubator | 10 | | Pick empty flask | 10 |
| Decap | 10 | | Decap | 10 |
| Spent media removal | 40 | | Dispense cells | 60 |
| Dispense PBS | 30 | | Dispense media | 30 |
| Swirl | 20 | | Cap | 10 |
| PBS removal | 40 | | Place flask in incubator | 10 |
| Dispense Trypsin | 30 | | - | |
| Cap | 10 | | - | |
| Trypsin incubation | 300 * | | - | |
| Tap flask | 15 | | - | |
| Swirl | 20 | | - | |
| Decap | 10 | | - | |
| Dispense media (quench trypsin activity) | 30 | | - | |
| Aspirate cell suspension | 40 | | - | |
| Cap | 10 | | - | |
| Place flask in waste chute | 10 | | - | |
| SUBTOTAL | 325 | | SUBTOTAL | 130 |
| TOTAL processing time for plant and harvest of one flask (seconds) | | | | 455 |
| TOTAL processing time required per flask (min) | | | 7.6 minutes | |

Table 2-3c. Estimated processing time available in an automated cell culture system. Downtime factors (†) were specified as advised by an experienced automation engineer. (‡) Data as for windows of operation case (A), figure 5-1 a.

| Quantity | Units | Value |
|---|---|---|
| Total time available | (h/day) | 24 |
| Maintenance downtime factor (†) | (-) | 0.25 |
| Changeover downtime factor (†) for cleaning, media change, fresh flask stocking etc. | (-) | 0.125 |
| Process time available [per day] | (h) | 15 |
| Process time available [per day] | (min) | 900 |
| Process time required per flask | (min/flask) | 7.6 |
| Specified **throughput** [per robot per day] (‡) | (**unit**) | 4 |
| Maximum throughput [per robot per day] | (flasks) | 118 |
| Maximum process time per unit | (min/**unit**) | 225 |
| Max. number of flasks per culture train (‡) | (flasks/**unit**) | 29 |

Table 2-4. Example cell culture train used to construct 'Windows of operation' figures (figures 5-1a-c). This example cell culture train corresponds to the set up of the 'operating line' in figure 5.1a. Initial calculations (equation 2-9, section 2.5.2., table 2-3a) indicate that we require a minimum final cell culture passage area of 6754cm$^2$ (a). This is achieved by specifying 13x500cm$^2$, 1x175cm$^2$, 4x25cm$^2$ flasks (b), resulting in total area for this passage of 6775cm$^2$ (c). It is assumed that cell number triples in each passage (including any losses in culture) with harvest cell density being constant (at 18000 cell/cm$^2$), thus the preceding passage must provide a minimum area of (6775 / 3) = 2258cm$^2$ at harvest (d, e). The rest of the passage train may then be constructed by repeating this calculation 'loop' (first iteration illustrated by arrows). Alternatively, rather than using cells taken from a preceding passage, each passage could be seeded using cells taken directly from a biopsy: the number of cells required to seed passage 5 (f) is given by the total area for this passage (c) multiplied by the seeding density (harvest density / 3 = 18000 / 3 = seeding density = 6000 cell/cm$^2$), i.e. 6775*6000 = 4.1x10$^7$ cells (f). As a peripheral vein biopsy provides 1.5x10$^5$ (cells / cm vein, table 2-3a), the biopsy size required is (4.1x10$^7$ / 1.5x10$^5$ ) = 271cm of vein (g). The total number of passages (h) is counted backwards from the final passage in the cell culture train. (*) Are the output data for the operating line; these data are presented as a histogram plot in the 'windows of operation' diagram (figure 5.1a).

| Arbitrary passage number | 1 | 2 | 3 | 4 | 5 |
|---|---|---|---|---|---|
| Minimum required final area (cm$^2$) | 92 | 258 | 758 | 2258 (e) | 6754 (a) |
| No. 500cm$^2$ flasks | - | - | 1 | 4 | 13 (b) |
| No. 175cm$^2$ flasks | - | 1 | 1 | 1 | 1 (b) |
| No. 25cm$^2$ flasks | 4 | 4 | 4 | 4 | 4 (b) |
| Total area in flasks i.e. final area (cm$^2$) | 100 | 275 | 775 | 2275 | 6775 (c) |
| Harvested flask area required to seed this passage (cm$^2$) | 33 | 92 | 258 | 758 | 2258 (d) |
| No. of cells required to seed this passage | 6x10$^5$ | 1.7x10$^6$ | 4.6x10$^6$ | 1.4x10$^7$ | 4.1x10$^7$ (f) |
| (*) **Biopsy size** required to seed this passage (cm) | 4 | 11 | 31 | 91 | 271 (g) |
| (*) **Number of passages** in the culture train | 5 | 4 | 3 | 2 | 1 (h) |

Illustration of flasks used in each cell culture passage:

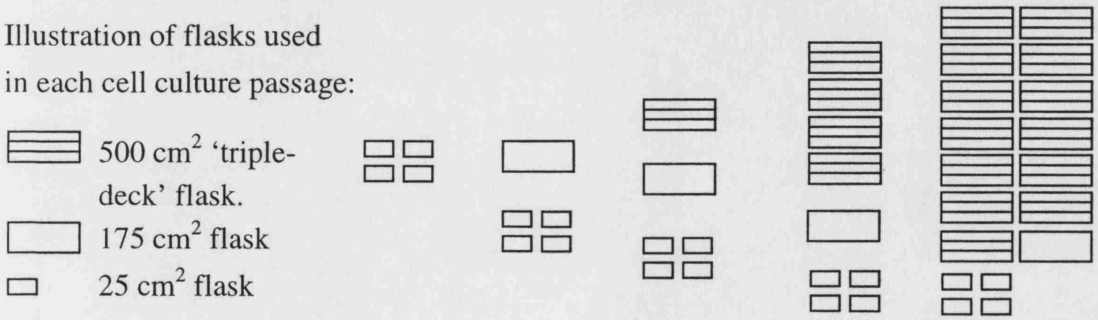

## Chapter 3: Sensitivity of cells to flow stress

### 3.0. Introduction

As automated systems are capable of operating at high speeds, throughput is likely to be constrained by sensitivity of biological materials to physical stress. Typical cell transfer steps such as aspirate, dispense (e.g. to or from pipettes) and pipe flow all involve exposure of cells to shear stress in approximate capillary geometry. For these types of processing operations, exposure of cells to flow stress is expected to last for a very short time (~ 0-1 second) but may be repeated many times during processing. It is anticipated that a combination of high flowrates and small pipe diameters will be preferred: higher flowrates reduce process times thus increasing apparatus capacity and reducing risk of detrimental changes in cellular process materials (e.g. hypoxia or aggregation), while smaller pipe diameters may reduce hold-up losses of cell suspensions in piping and on surfaces. As any adverse process impact on the functional characteristics of the cell population must be minimised, it is necessary to investigate the effect of repeated capillary shear on cells with a view to generating a design basis able to specify suitable flowrates and pipe sizes. As turbulent flow conditions are generally more damaging than laminar flow at the same shear stress magnitude [Chisti, 2001], it is assumed that the optimum conditions for cell yield will be found in the laminar capillary flow regime and so this regime has been investigated.

### 3.1. Effects of capillary shear flow on cells in media

Adherent cell harvest typically produces relatively large volumes of dilute cell suspension, of the order of ~$1x10^5$ cell/mL (cell volume fraction < 0.01); cell harvest volume per patient unit is expected to be of the order of 0.5-1.0 L. This volume must then be transferred to the subsequent process operation with minimal loss of cells and cell health. Key parameters chosen for assessment in this study are cell number, membrane integrity, growth rate and metabolism; in order to minimise culture time of tissue grafts, cells must be recovered intact and able to proliferate normally. Analysis of these parameters can provide a reasonable indication of the general health of a cell population. Trypan blue dye exclusion is the standard laboratory assay for the rapid assessment of mammalian cell number and membrane integrity and the characteristics of sheared cells in terms of growth and metabolism may be examined under standard culture conditions.

3.1.1. Effect of 0-20 capillary passes at high shear (120 Pa) on cell number

In order to quantify the (maximal) detrimental effect of repeated exposure to high laminar capillary shear stress on cell membrane integrity and cell growth characteristics, cell suspension was repeatedly passed through a hypodermic needle at a high flowrate (wall shear stress 120 Pa), approaching the onset of transition to turbulent flow (at $Re_p$ = 2000, wall shear ~130 Pa). It was anticipated that a decline in intact cell number would be observed with increasing shear exposure (number of capillary passes), possibly first order. Sheared cell samples were assayed for membrane integrity and cultured to investigate number of cells able to grow, growth rate and metabolism (section 3.1.2.). Briefly, cells retaining membrane integrity after ~20h in culture were denoted 'growing cells'. Results for total, intact and growing cell concentrations at increasing number of capillary passes are presented in figure 3-1.

For the 'no capillary control' (figure 2-1b) at 5 passes (figure 3-1), there is no loss in the number of total or intact cells and the decline in number of growing cells (not significant, Student's paired t-test $p = 0.14$) is small compared to the main results. The continued decline in cell number during repeated shearing shows that substantial cell loss or damage is occurring during each capillary pass. Many 'ghost cells' (i.e. lysed cell shells) and cell debris particles were observed following successive capillary passes at this flowrate. The decline in total cell number can be attributed at least in part to non-counting of 'ghost' cells and relatively large pieces of cellular debris. Combined with these observations, the decline in intact cell number demonstrates that cell lysis is occurring during exposure to these shear conditions. In addition, the decline in the number of growing cells is greater than the decline in the number of intact cells; while this indicates the occurrence of non-lytic cell death as a result of exposure to shear stress, it should be noted that estimates of cell viability by trypan blue assay have previously been shown to overestimate the cell population viability significantly [Altman et al., 1993], particularly below the 50% level [Mascotti et al., 2000]. Neither first nor second order decay curves provide good fits to the data ($R^2 < 0.9$). Although higher order decay curves present a reasonable fit to the data ($R^2 > 0.9$), there is no apparent mechanistic basis for this result. A proportion of cells are able to survive repeated exposure at this shear stress (120 Pa). This could be due to two main factors: (1) these cells have travelled along the centre of the capillary in all passes and so have not been exposed to damaging shear levels; (2) there exists a distribution of membrane strength (burst tension) within the cell population [Born et al., 1992]; the ~50% of cells

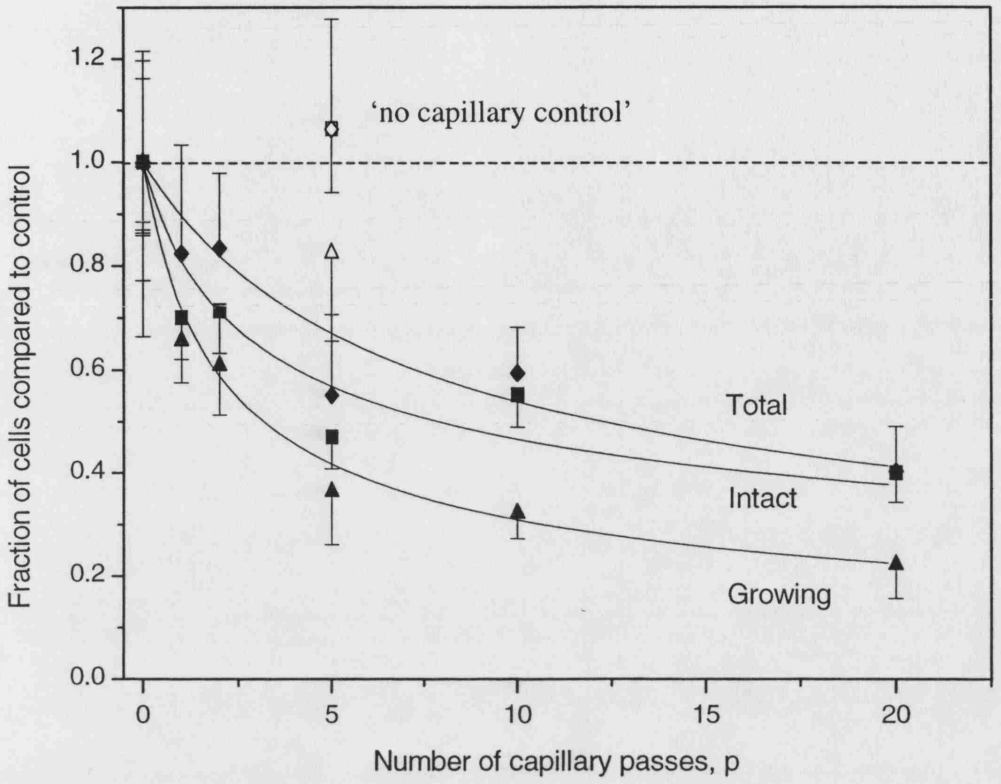


Figure 3-1. Fraction of cells remaining after 0-20 capillary passes at 120 Pa.

Rat aortic smooth muscle suspension was harvested normally from T150 flasks and aliquots (~15mL, ~1x10$^5$ cells/mL) were repeatedly taken up into a disposable syringe (25mL) and then expelled through a needle (0.45x23mm) into a 50mL sample tube. Flowrate was set at 50mL/min (capillary wall shear stress 120 Pa) using a syringe pump. Flow regime was calculated to be laminar ($Re_p$ = 1800). Data are expressed as the fraction of cells remaining compared to 'no flow reference sample' (figure 2-1a). (◆) total cells, (■) intact cells, (▲) growing cells. Number of total and intact cells was assayed by manual trypan blue count. Number of cells able to grow (after shear) was taken as the number of cells which attached normally to a T-flask during the first ~20h in culture, by trypan blue count (see figure 3-2). Open symbols represent a 'no capillary control' sample (figure 2-1b) 'sheared' by the same protocol (same flowrate) but with no capillary attached to the syringe.

(- - -) Null hypothesis. (—) 3$^{rd}$ or 4$^{th}$ order decay fits for clarity, $R^2 \geq 0.9$; attempts to fit 1$^{st}$ or 2$^{nd}$ order decay kinetics were unsuccessful, $R^2 < 0.9$). Error bars represent one standard deviation on quadruplicate cell counts, half only shown for clarity.

which remain intact at 5-20 passes are the 'stronger' cells in the population and will remain intact when exposed to 120 Pa, notwithstanding any secondary breakdown effect due to a gradual weakening of cells during each pass.

3.1.2. Effect of 0-20 capillary passes at high shear (120 Pa) on growth and metabolism

Following shearing, cells were planted in T25 culture flasks and cultures monitored over a six-day period. Linearised (by log plot) growth curves are presented in figure 3-2. For 'no flow reference sample' (figure 2-1a) flasks, the number of intact cells at day 1 (figure 3-2, open symbols) was not significantly different from the number of cells at inoculation (student's paired t-test, $p = 0.86$); hence the number of intact cells counted at day 1 may be used as a measure of the number of cells present at inoculation which were able to survive and grow, denoted 'growing cells'. Cells which were intact after shear but were no longer intact at day 1 were regarded as non-growing intact cells and presumed to have either failed to attach to the growth surface or lysed following death by necrosis or apoptosis. It has been previously reported that shear stress below that required for physical destruction of the cell can cause debilitating damage and loss of function [Chisti, 2001]. Comparing highly sheared samples (120 Pa, $p = 10, 20$) with 'no flow reference samples' (figure 2-1a), figure 3-2 clarifies the decline in intact cell density observed at ~20 hr in culture (i.e. number of growing cells following shear). All cultures reached a similar density after four or six days (~90 or 140 h) in culture.

Exponential growth rates in culture were calculated by linear regression on data between 10-110h ($R^2 > 0.95$ in all cases) and are presented in figure 3-3. The data indicate that there is no significant decline in growth rate associated with the shear-induced cellular damage and that all cultures ultimately reach similar cell densities, implying that cells which are able to grow do so normally. There is perhaps a slight trend towards increasing growth rate with increasing number of capillary passes (figure 3-3), although this is not strongly supported by the data ($R^2 = 0.34$). Apparent differences in growth rate may be due to 'crowding' retarding growth as cells approach confluence, effectively giving initially less dense cultures a chance to 'catch up' to the same cell number; the retardation effect would be more pronounced for cultures with higher initial growing cell density, thus yielding a lower apparent growth rate in these cultures. Alternatively, it is possible that a selection process occurs during exposure to shear stress: those cells with the highest membrane burst tension could be 'in better health' i.e. able to grow more quickly than weaker (possibly degenerating) cells.

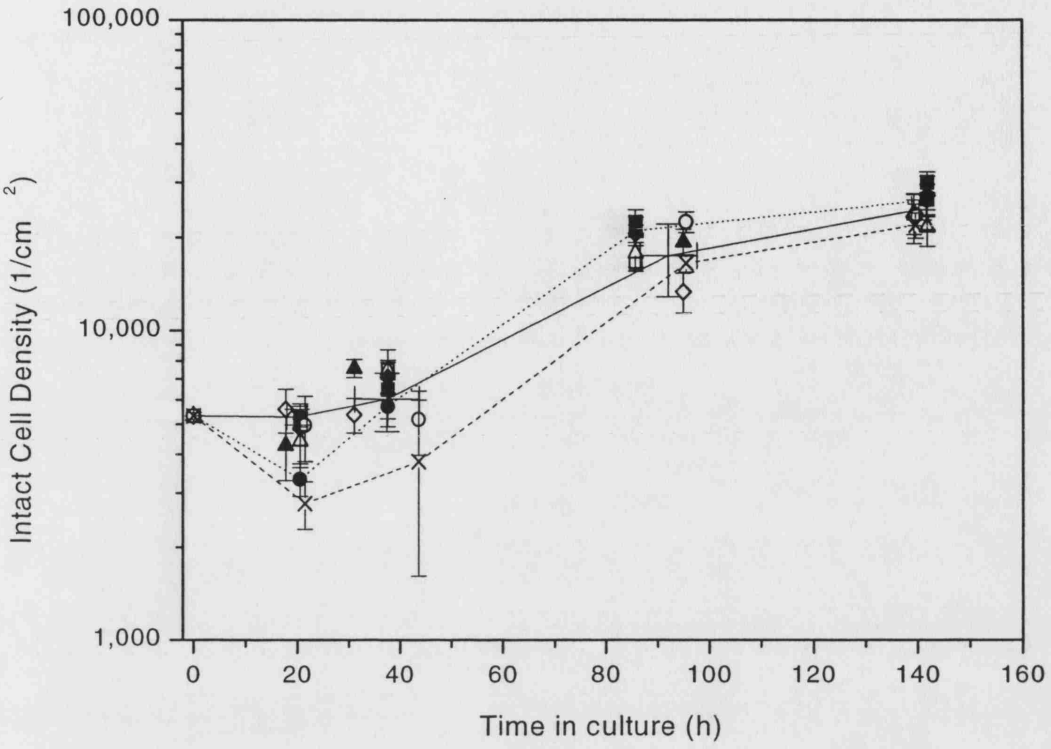


Figure 3-2. Cell growth curve following 0-20 capillary passes at 120 Pa.

Harvested rat aortic muscle cell suspension which had been subjected to repeated capillary shear (0-20 capillary passes, wall stress 120 Pa, see figure 3-1) was used to plant multiple T25 ($25cm^2$) culture flasks. Cell seeding density was standardised at 5300 intact cells per $cm^2$ by adding larger volumes of cell suspension where intact cell number was reduced. T25 flasks were harvested on days 1, 2, 4 and 6 of culture and cell density on the growth surface calculated via trypan blue count. The logarithmic y-axis presents exponential cell growth visually as a linear increase, observed to occur between ~20-100 h. There was no significant change in the number of intact cells in 'no flow reference samples' (figure 2-1a) between seeding and day 1 (students paired t-test, $p > 0.05$), indicating that the first ~20 hours are a lag phase; the number of cells surviving to day 1 was thus classified as the number of seeded cells which are subsequently able to grow (i.e. growing cells, figure 3-1). Number of capillary passes, p : Closed symbols (■) p = 1, (◆) p = 2, (▲) p = 5, (●) p = 10, (×) p = 20. Open symbols are 'no flow reference samples' on different days: (□, ◇, ○), except for (△) where p = 5 with no capillary fitted ('no capillary control' (figure 2-1b)). Lines shown to highlight culture behaviour for 'no flow reference sample' (—, mean of the three 'no flow reference samples') and highly sheared (···●···, p = 10 ; ---×---, p = 20) samples. Error bars represent one standard deviation on either quadruplicate assay repeats (p=1-20) or scatter between the 3 'no flow reference samples'.

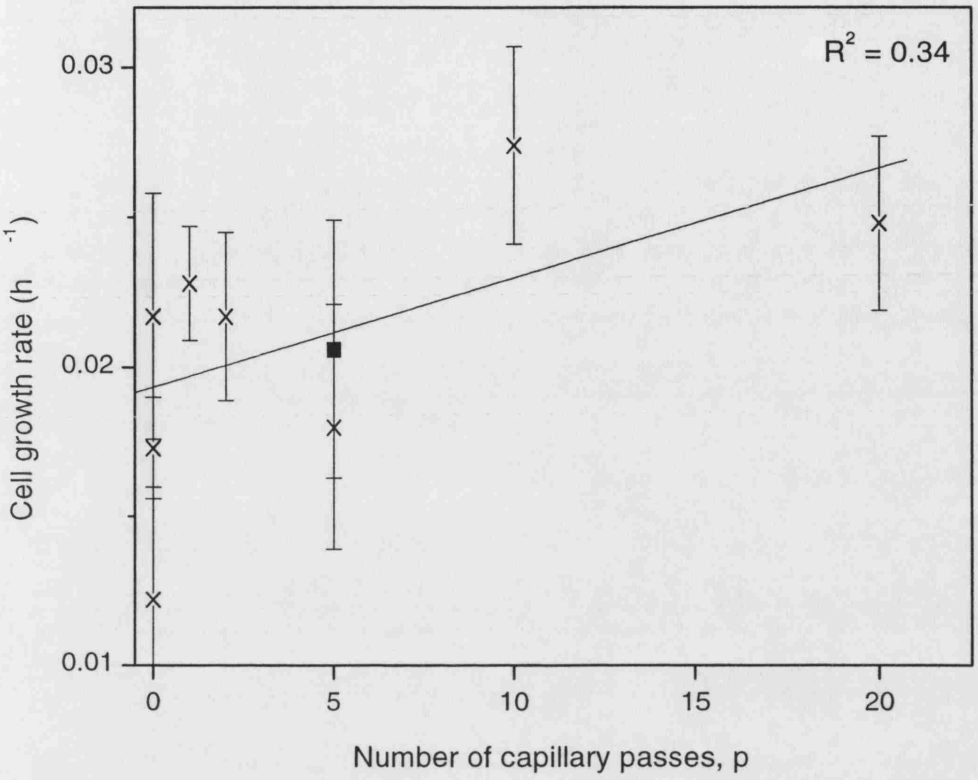


Figure 3-3. Cell growth rate following 0-20 capillary passes at 120 Pa.

Harvested rat aortic muscle cell suspension which had been subjected to repeated capillary shear (0-20 capillary passes, wall stress 120 Pa, see figure 3-1) was used to plant multiple T25 ($25cm^2$) culture flasks. T25 flasks were harvested on days 1, 2, 4 and 6 of culture and cell density on the growth surface calculated via trypan blue count. Exponential growth rate was calculated by linear regression on data between 10-100h in culture (figure 3-2), $R^2 > 0.95$ in all cases. (×) data for needle-sheared samples and the three 'no flow reference samples' (figure 2-1a, p = 0). (■) 'no capillary control' (figure 2-1b), 'sheared' for five passes. (—) Linear regression fit, excluding (■), $R^2 = 0.34$). Error bars derived manually by considering maximum and minimum slopes (growth rates) fitting within the range of observed error in cell surface density; error in cell surface density was standard deviation on quadruplicate trypan blue counts (figure 3-1).

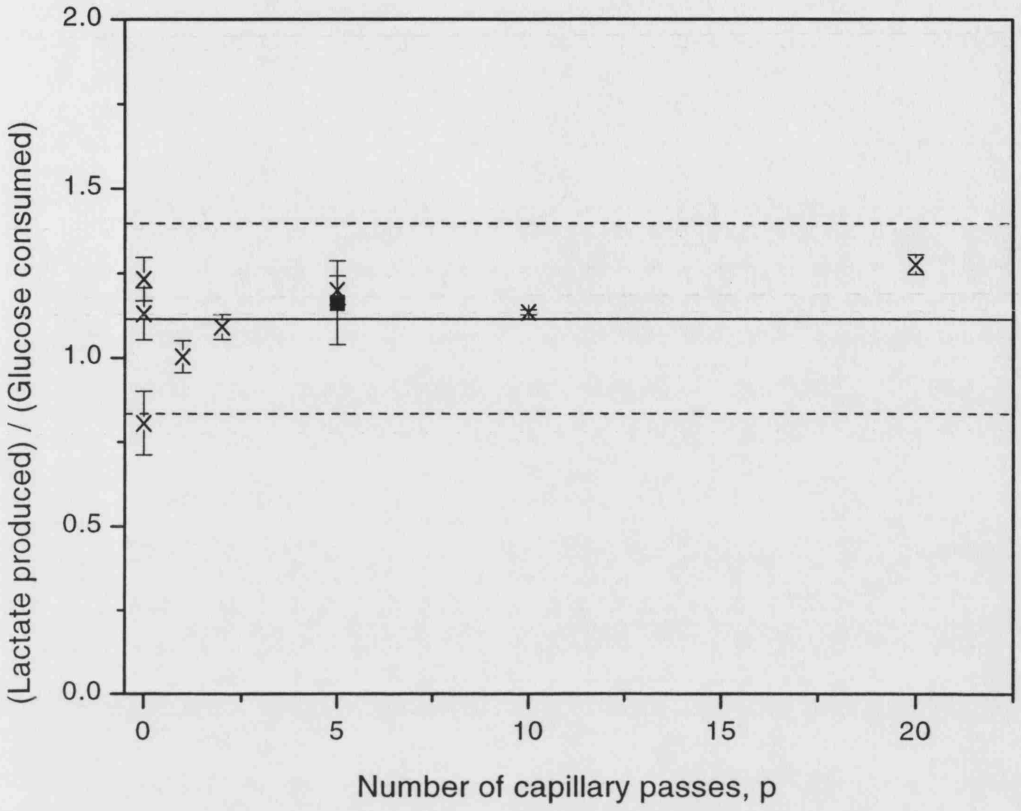


Figure 3-4. Metabolism of cells following 0-20 capillary passes at 120 Pa.

Harvested rat aortic smooth muscle cell suspension which had been subjected to repeated capillary shear (0-20 capillary passes, wall stress 120 Pa, see figure 3-1) was used to plant multiple T25 (25 $cm^2$) culture flasks. Concentrations of glucose and lactate in planted cell suspension (day 0 of culture) and spent media (day 6) were assayed twice by biochemical analyser. The ratio of lactate produced to glucose consumed over the six days in culture was calculated for each sample. Overall, glucose concentration in the medium fell from 3.4-3.7 g/L to 2.8-3.2 g/L, while lactate concentration rose from 0.15-0.17 g/L to 0.6-1.0 g/L, well away from levels associated with inhibition of mammalian cell growth (< 0.6 g/L glucose, > 2 g/L lactate, [Ozturk et al., 1997]). (×) data for needle-sheared samples and the three 'no flow reference samples' (figure 2-1a, p = 0). (■) 'no capillary control' (figure 2-1b), 'sheared' for five passes with no capillary fitted to the syringe. (—) Mean of all data. (- -) Two standard deviations about the mean, i.e. the range expected to include 95% of observations if data are normally distributed about the mean. Error bars represent one standard deviation on two assays repeats, combined from four raw data points (day 0 and 6 for both glucose and lactate) per point on the graph.

The ratio of lactate produced to glucose consumed was calculated over the full six days in culture and is presented in figure 3-4. The ratio is similar in all cases (excepting one 'no flow reference sample' (figure 2-1a) culture) indicating that there is no significant change in the overall metabolism of cells which have undergone shearing, although it is possible that the balance of individual metabolic pathways may have changed.

### 3.1.3. Effect of shear stress on membrane integrity

It was anticipated that laminar capillary shear stress would cause a decline in cell number and membrane integrity, with the magnitude of the effect being greatest at the higher shear stress. Results for total and intact cell number over a range of shear stresses (flowrates) are presented in figure 3-5a and 3-5b and the proportion of remaining cells which are intact presented in figure 3-5c. As expected a higher number of shear passes results in greater cell disruption and there is evidence of increased cell disruption at high shear (~100 Pa). This is consistent with a previous report which determined the critical shear stress for the onset of mammalian cell membrane disruption (TB/C3 hybridomas, exposure time 180s) to be around 100 Pa [Born et al., 1992]. In addition we observe a substantial loss in total and intact number of cells at low shear (2 Pa), an unexpected occurrence which has been previously reported [Mardikar and Niranjan, 2000]. While the mechanism of cell loss at low shear is uncertain, it is clear that this effect must be properly investigated and taken into account when specifying design and operational parameters for an automated tissue engineering process. The optimum shear stress for intact cell yield appears to be around 10 Pa, in close agreement with the previous report of the low shear phenomenon [Mardikar and Niranjan, 2000], although there is no significant decrease in cell concentration between 10-50 Pa. The apparent increase in the total number of cells present after 1 pass at 0-50 Pa could be due to shear-induced break-up of aggregates initially present, leading to increased cell counts. At all shear levels the vast majority of cells which are damaged are lost entirely, as can be seen from the high proportion of intact cells in all samples (figure 3-5c). This indicates that the mechanism of cell lysis under capillary shear is catastrophic, reducing the cell to debris particles which are necessarily excluded from the cell count.

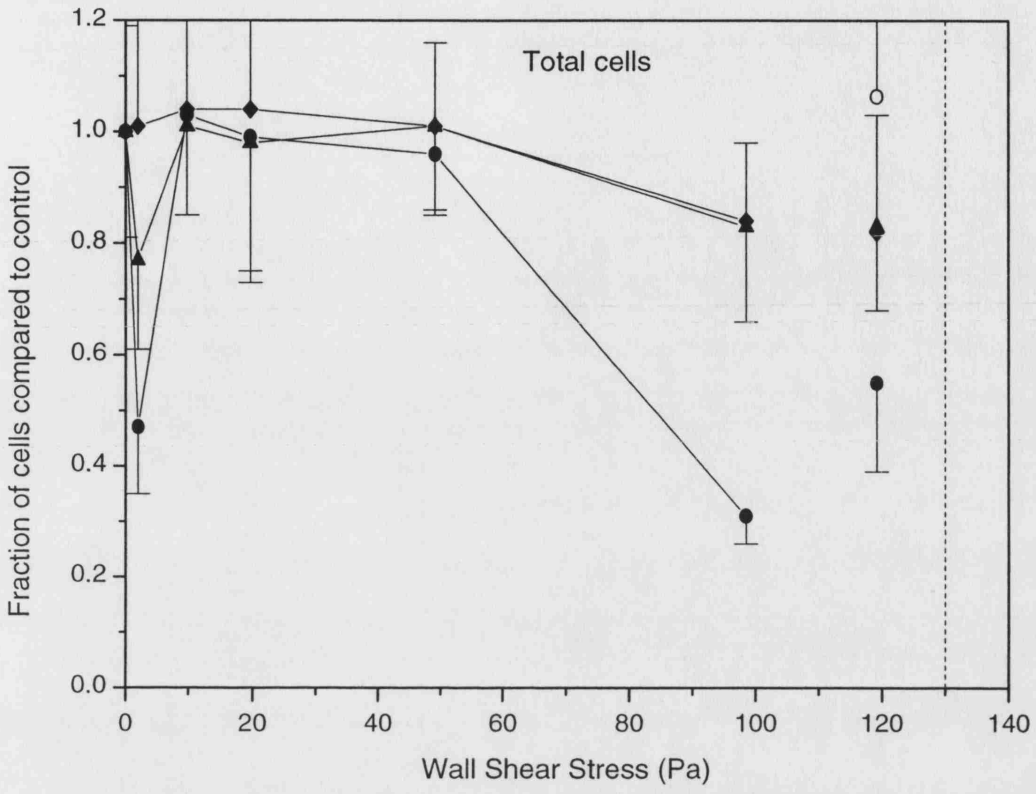


Figure 3-5a. Fraction of total cells remaining after 1, 2, 5, capillary passes at 0-120 Pa.
Rat aortic smooth muscle suspension was harvested normally from T150 flasks and divided into three aliquots for shearing (6mL, ~$1x10^5$ cells/mL) and a 'no flow reference sample' (figure 2-1a). Cell suspension was taken up into a disposable syringe (10mL) and then expelled through a needle (0.45x23mm) into a 15mL vial; this procedure was performed either 1, 2 or 5 times for sheared aliquots. Flowrate was fixed at a specified value in the range 0.8-41 mL/min (capillary wall shear stress 2-100 Pa) using a syringe pump. Data are expressed as the fraction of cells remaining compared to 'no flow reference samples', measured by manual trypan blue assay. Data at 120 Pa are brought forward from the preceding study (figure 3-1) for comparison. Flow regime was calculated to be laminar, $Re_p < 2000$; (---) wall shear stress corresponding to $Re_p = 2000$, the onset of transition to turbulent flow. Number of capillary passes, p : (—◆—) p = 1, (—▲—) p = 2, (—●—) p = 5, (O) p = 5 for a 'no capillary control' run (figure 2-1b). Error bars represent one standard deviation on quadruplicate cell count repeats; only half error bars are shown for clarity.

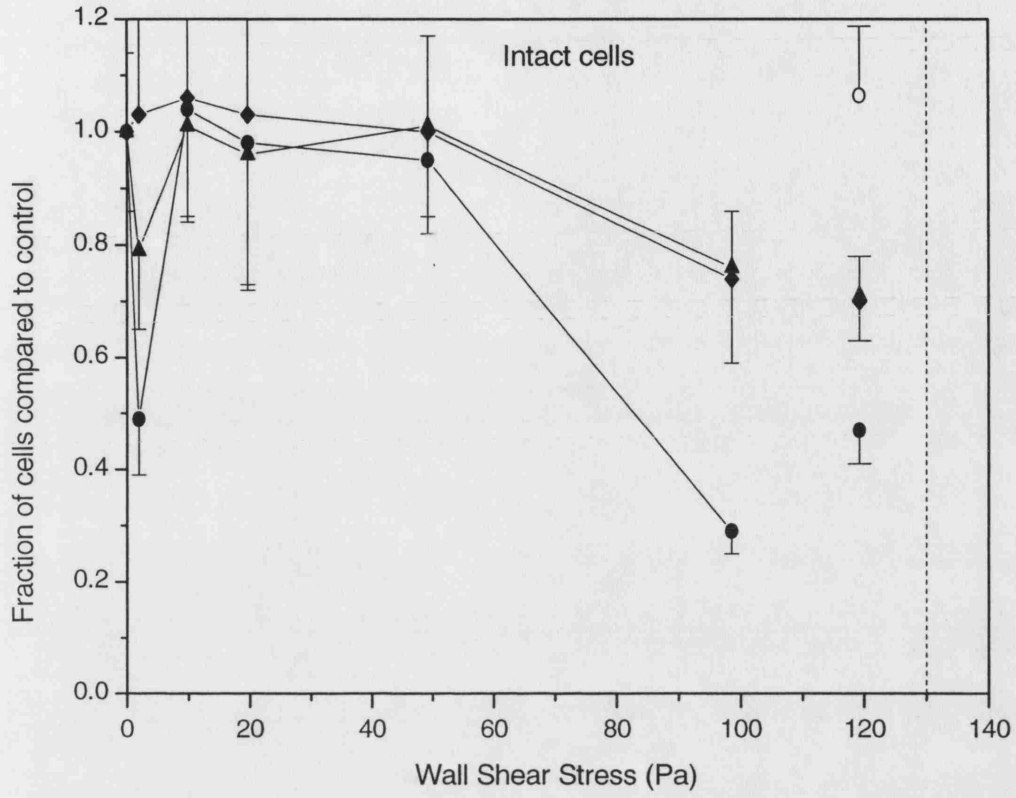


Figure 3-5b. Fraction of intact cells remaining after 1, 2, 5, capillary passes at 0-120 Pa
Rat aortic smooth muscle suspension was harvested normally from T150 flasks and divided into three aliquots for shearing (6mL, ~1x10$^5$ cells/mL) and 'no flow reference sample' (figure 2-1a). Cell suspension was taken up into a disposable syringe (10mL) and then expelled through a needle (0.45x23mm) into a 15mL vial; this procedure was performed either 1, 2 or 5 times for sheared aliquots. Flowrate was fixed at a specified value in the range 0.8-41 mL/min (capillary wall shear stress 2-100 Pa) using a syringe pump. Data are expressed as the fraction of cells remaining compared to 'no flow reference sample', measured by manual trypan blue assay. Data at 120 Pa are brought forward from the preceding study (figure 3-1) for comparison. Flow regime was calculated to be laminar, $Re_p$ < 2000; (---) wall shear stress corresponding to $Re_p$ = 2000, the onset of transition to turbulent flow. Number of capillary passes, p : (—◆—) p = 1, (—▲—) p = 2, (—●—) p = 5, (O) p = 5 for a 'no capillary control' run (figure 2-1b). Error bars represent one standard deviation on quadruplicate cell count repeats; only half error bars are shown for clarity.

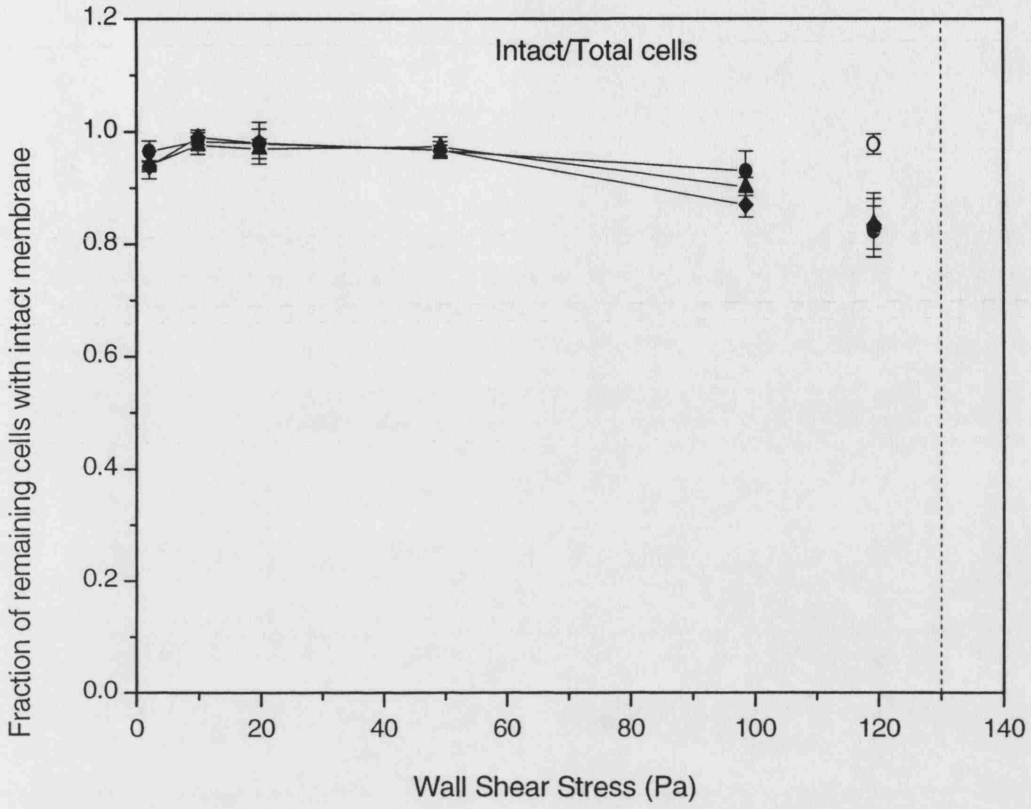


Figure 3-5c. Fraction of remaining cells with intact membrane after 1, 2, 5, capillary passes at 0-120 Pa

Rat aortic smooth muscle cell suspension was harvested normally from T150 flasks and divided into three aliquots for shearing (6mL, ~1x10$^5$ cells/mL) and 'no flow reference sample' (figure 2-1a). Cell suspension was taken up into a disposable syringe (10mL) and then expelled through a needle (0.45x23mm) into a 15mL vial; this procedure was performed either 1, 2 or 5 times for sheared aliquots. Flowrate was fixed at a specified value in the range 0.8-41 mL/min (capillary wall shear stress 2-100 Pa) using a syringe pump. Data are expressed as the fraction of remaining cells (compared to 'no flow reference sample') which are scored as 'intact' (i.e. cell membrane is intact; excludes dye), measured by manual trypan blue assay. Data at 120 Pa are brought forward from the preceding study (figure 3-1) for comparison. Flow regime was calculated to be laminar, $Re_p$ < 2000; (---) wall shear stress corresponding to $Re_p$ = 2000, the onset of transition to turbulent flow. Number of capillary passes, p : (—◆—) p = 1, (—▲—) p = 2, (—●—) p = 5, (O) p = 5 for a 'no capillary control' run (figure 2-1b). Error bars represent one standard deviation on quadruplicate cell count repeats; only half error bars are shown for clarity.

### 3.1.4. Discussion - effects of capillary shear flow on cells in media

It has been demonstrated that exposure to high laminar capillary shear (≥ 100 Pa) causes substantial damage to the suspended adherent cell population, apparently by catastrophic cell lysis. The decline in mammalian cell number with increased exposure to a given laminar shear stress is consistent with findings in the literature [Born et al., 1992]. Cells which are able to grow following exposure to high shear are able to grow normally with no significant changes in growth rate, achievable cell density or metabolism. This result is encouraging, suggesting that cells not taken beyond a lethal damage threshold are robust and able to recover from any subtle effects of transient flow stress not considered in this study. For 1-5 capillary passes it is possible to achieve intact cell yields of over 95% by operating in the range 10-50 Pa (equivalent flowrate ~ 4-20 mL/min for 0.45mm ID capillary); this is in agreement with previous findings (optimum shear stress 10 Pa, [Mardikar and Niranjan, 2000]). There is an indication that capillary shear in the range 10-50 Pa may be able to break up aggregates in harvested cell suspension; this effect could potentially be useful in terms of decreasing the heterogeneity of a harvested cell suspension. Substantial loss of cells is observed at both lower (2 Pa) and higher (100 Pa) shear stress; further studies are desirable to clarify both the mechanisms and thresholds of cell loss in these two regions. Understanding these factors is expected to enable construction of a robust basis for the design of automated capillary cell processing systems.

While assessment of cell membrane integrity by trypan blue assay provides an indication of cell damage, this assay systematically overestimates the number of cells able to grow following exposure to high shear, indicating that either sub-lytic capillary shear effects can cause delayed cell death, or that this assay is inherently inaccurate. In addition the poor precision observed with the trypan blue assay in this study makes it difficult to comment on small changes or any slight trends in shear damage in the shear stress range most relevant to process design (i.e. maximal intact cell yield, 10-50 Pa, figure 3-5b). Thus development of a more precise (more sensitive) assay is desirable for application in further studies, enabling clarification of any true optimum or loss thresholds between 0-100 Pa.

### 3.2. Flow cytometry assay development

The standard trypan blue assay has been shown to overestimate the number of cells able to grow following shear (section 3.1.2.). This is consistent with previous reports comparing manual microscopic assays using different dye systems: trypan blue assay has been shown to significantly overestimate cell population viability (membrane integrity) when compared with similar 2-colour fluorescent dye assays [Altman et al., 1993; Mascotti et al., 2000]. Previous reports have illustrated advantages of flow cytometry assays for cell membrane integrity as compared to trypan blue in terms of speed [Fiala at al., 1999], ease of use and increased precision due to increased sample size and reduced operator dependence [Al-Rubeai et al., 1997]. Flow cytometry was chosen as the platform for improved assay development due to these considerations, the availability of a flow cytometry system and the ability of flow cytometry to provide additional information on cell size distribution (on the basis of cell light scatter properties [Rieseberg et al., 2001]).

#### 3.2.1. Trypan blue assay and its limitations

Many problems were encountered during application of the trypan blue assay during shear studies. Only a relatively small number of cells can be counted by this method (~ 100 cells per assay replicate), leading to poor statistical precision associated with small sample size. High concentration samples require dilution (to ~$1x10^5$ cell/mL) for counting, possibly affecting the sample and introducing dilution error. Cell aggregates were generally excluded from counts, partially due to procedural issues (e.g. sampling or aggregate hold-up); in addition the number of cells within aggregates cannot be accurately counted and so must either be roughly estimated or excluded entirely. Ideally, stained cells are either bright white (unstained) or dark blue (stained). In reality, a distribution of staining intensities exists, along with various cell debris and other particles. The operator must determine whether objects are cells or not and classify a range of partially stained cells as either stained or unstained; these issues were observed to be particularly problematic with sheared cell samples. Due to the time taken for the assay (~10-15 min per sample, i.e. 4 replicates), assessment of many samples is a slow and laborious process requiring meticulous concentration and so error is likely to be introduced due to sample degeneration and operator fatigue.

### 3.2.2. Advantages of flow cytometry

According to the manufacturer, the flow cytometer used was able to accurately process cells at a rate of up to around 500-1000 'events' per second (depending on sample concentration), providing the possibility of assessing thousands of cells in a very short time. The flow cytometer is able to process sample cell concentrations up to around $1 \times 10^7$ cell/mL, with low-end sample concentration being limited only by the time taken to process sufficient sample volume; thus there is no requirement for changes in sample processing dependent on cell concentration (i.e. dilution). The flow cytometer measures fluorescence at up to four separate wavelengths (channels); inclusion of additional dyes within a single assay enables simultaneous examination of multiple cell properties, or parallel examination of a single property by alternative staining methods. As the flow cytometer quantifies the intensity of a fluorescence signal (i.e. the intensity of cell staining), precise intensity thresholds can be set for discrimination between negative and positive staining, eliminating subjectivity associated with a distribution of staining intensities. Signals due to debris and background particle counts may also be filtered ('gated') out on various parameters, or combinations of parameters such as size (light scatter properties).

Although it was unclear whether flow cytometry would be able to offer any advantages in terms of counting cells within aggregates, it was thought that hydrodynamic focusing of sample suspension into a single cell stream (prior to entering the excitation laser) could potentially cause aggregate break-up prior to cell assessment (i.e. counting). One disadvantage of the flow cytometer is the inherent inability to provide a direct volumetric count of cells in the sample. To overcome this it is necessary to add 'counting beads' of a known concentration to the sample at a known volume ratio; following assay, the concentration of cells in the initial sample can be calculated from the observed ratio of cells to beads and the initial bead concentration. The main disadvantage here is introduction of sampling error when combining beads with cell suspension in a precise ratio.

### 3.2.3. Assay development

Key improvements sought in the development of the new assay were a reduction in statistical counting error (~1 order of magnitude), elimination of operator-dependence, increased resolution (intact/permeable cells) and increased assay throughput (speed). Statistical error in a cell count may be approximated by the square root of the number of

cells counted [Biowhittaker, 2003]; for 100 cells this is 10% error (typical trypan blue count) while for 5000 or 10000 cells this is 1.4 or 1.0% error. The ceiling for the number of cells counted per assay was set at 5000; this number achieves good theoretical precision and could be achieved rapidly with the flow cytometer (typically ~1-2 min for a sample concentration of $2x10^6$ cell/mL as in capillary flow studies).

It was thought that using two dyes, both of which probe cell membrane integrity by alternative mechanisms, could increase assay accuracy and resolution compared to trypan blue; previous reports have advocated the superiority of 2-colour fluorometric dye assays over trypan blue [Altman et al., 1993; Mascotti et al., 2000]. The assay developed was adapted from a 2-dye fluorometric staining protocol using Fluorescein diacetate (FDA) and Propidium iodide (PI) [Darzynkiewicz et al., 1994]. 7-Amino-actinomycin D (7AAD) was substituted for PI and fluorospheres (counting beads) added for determination of absolute cell numbers. Incubation with both dyes was expected to provide increased resolution compared to a single dye alone, as cells should be labelled either +/- (intact) or -/+ (permeable) with respect to FDA/7AAD.

Setup of data acquisition and dye staining thresholds (i.e. data analysis protocol) was carried out using intact cells and cells permeabilised by either freeze-thaw or heating (60°C 15min) and incubated with neither, either or both dyes as appropriate. Following preliminary assay setup, a threshold ('discriminator') was set up to exclude small background particles from data acquisition on the basis of cell size (forward scatter), by comparing data gathered for cell suspensions with background readings.

### 3.2.4. Results – flow cytometry assay performance

The flow cytometry and trypan blue assays employed probe cell membrane integrity and so results are classified accordingly: a cell (membrane) is either 'intact' or 'permeable' and the proportion of cells which are intact is expressed as '% integrity'. Classification on the basis of cell 'viability' is considered unrepresentative of assay results and is avoided. For a typical experiment with 10 samples, the overall time taken for flow cytometry setup, sample assay and shutdown was comparable to trypan blue (~2h), however flow cytometry setup and shutdown could be performed before and after the main experiment, yielding a substantially reduced time for sample assessment (~1h).

An example of the raw output plots from the flow cytometry assay is presented in figure 3-6, showing both 'dot plot' and isometric views; for 'dot plots' a pixel is coloured

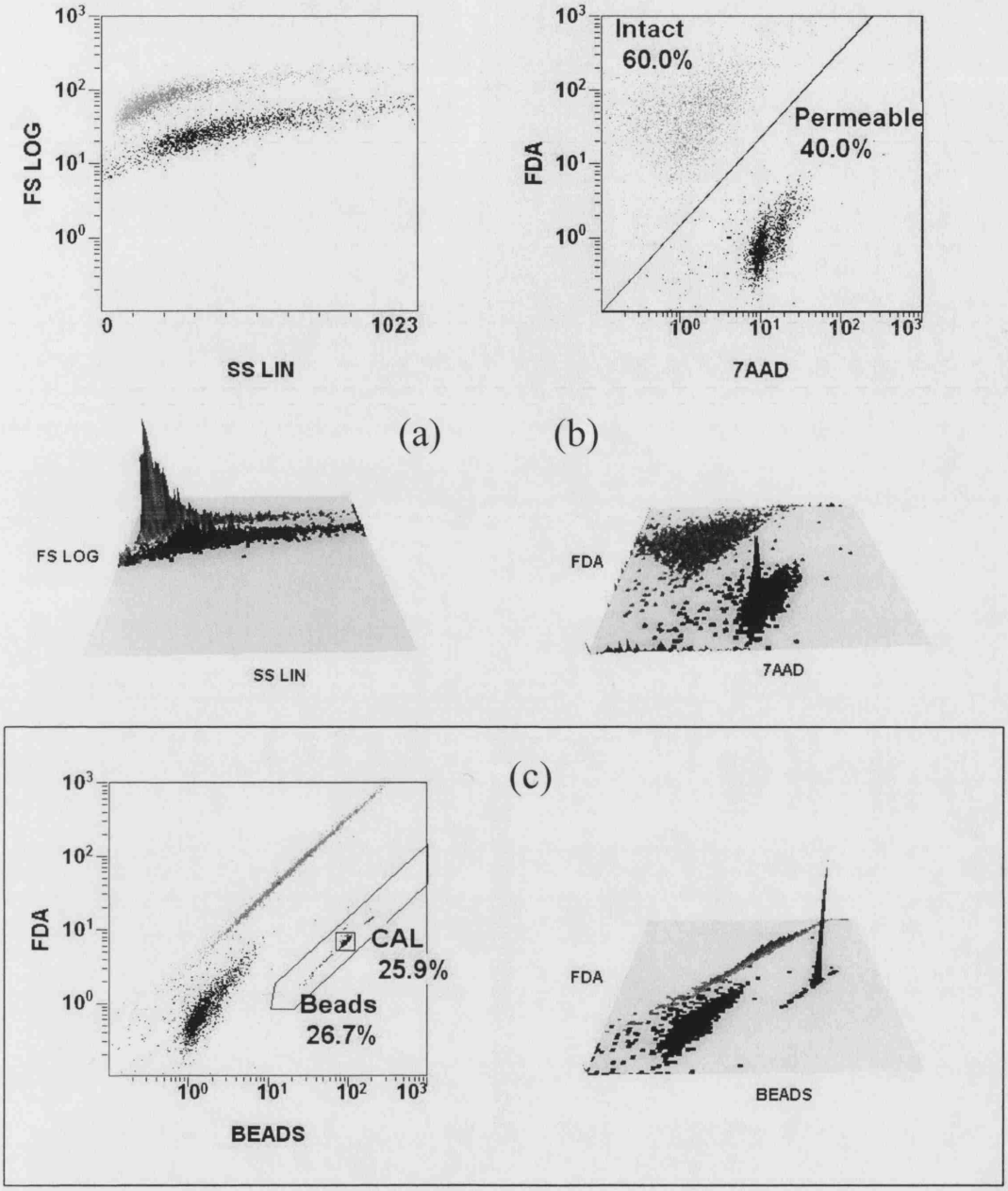


Figure 3-6. Example flow cytometry raw data – intact and heat-permeabilised cells.
Harvested rat aortic smooth muscle cell suspension was concentrated by protocol (B) (to ~2x10$^6$ cell/mL) and divided into two aliquots. One aliquot was permeabilised by heating (60°C 15min) and aliquots recombined in a 3:2 intact:permeable ratio (i.e. one data point taken from figure 3-8.). 3D plots included for clarity; z-axis is number of events (i.e. no. particles counted). In all plots grey colour indicates 'intact cells', black indicates 'permeable cells'. (a) Forward scatter vs. side scatter; beads excluded. (b) FDA intensity (525nm) vs. 7AAD intensity (675nm); beads excluded. (c) FDA intensity (525nm) vs. Beads intensity (620nm); NB bead events are shown in plot (c) (region marked 'Beads') and coloured black. 'CAL' is the bead population used for calculation of cell concentrations, other events within 'Beads' region are disregarded.

where one or more events (objects) occurs at that coordinate and in isometric views the number of events recorded at each coordinate is represented by peak height. The gates (i.e. dye staining thresholds) set up within the analysis protocol are shown. The high degree of spread observed the FDA/7AAD (fluorescence intensity) plot (figure 3-6b) is attributed to the wide cell size distribution in the cell population (section 4.1.2.); larger cells are expected to take up and retain more FDA and exhibit a higher background level with either dye. Due to the spread of fluorescence peaks and it was observed that the two peaks for intact and permeable cells were not well resolved by a single dye alone (data not shown). The 2-dye method clearly resolves the intact and permeable cell populations in the 2-colour plot (figure 3-6b). Counting beads formed a distinct population in a plot of FDA/Beads intensity (figure 3-6c) and were 'gated' accordingly. Permeable cells form a distinct population in the forward (light) scatter / side scatter (FS/SS) plot (figure 3-6a) at lower FS (cell size) than intact cells; observed reduction in the size of permeable cells is probably due to efflux of cytoplasm through membrane breaks [Mardikar and Niranjan, 2000].

Dilution curves were generated for both intact (figure 3-7) and heat-permeabilised (not shown) cells. Regression fits to the data indicate good assay linearity in the range $10^3$-$10^4$ cell/μL ($10^6$-$10^7$ cell/mL). Overall flow cytometry tended to return higher cell concentrations than trypan blue (average +25% for intact cells, +10% for permeable cells), with closest agreement between the two assays in the range $10^6$-$10^7$ cell/mL. Manual fits indicated flow cytometry background readings of ~1-2x$10^4$ cell/mL; this was confirmed by two further runs with 0.2μm-filtered saline solution as the sample.

A stepped curve of intact and heat-permeabilised cells was generated to compare values of '% integrity' between trypan blue and flow cytometry assays (figure 3-8). Flow cytometry counts agree very well with expected values (based on initial trypan blue counts), whereas trypan blue counts performed after flow cytometry report a significantly lower '% integrity' overall (1-18%).

Predicted and observed flow cytometry precision was investigated and compared with trypan blue assay (table 3-1). Manual trypan blue counts returned a much higher degree of variation than the flow cytometry assay. Predicted flow cytometry precision agrees well with observed values (excepting '% integrity') suggesting that sample heterogeneity was low and sampling (pipetting) error was within expected tolerances. Variability was much higher for permeable cells than total or intact cells; increased statistical error in the permeable cell count is due to the low concentration of permeable

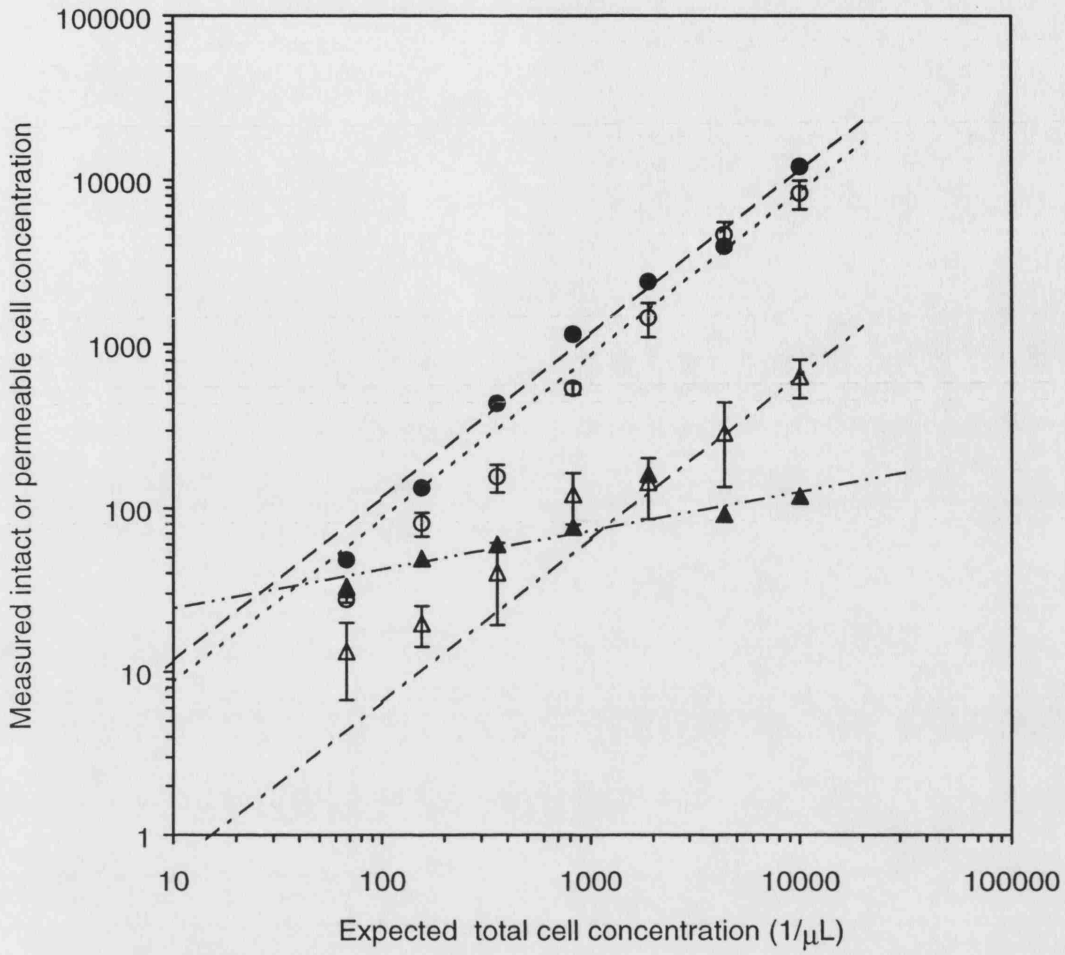


Figure 3-7. Intact cell concentration curve, assayed by flow cytometry and trypan blue.
Harvested rat aortic smooth muscle cell suspension was concentrated (to ~$1x10^7$ cell/mL) as for protocol (B), excepting a reduced volume of resuspension fluid (9g/L saline solution). Cell concentrate was serially diluted (dilution factor 2.3, 9g/L saline solution) and samples were assayed first by flow cytometry and then manually by trypan blue. 'Expected total cell concentration' (x-axis) represents the approximate expected total cell concentration after resuspension (~$1x10^7$ cell/mL) and linear declination thereof by the serial dilution. 'Measured cell concentration' (y-axis) are the assay results for the dilution curve samples: ( ● , ▲ ) Flow cytometry, (●) intact cells, (▲) permeable cells. ( O , △ ) Trypan blue assay, (O) intact cells, (△) permeable cells. Linear regression fits, forced through the origin: (— ● —) $R^2$ = 0.99, (— - O — -) $R^2$ = 0.98, (— -△— -) $R^2$ = 0.98. Manual fit: (— - -▲— - -), no $R^2$ value, Y-intercept = ~10-20 cell/μL = ~$1-2x10^4$ cell/mL. Error bars represent one standard deviation on quadruplicate trypan blue assay repeats. No error bars are shown for flow cytometry; flow cytometry assays were performed once only.

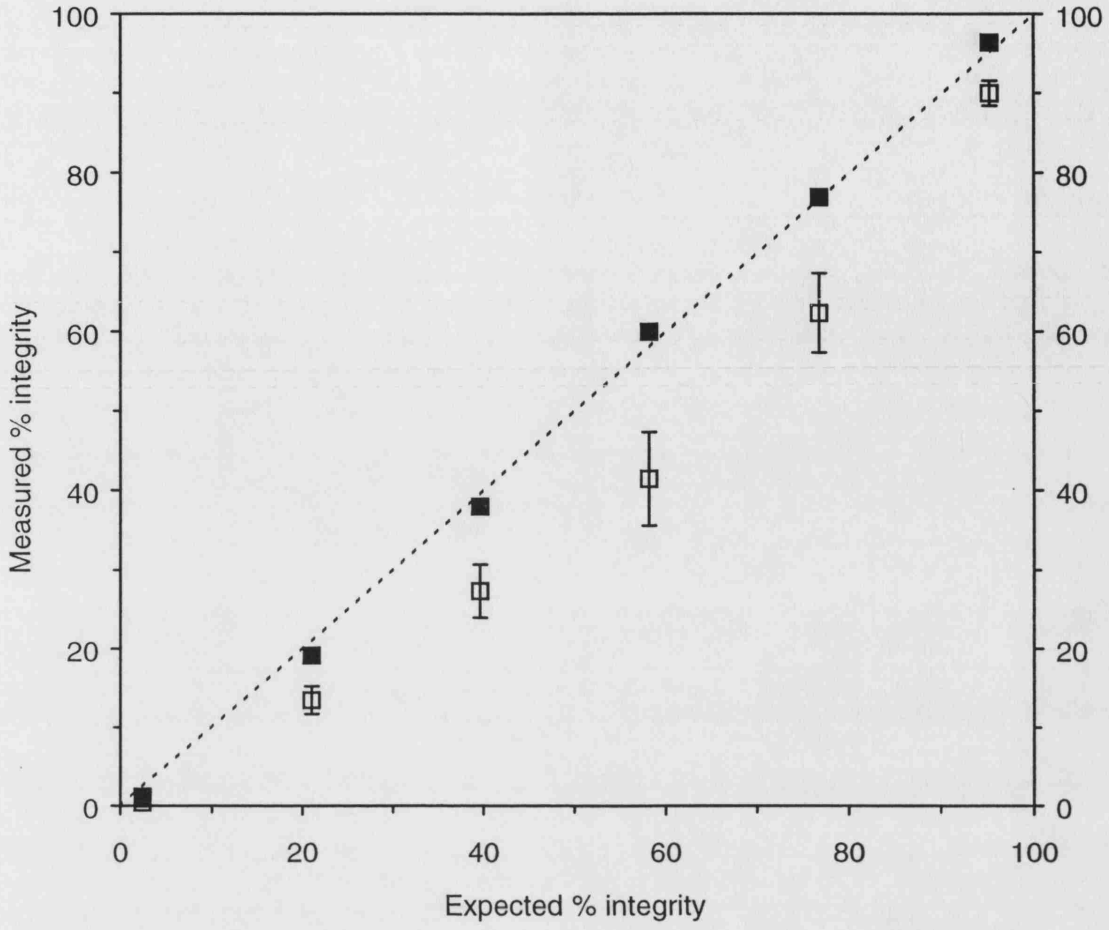


Figure 3-8. Intact and permeable cell stepped curve, assayed by flow cytometry and trypan blue.

Harvested rat aortic smooth muscle cell suspension was concentrated by protocol (B) (to ~$2x10^6$ cell/mL) and divided into two aliquots. One aliquot was permeabilised by heating (60°C 15min). The 'intact' and 'permeable' aliquots were then assayed by trypan blue (†) and then recombined to generate a six-sample stepped curve covering the range of '% integrity'. Stepped curve samples were then assayed (‡) first by flow cytometry and then manually by trypan blue assay.

'Expected %' (x-axis) was calculated from initial trypan blue counts (†) on the 'intact' and 'permeable' aliquots and the mixing ratios using to produce stepped curve samples. 'Measured %' (y-axis) are the assay results (‡) for the stepped curve samples, by (■) flow cytometry and (□) trypan blue. (---) 'Measured %' = 'Expected %'. Error bars represent one standard deviation on quadruplicate trypan blue assay repeats. No error bars are shown for flow cytometry; flow cytometry assays were performed once only.

Table 3-1. Assay precision – flow cytometry and trypan blue assays compared.
Assay precision was investigated by performing quintuplicate assay repeats on three different intact cell samples (~$2x10^6$ cell/mL, concentrated from normal cell harvest by protocol (B)). Standard deviation on quintuplicate assay repeats (expressed as a percentage of the mean) was averaged across the three samples to provide a coefficient of variance (CV, standard deviation expressed as % of the mean) for each assay. Predicted flow cytometry assay error was calculated based on statistical error (i.e. number of cells counted) and sampling error (pipette tolerances), according to error propagation formulae (Appendix C).

| Assay output | Flow cytometry predicted CV (%) | Flow cytometry observed CV (%) | Trypan blue observed CV (%) |
|---|---|---|---|
| | | | |
| Total cells/μL | 3.9 | 4.1 | 16.4 |
| Intact cells/μL | 3.9 | 4.1 | 16.7 |
| Permeable cells/μL | 8.9 | 9.9 | 33.8 |
| % of cells with intact membrane | 1.9 | 0.3 | 3.4 |

cells in the intact cell samples investigated (<5%) i.e. few cells counted hence small sample size. For flow cytometry, calculation of '% integrity' is internal to the cell suspension and so excludes all pipetting error and fluorosphere counting error, resulting in significantly reduced variation compared to volumetric counts. Overall the observed degree of variation for both trypan blue and flow cytometry agrees well with previously reported values [Al-Rubeai et al., 1997].

### 3.2.5. Discussion – flow cytometry assay performance

The systematic difference between the flow cytometry method and the trypan blue method was unexpected; typically flow cytometry methods do not exhibit systematic differences when compared to manual assay methods [Al-Rubeai et al., 1997; Fiala et al., 1999]. This disparity between cell count methods does not appear to be due to additional counting of cell debris by flow cytometry as background counts were relatively low (≤ 1% of total cells) and there is no evidence of a large debris population in raw flow cytometry plots (figure 3-6). The difference is thought to be due to release of cells from aggregates in the flow cytometry assay; cells within aggregates were generally excluded from trypan blue counts. Aggregate break-up could be due to two factors: (1) hydrodynamic conditions within the flow cytometer and (2) the presence of a surfactant within the flow cytometry counting bead suspension as supplied. For the further shear studies assayed by flow cytometry (section 3.3.), total cell concentration is ~1-2x$10^6$ cells/mL, within the observed range of optimal assay performance and closest agreement with trypan blue ($10^6$ – $10^7$ cell/mL); thus the flow cytometry assay is expected to perform well in the further shear studies. In any case flow cytometry results are expected to be internally consistent with respect to any systematic or background error and thus comparative data are meaningful (i.e. data generated during capillary shear studies: fraction of cells remaining after shear).

Given that the '% integrity' stepped curve results (figure 3-8) for flow cytometry match well to *initial* trypan blue counts (prior to flow cytometry assay) and that the *subsequent* trypan blue counts (performed 1-2h later, after flow cytometry) returned a reduced % integrity, it is most likely that sample degeneration (e.g. cell aggregation, surface adhesion, breakdown) occurred during this lag time, leading to skewed manual counts.

This implies that, when performed promptly, both assays may return similar results for % integrity, indicating that the shorter time taken to perform flow cytometry counts provides reduced inter-sample variability when processing batches of samples.

While is was anticipated that the 2-colour fluorometric assay might yield reduced '% integrity' values compared to trypan blue [Altman et al., 1993; Mascotti et al. 2000], results indicated either good agreement (when performed promptly) or reduced '% integrity' values by trypan blue (following 1-2h lag time). The clear resolution between intact and permeable cell populations, consistent with changes in cell size (figure 3-6) provides a high level of confidence in ability of the flow cytometry assay to accurately discriminate between and classify intact and permeable cells.

The flow cytometry assay exhibits around one quarter of the variation observed with trypan blue (table 3-1) and is thus able to detect changes in the cell population with much greater sensitivity. It is expected that trypan blue assay variability would further increase if processing large batches of samples, due to operator fatigue and sample deterioration. The close agreement of flow cytometry assay precision with predictions and literature values [Al-Rubeai at al., 1997] suggests that the method developed approaches the practicable limit of precision for flow cytometry cell counting assays.

Overall the flow cytometry assay satisfied all the key improvements sought: (1) assay precision was substantially improved (~4-fold) by increasing the number of cells counted (>10-fold), (2) operator-dependence (subjectivity) was eliminated by specification of a precise machine-read analysis procedure, (3) a high degree of resolution between intact and permeable cells was attained by 2-dye staining and (4) the time taken for sample assay was substantially reduced (for 10 samples, ~2h by trypan blue reduced to ~1h for flow cytometry). In addition it was suggested that increased counts recorded by flow cytometry may be due to release of cells from aggregates, which would represent a significant improvement in assay accuracy.

### 3.3. Effects of capillary shear flow on cells in saline

Following on from the earlier capillary shear studies, it was decided to investigate in more detail cell loss at very low shear stresses, with a view to determining the threshold and mechanism of cell loss in this range. In addition, a range of moderate to high laminar shear stresses (flowrates) were also investigated to clarify any threshold for the onset of damage at high shear and determine the optimum range for recovery of intact cells. Rather than using the same suspension conditions as in the previous study (~$10^5$ cell/mL in harvest medium) it was decided to examine shear effects on cells following cell concentration. The key issue is whether the concentration process itself and the

altered suspension conditions (higher cell density; absence of serum in the suspending saline solution) affect the shear-susceptibility of the cells; thus these conditions were investigated in the interests of gaining information over the whole (envisaged) process.

### 3.3.1. Experimental development

Following concentration of cell harvest, only very small volumes of cell concentrate require processing; in the envisaged model process, cell concentrate volume is of the order of 2-4 mL, $2x10^7$ cell/mL (cell volume fraction 0.12) in a 9g/L NaCl solution. The conditions in this study were chosen to mimic this as far as practically possible: concentrate volume was 2.5 or 5 mL with 2 or $1x10^6$ cell/mL respectively (cell volume fraction ~0.01), being the maximum practicable cell concentration. Custom-made capillaries were commissioned: process-grade stainless steel (304), sufficient length to reach into a 50mL centrifuge tube (120mm), carefully polished capillary ends to minimise flow disturbance (e.g. turbulence) at capillary entry and exit. The capillary geometry mimics both aspirate-dispense and flow-through cell transfer operations; aspirate-dispense steps could also be employed in cell pellet resuspension, break-up of residual aggregates within cell concentrate and mixing of cell concentrate with alginate solution. As the primary focus of this investigation is the effect of laminar capillary shear on a well-dispersed cell suspension, any large aggregates formed during cell concentration were removed by pipette prior to shear studies to exclude potential skew of results due to shear-induced break-up of aggregates. The shear stress conditions used were selected to investigate the ranges of interest suggested by earlier findings (section 3.1.) with a view to clarifying the shear stress range providing maximal yield of intact cells; this range was expected to be bounded by cell loss at both low ($< 5$ Pa) and high ($\geq 100$ Pa) shear stress (previously observed, section 3.1.). Maximum shear stress investigated (75 Pa) was limited by practical considerations with the small volumes of cell concentrate used. Within the flowrate ranges investigated, a higher number of distinct flowrates investigated was prioritised over multiple experimental repeats, with a view to resolving trends in the overall data set and revealing shear stress thresholds for low and high shear cell loss effects. Flowrate, wall shear stress and capillary residence time was calculated for all conditions investigated and is summarised in table 3-2.

Table 3-2. Capillary residence times at various flowrates.

Values refer to 0.51x120mm capillaries and include all data points investigated using this capillary size (i.e. all shear studies assayed by flow cytometry). Calculations for superficial fluid velocity and capillary residence time assume plug flow in the capillary.

'Capillary entry length' is the distance from the capillary inlet where the laminar flow profile is fully developed (see figure 1-3). 'Capillary entry length' is calculated as ( $0.0575.d.Re_p$ ) where 'd' is the capillary internal diameter [Cousin and Richardson, 1991].

| Syringe pump flowrate | Capillary wall shear stress | Superficial fluid velocity | Capillary residence time per pass | Cumulative residence time for 9 capillary passes | Capillary entry length |
|---|---|---|---|---|---|
| (mL/min) | (Pa) | (m/s) | (s) | (s) | (mm) |
| | | | | | |
| 0.36 | 0.5 | 0.03 | 4.1 | 37 | 0.4 |
| 0.71 | 1.0 | 0.06 | 2.1 | 19 | 0.9 |
| 1.4 | 2.0 | 0.12 | 1.0 | 9.3 | 1.8 |
| 2.5 | 3.5 | 0.20 | 0.59 | 5.3 | 3.0 |
| 3.6 | 5.0 | 0.29 | 0.41 | 3.7 | 4.3 |
| 5.3 | 7.5 | 0.43 | 0.28 | 2.5 | 6.4 |
| 7.1 | 10 | 0.58 | 0.21 | 1.9 | 8.7 |
| 11 | 15 | 0.87 | 0.14 | 1.2 | 13.0 |
| 17 | 25 | 1.5 | 0.09 | 0.78 | 22.4 |
| 25 | 35 | 2.0 | 0.06 | 0.53 | 29.9 |
| 32 | 45 | 2.6 | 0.05 | 0.41 | 38.9 |
| 39 | 55 | 3.2 | 0.04 | 0.34 | 47.9 |
| 46 | 65 | 3.8 | 0.03 | 0.29 | 56.8 |
| 53 | 75 | 4.3 | 0.03 | 0.25 | 64.3 |
| 71 | 100 | 5.8 | 0.02 | 0.19 | 86.7 |

3.3.2. Effect of repeated capillary passes at low shear (0-15 Pa)

The number of cells remaining after shear (0-9 capillary passes) was quantified by flow cytometry and expressed as a fraction of cells remaining compared to the 'no flow reference sample' (figure 2-1a). 'No capillary control' runs (figure 2-1b) were not performed as this was precluded by the geometry of the apparatus setup. Examining the total number of cells remaining after shear (figure 3-9a) we see no significant change for 2-15 Pa; data is scattered around the null hypothesis, within the expected 95% range for a normal distribution. At the two lowest stresses investigated (0.5 and 1.0 Pa) the fraction of total cells remaining decreases significantly and is lowest after 9 passes (0.75 and 0.82 respectively); curve fits are based on exponential cell depletion saturating at remaining cell fractions of 0.74 and 0.79 respectively. While the decline in total cell number following shear is mirrored in the number of intact cells remaining after shear (figure 3-9b), the number of permeable cells remaining after shear is not significantly altered, data mostly being scattered within the expected 95% range for a normal distribution, with no apparent trend (figure 3-9c). This suggests that, at low shear, intact cells are being selectively lost by an unspecified mechanism, possibly adsorption to apparatus surfaces. As the samples have initially high % integrity ($\geq$ 92 %), data for total number of cells is dominated by number of intact cells. For *all* samples assayed, % integrity was in the range 92-97%, and even after significant loss of intact cells, no significant change in the % integrity of samples is evident (data not shown).

Microscopic observation of sheared samples before and after low (0.5 Pa) and high (75 Pa) shear were compared (figure 3-10). After exposure to high shear, typical characteristics of shear-induced cell damage were observed: cell fragments, large quantities of small debris particles, permeable (stained) cells with distorted morphology, cells leaking cytoplasm and ghost cells. Following low shear, little debris or other changes in the cell population morphology were evident, suggesting that the predominant mechanism of cell loss at low shear does not involve extensive cell disruption or lysis.

It appears that the observed cell loss at low shear tends towards saturation at around 20-25% loss, (figure 3-9a-b). This could imply that losses are due to, for example, adsorption of a monolayer of cells onto the capillary wall. A calculation was performed to examine the percentage of the total cells in each sample which could be lost by adsorption to the internal surfaces of the apparatus, based on cubic monolayer packing of spherical cells. The percentage of the total cells which could potentially be lost in

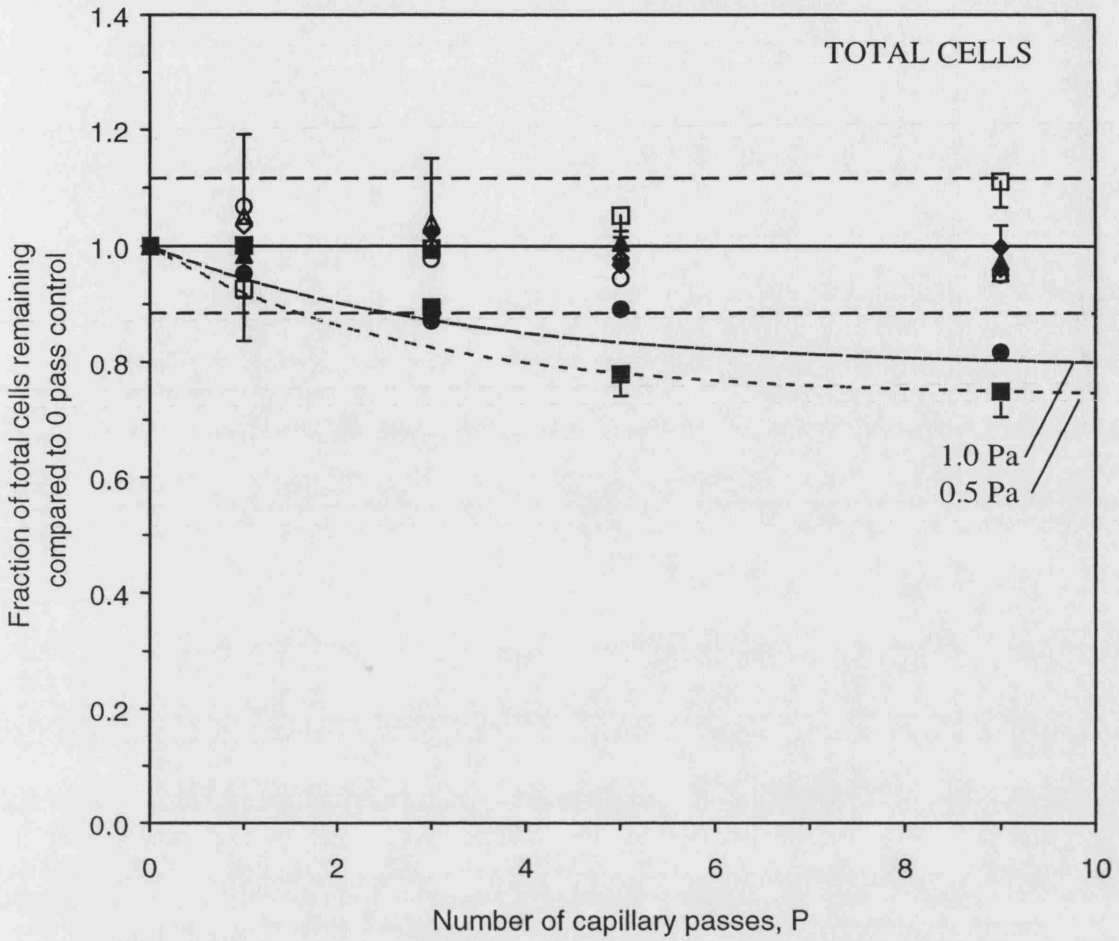


Figure 3-9a. Low shear stress studies: fraction of total cells remaining after 0-9 capillary passes (0-15 Pa).

Harvested rat aortic smooth muscle cell suspension was concentrated by protocol (B); for each sample cell concentrate was ~2.5mL, ~$2x10^6$ cell/mL in 9g/L saline solution. Each 2.5mL sample was taken up into a syringe (2.5mL) and subjected to four dispense-aspirate cycles through a capillary (0.51x120mm) and a final dispense (total of 9 capillary passes). Samples (100µl) were taken before shearing ('no flow reference sample' figure 2-1a) and after 1, 3, 5 and 9 capillary passes. After shearing all samples were assayed by flow cytometry. The fraction of cells remaining in each sample was calculated relative to the 'no flow reference sample' (figure 2-1a). Wall shear stress (Pa = $N/m^2$): (■) 0.5, (●) 1, (▲) 2, (◆) 3.5, (□) 5, (O) 7.5, (△) 10, (◇) 15. Saturating exponential decay fits: (– –●– –) 1 Pa, $R^2$ = 0.89. (- -■- -) 0.5 Pa, $R^2$ = 0.94. (—) Null hypothesis. (– –) Two standard deviations about the null hypothesis, based on flow cytometry assay precision (table 3-1), i.e. the range expected to include 95% of observations if data are normally distributed about the null hypothesis. Error bars (half only for clarity) are one standard deviation on duplicate repeat experiments, performed for (■) 0.5, (□) 5 and (△) 10 Pa conditions only.

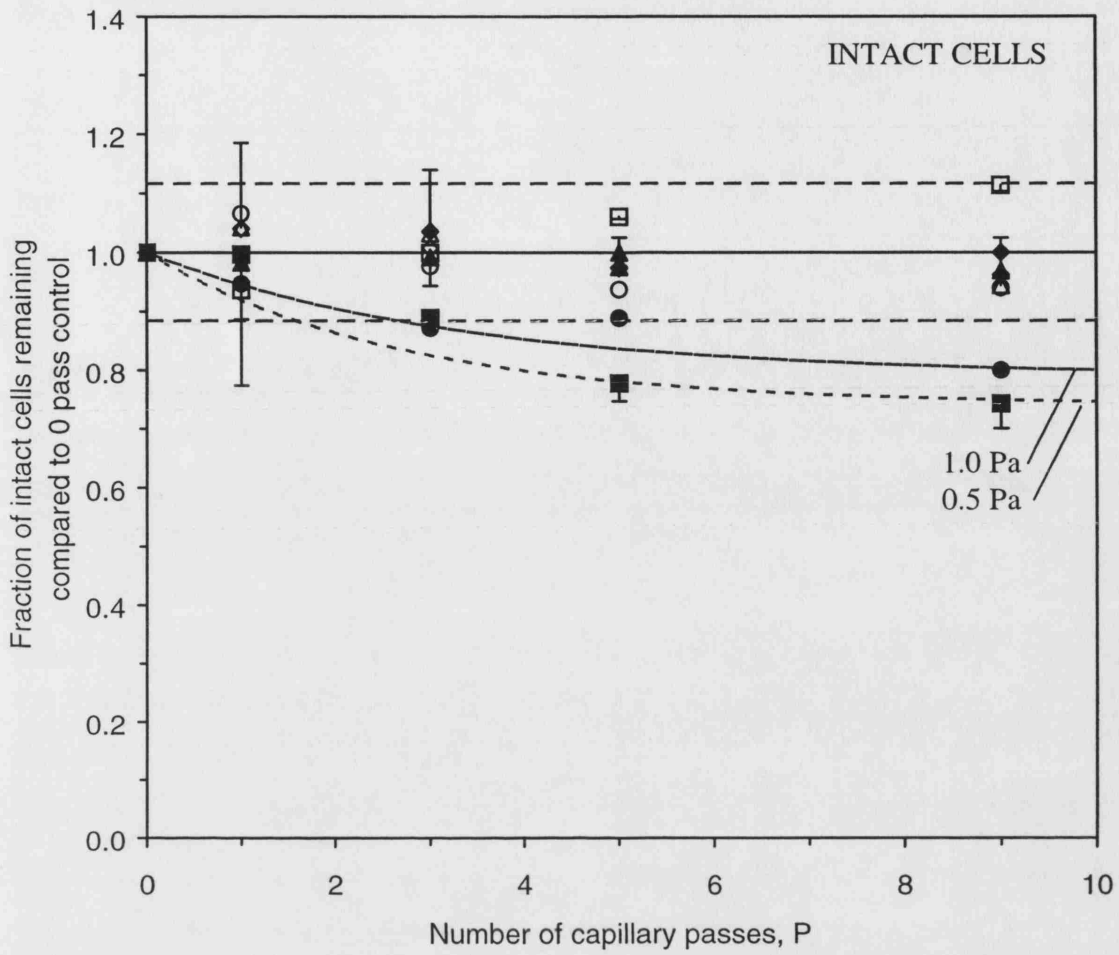


Figure 3-9b. Low shear stress studies: fraction of intact cells remaining after 0-9 capillary passes (0-15 Pa).

Harvested rat aortic smooth muscle cell suspension was concentrated by protocol (B); for each sample cell concentrate was ~2.5mL, ~$2x10^6$ cell/mL in 9g/L saline solution. Each 2.5mL sample was taken up into a syringe (2.5mL) and subjected to four dispense-aspirate cycles through a capillary (0.51x120mm) and a final dispense (total of 9 capillary passes). Samples (100µl) were taken before shearing ('no flow reference sample' figure 2-1a) and after 1, 3, 5 and 9 capillary passes. After shearing all samples were assayed by flow cytometry. The fraction of intact cells remaining in each sample was calculated relative to the 'no flow reference sample' (figure 2-1a). Wall shear stress (Pa = $N/m^2$): (■) 0.5, (●) 1, (▲) 2, (◆) 3.5, (□) 5, (O) 7.5, (△) 10, (◇) 15. Saturating exponential decay fits: (– –●– –) 1 Pa, $R^2$ = 0.88. (- -■- -) 0.5 Pa, $R^2$ = 0.94. (—) Null hypothesis. (– –) Two standard deviations about the null hypothesis, based on flow cytometry assay precision (table 3-1), i.e. the range expected to include 95% of observations if data are normally distributed about the null hypothesis. Error bars (half only for clarity) are one standard deviation on duplicate repeat experiments, performed for (■) 0.5, (□) 5 and (△) 10 Pa conditions only.

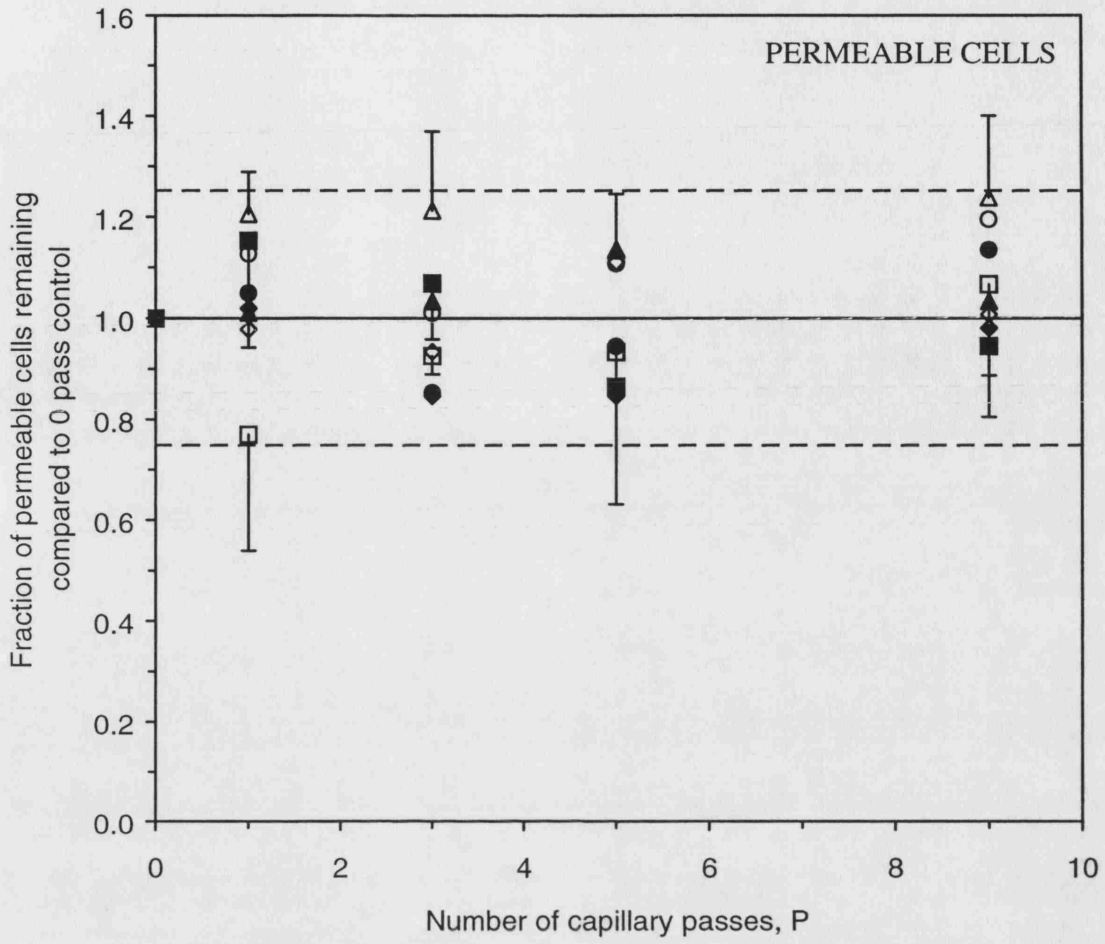


Figure 3-9c. Low shear stress studies: fraction of permeable cells remaining after 0-9 capillary passes (0-15 Pa).

Harvested rat aortic smooth muscle cell suspension was concentrated by protocol (B); for each sample cell concentrate was ~2.5mL, ~$2x10^6$ cell/mL in 9g/L saline solution. Each 2.5mL sample was taken up into a syringe (2.5mL) and subjected to four dispense-aspirate cycles through a capillary (0.51x120mm) and a final dispense (total of 9 capillary passes). Samples (100µl) were taken before shearing ('no flow reference sample' figure 2-1a) and after 1, 3, 5 and 9 capillary passes. After shearing all samples were assayed by flow cytometry. The fraction of permeable cells present in each sample was calculated relative to the 'no flow reference sample' (figure 2-1a). Wall shear stress (Pa = $N/m^2$): (■) 0.5, (●) 1, (▲) 2, (◆) 3.5, (□) 5, (○) 7.5, (△) 10, (◇) 15. (—) Null hypothesis. (– –) Two standard deviations about the null hypothesis, based on flow cytometry assay precision (table 3-1), i.e. the range expected to include 95% of observations if data are normally distributed about the null hypothesis. Error bars (half only for clarity) are one standard deviation on duplicate repeat experiments, performed for (■) 0.5, (□) 5 and (△) 10 Pa conditions only.

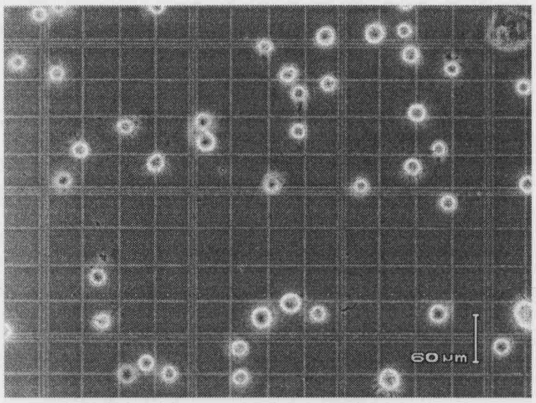


(a) Low shear control
0.5 Pa (0.36 mL/min)

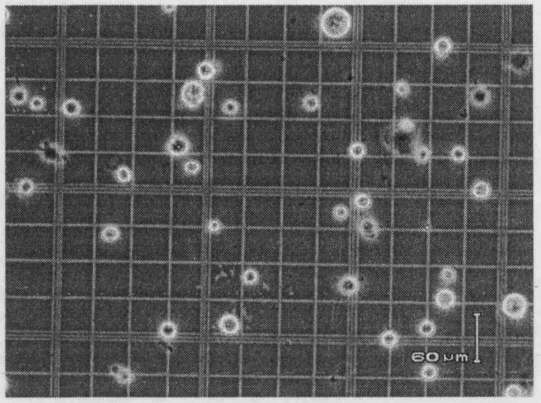


(b) After low shear, 9 capillary passes
0.5 Pa (0.36 mL/min)

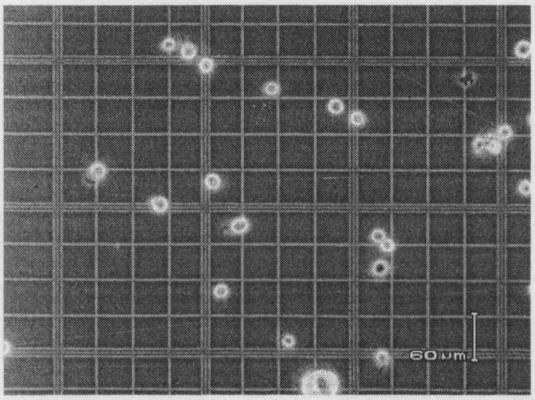


(c) High shear control
75 Pa (53 mL/min)

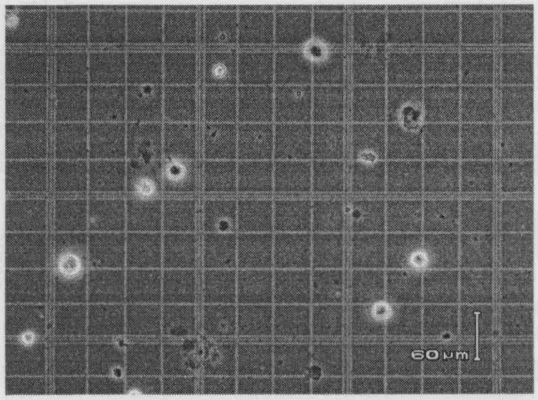


(d) After high shear, 9 capillary passes
75 Pa (53 mL/min)

Figure 3-10. Sample images of cells before and after low and high shear.
Harvested rat aortic smooth muscle cell suspension was concentrated by protocol (B) ((a) to ~$2x10^6$ cell/mL, (c) to ~$1x10^6$ cell/mL) and samples divided into one aliquot for shearing and a 'no flow reference sample' (figure 2-1a). Each sample for shearing was taken up into a syringe [(a-b) 2.5mL, (c-d) 20mL] and subjected to four dispense-aspirate cycles through a capillary (0.51x120mm) and a final dispense (total of 9 capillary passes). Flowrate was fixed as specified using a syringe pump. Cell suspension was mixed 1:1 with trypan blue stain (0.4%) and visualised on a standard haemocytometer slide. Photographs were taken with a digital camera and inverted phase contrast microscope, 100x magnification, scale bar 60µm. (a), (c) the vast majority of cells exhibit intact membranes i.e. appear white. (b) low shear (0.5 Pa): few cells stained, no cell lysis (little or no debris, stained cells exhibit coherent morphology). (d) high shear (75 Pa): many cells stained, substantial cell lysis occurs (many debris particles, stained cells exhibit varying degrees of disrupted morphology).

each apparatus section was calculated: capillary 15%, reservoir 53%, syringe 103% (i.e. if *all* cells (100%) adhered to the syringe as a monolayer, 3% *more* cells would be required to form a *complete* monolayer). A control experiment found that no significant decline in the number of cells in the shearing reservoir occurred over the time taken to perform shearing experiments (data not shown), indicating that cells are not lost by adhesion to the reservoir. As the conditions in the syringe are very similar to those in the reservoir, experimental conditions for all samples are similar except for the residence time and shear stress level in the capillary (table 3-2). Attempts (n = 4) to quantify the number of cells attached to the capillary (by rinsing with trypsin solution and performing a cell count) could only account for a total cell loss of less than 1 %.

3.3.3. Effect of repeated capillary passes at high shear (15-75 Pa)

The moderate to high (15-75 Pa) shear range was investigated by the same procedure as low shear (0.5-15 Pa) except a larger syringe and sample volume (20mL syringe, 5mL sample at ~$1x10^6$ cell/mL) was used to attain the higher flowrates. 'No capillary control' runs (figure 2-1b) were possible with this larger syringe and were performed as for 15 and 75 Pa capillary runs. The fraction of total and intact cells remaining after shear (figure 3-11a-b) exhibited a greater degree of scatter than the low shear study (section 3.3.2.). Although there was no significant difference in cell loss observed for any high shear conditions (including 'no-capillary controls'), overall the fraction of cells remaining dropped by around 10 % after 9 passes, indicating that some cell loss was occurring.

The number of permeable cells remaining after shear (figure 3-11c) remained unchanged (at ~$10^5$ cell/mL) for experiments at moderate shear (15-25 Pa) and for 'no-capillary control' runs (figure 2-1b) at moderate (15 Pa) and high (75 Pa) shear. There is some indication of an increase in the number of permeable cells generated at higher shear levels (35-75 Pa) particularly at the highest shear levels (65, 75 Pa). Although this increase in the number of permeable cells at higher shear levels does not appear to follow a consistent pattern, either with shear level or number of capillary passes, it does provide evidence that some shear damage is occurring within the cell suspension, particularly at the higher flowrates (65-75 Pa). Photographs taken before and after capillary shear at the highest flowrate (75 Pa, figure 3-10) provides supporting evidence for the occurrence of shear damage at the higher flowrates. '% integrity' data for sheared suspensions (not shown) reflected the observed increase in permeable cell

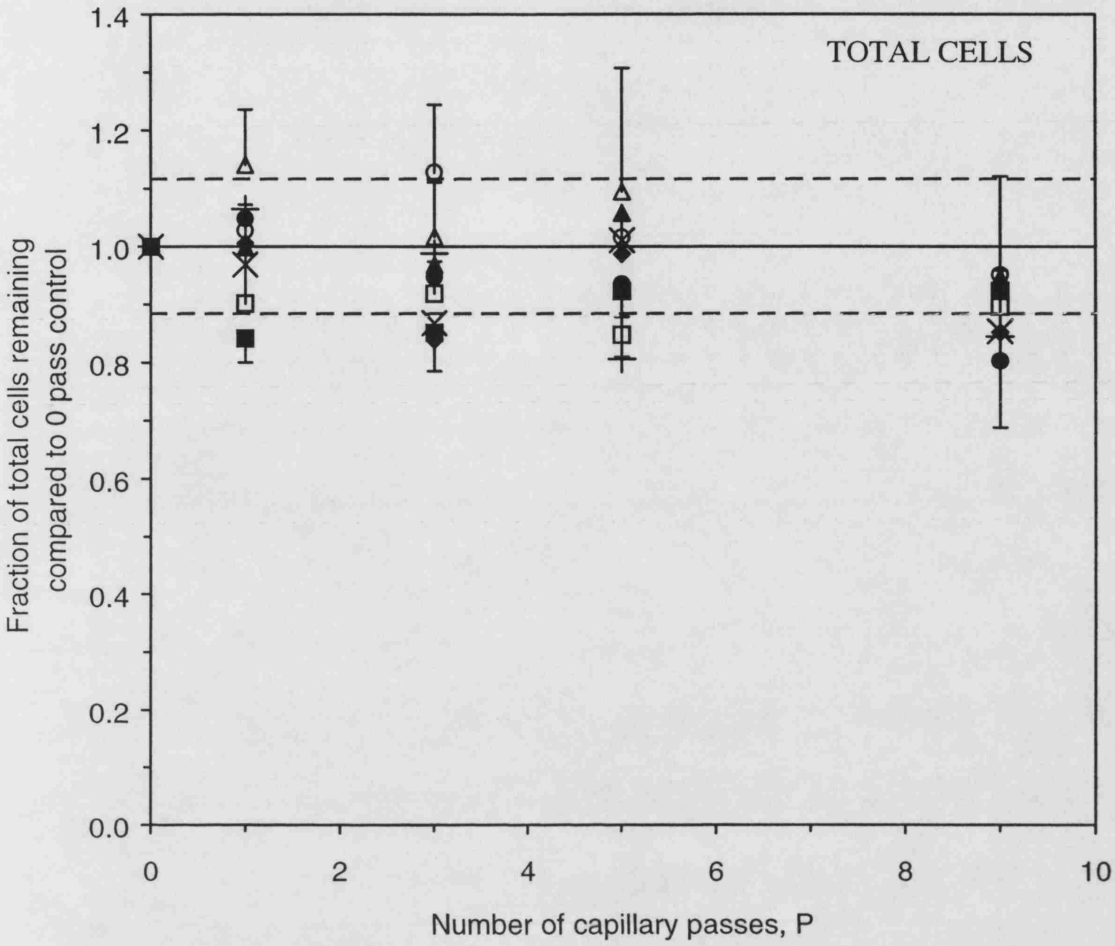


Figure 3-11a. High shear stress studies: fraction of total cells remaining after 0-9 capillary passes (15-75 Pa).

Harvested rat aortic smooth muscle cell suspension was concentrated by protocol (B), except a final volume of 5mL (~$1x10^6$ cell/mL in 9g/L saline solution) was used. Each 5mL sample was taken up into a syringe (20mL) and subjected to four dispense-aspirate cycles through a capillary (0.51x120mm) and a final dispense (total of 9 capillary passes). Samples (100µl) were taken before shearing ('no flow reference sample', figure 2-1a) and after 1, 3, 5 and 9 capillary passes. After shearing all samples were assayed by flow cytometry. The fraction of cells remaining in each sample was calculated relative to the 'no flow reference sample'. Wall shear stress (Pa = $N/m^2$): (■) 15, (●) 25, (▲) 35, (◆) 45, (□) 55, (O) 65, (△) 75. 'No capillary control' runs (figure 2-1b): (×) 15, (+) 65 Pa. (—) Null hypothesis. (– –) Two standard deviations about the null hypothesis, based on flow cytometry assay precision (table 3-1), i.e. the range expected to include 95% of observations if data are normally distributed about the null hypothesis. Error bars (half only for clarity) are one standard deviation on duplicate repeat experiments, performed for (■) 15, (□) 55, (O) 65 and (△) 75 Pa conditions only.

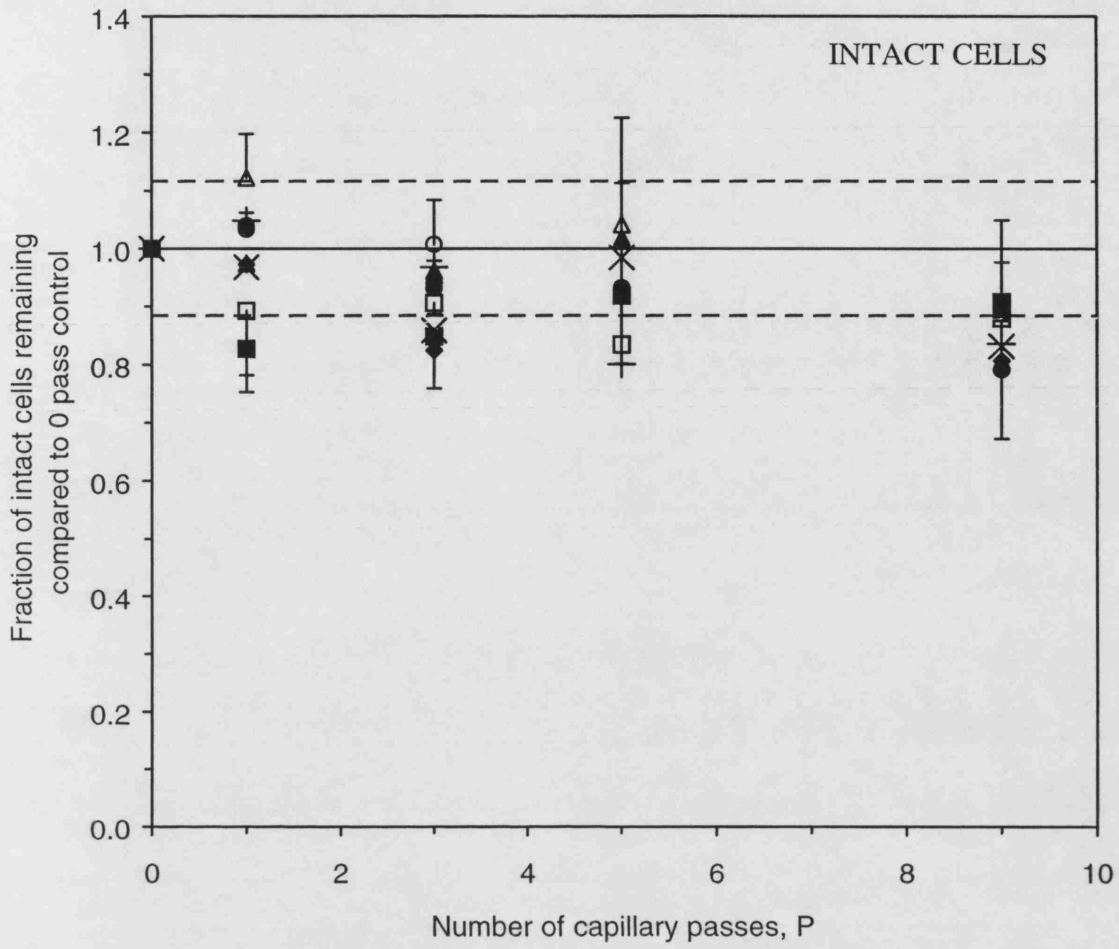


Figure 3-11b. High shear stress studies: fraction of intact cells remaining after 0-9 capillary passes (15-75 Pa).

Harvested rat aortic smooth muscle cell suspension was concentrated by protocol (B), except a final volume of 5mL (~$1x10^6$ cell/mL in 9g/L saline solution) was used. Each 5mL sample was taken up into a syringe (20mL) and subjected to four dispense-aspirate cycles through a capillary (0.51x120mm) and a final dispense (total of 9 capillary passes). Samples (100µl) were taken before shearing ('no flow reference sample', figure 2-1a) and after 1, 3, 5 and 9 capillary passes. After shearing all samples were assayed by flow cytometry. The fraction of cells remaining in each sample was calculated relative to the 'no flow reference sample'. Wall shear stress (Pa = $N/m^2$): (■) 15, (●) 25, (▲) 35, (◆) 45, (□) 55, (O) 65, (△) 75. 'No capillary control' runs (figure 2-1b): (×) 15, (+) 65 Pa. (—) Null hypothesis. (– –) Two standard deviations about the null hypothesis, based on flow cytometry assay precision (table 3-1), i.e. the range expected to include 95% of observations if data are normally distributed about the null hypothesis. Error bars (half only for clarity) are one standard deviation on duplicate repeat experiments, performed for (■) 15, (□) 55, (O) 65 and (△) 75 Pa conditions only.

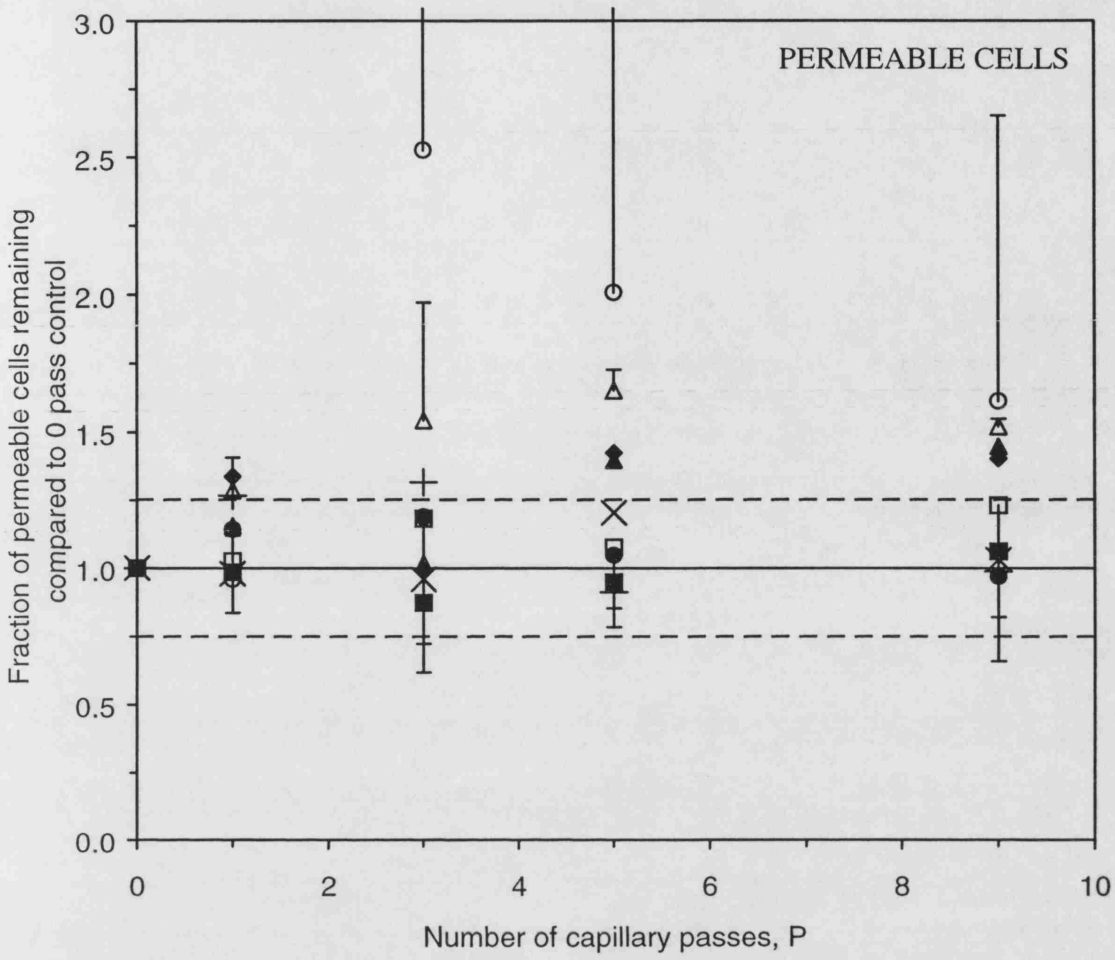


Figure 3-11c. High shear stress studies: fraction of permeable cells remaining after 0-9 capillary passes (15-75 Pa).

Harvested rat aortic smooth muscle cell suspension was concentrated by protocol (B), except a final volume of 5mL (~1x10$^6$ cell/mL in 9g/L saline solution) was used. Each 5mL sample was taken up into a syringe (20mL) and subjected to four dispense-aspirate cycles through a capillary (0.51x120mm) and a final dispense (total of 9 capillary passes). Samples (100µl) were taken before shearing ('no flow reference sample', figure 2-1a) and after 1, 3, 5 and 9 capillary passes. After shearing all samples were assayed by flow cytometry. The fraction of cells remaining in each sample was calculated relative to the 'no flow reference sample'. Wall shear stress (Pa = N/m$^2$): (■) 15, (●) 25, (▲) 35, (◆) 45, (□) 55, (○) 65, (△) 75. 'No capillary control' runs (figure 2-1b): (×) 15, (+) 65 Pa. (—) Null hypothesis. (– –) Two standard deviations about the null hypothesis, based on flow cytometry assay precision (table 3-1), i.e. the range expected to include 95% of observations if data are normally distributed about the null hypothesis. Error bars (half only for clarity) are one standard deviation on duplicate repeat experiments, performed for (■) 15, (□) 55, (○) 65 and (△) 75 Pa conditions only.

number at higher shear conditions ( ≥ 35 Pa); at 9 passes there was an average drop in '% integrity' of 1.6% for 'no-capillary controls' (figure 2-1b) and ≤ 25 Pa, with an average drop of 4.4 % for ≥ 35 Pa.

3.3.4. Effect of 9 capillary passes over the full range of shear (0-75 Pa)

In order to compare the maximal effect of shearing over the range of flowrates investigated, the fraction of cells remaining after 9 capillary shear passes is presented in figures 3-12a-c, with % integrity shown in figure 3-12d. Overall there was a loss in total and intact cell number of around 5-10 %. Cell loss observed in the 'no capillary control' runs (figure 2-1b) is similar to the loss for the capillary shear runs in the same flowrate range, any difference being within the observed level of data scatter. The greatest loss in total and intact cell number occurred at very low shear (0.5 Pa, ~25 % loss), indicating that very slow flow of cell suspension (<1 mL/min) should be avoided. There was no significant increase in either total or intact cell loss with increasing shear stress up to 75 Pa. The fraction of permeable cells following 9 capillary passes did not change significantly up to 25 Pa. At 35 Pa and above, the number of permeable cells after 9 passes increased by around 50 %; although the error bars at 55 and 65 Pa detract from confidence in any conclusion, the relative consistency of the results both above and below ~30 Pa indicates that a threshold for shear damage may exist in the range 25-35 Pa. In addition, while total and intact cell loss occurs in the 'no capillary control' (figure 2-1b) at 65 Pa (figure 3-12a-b), there is no increase in the number of permeable cells (figure 3-12c), indicating that the presence of the capillary at the higher flowrates is responsible for generation of permeable cells. The increase in the number of permeable cells produced during shear (at ≥ 35 Pa) is also reflected in the (normalised) % integrity values (figure 3-12d): for shear stress ≤ 25 Pa there is little or no significant drop in % integrity (≤ 2%), while for shear stress ≥ 35 Pa, there is a more substantial drop in % integrity (4.4 % on average).

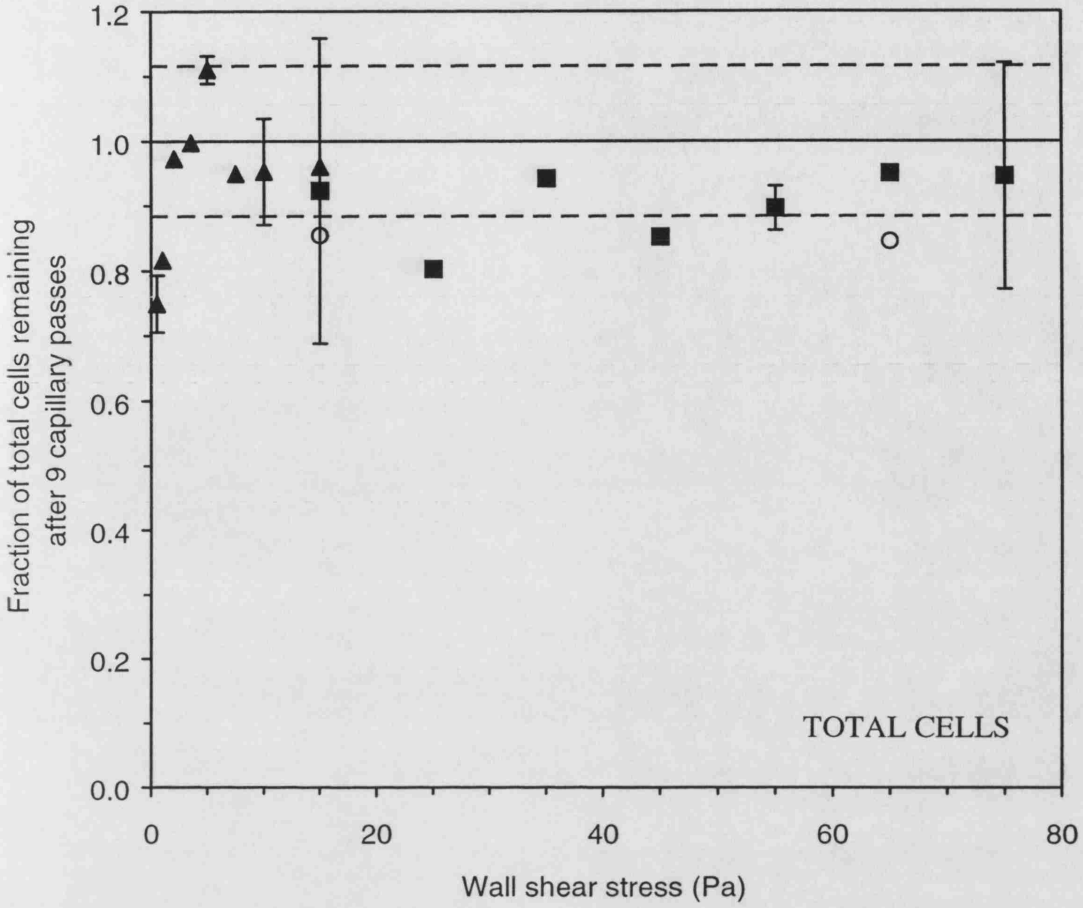


Figure 3-12a. Effect of wall shear stress on fraction of total cells remaining after 9 capillary passes (0-75 Pa).

Harvested rat aortic smooth muscle cell suspension was concentrated by protocol (B), to a specified volume of cell concentrate (below). Each concentrate sample was taken up into a syringe (see below) and subjected to four dispense-aspirate cycles through a capillary (0.51x120mm) and a final dispense (total of 9 capillary passes). Flowrate was controlled using a syringe pump. Samples taken before shearing ('no flow reference sample', figure 2-1a) and after 9 capillary passes had been assayed by flow cytometry and the fraction of cells remaining after 9 passes was calculated relative to the 'no flow reference sample'. Experimental conditions varied according to the shear range investigated: (▲) 'Low shear', cell concentrate volume 2.5mL at ~$2x10^6$ cell/mL, 2.5mL syringe, 0-15 Pa. (■) 'High shear' cell concentrate volume 5mL at ~$1x10^6$ cell/mL, 20mL syringe, 15-75 Pa. (O) were 'no capillary control' runs (figure 2-1b) performed exactly as for (■) data points at 15 and 65 Pa, except without a capillary attached to the syringe. (—) Null hypothesis. (– –) Two standard deviations about the null hypothesis, based on flow cytometry assay precision (table 3-1), i.e. the range expected to include 95% of observations if data are normally distributed about the null hypothesis. Error bars represent one standard deviation on duplicate repeat experiments, where performed.

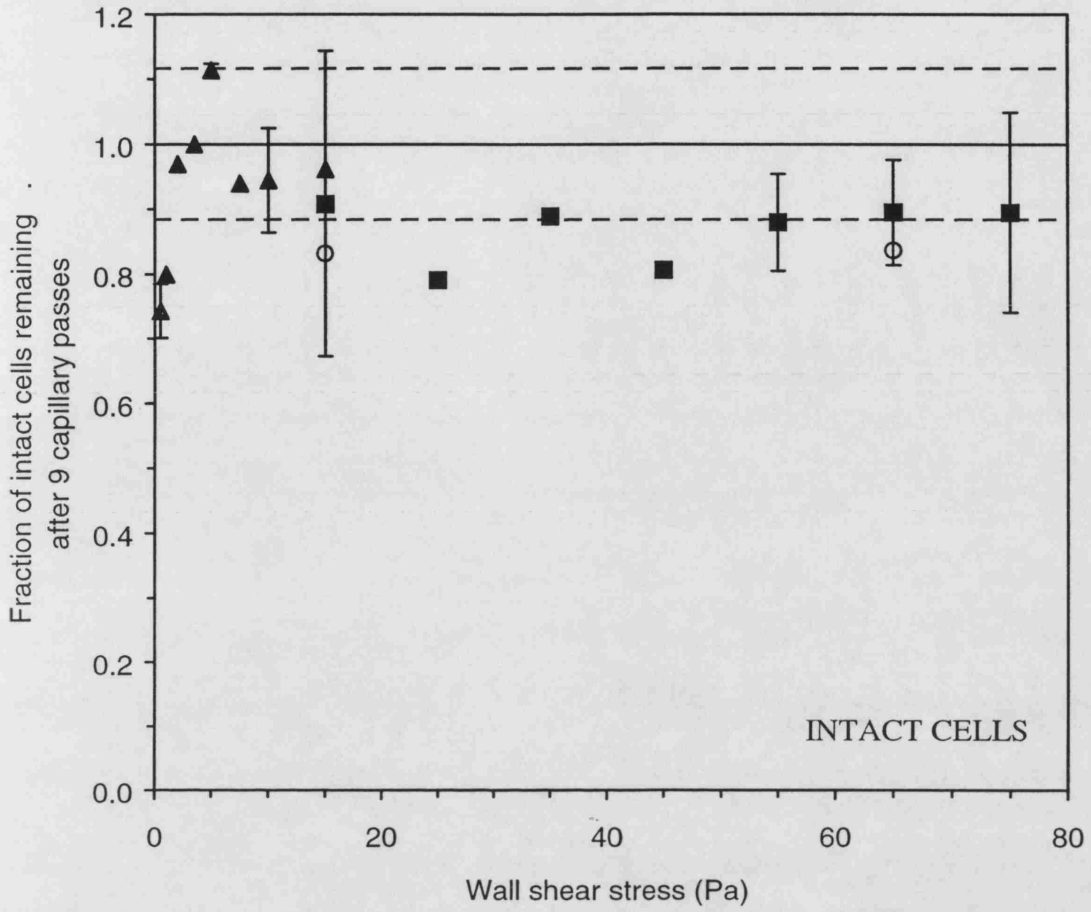


Figure 3-12b. Effect of wall shear stress on fraction of intact cells remaining after 9 capillary passes (0-75 Pa).

Harvested rat aortic smooth muscle cell suspension was concentrated by protocol (B), to a specified volume of cell concentrate (below). Each concentrate sample was taken up into a syringe (see below) and subjected to four dispense-aspirate cycles through a capillary (0.51x120mm) and a final dispense (total of 9 capillary passes). Flowrate was controlled using a syringe pump. Samples taken before shearing ('no flow reference sample', figure 2-1a) and after 9 capillary passes had been assayed by flow cytometry and the fraction of cells remaining after 9 passes was calculated relative to the 'no flow reference sample'. Experimental conditions varied according to the shear range investigated: (▲) 'Low shear', cell concentrate volume 2.5mL at ~$2x10^6$ cell/mL, 2.5mL syringe, 0-15 Pa. (■) 'High shear' cell concentrate volume 5mL at ~$1x10^6$ cell/mL, 20mL syringe, 15-75 Pa. (O) were 'no capillary control' runs (figure 2-1b) performed exactly as for (■) data points at 15 and 65 Pa, except without a capillary attached to the syringe. (—) Null hypothesis. (– –) Two standard deviations about the null hypothesis, based on flow cytometry assay precision (table 3-1), i.e. the range expected to include 95% of observations if data are normally distributed about the null hypothesis. Error bars represent one standard deviation on duplicate repeat experiments, where performed.

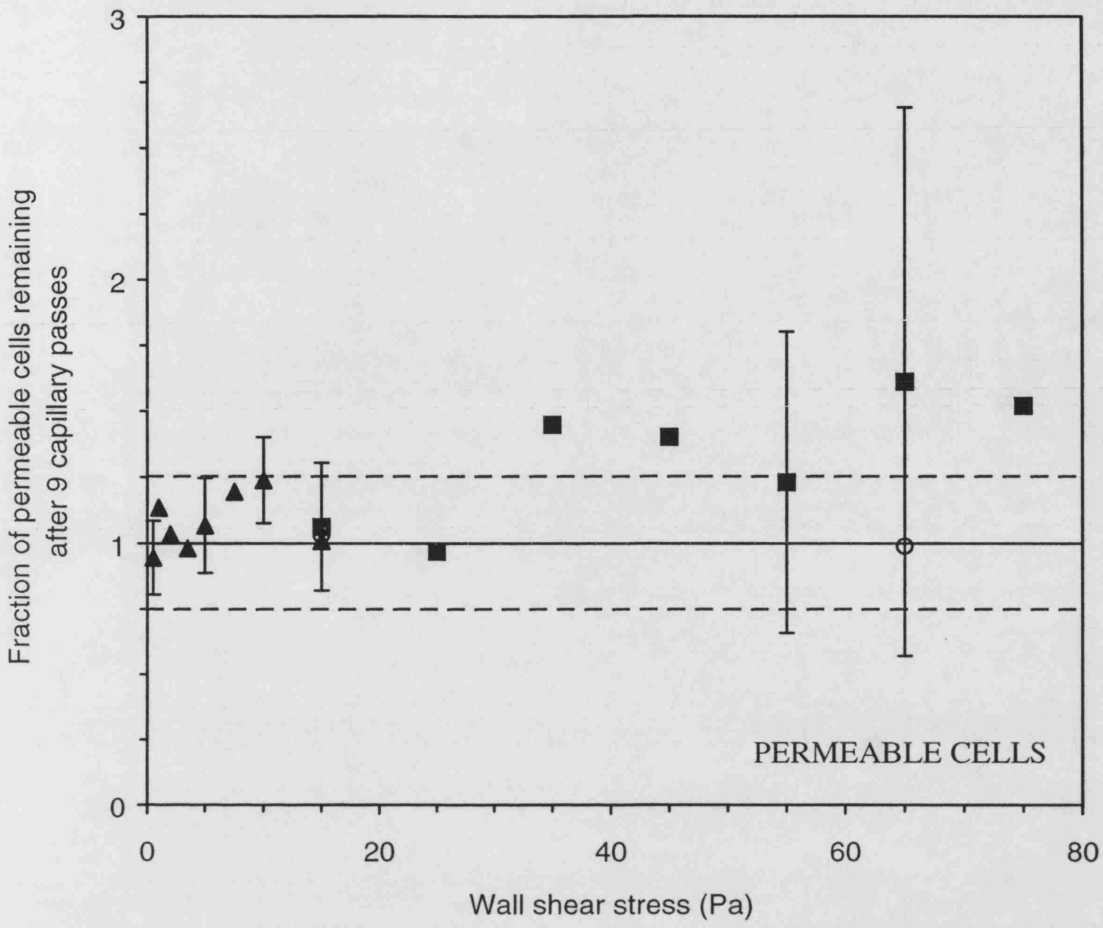


Figure 3-12c. Effect of wall shear stress on fraction of permeable cells remaining after 9 capillary passes (0-75 Pa).

Harvested rat aortic smooth muscle cell suspension was concentrated by protocol (B), to a specified volume of cell concentrate (below). Each concentrate sample was taken up into a syringe (see below) and subjected to four dispense-aspirate cycles through a capillary (0.51x120mm) and a final dispense (total of 9 capillary passes). Flowrate was controlled using a syringe pump. Samples taken before shearing ('no flow reference sample', figure 2-1a) and after 9 capillary passes had been assayed by flow cytometry and the fraction of cells remaining after 9 passes was calculated relative to the 'no flow reference sample'. Experimental conditions varied according to the shear range investigated: (▲) 'Low shear', cell concentrate volume 2.5mL at ~$2x10^6$ cell/mL, 2.5mL syringe, 0-15 Pa. (■) 'High shear' cell concentrate volume 5mL at ~$1x10^6$ cell/mL, 20mL syringe, 15-75 Pa. (O) were 'no capillary control' runs (figure 2-1b) performed exactly as for (■) data points at 15 and 65 Pa, except without a capillary attached to the syringe. (—) Null hypothesis. (– –) Two standard deviations about the null hypothesis, based on flow cytometry assay precision (table 3-1), i.e. the range expected to include 95% of observations if data are normally distributed about the null hypothesis. Error bars represent one standard deviation on duplicate repeat experiments, where performed.

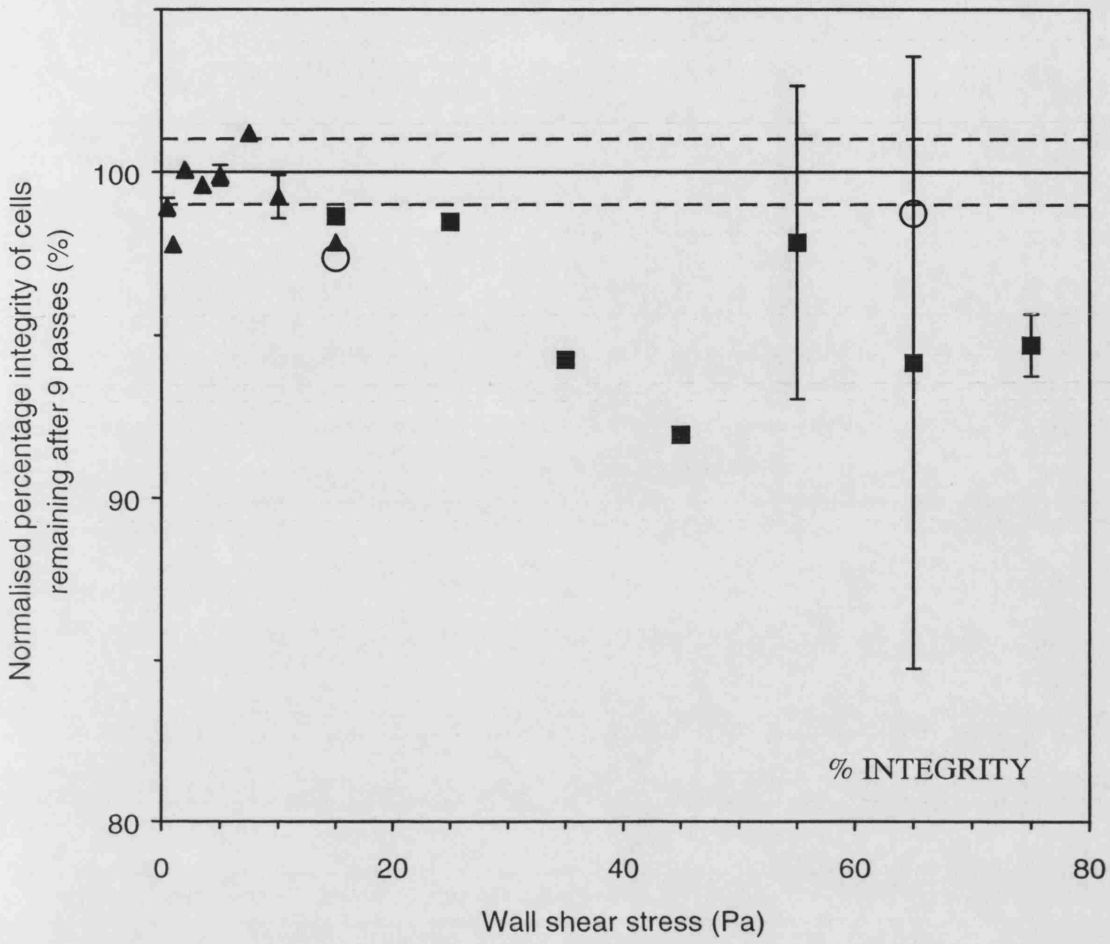


Figure 3-12d. Effect of wall shear stress on % integrity of cells remaining after 9 capillary passes (0-75 Pa).

Harvested rat aortic smooth muscle cell suspension was concentrated by protocol (B), to a specified volume of cell concentrate (below). Each concentrate sample was taken up into a syringe (see below) and subjected to four dispense-aspirate cycles through a capillary (0.51x120mm) and a final dispense (total of 9 capillary passes). Flowrate was controlled using a syringe pump. Samples taken before shearing ('no flow reference sample', figure 2-1a) and after 9 capillary passes had been assayed by flow cytometry and the '% integrity' of cells remaining after 9 passes was calculated, normalised relative to 100% for the 'no flow reference sample' (initial '% integrity' of cell concentrate was in the range 87-97 %). Experimental conditions varied according to the shear range investigated: (▲) 'Low shear', cell concentrate volume 2.5mL at ~$2x10^6$ cell/mL, 2.5mL syringe, 0-15 Pa. (■) 'High shear' cell concentrate volume 5mL at ~$1x10^6$ cell/mL, 20mL syringe, 15-75 Pa. (O) were 'no capillary control' runs (figure 2-1b) performed exactly as for (■) data points at 15 and 65 Pa, except without a capillary attached to the syringe. (—) Null hypothesis. (– –) Two standard deviations about the null hypothesis, based on flow cytometry assay precision (table 3-1), i.e. the range expected to include 95% of observations if data are normally distributed about the null hypothesis. Error bars represent one standard deviation on duplicate repeat experiments, where performed.

### 3.3.5. Discussion – effect of shear on cells in saline solution (0.5-75 Pa)

The aims of this study were to confirm the existence of a low shear loss effect and clarify the mechanisms and thresholds for shear loss at low and high shear, with a view to characterizing the optimum shear range for laminar capillary flow of cell suspensions. In addition the study was designed to mimic envisaged process conditions and potential process operations relevant to the automated handling of cell concentrates. Previous studies have attributed a decrease in total and intact cell number to cell damage, both at high (>100 Pa) [Born et al., 1992] and low (<5 Pa) [Mardikar and Niranjan, 2000] laminar shear stress. This conclusion may be problematic for low shear conditions as it is can be difficult to distinguish between cell loss by total lysis (annihilation) or surface attachment.

#### 3.3.5.1. Discussion – low shear (0.5-15 Pa)

Significant cell loss (~20-25%) was observed at low shear stress (≤ 1.0 Pa) but was not associated with generation of permeable cells. It is known that low shear stress (0.25-0.60 Pa in laminar flow) can interfere with the process of cell attachment to surfaces and laminar shear stress of the order of 0.5-10 Pa may remove adherent cells from surfaces [Chisti, 2001]. Adherent BHK cells may be torn away from their substratum at between 0.5 - 2.5 Pa, destroying their membranes [Kretzmer, 2000]. Olivier and Truskey [1993] predicted that surface shear stress required to detach adsorbed (not spread; not attached) bovine aortic endothelial cells is in the range 2-6 Pa. These reports suggest that surface fluid shear stress permitting surface attachment of cells is of the order of <5 Pa, corresponding to the range of wall shear stress resulting in cell loss in this study (<2 Pa). Although cell loss due to adhesion is likely to be influenced by kinetics, implying that loss may be observed only at low shear due to increased capillary residence time (table 3-2), the reports above suggest that there is a threshold shear stress permitting attachment (at around 0.5-5 Pa); above such a threshold the effect of fluid-surface contact time on cell adhesion would be minimal.

We have presented circumstantial evidence that, in this study, a major cause of cell loss at low shear (<2 Pa) is surface adhesion rather than cell damage, although we have not been able to been able to locate lost cells to confirm this hypothesis. Following exposure to low shear there is no significant change in the number of permeable cells, and little or no generation of cell debris normally associated with cell rupture and some indication of a saturation in observed intact cell loss, indicating an apparent selective

depletion of intact cells. In addition the level of shear corresponding to cell loss is consistent with that expected to permit surface attachment, sufficient surface area is available within the apparatus to account for losses by cell monolayer deposition and at intermediate shear (2-15 Pa) neither significant cell loss nor damage was observed. The evidence suggests that loss (adsorption) of cells may be reversible; cells which adsorb at low shear might be recovered (detached) at intermediate shear, although 'tearing' cells away from a surface could be damaging. We may consider the possibility of a low shear damage mechanism involving partial or transient surface adsorption or 'rolling', although there is no evidence to support such an effect in this study.

The range of low shear associated with cell loss matches with a previous report of the phenomenon (1 Pa, [Mardikar and Niranjan, 2000]) and is very close to previous findings in this work (2 Pa), although the magnitude of cell loss found in this study was relatively low. One major difference in this study was the use of a saline solution, rather than 10% serum-supplemented cell culture medium, as the suspending fluid; it is conceivable that serum proteins could assist surface attachment of cells (e.g. a protein-coated surface might be more adhesive to cells) and that the absence of serum proteins from the suspension attenuates cell losses by surface attachment.

It has been reported that up to 20% of cells depleted from a cell seeding suspension may be lost due to apparatus surface attachment and cell precipitation, rather than attachment to the scaffold [Li et al., 2001]. This highlights the potential severity of successive losses by surface attachment, particularly for concentrated suspensions where kinetics of adhesion will be increased. In order to avoid loss of cells due to surface adsorption, it seems prudent to operate cell suspension handling processes such that wall shear stress is in excess of ~5 Pa (~3.5mL/min for 0.5mm capillary). Process wait times should be reduced or eliminated such that fluid-surface contact time at zero shear is minimised. An alternative (additional) strategy would be to coat apparatus surfaces with 'non-stick' materials (e.g. Teflon, polyethylene glycol) to reduce risk of cell loss by adhesion.

3.3.5.2. Discussion – high shear (15-75 Pa)

Overall no significant decline in the number of intact cells was observed in the range 15-75 Pa, indicating that the conditions investigated are not seriously detrimental to a suspended cell population. There was an indication of a small increase in the number of permeable cells generated at higher shear stress (flowrate) (≥ 35 Pa), particularly the highest shear stress (≥ 65 Pa), indicating that a small amount of shear damage occurred

in this range. The small increase in permeable cells (~$5x10^4$ cell/mL) was large (~ +50%) relative to the low concentration of permeable cells (~$1x10^5$ cell/mL) and outside the observed range of assay variation for permeable cells (~10%). A corresponding reduction in intact cell number would represent a small change (~ 2-5%) relative to the high concentration of intact cells (~$1\text{-}2x10^6$ cell/mL); as this is of the order of assay variability for intact cell number (~4%), such a change is unlikely to appear significant (be detected). The ability of the flow cytometry assay to detect low-level changes in the permeable cell concentration has revealed apparent shear damage at laminar shear levels much lower than would have been seen with the trypan blue assay.

Reported values vary for the level and exposure time of high laminar shear causing damage to mammalian cells, with shear-susceptibility depending on cell type; two literature reports using the trypan blue assay with suspension cell types sheared under laminar conditions (cone and plate rheometer) reported substantial cell damage in the range 50-100 Pa, 5-20min [Mardikar and Niranjan, 2000], and ≥ ~100 Pa, 3 min, [Born et al., 1992]. While direct comparisons are not possible due to differences in experimental method, shear exposure time and assay, there is some overlap with the shear range causing cell damage. The very low level of damage observed in this study may be attributed to the relatively short exposure times (~0.1-10s, table 3-2). Observed results are consistent with the earlier shear studies in this work (section 3.1.); the threshold for substantial shear damage may be above 75 Pa (i.e. 75-100 Pa). In addition the custom capillaries used for this study (polished entry and exit) may have reduced the level of damage caused at the same shear rates due to reduced end effects.

While there is an indication of shear damage in the range 35-75 Pa, there does not appear to be a consistent trend for with increasing number of passes or shear stress. Any dependence on shear stress may be masked by reciprocal reduction in capillary residence time with increasing shear stress (flowrate); shear damage at a constant shear stress has been shown to increase with exposure time [Born et al., 1992; Chisti, 2001].

3.3.5.3. Discussion – low and high shear, 9 capillary passes (0.5-75 Pa)

When considering the effect of 9 capillary passes over the range of shear, we see (figure 3-12b) some indication of a generalised background intact cell loss of ≤ 5% for the low shear study and ~10% for the high shear study (including 'no capillary controls' (figure 2-1b)). Aside from shear level (flowrate), the only difference in procedure was the sample volume and syringe size used (low shear 2.5 mL sample, 2.5 mL syringe; high

shear 5 mL, 20 mL). The larger fluid-surface contact area for the high shear study may have enabled greater losses by generalised cell surface adhesion under low surface shear conditions in the syringe or reservoir.

Overall, after 9 capillary passes, there is an indication of cell loss occurring at $\leq 1$ Pa, reflected by changes in intact cell number (figure 3-12b); there is also some indication of low-level cell damage occurring between 35-75 Pa, reflected by changes in permeable cell number (figure 3-12c) and % integrity (figure 3-12d). Generally these results for capillary processing of cell suspensions are encouraging; it appears that only low-level cell damage occurs up to 75 Pa (equivalent flowrate 53 mL/min in 0.51mm capillary) and by operating at $\leq 25$ Pa (17 mL/min) shear damage will be minimal. Given that the volume of cell concentrate produced per patient is envisaged to be around 2-4mL, these results suggest that process operations such as cell transfer by aspirate-dispense could be performed rapidly (~20s), with little or no risk of cell damage. These studies consider only relatively dilute cell suspensions ($1\text{-}2\text{x}10^6$ cell/mL, cell volume fraction ~0.01), while cell concentration in the envisaged process is around one order of magnitude higher ($\sim 2\text{x}10^7$ cell/mL, cell volume fraction 0.12), with an associated increase in suspension viscosity (section 4.1.5.). The shear stress ranges associated with cell loss described here may or may not translate to the higher concentration range; the 'nature' of shear stress, as experienced by suspended cells, may alter as changes in apparent viscosity (i.e. cell concentration) become significant, possibly giving rise to alternative mechanisms of cell damage. Potential cell loss by surface adhesion is likely to increase with cell concentration due to kinetic effects, i.e. the number of cells in the vicinity of apparatus surfaces will rise.

### 3.4. Summary

Hydrodynamic (shear) stress is widely recognised as being able to cause significant mechanical damage to a suspended cell population, with turbulent shear stress being more damaging to cells than laminar shear stress of the same magnitude [Chisti, 2001]. Automated processing of cell suspensions for regenerative medicine is likely to include laminar capillary flow as a common operation. Various capillary flow and suspension conditions were investigated to determine effects of processing on cell health and yield, and to determine optimal capillary flow conditions for healthy cell survival.

Initial studies with cell harvest suspension (~$1x10^5$ cell/mL), showed that repeated exposure to high laminar capillary shear (≥ 100 Pa) causes serious damage to suspended adherent cells by mechanical cell lysis. Substantial apparent cell loss also occurred at low shear stress (2 Pa), by an uncharacterised mechanism. The optimum wall shear stress for cell survival was found to be ~10 Pa (equivalent flowrate 4mL/min) and is in close agreement with previous findings [Mardikar and Niranjan, 2000]. The decline in mammalian cell number with increasing exposure to laminar shear stress is consistent with that found in the literature [Born et al., 1992]. Cells which were able to grow following exposure to high shear were able to grow normally with no significant changes in growth rate, achievable cell density or metabolism. As the trypan blue assay used in these studies was slow, laborious, subjective and exhibited poor precision, it was deemed unsuitable for further studies.

Development of a flow cytometry assay quantifying the concentration of intact and permeable cells accomplished the principal aims of providing substantial increases in assay precision (~4-fold) and speed (~2-fold), achieving a high degree of resolution between intact and permeable cells by means of two-dye staining, and elimination of operator involvement (subjectivity) in cell classification and counting. Improvement in assay speed reduces time for sample deterioration; increased assay precision increases assay sensitivity to small changes in the suspended cell population. In addition increased cell counts recorded by flow cytometry (compared to trypan blue) may have been due to release of cells from aggregates, which would represent an improvement in assay accuracy over trypan blue.

Shear studies with concentrated cell suspension (~$1\text{-}2x10^6$ cell/mL in 9g/L saline solution) indicated that moderate shear stress (2-25 Pa) did not cause significant loss of, or damage to, cells. At very low shear stresses (<2 Pa) significant intact cell loss occurred, apparently by surface adhesion. At moderate-high shear stresses (≥ 35 Pa), particularly the highest shear stresses (≥ 65 Pa), there was some indication of a low level of cell membrane damage. Overall the recommended range for maximal healthy cell yield would be ~5-25 Pa (equivalent flowrate 4-17 mL/min, 0.5 mm capillary) corresponding to reasonable capillary transfer times (~20 s) for the envisaged volume of cell concentrate (2-4 mL). If necessary, higher flowrates could be achieved by changes in capillary diameter, or by accepting a low level of cell damage (e.g. as observed in the range 35-75 Pa). For the high shear study (15-75 Pa), an apparent background cell loss

of ~10% indicated that generalised surface adhesion of cells to apparatus may be a significant loss factor during processing and that appropriate steps should be taken at the process design stage to reduce risk of cell loss: minimisation of fluid-surface contact areas and times, careful materials selection for contact surfaces to reduce surface adhesiveness.

Overall, these studies were very encouraging, illustrating that automated processing of adherent cell suspensions can be achieved at reasonable flowrates and capillary diameters with little or no loss of, or damage to, suspended cells. Unfortunately, practical considerations limited studies to relatively dilute cell suspensions (~1-2x$10^6$ cell/mL, volume fraction ~0.01); it was not possible to investigate shear damage effects in highly concentrated cell suspensions as envisaged in a real process (e.g. $\geq$ 1x$10^7$ cell/mL, cell volume fraction $\geq$ 0.1); further studies are required to determine how current results translate to a different flow regime where rheology (and possibly shear damage mechanisms) are controlled by cell concentration and cell-cell interactions.

# Chapter 4: Cell concentration

## 4.0. Introduction

Cell concentration is a generic processing operation, present in most, if not all, tissue engineering processes. Following harvest, cells must be concentrated before they can be seeded, or otherwise formed, into a tissue construct. Within a nascent tissue construct, a high number of initially seeded cells can improve structural stability and biochemical composition of engineered tissues [Li et al., 2001] and reduced cell density within blood vessel tissue constructs has been associated with decreased contractility [L'Heureux 2001]. Cell seeding suspension concentrations reported range from around $10^5$ cells/mL [Li et al., 2001] up to typical *in vivo* cell densities of $0.5\text{-}1x10^8$ cells/mL for cardiac myocytes [Radisic et al, 2003] or higher $3x10^8$ cells/mL [Dar et al., 2002]; very high cell concentrations may be desirable in many applications.

While previous reports have tended to focus on the process downstream of cell concentrate preparation (cell seeding efficiency, construct growth and morphology etc.), it is also necessary to characterise the behaviour, performance and impact of the concentration process and the physical and biochemical properties of cell concentrates generated. Principal performance criteria for the cell concentration operation include concentration factor, total cell yield, health of concentrated cells and process reproducibility.

In this chapter cell size and concentrate rheology are investigated, along with development and performance characterisation of two semi-automated concentration protocols. In addition consideration is given to potential impact of nutrient (oxygen) depletion in cell concentrates.

## 4.1. Processing characteristics of cell suspension

Knowledge of cell concentrate rheology is essential for engineering design of concentrate handling systems and it is likely to be an important factor in many tissue seeding or other formation processes. In addition the biochemical requirements of live biological materials must be considered, in this case the principal factor is oxygen consumption rate of the cells.

4.1.1. Experimental development – cell culture

As studies on the rheology of highly concentrated cell suspensions were estimated to require up to around 100 million cells, manual cell culture was converted from T150 ($150cm^2$) flasks into larger capacity T500 'triple-decker' ($500cm^2$) flasks, to reduce manual cell culture labour and enable investigation of the highest practicable cell concentrations. T500 was selected as the largest available flask which could be accommodated in the available cell culture facilities without additional equipment. In addition T500 are externally identical to T175 flasks and as such are geometrically compatible with automated cell culture systems such as SelecT (see table 2-2a); the manual T500 cell culture process could thus be easily transferred directly into such a system for process scale-up (scale-out). In moving from T150 to T500, the volume of harvest enzyme solution (trypsin/EDTA) was scaled directly as cell culture area (to 20mL/T500), while the volume of quenching media was reduced (to 20mL/T500) so that the total volume of the cell harvest suspension (~40mL per T500) would fit into a standard laboratory centrifuge tube (50mL).

Cell culture trains using the standard T150 and newly developed T500 passage protocols were carried out in parallel to compare the productivity of cell cultures in the two flask types. Harvested cell density and glucose/lactate metabolism of cells in duplicate flasks were monitored over seven passages (figures 4-1a and 4-1b respectively). Overall, mean harvested cell density was 23% higher in T150 flasks, this difference being significant at the 95% but not the 99% confidence level (table 4-1a). While there was no significant difference in cell density after three days in culture, cell density in T150 flasks was significantly higher after four days in culture. Possible reasons contributing to this relative reduction in cell proliferation in the four-day T500 cultures could be: gas transfer limitation in the T500 flasks (both flasks have similar gas-exchange filter caps for very different culture areas); differences in the growth surface characteristics of the two flask types (supplied by different manufacturers); uneven media distribution between 'decks' in the T500 leading to slight differences in nutrient/waste concentrations at the longer time point. During all passages the ratio of lactate produced to glucose consumed was very similar between the two flask types (figure 4-1b) with no significant difference (table 4-1b). The similarity between fluctuations in metabolism suggests that any variable factors had affected both cultures equally (for example incubator gas or temperature fluctuations, media batch variation). Although the time taken to process T150 and T500 flasks manually was not compared

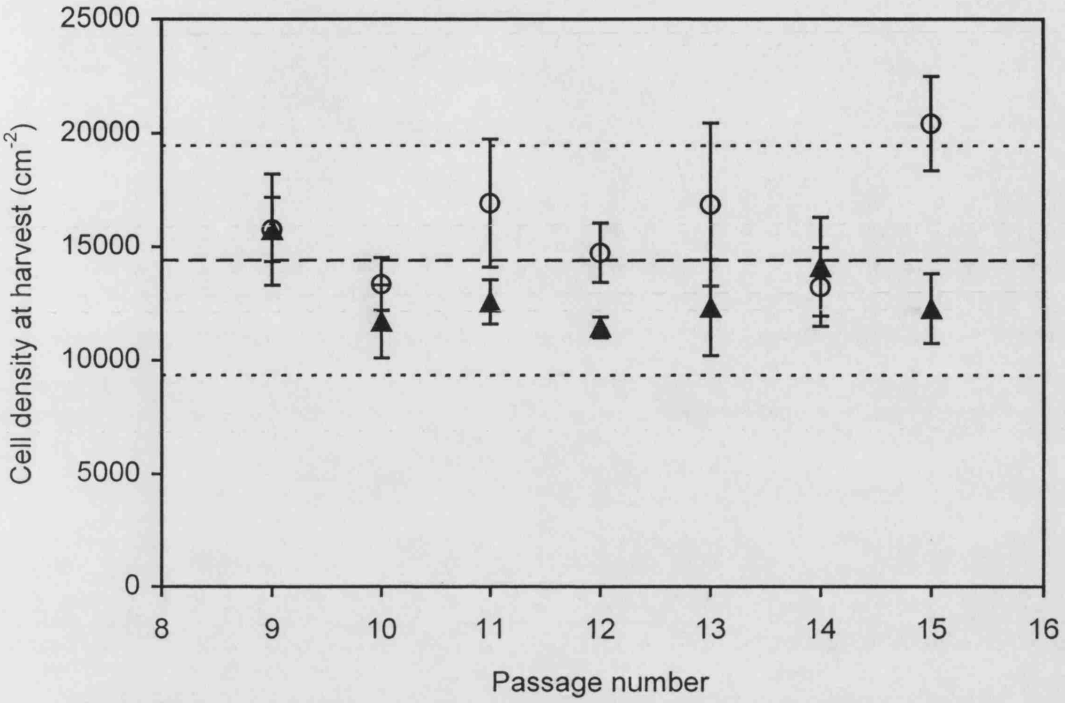


Figure 4-1a. Culture flask comparison – cell density

Harvest cell density on T-flask growth surfaces during parallel cell culture trains. Rat aortic smooth muscle cells (revived from cryopreservation at passage 6) were initially expanded in T150 (150cm$^2$ culture area) flasks and planted (passage 9) at 6000 cells/cm$^2$ into T150 and T500 ('triple-deck', 500cm$^2$ culture area) culture flasks. Flasks were then passaged alternately every 3 or 4 days at a 1 to 3 split ratio; for passages 10-15, two flasks of each type were planted and pooled for analysis/harvest. Cell density on the culture surface, (O) T150, (▲) T500, was calculated from cell concentration (haemocytometer count) in a measured volume of harvested cell suspension. (— —) mean of all data, (- -) two standard deviations about the mean, i.e. the range expected to include 95% of observations if data are normally distributed about the mean. Error bars represent one standard deviation on quadruplicate haemocytometer cell counts.

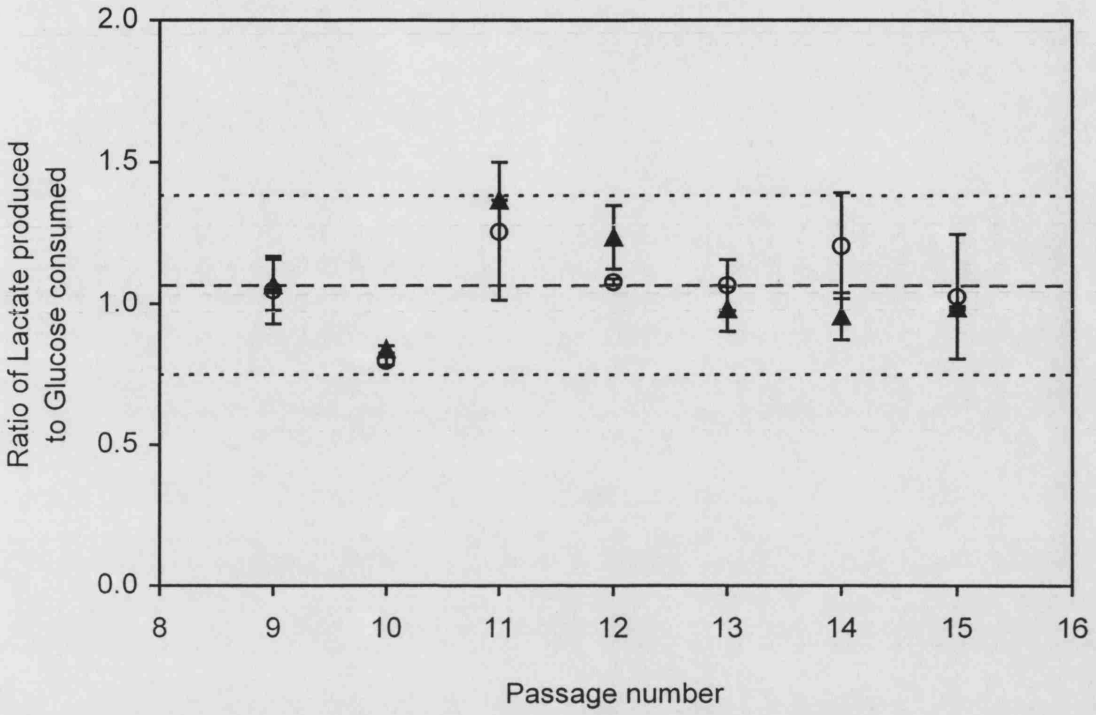


Figure 4-1b. Culture flask comparison – cell metabolism

The ratio of lactate produced to glucose consumed during each cell culture passage, throughout parallel cell culture trains in T150 (150cm$^2$) or T500 ('triple-deck', 500cm$^2$) culture flasks. Rat aortic smooth muscle cells were initially planted at 6000 cells/cm$^2$ (passage 9) into T150 and T500 flasks. Flasks were then passaged alternately every 3 or 4 days at a 1 to 3 split ratio; for passages 10-15, two flasks of each type were planted and pooled for analysis/harvest. Samples (0.5mL) of cell culture medium for analysis were taken from all flasks following cell planting and immediately prior to cell harvest.

The ratio of lactate produced to glucose consumed was calculated: (O) T150, (▲) T500, (— —) mean of all data, (- - -) two standard deviations about the mean, i.e. the range expecte to include 95% of observations if data are normally distributed about the mean. Error bars represent one standard deviation on duplicate assay repeats.

Table 4-1a. Cell culture flask comparison: statistical analysis of cell density on culture surface (cells/cm$^2$) at flask harvest; performed using Student's t-test (unpaired). Significant difference between the cell density in T150 and T500 culture flasks (day 3 or 4) is observed at the 95% confidence level ($P<0.05$) but not at the 99% confidence level ($P<0.01$). No significant difference is observed between the flask types after three days in culture. Significant difference between the T150 and T500 culture flasks is observed (at the same level as above) where culture duration extended to four days.

| Days per passage | n | Surface cell density at harvest, T150 flask (x10$^3$ cells/cm$^2$) | | Statistical comparison | Surface cell density at harvest, T500 flask (x10$^3$ cells/cm$^2$) | |
|---|---|---|---|---|---|---|
| | | Mean | SD | P-value | Mean | SD |
| | | | | | | |
| 3 or 4 | 7 | 15.9 | 2.5 | **0.02** | 12.9 | 1.5 |
| 3 | 3 | 13.8 | 0.8 | 0.24 | 12.4 | 1.5 |
| 4 | 4 | 17.5 | 2.0 | **0.02** | 13.2 | 1.7 |

Table 4-1b. Cell culture flask comparison: statistical analysis of the ratio of Lactate produced to Glucose consumed (L:G ratio), performed using Student's t-test (unpaired). No significant difference is observed between the T150 and T500 culture flasks at the 95% confidence level ($P<0.05$).

| Days per passage | n | T150 flask (L:G ratio) | | Statistical comparison | T500 flask (L:G ratio) | |
|---|---|---|---|---|---|---|
| | | Mean | SD | P-value | Mean | SD |
| | | | | | | |
| 3 or 4 | 7 | 1.07 | 0.15 | 0.92 | 1.06 | 0.18 |
| 3 | 3 | 1.03 | 0.21 | 0.93 | 1.01 | 0.20 |
| 4 | 4 | 1.10 | 0.11 | 0.98 | 1.10 | 0.18 |

quantitatively, it was observed that the labour required when producing large numbers of cells was reduced by around half (T500 vs. T150).

### 4.1.2. Size distribution of cells

Optical microscopy with a graticule was the method selected to measure cell size distribution. Although labour-intensive, this simple, direct method offers suitable resolution (1.7μm per graticule division at 60x magnification) and does not require substantial calibration or verification. Qualitatively, cell size distribution was observed to be consistent across the four samples taken (from passages 10, 12 and 13, harvested on days 3, 4, or 5; >100 cells per sample, total n = 483). The total data set is presented as number frequency, cumulative number% and cumulative volume% (figure 4-2); the cumulative volume curve is skewed with respect the cumulative number curve due to the cubic dependence of cell volume on diameter. The vast majority of cells were observed to be spherical and within the 10-40μm size range, although a few very large cells (>40μm) were seen (figure 4-2). It was observed that many cells exhibited fibrillar surface protrusions of the order of cell radius which tend to be arranged in bundles at two opposing ends of the cells. Cell aggregates were not observed; any aggregates may have been excluded by the method or small sample volume examined. The volume mean cell volume was calculated as (total volume of all measured cells)x(total number of measured cells)$^{-1}$ and found to be $5.8 \times 10^{-15}$ m$^3$, corresponding to a volume mean cell diameter of 22.4μm. The volume mean cell diameter corresponds to the 50$^{th}$ percentile on the cumulative volume curve (figure 4-2); half of the total cell volume lies either side of the mean cell volume. The theoretical maximum cell volume fraction, $\phi = 1.0$, corresponds to a cell concentration of $1.71 \times 10^8$ cell/mL. While less than 5% of cells are over 30μm in diameter, approximately 20% of cell volume (or mass) is contained within these large cells.

### 4.1.3. Rheology of cell concentrates

A key bulk physical property of a suspension is viscosity, which is typically a strong function of suspended solids volume fraction [Matijasic and Glasnovic 2002]. As different cell types exhibit different sizes and it is useful to relate cell suspension rheology results to the established literature, it is necessary to express suspension cell concentrations in terms of cell volume fraction. This was achieved by conversion from

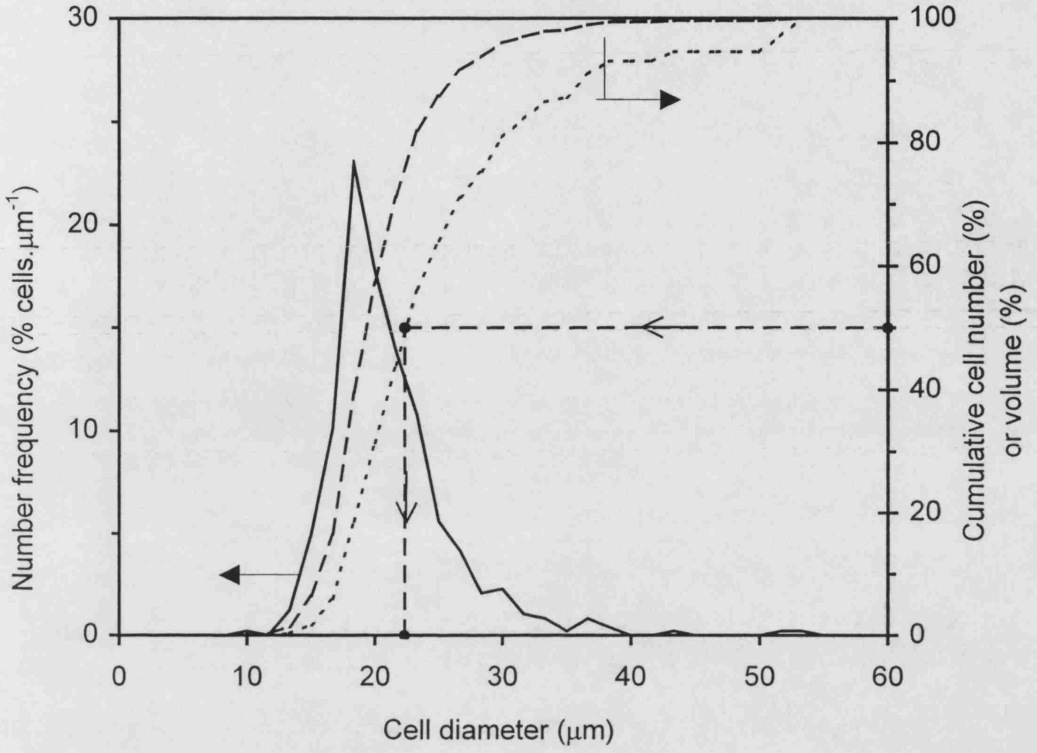


Figure 4-2. Cell size distribution of harvested rat aortic smooth muscle cells.

RSMC suspended in trypsin quenched with culture medium as for the normal passage protocol. Cell diameters measured with 100-division graticule and inverted phase contrast microscope (600x magnification), corresponding to a resolution of 1.7μm per graticule division. Four samples taken from separate culture flask harvests, >100 cells per sample, n = 483 cells in total). (—) Number frequency expressed as percentage of all cells counted. (– –) Cumulative cell number (as % of total), (---) cumulative cell volume (as % of total), (–•–) volume mean cell diameter (22.4 μm) corresponds to the 50$^{th}$ percentile on the cumulative volume curve.

numerical cell concentrations (manual haemocytometer cell count) via measured volume mean cell volume:

$$\phi = c / c_{max} \qquad \text{(eq. 4-0)}$$

Where:

$\phi$ = cell volume fraction (v/v)

$c$ = cell concentration (cell/mL)

$c_{max}$ = theoretical cell concentration at $\phi = 1.0$ ($1.71 \times 10^8$ cell/mL)

4.1.4. Predicted rheology of cell suspensions

Many mechanistic models and correlations are available in the literature which may be used to describe the behaviour of suspensions as a function of parameters such as shear rate, solids volume fraction, particle shape and size distribution. In this study generation of simple correlations was attempted in two distinct situations: (1) response of apparent suspension viscosity to changes in shear rate (fixed cell volume fraction); (2) effect of cell volume fraction as a function of cell volume fraction (fixed shear rate). As harvested cells are approximately spherical, shape is not expected to be a major factor and effects of particle size distribution are not considered. Simple equations are considered for rheology at fixed cell concentration: Newtonian, Power Law or Bingham plastic fluids:

Newtonian: $\tau = \mu.\gamma$ (eq. 4-1)

Power law: $\tau = k.\gamma^n$ (eq. 4-2)

Bingham plastic: $\tau = \tau_y + \mu_b.\gamma$ (eq. 4-3)

Where:

$\tau$ = shear stress (Pa = $N/m^2$)

$\mu$ = Newtonian viscosity (Pa.s)

$\gamma$ = shear rate ($s^{-1}$)

$k$ = consistency index ($Pa.s^n$)

$n$ = power law index (-)

$\tau_y$ = Bingham yield stress ($N/m^2$)

$\mu_b$ = 'Bingham viscosity' (Pa.s)

Simple theoretical models for suspension behaviour as a function of cell volume fraction were reported by Einstein (1905) and Vand (1948) [Sherman, 1970], for dilute suspensions of uniform hard spheres, based on viscous interactions alone (Einstein) and

additional surface interactions (Vand); the mechanistic basis for these equations are generally considered to be valid only for dilute suspensions ($\phi < 0.05$).

Einstein: $\mu_r = (1+ 2.5\phi)$ (eq. 4-4)

Vand: $\mu_r = (1 + 2.5\phi + 7.35\ \phi^2)$ (eq. 4-5)

Where: $\mu_r$ = relative suspension viscosity (relative to diluent viscosity)

$\phi$ = solids (or cell) volume fraction (v/v)

Many alternative correlations of various forms exist for a wide variety of suspension types; detailed consideration of such correlations is beyond the scope of this work.

### 4.1.5. Rheology results

The rheology of rat aortic smooth muscle cell (RSMC) concentrates was analysed over the maximum range of shear rates possible with the cone and plate rheometer used; measurable shear rates were lower with more viscous samples. Cell volume fraction was calculated from cell concentration (by haemocytometer cell count) and volume mean cell volume (section 4.1.2.). Results for apparent viscosity of various concentrates over the measured range of shear are shown in figure 4-3 along with example data for yeast cell suspensions [Ward, 1989]; some RSMC data sets are omitted for clarity. There is a clear reduction in apparent viscosity with increasing shear rate (shear thinning) which is not fully attenuated when returning to lower shear rates, indicating time-dependent or irreversible alteration of the suspension microstructure. RSMC suspension viscosity is much higher than reported for yeast cell suspensions at similar volume fraction. RSMC suspension does not exhibit shear thickening behaviour in the range of concentration and shear rate examined.

Bingham plastic and Power law fluid parameters were determined for all RSMC suspensions by linear regression analysis; this analysis was performed separately for data taken stepping shear rate up and down (tables 4-2a, 4-2b) and for combined data sets (table 4-2c). Suspensions are observed to be Newtonian where $\phi < 0.03$, with deviations from Newtonian behaviour increasing with $\phi$ ($\phi \geq 0.03$). From $\phi = 0.03$ - 0.07, both Power law and Bingham plastic fits accurately describe suspension rheology for separate 'up' and 'down' data ($R^2 \geq 0.99$). Where $\phi \geq 0.03$ the combined (up and down) data sets show reduced accuracy ($R^2 < 0.99$ in most cases); this indicates that the suspension characteristic responsible for non-linear behaviour (e.g. cell-cell interaction) is degraded at higher shear levels and so 'up' and 'down' measurement conditions must

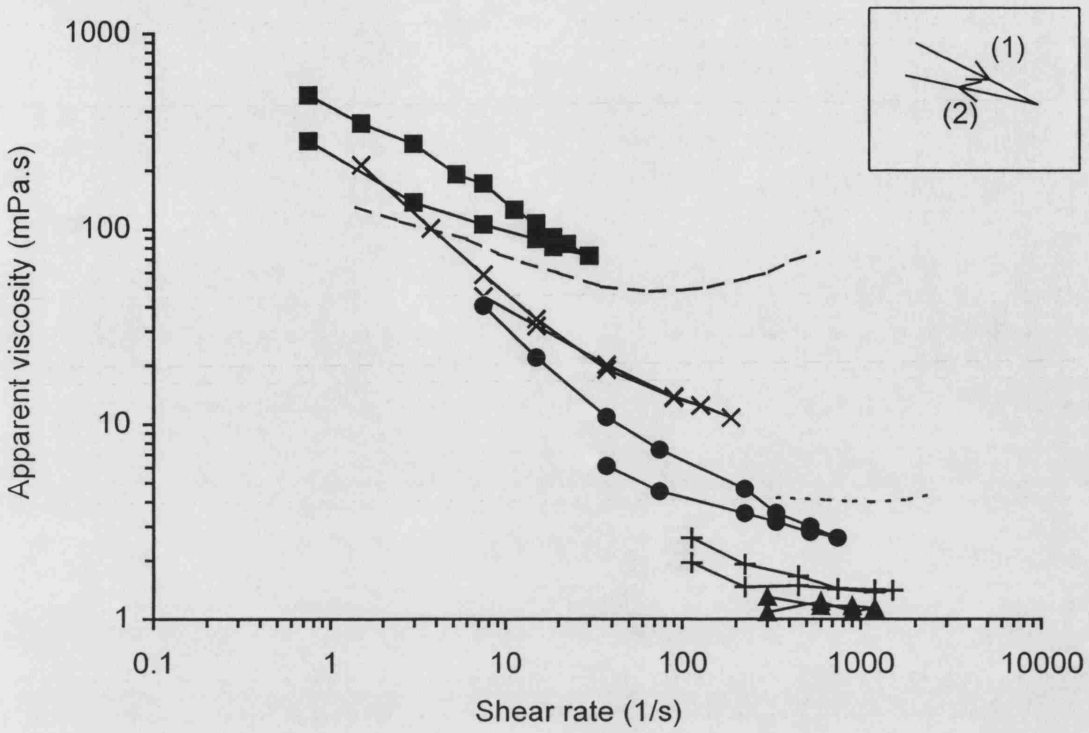


Figure 4-3. Apparent viscosity of rat aortic smooth muscle cell suspension as a function of shear rate.

Concentrated rat cell suspensions generated by centrifugation and resuspension in 9g/L $NaCl/H_2O$. Apparent viscosity of 0.5mL samples was measured in a cone and plate rheometer (25 ± 0.5°C) over the maximum measurable range of shear rate. Inset box: cone angular velocity was first stepped up (1) and then down (2) allowing the viscosity readout to stabilise before recording each data point. Data for non-flocculated yeast cell suspensions [Ward, 1989] is included for comparison. For rat cell suspensions, cell volume fraction, $\phi$ = (▲) 0.01, (+) 0.03, (●) 0.09, (×) 0.25, (■) 0.34 (wet cell pellet); other rat cell data sets collected are omitted for clarity. For yeast cell suspensions, $\phi$ = (- -) 0.32, (— —) 0.54; yeast suspension viscosity was measured using concentric cylinder or cup and bob rheometers respectively.

Table 4-2a. Bingham plastic fluid parameters for rat aortic smooth muscle cell suspension in 9g/L saline solution at 25 ± 0.5 °C. Shear rate (motor speed) in the rheometer was first stepped up through the specified range and then stepped back down.

| | | Stepping shear rate UP | | | Then stepping shear rate DOWN | | | |
|---|---|---|---|---|---|---|---|---|
| Cell volume fraction | Cell concentration | Slope 'Bingham viscosity' | Bingham yield stress | Linearised Fit $R^2$ | Slope 'Bingham viscosity' | Bingham yield stress | Linearised Fit $R^2$ | Shear rate range |
| - | ($10^6$/mL) | (mPa.s) | ($N/m^2$) | - | (mPa.s) | ($N/m^2$) | - | (1/s) |
| | | | | | | | | |
| 0.00 | 0.0 | 1.0 | - | 1.00 | 1.0 | - | 0.99 | 300 - 1200 - 300 |
| 0.007 | 1.2 | 1.1 | - | 0.99 | 1.1 | - | 0.99 | 263 - 1200 - 263 |
| 0.012 | 2.2 | 1.1 | - | 0.99 | 1.1 | - | 0.99 | 300 - 1200 - 300 |
| 0.03 | 4.7 | 1.3 | 0.14 | 1.00 | 1.4 | 0.05 | 1.00 | 113 - 1500 - 113 |
| 0.07 | 12.6 | 1.9 | 0.22 | 0.99 | 1.9 | 0.10 | 1.00 | 75 - 1000 - 75 |
| 0.09 | 15.6 | 2.1 | 0.43 | 0.98 | 2.4 | 0.19 | 0.99 | 37.5 - 750 - 37.5 |
| 0.25 | 42.4 | 9.3 | 0.35 | 0.99 | 9.0 | 0.39 | 1.00 | 7.5 - 188 - 7.5 |
| 0.34 | 58.4 | 58.7 | 0.60 | 0.93 | 67.8 | 0.23 | 0.99 | 0.75 - 30 - 0.75 |

Table 4-2b. Power law fluid parameters for rat aortic smooth muscle cell suspension in 9g/L saline solution at 25 ± 0.5 °C. Shear rate (motor speed) in the rheometer was first stepped up through the specified range and then stepped back down.

| | | Stepping shear rate UP | | | Then stepping shear rate DOWN | | | |
|---|---|---|---|---|---|---|---|---|
| Cell volume fraction | Cell concentration | Consistency index, k | Power law index, n | Linearised Fit $R^2$ | Consistency index, k | Power law index, n | Linearised Fit $R^2$ | Shear rate range |
| - | ($10^6$/mL) | (mPa.s$^n$) | - | - | (mPa.s$^n$) | - | - | (1/s) |
| | | | | | | | | |
| 0.00 | 0.0 | 1.7 | 0.92 | 0.99 | 1.3 | 0.96 | 1.00 | 300 - 1200 - 300 |
| 0.007 | 1.2 | 1.7 | 0.93 | 1.00 | 0.8 | 1.05 | 1.00 | 263 - 1200 - 263 |
| 0.012 | 2.2 | 1.0 | 1.02 | 0.99 | 2.2 | 0.91 | 1.00 | 300 - 1200 - 300 |
| 0.03 | 4.7 | 7.2 | 0.77 | 0.99 | 2.9 | 0.89 | 0.99 | 113 - 1500 - 113 |
| 0.07 | 12.6 | 12.1 | 0.74 | 1.00 | 5.4 | 0.86 | 0.99 | 75 - 1000 - 75 |
| 0.09 | 15.6 | 60.3 | 0.52 | 1.00 | 15.8 | 0.72 | 1.00 | 37.5 - 750 - 37.5 |
| 0.25 | 42.4 | 107.6 | 0.55 | 1.00 | 146.6 | 0.48 | 0.97 | 7.5 - 188 - 7.5 |
| 0.34 | 58.4 | 442.6 | 0.48 | 0.99 | 222.9 | 0.66 | 0.99 | 0.75 - 30 - 0.75 |

Table 4-2c. Bingham plastic and Power law fluid parameters for rat aortic smooth muscle cell suspension in 9g/L saline solution at 25 ± 0.5 °C. Shear rate was first stepped up through the specified range and then stepped back down; values here were calculated using the entire data set.

| Cell volume fraction | Cell concentration | Bingham plastic fluid parameters | | | Power law fluid parameters | | | Shear rate range |
|---|---|---|---|---|---|---|---|---|
| | | Slope 'Bingham viscosity' | Bingham yield stress | Linearised Fit $R^2$ | Consistency index, k | Power law index, n | Linearised Fit $R^2$ | |
| - | ($10^6$/mL) | (mPa.s) | ($N/m^2$) | - | (mPa.$s^n$) | - | - | (1/s) |
| | | | | | | | | |
| 0.00 | 0.0 | 1.0 | - | 0.99 | 1.0 | 1.03 | 0.99 | 300 - 1200 |
| 0.007 | 1.2 | 1.1 | - | 0.99 | 1.1 | 1.00 | 0.99 | 300 - 1200 |
| 0.012 | 2.2 | 1.1 | - | 0.99 | 1.5 | 0.96 | 0.99 | 300 - 1200 |
| 0.03 | 4.7 | 1.3 | 0.10 | 1.00 | 5.0 | 0.82 | 0.98 | 113 - 1500 |
| 0.07 | 12.6 | 1.9 | 0.17 | 0.99 | 10 | 0.76 | 0.98 | 75 - 1000 |
| 0.09 | 15.6 | 2.3 | 0.30 | 0.97 | 79 | 0.45 | 0.85 | 7.5 - 750 |
| 0.25 | 42.4 | 9.5 | 0.35 | 0.99 | 130 | 0.51 | 0.98 | 1.5 - 188 |
| 0.34 | 58.4 | 63.9 | 0.45 | 0.90 | 340 | 0.55 | 0.91 | 0.75 - 30 |

be considered separately. Where $\phi$ = 0.09 - 0.34, Power law fits (table 4-2b) describe 'up' and 'down' data sets more accurately overall than Bingham plastic fits (table 4-2a). The flow behaviour of the most concentrated suspension ($\phi$ = 0.34), is visualised with a shear stress vs. shear rate plot (figure 4-4). For 'up' data, Power law clearly provides the better fit; for 'down' data, although there is no statistical difference between the accuracy of the fits; overall the pattern of curvature in the data indicates that the Power law equation provides the appropriate fluid description.

The dependence of RSMC suspension apparent viscosity (extrapolated to shear rate = $200s^{-1}$ using figure 4-3) on suspended cell volume fraction is presented (figure 4-5) alongside reported correlations for plant cells [Curtis and Emery, 1993] and yeast cells [Ward, 1989; Reuss et al., 1979] (shear rates unspecified). Over the range of volume fraction examined, apparent viscosity of RSMC suspension is similar to plant cells but up to an order of magnitude higher than reports for yeast. It should be noted however that comparisons between studies are limited due to non-standardisation of measuring systems and shear rate. Both the Einstein and Vand equations (section 4.1.4.) underestimated relative viscosity by a large margin (data not shown): at the highest cell concentration ($\phi$ = 0.34), predicted values for relative viscosity were 1.9 (Einstein), 2.7 (Vand), while measured relative viscosity was 32. A correlation for yeast viscosity based on that used by Reuss et al. [1979] was adapted and provided a reasonable fit for concentrated RSMC suspension where $\phi > 0.05$ (figure 4-5):

$$\mu_r = \mu_s / \mu_o = ( 1 - ( 2.5\, \phi )^{0.2} )^{-1} \qquad \text{(eq. 4-6)}$$

Where:

$\mu_s$ = suspension viscosity

$\mu_o$ = diluent viscosity where $\phi = 0$

$\mu_r$ = relative suspension viscosity (relative to diluent viscosity)

The form of this curve fit is similar to reported correlations for yeast and plant cells, indicating that although there are some differences between the suspension properties of specific cell types, generally the behaviour of all these cell suspensions is similar. Equation (4-6) implies relative viscosity is asymptotic at $\phi$ = 0.4, suggesting complex suspension behaviour would be expected as $\phi \rightarrow 0.4$ or for $\phi > 0.4$ , possibly including a transition to 'solid-like' or 'gel-like' behaviour.

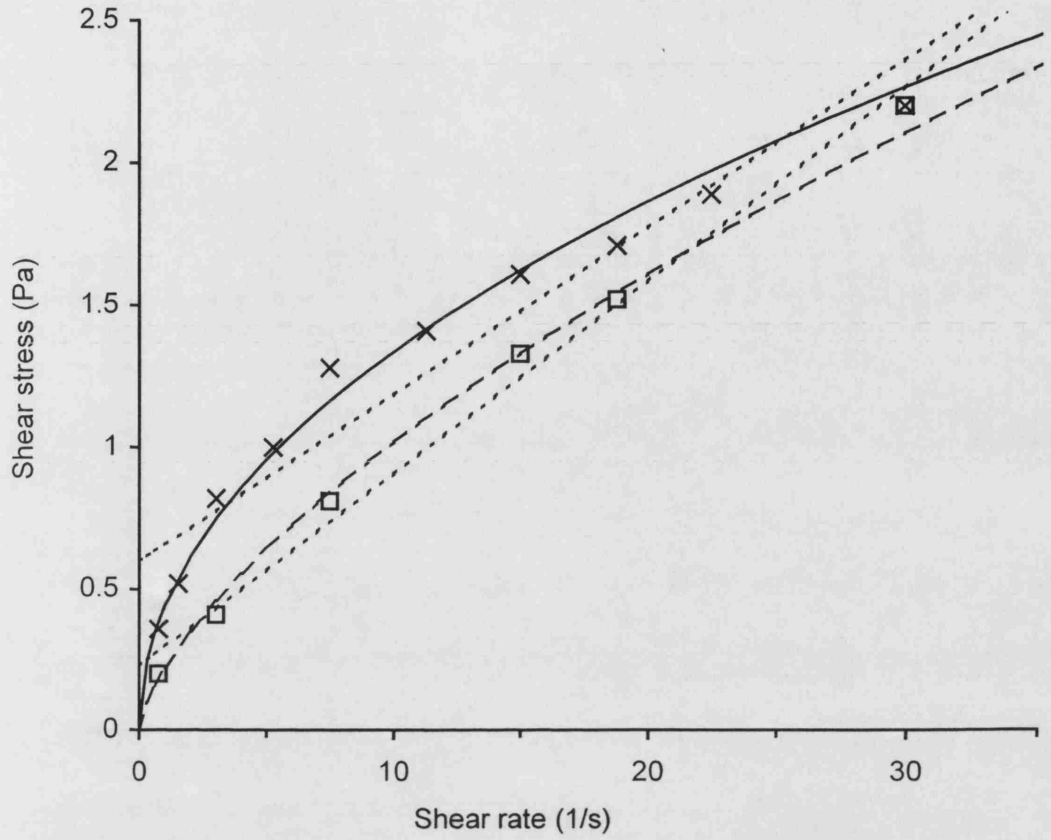


Figure 4-4. Shear stress-shear rate plot illustrating the rheological behaviour of highly concentrated rat aortic smooth muscle cell suspension (25 ± 0.5 °C).

Rheology measurements were first taken stepping shear rate up (×) and then down (□). This sample was prepared by concentration protocol (A) (section 4.3.2.); in this case no resuspending fluid was added to the cell pellet, i.e. the cell pellet was diluted only by the remaining supernatant associated with the pellet surface. Cell volume fraction, $\phi$ = 0.34, was calculated from a numerical cell count and known mean cell volume (section 4.1.2.). Power law (curve) and Bingham plastic (straight line) fits are shown. For the stepping up data (×), Power law (——, $R^2$ = 0.99) fits the data more closely than Bingham plastic (- - - , $R^2$ = 0.93), while for stepping down data (□), both the Bingham plastic (- - -) and Power law (— —) provide similar accuracy; $R^2$ = 0.99 in both cases.

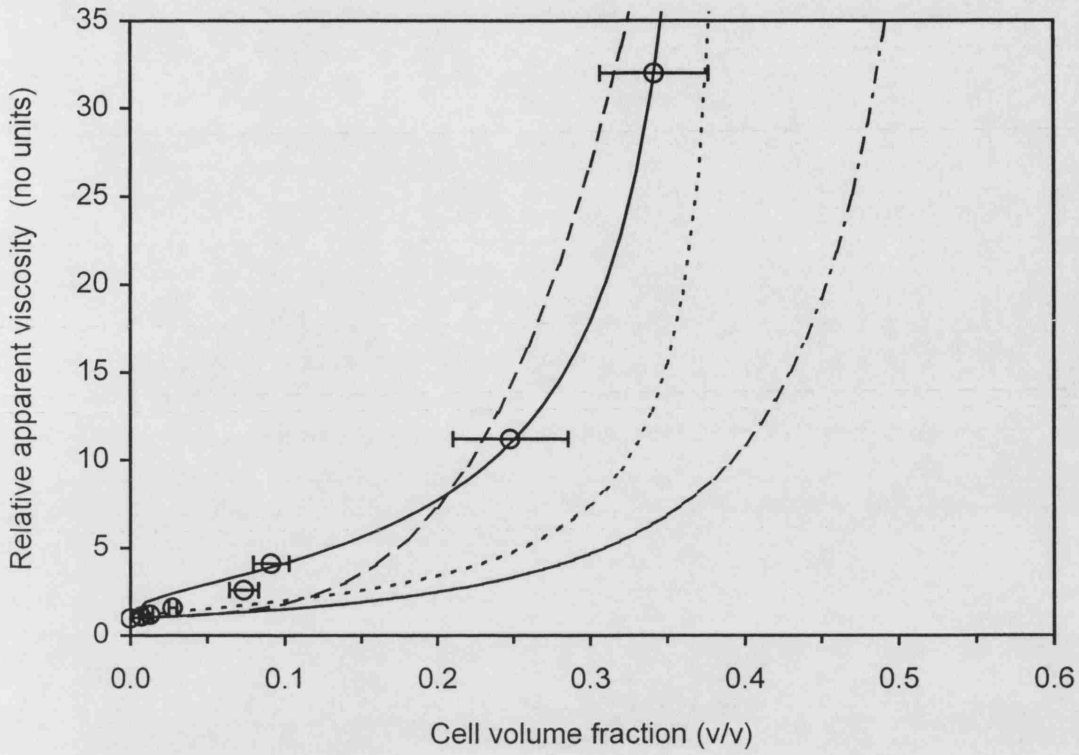


Figure 4-5. Relative apparent viscosity of concentrated rat aortic smooth muscle cell suspension (in 9g/L $NaCl/H_2O$) as a function of cell volume fraction.

Several reported correlations for other cell types are included for comparison. (O) Rat cell suspension apparent viscosity at 200 $s^{-1}$ (extrapolated where necessary via figure 4-3), (— curve fit to rat cell data, (- – -) reported correlation for yeast cell suspensions [Ward, 1989], (- - reported correlation for yeast cell suspensions at an osmotic pressure of 18.7 bar [Reuss et al., 1979], (– –) reported correlation for poppy cell suspensions [Curtis and Emery, 1993]. Horizontal error bars represent one standard deviation on quadruplicate cell counts quantifying numerical cell concentration; cell volume fraction converted from numerical cell count via known mean cell volume, section 4.1.2..

4.1.6. Visualising cell pastes

Figure 4-6 illustrates the appearance of cell concentrate of various $\phi$, providing a reference point for understanding and visualising the nature of the process material. From this we can gain a qualitative appreciation for the nature of material behaviour: (a) dilute suspension, little cell-cell interaction, viscosity similar to suspending fluid; (b) significant cell-cell interactions, approximately corresponds to the onset of non-Newtonian behaviour; (c) extensive cell-cell interactions, apparent viscosity rises substantially and significant deviations from Newtonian behaviour observed; (d) highly concentrated, vast majority of suspension appears homogeneous (1), with a few rarefactions (3), and dense areas (2) - dense areas are thought to be tightly packed cells or dense cell and secreted matrix flocs; (e) as (d) following rheological assessment (at shear rate up $30s^{-1}$) - dense areas are now absent, probably due to either aggregation (hence absence due to sampling issues) or break-up of dense areas.

4.1.7. Discussion

4.1.7.1. Cell size distribution

Having determined mean cell volume it is possible to calculate cell volume fraction from cell concentration in any suspension, or create a simple conversion chart. In addition to providing a bridge to standard equations describing suspension properties in terms of volume fraction, this conversion enables the investigator to immediately visualise the nature of the material at the microscale. A significant proportion of the total cell mass or volume is present in relatively few very large cells; achieving cell mass or volume yields of the order of 90-100% may require consideration of potential factors preferentially affecting these larger cells, such as increased sensitivity to shear stress due to their large size or hypoxia due to relatively low surface area to volume ratio.

4.1.7.2. Rheology

Aggregating suspensions are know to exhibit shear thinning behaviour even with Newtonian matrix liquids and at low shear rates they can be approximated by Power law relationships [Barthelmes, 2003]. Flocculation or aggregation of suspensions influences rheological properties; marked time-dependence, shear thinning and yield stress are due to breakdown and rearrangement of inter-particle bonds [Ward, 1989]. RSMC suspensions in this study were observed qualitatively to be aggregating

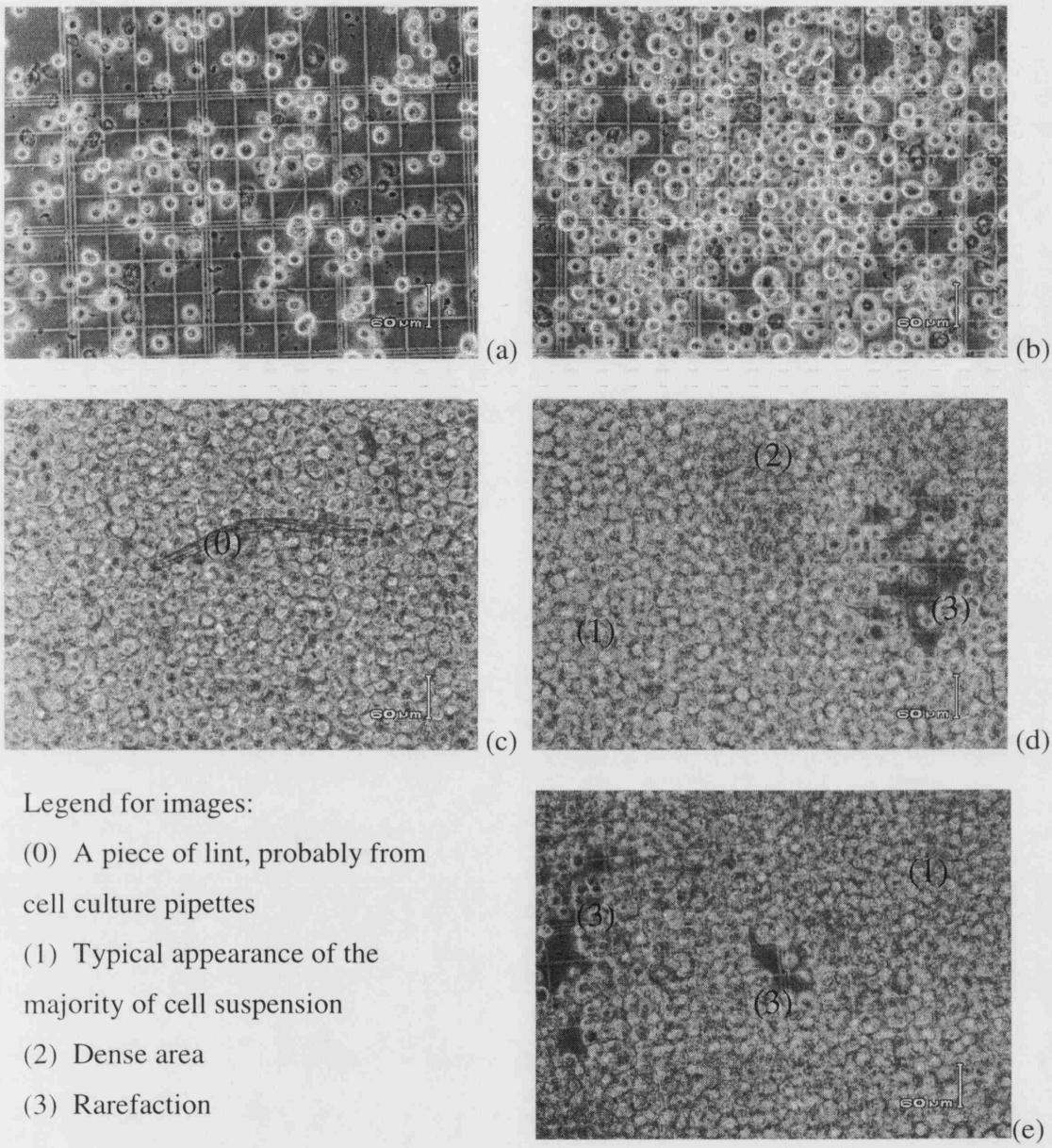


Figure 4-6. Images of concentrated rat aortic smooth muscle cell suspension.

Cells were concentrated using protocol (A) (section 4.3.2.). Unstained cell suspension was imaged on a standard haemocytometer slide using a digital camera and inverted phase contrast microscope at 100x magnification; scale bar 60μm. Cell volume fraction (ϕ), converted from (quadruplicate) numerical cell count via known mean cell volume, section 4.1.2. ϕ = (a) 0.02, (b) 0.04, (c) 0.18, (d) 0.34. (d) is undiluted cell pellet. (e) is taken from the same sample as (d) but images following rheology measurements (maximum shear rate $30s^{-1}$).

suspensions and RSMC suspension rheology can be accurately described by the Power law equation, indicating a close agreement with the expected fluid behaviour. Observed non-linear fluid properties are most likely due to cell-cell interactions, which could be mediated by cell surface fibrils, charge, proteins or flocculation-type processes involving extracellular matrix deposits carried over from cell culture. Such interactions are shown to be reduced when shear is applied (in the rheometer), resulting in both shear thinning behaviour and time-dependent or irreversible changes in suspension behaviour. Further investigation might yield information regarding the strength of cell-cell interactions and the potential for cell damage during breakdown of such bonds.

The degree of homogeneity achieved in concentrated cell suspensions is an issue as it may directly affect the homogeneity of formed tissue, either simply due to seeding of aggregates or due to the impact of heterogeneous suspension rheology on the dynamics of a tissue forming or seeding process. Recently, models have been developed predicting aggregate size distribution and rheological behaviour of concentrated suspensions due to shear-induced coagulation and fragmentation [Barthelmes, 2003; Usui, 2001]. Thus there exists the possibility of describing concentrated suspensions of adherent mammalian cells using a related approach. Such analysis could potentially provide important design information regarding the shear profile and timescales required to generate the desired aggregate size distribution (degree of homogeneity) in a concentrated cell suspension, and ensure undesirable changes in the suspension (e.g. aggregation) do not occur during process timescales.

Overall, the similarity of RSMC suspension rheology to the other cell concentrates considered suggests that useful parallels may be drawn with the body of established literature on various cell concentrates. Work with yeast suspensions [Ward, 1989] illustrates the possibility of encountering shear thickening properties of concentrated ($\phi > 0.3$) adherent cell suspensions at higher shear rates ($> 50s^{-1}$). This is of particular interest as the shear/concentration range associated with shear thickening has not been investigated with respect to either rheology or shear-induced cell damage; this fluid flow regime may be highly relevant to certain process operations e.g. high flowrate pumping, tissue formation or porous scaffold seeding at very high cell concentrations.

## 4.2. Biochemical effects

In addition to the mechanical effects of concentration processes on cells and the structure and handling properties of cell suspension, consideration must also be given to any biochemical constraints associated with very high cell concentrations. The worst conditions are expected to occur within cell pellets; availability of nutrient species and the dilution of metabolites may become severely limited as the volume of cells approaches the volume of intercellular medium.

### 4.2.1. Biochemical activity and requirements

Cells may exist within a variety of metabolic states, each having specific nutrient and energetic requirements: rest or repair, growth or proliferation, secretion of extracellular matrix or other molecules, and other specific functions such as muscular contraction. Within hybridoma cell cultures, depletion of serum, glucose, glutamine and oxygen are known to cause very high levels of apoptosis within the cell population [Singh et al., 1997]. Due to the low solubility of oxygen in culture media and other fluids, and associated poor mass transfer kinetics, oxygen is generally considered to be a key limiting substrate which requires continuous supply to avoid rapid depletion within cell cultures or tissue constructs [Foy et al., 1994; Peng and Palsson, 1996; Tilles et al., 2001]. The effects of low-oxygen culture on vascular smooth muscle include rapidly decreased contractile force and a shift from oxidative to glycolytic metabolism with build-up of large glycogen stores; chronic hypoxia *in vivo* has been implicated in the development of atherosclerosis [Lindqvist et al., 2002].

### 4.2.2. Oxygen Consumption

In this study oxygen solubility in the suspending fluid was assumed to be as for air-saturated water at 37°C ($7.3 g/m^3$, [Doran, 1995]), as an approximation for the resuspending fluid (9g/L $NaCl/H_2O$) used in concentration protocols (A) and (B) (section 4.3.2., table 4-4); this value for water is slightly higher than that reported for aqueous cell culture media ($6.72 g/m^3$, [Peng and Palsson, 1996]). There is a large range in reported values of oxygen uptake rate (OUR) for various mammalian cell types and culture conditions (table 4-3b). Reports cover a wide variety of measurement techniques, cell types and culture geometries (e.g. suspended cells, 2D sheet, 3D tissue construct); different cell types may have different oxygen requirements depending on additional factors including cell size, number of mitochondria present, growth rate, cell

Table 4-3a. Values of oxygen uptake rate (OUR) used in oxygen depletion calculations (figure 4-7.). Three 'OUR Scenarios' are considered to cover the approximate order of magnitude range of OUR reported in the literature. These data were adapted from reported literature values (table 4-3b.) observed with various mammalian cell types and culture conditions.

| OUR Scenario | Approx. OUR $10^{-6}$g/($10^6$ cell . h) | Cell Type | Reference |
|---|---|---|---|
| | | | |
| Low | 1 | Adherent human bone marrow mononuclear cells | [Peng and Palsson, 1996] |
| Moderate | 5 | Suspended mouse aortic endothelial | [Pandian et al., 2003] |
| High | 50 | Primary rat hepatocytes | [Foy et al., 1994] |

Table 4-3b. Reported literature values for oxygen uptake rate (OUR) of mammalian cell lines or primary cells. Units have been standardised to enable comparison. (Low/Moderate/High) refer to OUR scenarios presented in table 4-3a and figure 4-7.

| Cell type and conditions | Approx. OUR $10^{-6}$g/($10^6$ cell.h) | Reference |
|---|---|---|
| | | |
| Full range of all those below | 0.16 - 170 | - |
| Adherent human bone marrow mononuclear cells | 0.16 - 1.2 (Low) | [Peng and Palsson, 1996] |
| Full range of OUR reported for endothelial cells | 0.25 - 170 | [Pandian et al, 2003] |
| Porcine thoracic aorta endothelial cells | 1.92 | [Pandian et al, 2003] |
| Rat pulmonary artery endothelial cells | 2.78 | [Pandian et al, 2003] |
| Suspended mouse aortic endothelial cells | 5.9 (Moderate) | [Pandian et al, 2003] |
| Primary rat hepatocytes cultured on a 50 μm thick collagen gel sheet | 17 – 50 (High) | [Foy et al, 1994] |
| Primary rat hepatocytes on a collagen gel sheet | 46.1 | [Rotem et al, 1994] |
| Rat and porcine hepatocytes in 3D culture (within a gel) | 5.5 – 9.6 | [Patzer, 2004] |
| Microcarrier-attached porcine hepatocytes | 3.8 – 6.6 | [Patzer, 2004] |
| CHO cells, 2L stirred tank batch culture | 6.5 - 9.1 | [Ducommun et al, 2000] |
| Murine hybridoma cells | 14.1 | [Ozturk & Palsson, 1991] |
| Murine hybridoma cells | 6.4 – 14.4 | [Xui et al, 1999] |

function and metabolic state. Data were adapted to represent the range of literature reported values (table 4-3b) with three cases: low, moderate and high OUR (table 4-3a). The oxygen uptake rate and kinetics of the rat aortic smooth muscle cells (RSMC) used in this study are unknown, although it has been reported that smooth muscle cells typically exhibit higher OUR than endothelial cells [Pandian et al., 2003].

Predicted time taken for total oxygen depletion in the three cases is presented as a function of cell volume fraction in cell suspension, (figure 4-7). During cell concentration performed by protocol (B) (table 4-4), the average calculated cell volume fraction in the (wet) cell pellet was ~0.3-0.4 and the minimum time taken to perform cell concentration was 7 minutes. We can see from figure 4-7 that for a cell volume fraction of ~0.3, the low, moderate and high OUR cases correspond to a predicted oxygen depletion time of approximately 5.5, 1.0 and 0.1 minutes respectively. In the case of low OUR, the timescale of oxygen depletion (5.5 min) is similar to the timescale of the process operation (7 min), whereas for the moderate and high OUR cases, the cell pellet is predicted to be completely anoxic for the majority of the processing time. It is conceivable that at high centrifugation force, the volume fraction in a cell pellet could reach 0.5 or higher (regular close packing arrangements of uniform spheres, $\phi = 0.524 - 0.74$ (cuboidal – rhombohedral) [Coulson and Richardson, 1991]); in this case even with low OUR, hypoxia in the cell pellet is predicted to occur after ~1-2 minutes. Considering a resuspended pellet (i.e. cell suspension for tissue seeding or formation) at a moderate cell concentration of $1.7 \times 10^7$ cells/mL (cell volume fraction, $\phi = 0.1$), oxygen depletion for the low, moderate or high OUR cases is predicted to occur in around 20, 4 or 0.4 minutes respectively.

### 4.2.3. Implications for process design

According to the predictions made, total oxygen depletion is likely to occur in the cell pellet during the cell concentration process and may persist during subsequent processing steps, being cell suspension transfer and tissue seeding/formation. Qualitatively, the design indication is then to mitigate oxygen depletion, for example by ensuring supply of oxygen during cell concentration and transfer (e.g. use centrifuge tubes and transfer tubing/pipettes with high gas permeability), cooling cell suspension (i.e. reduce metabolic activity, increase gas solubility), or reduce processing time (e.g. increase centrifuge speed, apply high speed process automation). In order to establish the design heuristics quantitatively, it would be necessary to determine the oxygen

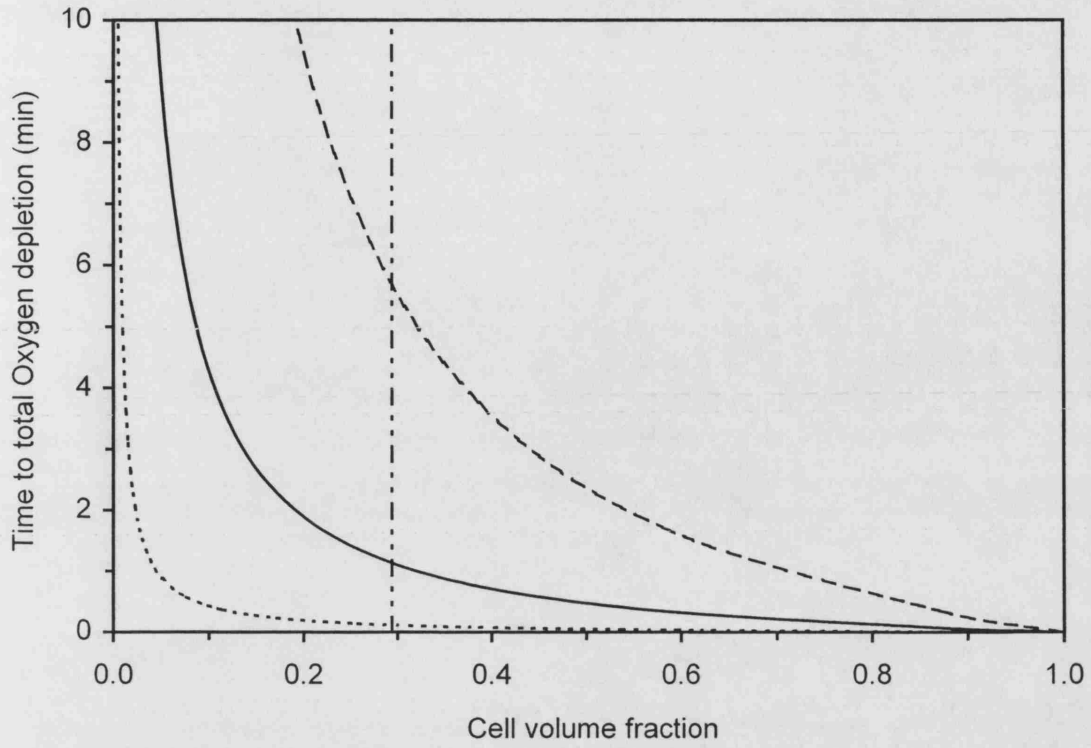


Figure 4-7. Estimated time taken for oxygen depletion in concentrated rat aortic smooth muscle cell suspension.

Key assumptions used in the analysis: No mass transfer to or from the system; mass transfe within the system is not limiting (i.e. the suspension is well-mixed); initial dissolved oxygen content is equal to the saturated oxygen content of water at 37°C, 7.3 g/m$^3$ [Doran, 1995]. Conversion from numerical cell concentration to cell volume fraction was calculated using the volume mean cell volume for rat aortic smooth muscle cells (section 4.1.2.). Three constant values are considered for oxygen uptake rate (OUR) of cells (table 4-3a), being representative of the range of OUR reported in the literature for mammalian cells (table 4-3b); values are quoted here as [x], with units of x10$^{-6}$g/(10$^6$ cell.h). (---) High OUR [50], (—) moderate OUR [5], (– –) low OUR [1]. (– - - –) Mean cell volume fraction of rat aortic smooth muscle cells observed in centrifuge pellets (concentration protocol (B), section 4.4.5., based on number of cells recovered). This cell volume fraction, $\phi \sim 0.3$, represents the approximate maximal cell volume fraction which could be achieved using the semi-automated cell concentration protocol developed in this work.

uptake rate and kinetics of the cell type in question and the effect of temperature thereon, and analyse the impact of transient hypoxia and/or cooling on cell health, metabolism and function. Further analyses could investigate the mass transfer properties of apparatus and predict oxygen penetration into cell pellets and/or concentrates under a diffusion-reaction regime.

4.2.4. Discussion – oxygen depletion

Substantial decline in cell viability following seeding and culture of a hypoxia-sensitive cell type (cardiac myocytes) at high density ($0.5\text{-}1x10^8$ cell/mL) has been previously reported and attributed to hypoxia [Radisic et al., 2003]. Typically effects of hypoxia in hybridoma cell cultures normally manifest after about 10h [Mercille and Massie, 1994]. Transient hypoxia is thus not expected to cause rapid loss of cell membrane integrity and so is unlikely to be responsible for apparent loss of cells during cell concentration in this study. The predictions for oxygen depletion time indicate that hypoxia during cell concentration and concentrate processing is potentially a serious concern (section 4.2.2.), even at cell suspension densities as low as $\phi = 0.05$ ($\sim 1x10^7$ cell/mL). Another consideration is that abnormally high levels of oxygen can be toxic [Peng and Palsson, 1996]. If it is necessary to control oxygen concentration within a relatively narrow range to avoid deleterious effects, there may be significant further process development challenges to address. In addition the dependence of OUR on cell concentration should be investigated as 'cell crowding' effects (section 1.4.3.) could lead to a reduced OUR at high cell concentrations.

## 4.3. Cell concentration process development

Alternatives for cell concentration include filtration and centrifugation techniques; although the method employed is rarely reported in literature studies, centrifugation and pellet resuspension is likely to be the method of choice due to the ease of use, availability of centrifuges within research laboratories and the high concentration factors and small final volumes which can be achieved with cell pellets. Principal performance parameters for a cell concentration process in the context of tissue engineering are recovery and health of intact cells, achievable concentration factor and process robustness (i.e. variability). The aim of this study was to develop and examine the performance of two semi-automated cell concentration (centrifuge and resuspend) protocols, with a view to demonstrating the feasibility of fully automated cell

concentration by centrifuge-resuspend and elucidating process development issues arising for this unit operation.

4.3.1. Predicted cell sedimentation time

Centrifugation parameters used for protocols (M, manual) and (A), (100g, 7min) had been established previously. In order to establish a theoretical design basis for the development of new centrifugation conditions, the time taken to sediment all cells (minimum cell size 12.5μm, figure 4-2) in a typical centrifuge run (40mL cell suspension) was calculated based on Stokes' law (section 2.3.1.). The results (figure 4-10) indicate that the initial conditions (100g, 7min) were expected to sediment all cells with a safety margin of 2.2 minutes (~45%). Around half of this safety margin would be taken up if feed volumes were increased up to the centrifuge tube maximum capacity of 50mL.

For further centrifugation conditions considered at higher sedimentation force (section 4.3.2.), centrifugation time was specified to be a minimum of +25% relative to the predicted sedimentation time for 40mL of cell suspension. As the minimum run time input resolution for the centrifuge used was one minute, centrifugation times used were well in excess of the predicted sedimentation time required in all cases. The centrifuge parameters chosen for protocol (B) (300g, 3min) correspond to a safety margin of 83% over the predicted sedimentation time for 40mL of cell suspension, or 58% over the predicted time for 50mL of cell suspension.

4.3.2. Concentration protocol development

A process flow diagram for the two developed protocols (A) and (B) is given in figure 4-8, aspirate/dispense procedures are shown schematically in figure 4-9 and process parameters are listed in table 4-4.

Protocol (A): The principal logic in the development of protocol (A) was to move from a manual pipette-based resuspension to a procedure more amenable to automation. Vortex mixing was chosen as automation of orbital shaking would be straightforward and a vortex mixer was immediately available in the laboratory. Key developments implemented in protocol (A) were:

(1) A protocol for minimising any disturbance of the cell pellet during supernatant aspiration (figure 4-9); the bulk of the supernatant was aspirated rapidly by pipette with the pipette tip near the surface of the supernatant. The centrifuge tube was then angled

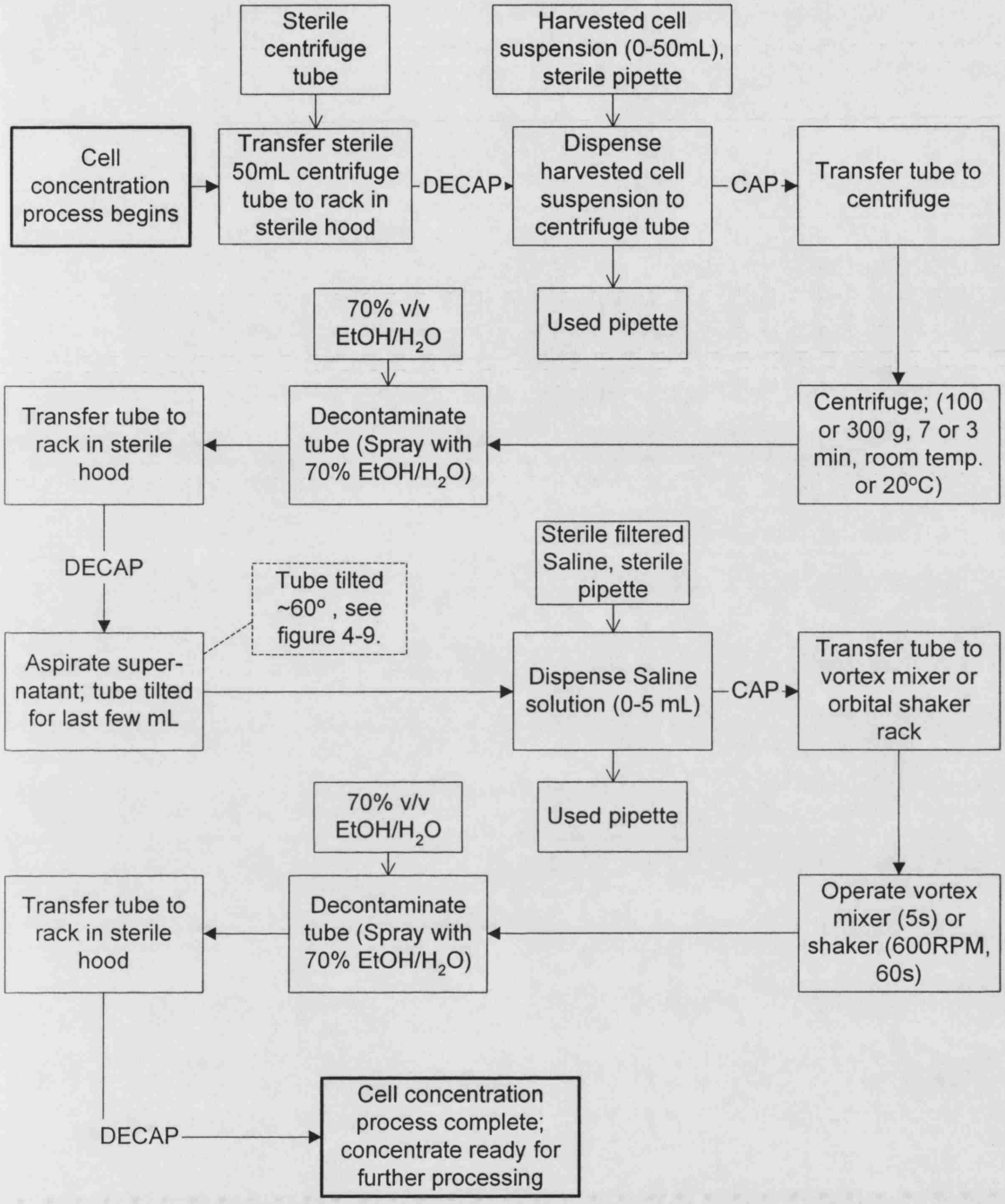


Figure 4-8. Process flow diagram for cell concentration protocols A and B. Process parameters for the two protocols are denoted (A or B) here and given in full in table 4-4. (→) denotes materials or equipment which must be transferred to/from the process. Processing systems/modules required: Tube transfer, sterile laminar flow hood with tilting tube rack, capping/decapping, liquid supply, liquid handling (pipetting), pipette supply, pipette disposal, centrifuge load/unload, refrigerated centrifuge, 70% Ethanol spray, supernatant waste disposal, orbital shaker.

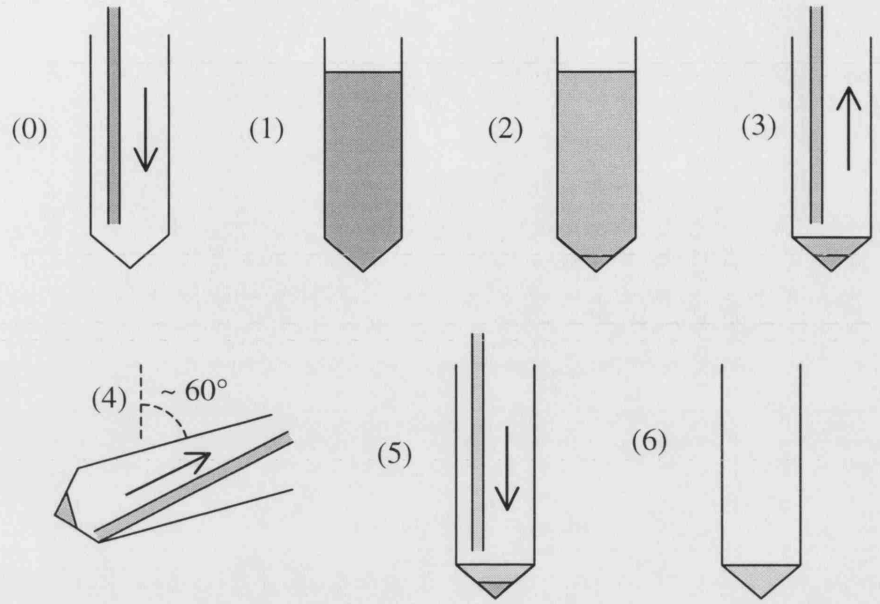


Figure 4-9. Schematic diagram of the semi-automated cell concentration process.

This schematic describes both protocols (A) and (B); process parameters are given in table 4-4. (0-1) Dispense harvested cell suspension to centrifuge tube. (1-2) Centrifuge (swing bucket centrifuge). (2-3) Keeping the pipette tip just below the supernatant surface, rapidly aspirate the supernatant, leaving the last ~5mL. (3-4) Gently angle the centrifuge tube ~60° to the vertical and slowly aspirate remaining supernatant from the side 'corner' of the tube, to prevent disturbing the cell pellet. (4-5) Right the centrifuge tube and dispense resuspension buffer, 9g/L $NaCl/H_2O$, onto the cell pellet. (5-6) Orbital shaking to resuspend cells. (6) Resuspended cell concentrate.

Table 4-4. Process parameters for cell concentration protocols.

All protocols employed standard 50mL Polypropylene centrifuge tubes and a swing-bucket centrifuge. Initial manual protocol parameters were not well characterised or monitored; this protocol is included for comparison only.

| Protocol Code | - | M (manual) | A | B |
|---|---|---|---|---|
| Feed volume | (mL) | ≤ 50 | 12 - 50 | 40 ± 2 |
| Centrifuge force | (g) | 100 | 100 | 300 |
| Centrifuge time | (min) | 7 | 7 | 3 |
| Centrifuge temperature | (°C) | 25 ± 4 | 25 ± 4 | 20 |
| Resuspend device | - | Manual or electric pipette | Vortex mixer | Orbital shaker |
| Orbital throw | (mm) | n/a | 7 | 4.5 |
| Added volume of resuspension fluid | (mL) | not recorded | 0.5 - 5 | 2.4 ± 0.1 |
| Resuspend speed | (RPM) | n/a | estimate ~1000 | 600 |
| Resuspend time | (s) | ~ 30 - 120 | 5 | 60 |

such that the supernatant would naturally drain away from the pellet as the last ~5mL were aspirated very slowly, minimising fluid flow and shear forces at the pellet surface.
(2) The resuspension solution used was always sterile filtered 9g/L $NaCl/H_2O$.
(3) Following addition of resuspension solution, pellet resuspension was carried out by manually applying the centrifuge tube to a vortex mixer for 5 seconds; the vortex mixer was always set to the same power setting.

Protocol (B): The principal logic in the development of protocol (B) was to: (a) minimise variability in the process by controlling as many process parameters as possible as tightly as possible - as the intensity of vortex mixing was observed to be variable depending on the pressure applied manually with the centrifuge tube, it was decided to move to a 'hands free' orbital shaker; (b) reduce the overall process time in order to minimise potential oxygen depletion issues in the cell pellet; (c) increase the intensity of cell sedimentation to 'harden' the cell pellet, thus potentially improving cell recovery - during execution of protocol (A) the surface layer of the cell pellet was observed to be quite soft and tended to be drawn away with the last fraction of the supernatant; (d) reduce the intensity of resuspension (relative to vortex mixing) to reduce shear forces and hence cell injury.

In order to simultaneously achieve points (b), (c) and (d), preliminary studies were performed to evaluate qualitatively various combinations of centrifuge and resuspend conditions. Additional centrifugation conditions used were selected based on predictions for cell sedimentation time (section 4.3.1., figure 4-10) and considering point (c) above. The orbital shaker used (4.5mm throw) was selected as it offered a wide range of resuspension speeds (0-1200 RPM) and was observed to generate an orbital (as opposed to chaotic) flow pattern with ~5 mL fluid in a 50mL centrifuge tube.

The preliminary study examining various centrifugation conditions (table 4-5a) showed that resuspension intensities of 100 and 300 RPM were insufficient to resuspend any cell pellets in a reasonable time. At 500 RPM all cell pellets were resuspended, with resuspension time required tending to increase with sedimentation force. Centrifugation conditions selected for protocol (B) (300g, 3min) were selected as providing a significant reduction in centrifugation time (compared to 100g, 7min), observations of a sufficiently 'hard' cell pellet, and rapid resuspension at a relatively low resuspension intensity. The preliminary study examining various resuspension conditions (table 4-5b) applied these new centrifugation conditions and qualitatively examined the time-course of pellet resuspension under a variety of resuspension intensities. Resuspension speeds

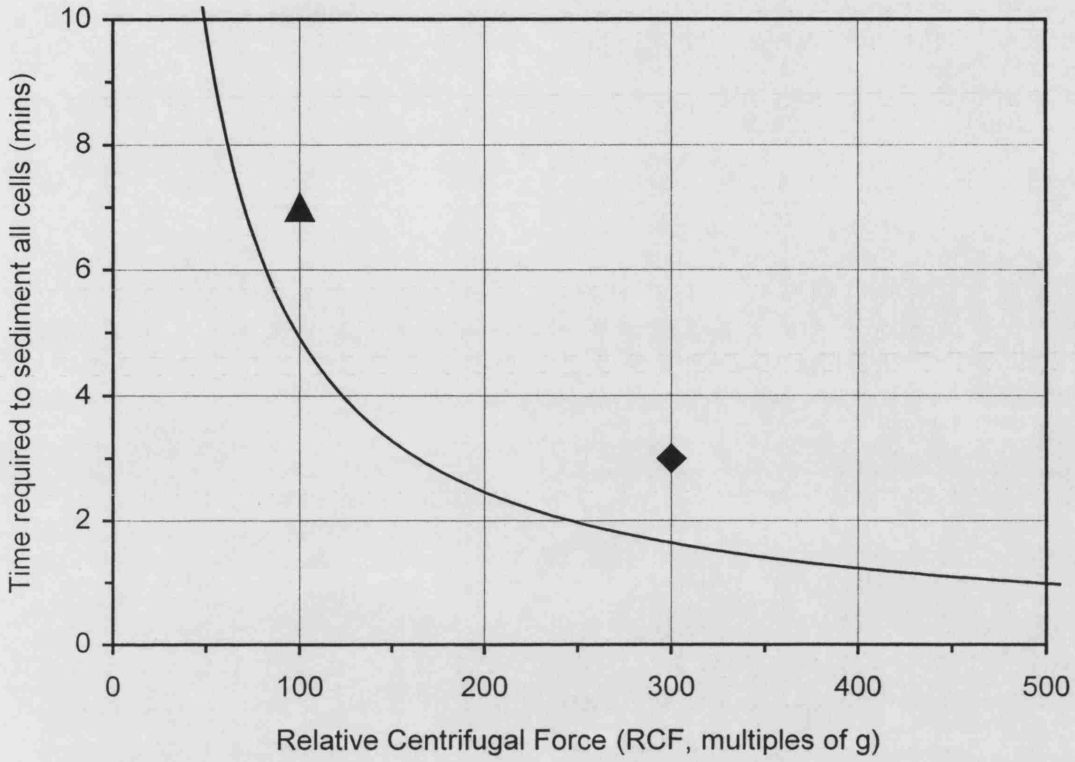


Figure 4-10. Predicted time taken to sediment all rat aortic smooth muscle cells during centrifugation (—).

Sedimentation time was calculated using Stokes' Law (section 2.3.1.) considering a cell diameter of 12.5 μm (only 1 of 483 measured cell diameters was <12.5μm, figure 4-2.) falling through 40mL of supernatant (equivalent to harvested cell suspension from one T500 flask, section 4.1.1.) in a standard 50mL centrifuge tube. The viscosity (1.25 mPa.s, section 2.2.5.) and density (1008 $kg/m^3$, section 2.3.1.) of cell culture supernatant had been measured previously and the density of cells was assumed to be 1050 $kg/m^3$ (section 2.3.1.). Symbols indicate the parameters used for semi-automated cell concentration protocols (A) (▲, 100g, 7min) and (B) (◆, 300g, 3min).

Table 4-5a. Centrifugation preliminary method development.

Rat aortic smooth muscle cells were harvested from T500 flasks, aliquoted into 50mL centrifuge tubes (50mL harvested cell suspension per tube) and centrifuged (swing bucket centrifuge). The supernatant was aspirated, being careful not to disturb cell pellets (figure 4-9) and cell pellets were subsequently resuspended by orbital shaking (4.5 mm orbital throw) with 0.5 mL of supernatant. Shaking was briefly interrupted after 30, 60, 120, 240 and 360 seconds, to allow visual inspection of pellets and estimation of remaining pellet fraction. Where pellets were not easily resuspended (i.e. no further progression of resuspension observed), resuspend time is denoted 'incomplete resuspension' (IR) and figures in square brackets [X, Y] represent (X) the longest resuspend time investigated for that sample (in seconds); (Y) the approximate fraction of cell pellet remaining at that time (by eye). (-) this combination of conditions was not investigated. Centrifugation parameters of 300g, 3min were chosen for the final protocol (protocol (B), table 4-4) due to a good balance of centrifugation time and ease of pellet resuspension.

| Resuspend speed (RPM) ↓ | Centrifuge sedimentation force (g), centrifuge time (minutes) | | | |
|---|---|---|---|---|
| | 100, 7 | 300, 3 | 500, 2 | 1000, 2 |
| | Time taken to resuspend centrifuge pellet (s) | | | |
| 100 | IR [120, 1.0] | - | - | - |
| 300 | IR [360, 0.2] | IR [360, 0.3] | IR [240, 0.5] | IR [240, 0.8] |
| 500 | 60 | 30 | 120 | 240 |

Table 4-5b. Cell pellet resuspension preliminary method development.

Rat aortic smooth muscle cells were harvested from T500 flasks, aliquoted into 50mL centrifuge tubes (50mL harvested cell suspension per tube) and centrifuged (swing bucket centrifuge) at 300g for 3 minutes. The supernatant was aspirated, being careful not to disturb cell pellets (figure 4-9) and cell pellets were subsequently resuspended by orbital shaking (4.5 mm orbital throw) with 0.5 mL of supernatant. Shaking was interrupted and pellets examined after 7.5, 15, 30, 60, 120 seconds. The fraction of cell pellet remaining (not resuspended) was estimated by eye. (-) this combination of conditions was not investigated. Resuspension parameters of 600 RPM, 60 seconds were chosen for the final protocol (protocol (B), table 4-4) due to a good balance of resuspension intensity and time.

| Resuspend Speed (RPM) ↓ | Resuspension time (s) | | | | |
|---|---|---|---|---|---|
| | 7.5 | 15 | 30 | 60 | 120 |
| | Approx. fraction of cell pellet remaining | | | | |
| 400 | - | 0.6 | 0.3 | 0.1 | 0 |
| 600 | - | 0.5 | 0.2 | 0 | 0 |
| 800 | 0.2 | 0.1 | 0 | 0 | 0 |

selected for investigation (400, 600, 800 RPM) were above the highest speed not enabling pellet resuspension (300RPM) and the below the speed corresponding to observed intensity of vortex mixing in protocol (A) (~1000RPM). All resuspension speeds provided total pellet resuspension within 2 minutes. Resuspension speed selected for protocol (B) (600RPM) was selected as providing a good balance between intensity (shear forces on cells) and time required (oxygen depletion concerns); the corresponding minimum observed resuspension time (60s) was specified for protocol (B).

Key modifications to protocol (A) implemented in protocol (B) were:

(1) Feed volume of harvested cell suspension was set at one T500 flask per 50mL centrifuge tube. In practice the feed volume was measured to be in the range $40 \pm 2$mL.

(2) The (refrigerated) centrifuge was pre-cooled to 20°C; 20°C was chosen as the maximum temperature which could be reliably set due to fluctuations in ambient temperature.

(3) Sedimentation parameters were set at 300g (300RCF) and 3minutes.

(4) Target volume of resuspended cell concentrate was 2.5mL; in practice the volume of resuspension solution (sterile filtered 9g/L $NaCl/H_2O$) was in the range $2.4 \pm 0.1$ mL.

(5) Following addition of resuspension solution, pellet resuspension was carried out by placing the centrifuge tube within a rack attached to an orbital shaker; the orbital shaker was always set to 600RPM and resuspension carried out for 60s.

### 4.3.3. Discussion – cell concentration protocol development

The predictions for cell sedimentation time formed a theoretical design basis which enabled selection of centrifugation conditions (i.e. combinations of force and time) without recourse to experimentation. All centrifugation conditions employed were expected to achieve total cell sedimentation with a large safety margin ($\geq 20\%$). Key steps for improving the theoretical analysis and optimising cell sedimentation would include measuring the density of the cells (e.g. quantitative density gradient centrifugation), incorporating centrifuge acceleration/deceleration time in calculations, performing experimental studies to correlate predicted with actual system behaviour, and employing a centrifuge in which run time may be programmed in seconds rather than minutes.

Both semi-automated protocols (A) and (B) demonstrated simple, effective laboratory procedures for cell concentration which did not require operator feedback control inputs in-process. Variability in input parameters was largely eliminated for protocol (B). Principal aspects of the process not tightly controlled in protocol (B) were: (a) times required for intermediate manual operations (e.g. centrifuge transfer, supernatant aspiration); (b) ambient and fluid temperatures; (c) cell density in T-flasks at harvest, i.e. cell concentration and possibly composition (i.e. extracellular matrix) of feed suspension. It is expected that variability in process times and temperatures could be reduced or eliminated during implementation of an automated system for cell concentration, and automation of upstream cell culture processes could reduce feed suspension variability [Archer and Wood, 1992]. However, inherent variability in biological cultures, especially autologous cells, is expected to remain. In addition there may be some degree of inherent process variability (e.g. cell aggregation) which is difficult to eliminate. It is important to quantify the nature, scale and impact of such variability on concentration process performance, develop strategies for process improvements where possible and otherwise establish the bounds of process robustness.

### 4.4. Cell concentration process performance

Principal performance parameters for a cell concentration process in the context of tissue engineering are the recovery and the health of the cells, the achievable concentration factor and the process robustness (i.e. variability). In this section data gathered for the two protocols (A) and (B) are compared and possible causes of cell loss, damage and process variability are discussed with a view to developing strategies for process improvement.

#### 4.4.1. Yield and integrity of cells

The performance of the two semi-automated protocols developed was evaluated using trypan blue counts before and after cell concentration; '% integrity' of cells prior to concentration was $\geq 98\%$ in all cases. A comparison of averaged data ($n = 15$ for each protocol) is presented in figure 4-11. Protocol (B) exhibits significant improvements in 'total cell yield', 'intact cell yield' and '% integrity of recovered cells' but not 'cell volume fraction in wet pellet'. For protocol (B) '% integrity of recovered cells' approaches 100% ($93 \pm 3\%$), although the apparent 'total cell yield' is low at $80 \pm 13\%$,

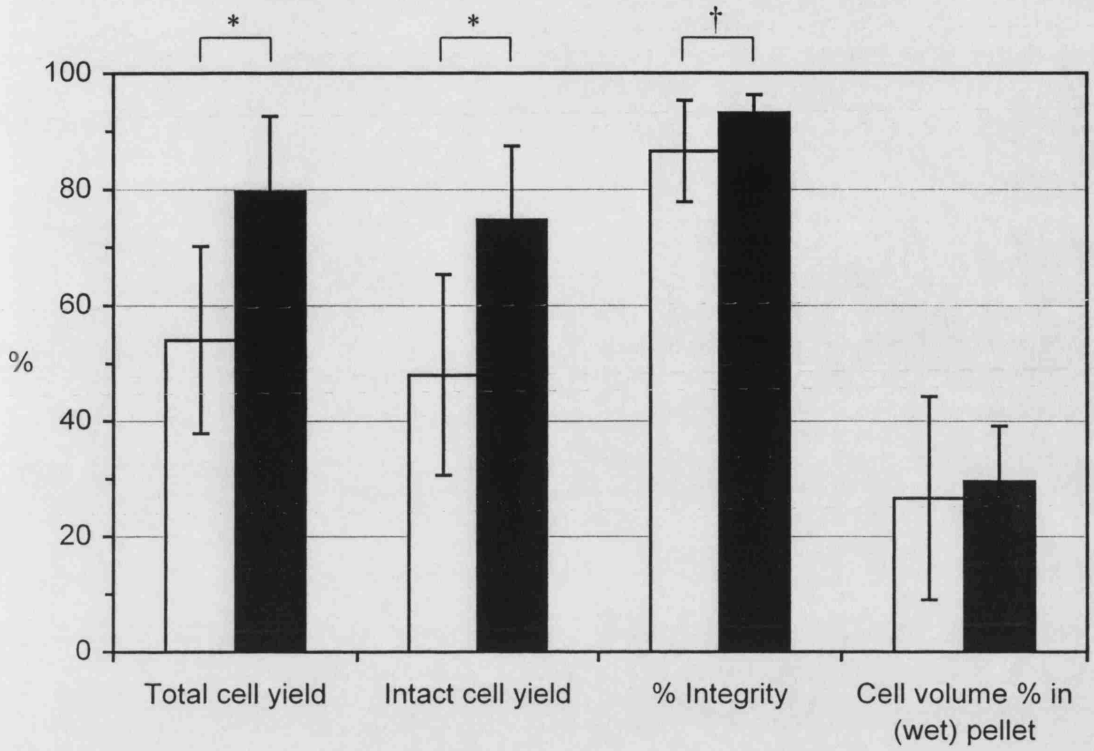


Figure 4-11. Performance comparison between two semi-automated cell concentration protocols.

Rat aortic smooth muscle cell suspension harvested from T500 flasks was concentrated by either protocol (A) or (B) (table 4-4). 'Total cell yield' is the total number of cells recovered, whereas 'intact cell yield' is the number of cells recovered intact, both expressed as percentage of cells initially dispensed to each centrifuge tube (quadruplicate trypan blue haemocytometer counts). '% Integrity' is the proportion of recovered cells which are intact, i.e. (intact cell yield) / (total cell yield). 'Cell volume % in (wet) pellet' is the volume fraction of cells in the cell pellet including residual supernatant, as converted from a haemocytometer cell count (on recovered cell concentrate) via mean cell volume (section 4.1.2.). (□) Protocol (A), n = 15 ; (■) protocol (B), n = 15. Error bars are 1 standard deviation on 'n' repeat experiments. [*] Significant difference (student's unpaired t-test) was found at the 99% level ($P < 0.01$). [†] Significant difference was found at the 95% level but not at the 99% level ($0.01 < P < 0.05$).

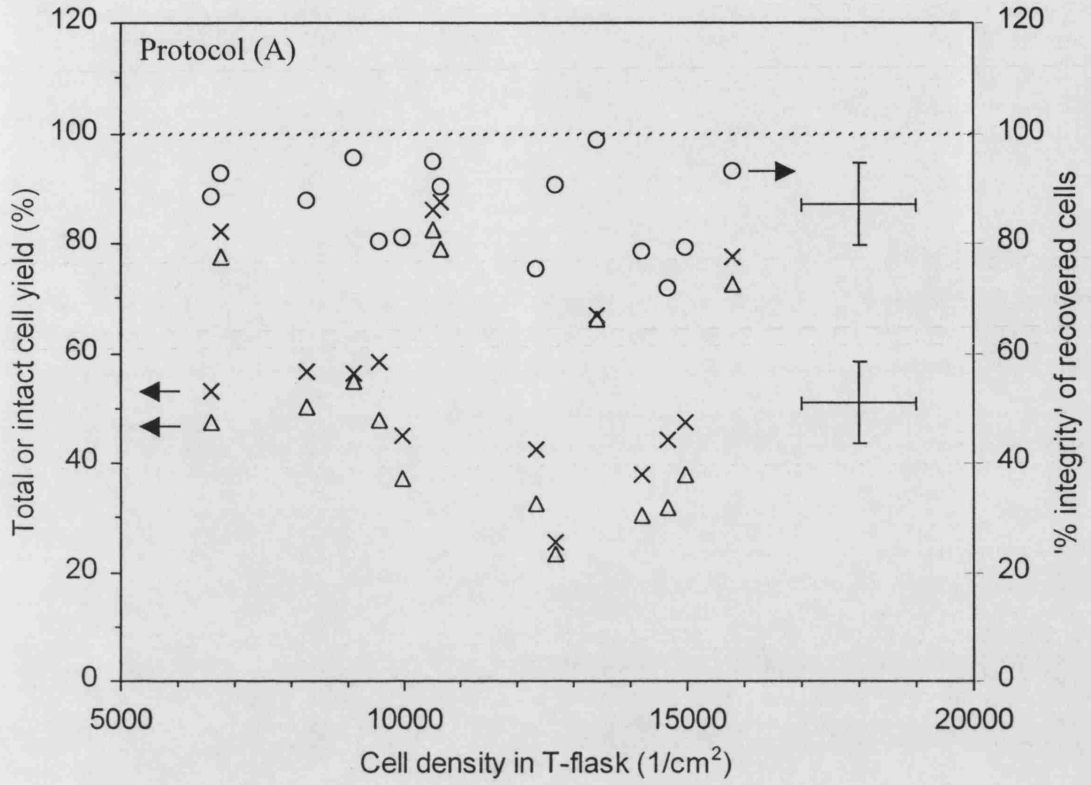


Figure 4-12a. Yield and membrane integrity of cells following concentration, as a function of cell density at harvest.

Rat aortic smooth muscle cell suspension harvested from T500 flasks was concentrated by protocol (A) (table 4-4), n = 15. 'Total cell yield' (×) is the total number of cells recovered, whereas 'intact cell yield' (△) is the number of cells recovered intact; both are expressed as percentage of cells initially dispensed to each centrifuge tube (quadruplicate trypan blue haemocytometer counts). '% Integrity of recovered cells' (○) is the proportion of recovered cells which are intact, i.e. ('intact cell yield') / ('total cell yield'). (- - -) 100% marker indicates desired (maximal) output for all quantities. Error bars shown are not data points, but represent approximate estimated error for all data.

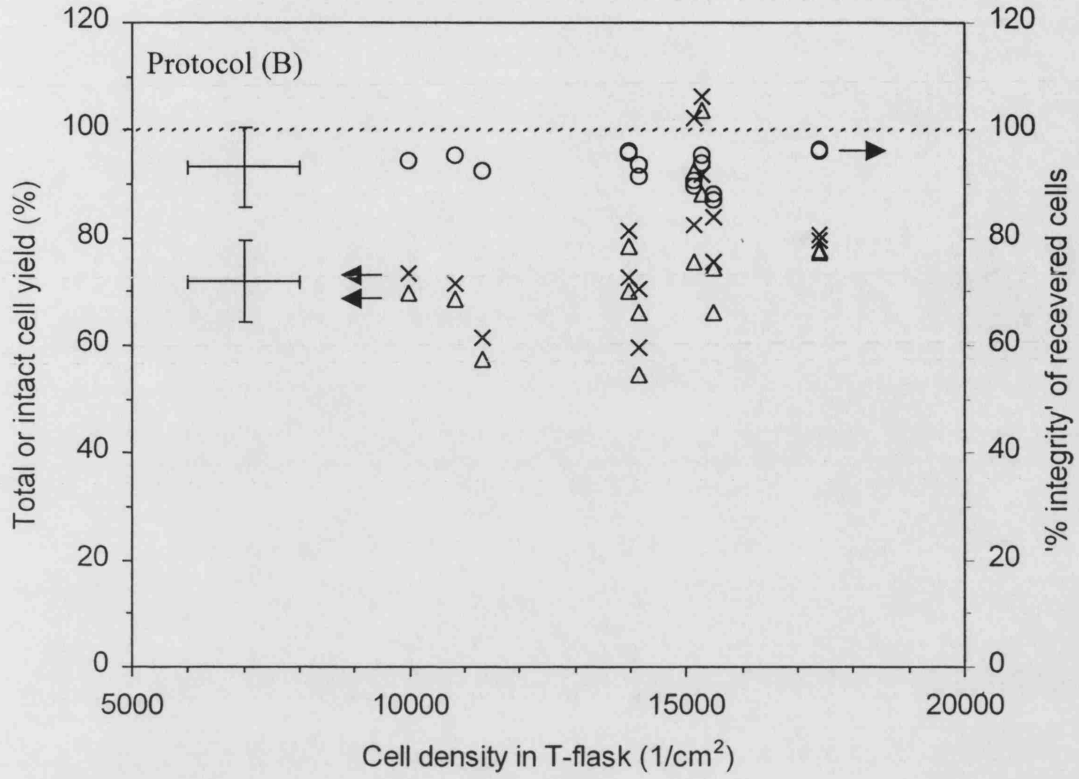


Figure 4-12b. Yield and membrane integrity of cells following centrifugation, as a function of cell density at harvest.

Rat aortic smooth muscle cell suspension harvested from T500 flasks was concentrated by protocol (B) (table 4-4), n = 15. In all cases centrifuge tubes were initially loaded with 40 ± 2mL of harvested cell suspension. Data with coincident x-values represent cell concentration performed in parallel with separate aliquots of a pooled cell harvest. 'Total cell yield' (×) is the total number of cells recovered, whereas 'intact cell yield' (△) is the number of cells recovered intact; both are expressed as percentage of cells initially dispensed to each centrifuge tube (quadruplicate trypan blue haemocytometer counts). '% integrity of recovered cells' (O) is the proportion of recovered cells which are intact, i.e. ('intact cell yield') / ('total cell yield'). (- - - 100% marker indicates desired (maximal) output for all quantities. Error bars shown are not data points, but represent approximate estimated error for all data.

with only 75 ± 13 % of initial cells remaining present and intact after concentration. Further examination of the possible mechanism of cell loss is necessary in order to develop a design basis for improvement in overall cell recovery. Concentration factor (i.e. 'cell volume fraction in wet pellet') is considered further in section 4.4.5.. Measured cell loss could be caused by cell hold-up or adhesion on surfaces of the process apparatus, aspiration with supernatant following either incomplete sedimentation or inadvertent premature pellet resuspension, annihilation due to shear during resuspension and apparent loss due to cell sequestration into aggregates. Cells held within aggregates may not be counted due to assay sampling and methodological constraints. Deleterious effect on cells could be caused by mechanical shear forces during pellet resuspension (section 4.4.3.) or biochemical effects (e.g. oxygen starvation) in cell pellet or concentrate (section 4.2.), although hypoxia is not expected to immediately affect cell membrane integrity (section 4.2.4.).

4.4.2. Process variability

It is evident that the variability in '% integrity of recovered cells' in protocol (B) (93 ± 3 %) is two-thirds lower than in protocol (A) (87 ± 9%); this represents a substantial improvement in process robustness and is consistent with gains hoped for when moving from the variable vortex mixing to the consistent orbital shaking procedure. The reduction of variation in '% integrity' can be more clearly seen by comparing figures 4-12a and 4-12b (see below). The variability in 'total cell yield', 'intact cell yield' and 'cell density in the pellet' are lower for protocol (B) but similar to protocol (A) in all cases. While assay imprecision may explain some of the apparent process variability, it is unlikely to account for the full spread in observed cell yields and recovered cell membrane % integrity. Thus further thought is required in order to develop strategies for improving robustness in process performance.

One of the main uncontrolled factors in both protocols was the behaviour of the upstream cell culture process. It was postulated that increased cell density on the growth surface (at cell harvest) might influence the performance of the concentration process due to variations in the composition of harvested cell suspension. Principally it was thought that increased cell density at cell culture harvest may correspond to increased extracellular matrix deposition during cell culture, leading to matrix carryover in harvested cell suspension and potential aggregation problems (see below, section

4.4.6.). The '% recovery' and '% integrity' of cells following concentration is presented as a function of cell density at harvest (figures 4-12a and 4-12b). Linear regression 'best fits' were added to the data in order to examine the possibility of any trends. A high level of scatter exists in the data and very low $R^2$ values ( $\leq 0.2$ ) were found for lines fit to 'total cell yield' and '% integrity', indicating that process variability is not directly related to 'cell density (in T-flask) at harvest'. In addition, similar plots were generated for percentage cell yield and integrity as a function of 'total number of cells in centrifuge feed suspension' (data not shown); these plots showed similar characteristics: a high level of scatter and no significant trends ($R^2 < 0.2$).

When examining parallel concentration of apparently identical aliquots of pooled cell suspension in figure 4-12b (data with coincident x-values), little variation in '% integrity of recovered cells' is evident, with much greater variation in 'cell yield'. The variation in cell yield indicates heterogeneity between separate aliquots of initial cell suspension; while this is of the order of assay precision and could simply be due to cell settling in the pool prior to aliquoting out, it could also indicate a level of inherent process variability independent of other potential factors such as the influence of upstream cell culture. This suggests that further studies, using much larger pools of cell suspension to perform many parallel 'identical' replicates, could evaluate the variability inherent in the concentration process itself, by excluding variation in factors relating to the upstream cell culture process and the precise composition of the cell suspension.

4.4.3. Shear forces during cell concentration

To evaluate the order of magnitude of potential shear forces during pellet resuspension, with a view to drawing parallels with chapter 3, a first order approximation for the shear stress in the centrifuge tube during resuspension was made based on an analysis of power dissipation in shaking flasks by Buchs et al. [2000]. Briefly, shear stress, $\tau$, assuming turbulent flow in an undisturbed hydrodynamic system, may be correlated by:

$$\tau = C.\rho.r^2.(2.\pi.n)^2 \, \mathrm{Re}_f^{-0.2} \qquad \text{(eq. 4-7)}$$

with Reynolds number in a shaking flask, $\mathrm{Re_f}$ given by:

$$\mathrm{Re}_f = \frac{\rho.n.d^2}{\mu} \qquad \text{(eq. 4-8)}$$

where: C = constant ( = 1.94, [Buchs et al. 2000])

$\rho$ = fluid density ($kg/m^3$)

r = radius of gyration, i.e. orbital throw (m)

n = orbital shaking speed (1/s)

d = maximum internal diameter of shaken vessel (m)

$\mu$ = fluid viscosity ($N.s/m^2$)

This calculation was performed (retrospectively) for the two systems investigated: (A) vortex mixer, 7mm throw, estimated ~1000 RPM; (B) orbital shaker, 4.5mm throw, 600RPM. The 50mL centrifuge tube internal diameter was 3cm and fluid viscosity assumed to be as for the resuspension solution (1 mPa.s). The predicted shear stress values for the two resuspension procedures were (A) 84 Pa and (B) 12 Pa. According to the observations in chapter 3 (section 3.4.), we would expect to see little or no cell damage at 12 Pa, with the onset of shear damage being in the range 50-100 Pa , i.e. some cell damage and loss is likely to occur at 84 Pa. Significant difference was observed in '% integrity of recovered cells' between the two protocols (A) 87 ± 9% and (B) 93 ± 3%, indicating that the change in the resuspension protocol has resulted in lower shear forces and lower cell damage. While the validity (e.g. assumption of turbulence) and hence expected accuracy of this calculation may be debatable, it does yield results which appear to be in accord with other findings in this work and also presents an analytical basis for comparison of different resuspension systems and conditions. Further development and validation of this (type of) correlation represents a good approach for the generation of a rigorous design basis for the optimisation and scale-up of pellet resuspension conditions.

### 4.4.4. Cell location following concentration

A small study was carried out to analyse the location of cells following concentration, with a view to determining the magnitude of apparent cell losses due to cell non-sedimentation, premature resuspension and fluid hold-up on the apparatus. In addition, the number of cells which could be lost due to adhesion to the centrifuge tube was estimated, based on formation of a spherical cell monolayer over the area of fluid-surface contact during shaking.

A mass balance on the number of cells before and after concentration was performed by trypan blue count and flow cytometry assays. The proportion of initial cells in various locations is presented in figure 4-13.

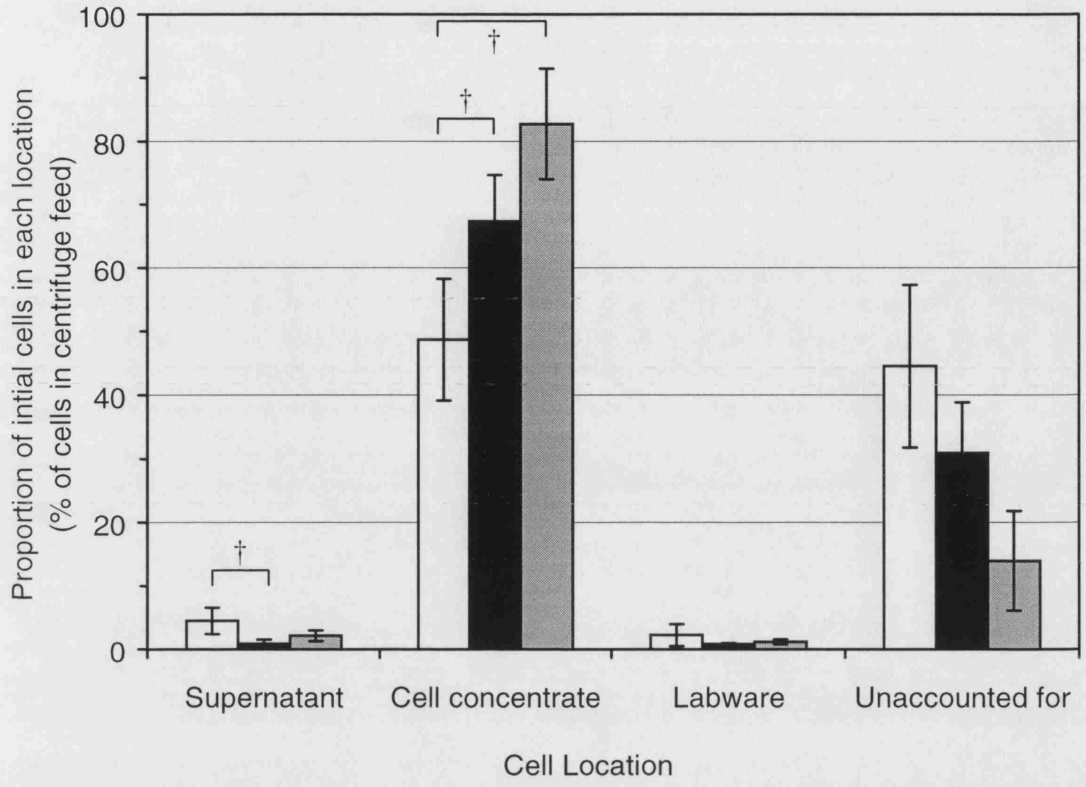


Figure 4-13. Analysis of cell location following cell concentration.

Rat aortic smooth muscle cell suspension harvested from T500 flasks (one T500, ~40mL cell suspension per sample) were concentrated by either protocol (A) or (B) (table 4-4). A pipette was used to aspirate cell concentrate from the centrifuge tube and saline solution (9g/L $NaCl/H_2O$, 2mL) was used to rinse out any retained cells from the centrifuge tube. The number of cells in the harvest cell suspension, centrifuge supernatant, final cell concentrate and saline rinse were assayed, either by trypan blue assay or flow cytometry. The number of cells in each 'location' was calculated as a percentage of the initial number of cells in the centrifuge tube prior to cell concentration. (□) Protocol (A), trypan blue assay, n = 3. (■) Protocol (B), trypan blue assay, n = 4. (▩) protocol (B), flow cytometry assay, n = 3. Error bars indicate 1 standard deviation on 'n' repeat experiments. [†] Significant difference (student's unpaired t-test) was found at the 95% level but not at the 99% level ($0.01 < P < 0.05$).

Comparing protocols (A) and (B) assayed by trypan blue counts, we observe a significant increase in number of cells recovered in the cell concentrate, with the magnitude of improvement being in agreement with findings above (section 4.4.1.). The significant decrease in cells found in the aspirated supernatant is attributed to a reduction in cell pellet aspiration during supernatant removal due to increased pellet hardness (expected, section 4.3.2.). Overall, the proportion of cells found in the supernatant and held-up in labware is very low, while the number of cells 'unaccounted for' is substantial, indicating that the major factor in apparent cell loss has not yet been considered.

Further analysis of protocol (B) by flow cytometry suggests that around half of the remaining apparent loss is due to differences between assays. The higher number of cells in the concentrate recorded by flow cytometry is consistent with assay behaviour observed in chapter 3 (sections 3.2.4., 3.2.5.); this difference was attributed to release of cells from aggregates during flow cytometry.

For the cell surface adhesion calculation, each cell (diameter 22.4μm, section 4.1.2.) was assumed to occupy a square area of $(22.4\mu m)^2$ in a monolayer. For a typical resuspension run by protocol (B) (concentrate volume ~2.5mL, $\sim 2 \times 10^6$ cell/mL, contact area $3 \times 10^{-3}$ $m^2$) it was estimated that a cell monolayer would correspond to 115% of all cells in the concentrate, thus cell loss by surface adhesion could be a significant factor. A visual (microscopic) check would be advisable to determine the extent of any actual cell adhesion and hence whether it would be appropriate to consider anti-adhesive materials or coatings (e.g. Silicone, Teflon) for the centrifuge tube.

### 4.4.5. Concentration factor

In both protocols (A) and (B), residual supernatant of the order of cell pellet volume remained associated with the cell pellet following supernatant aspiration, together denoted here as 'wet cell pellet'. Cell volume fraction in the wet pellet was calculated for all data points and the average calculated for both protocols, based on cell concentration in either the recovered cell concentrate or the initial harvested cell suspension (table 4-6). In addition, cell volume fraction in the wet pellet was determined graphically (from inverse slope, figure 4-14; table 4-6). Overall the calculated range of cell volume fraction in the pellet was 0.27 – 0.46, which is relatively low compared to theoretical volume fraction for regular packing arrangements of

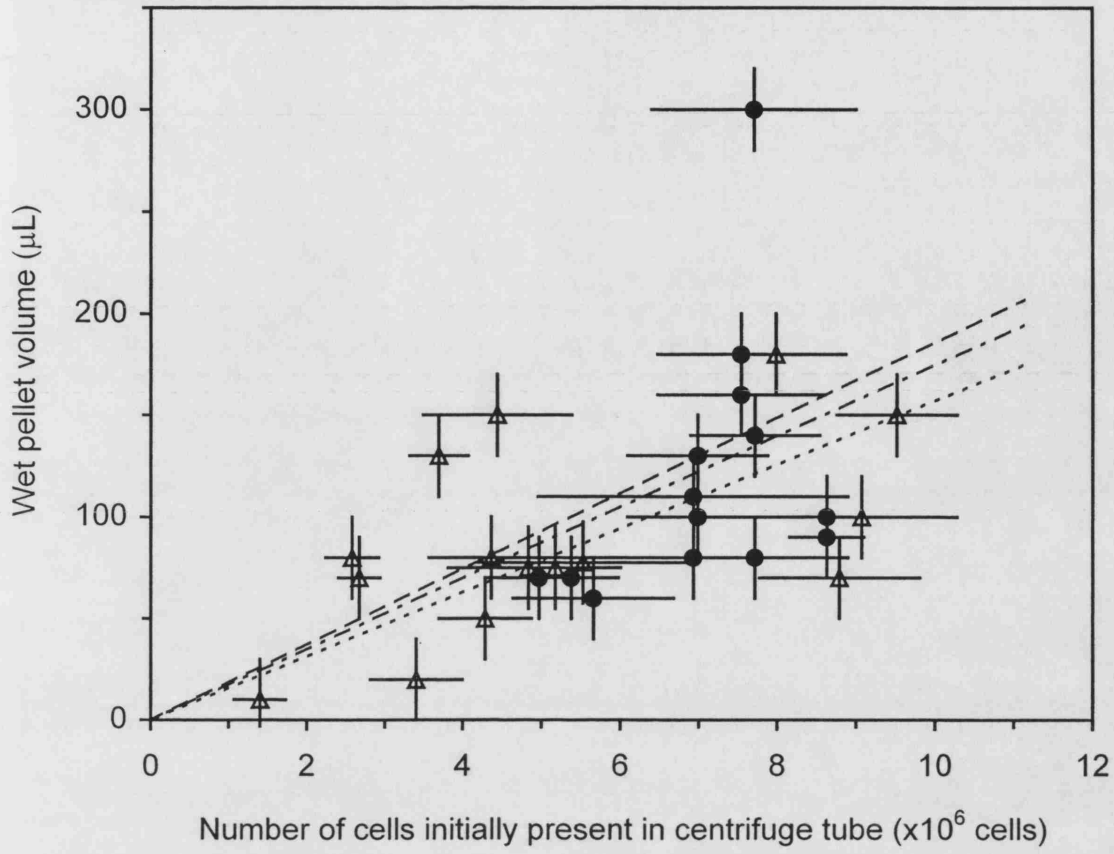


Figure 4-14. Centrifuge pellet volume as a function of the number of cells present prior to centrifugation.

Rat aortic smooth muscle cell suspension harvested from T500 flasks was concentrated by either protocol (A) or (B) (table 4-4). 'Wet pellet' denotes centrifuge pellet including the small residual layer of supernatant associated with the pellet surface. Wet pellet volume wa determined by subtracting (the volume of resuspension solution added) from (the volume of final cell concentrate produced), both measured by graduated pipette. Number of cells initially present in the centrifuge tube was determined from a manual count for cell concentration and graduated pipette measurement for suspension volume. Data: (△) protocol (A), (●) protocol (B). Linear regression fits: (— —) protocol (B), slope = 15.7, $R^2$ = 0.2 ; (- -) protocol (A), slope = 18.6, $R^2$ = 0.14 ; (– - –) protocols (A) and (B) combined data set, slope = 17.5, $R^2$ = 0.23 ; see table 4-6 for further analysis. Vertical error bars are twice the size of graduations on the pipette used to determine pellet volume. Horizontal error bars represent one standard deviation on quadruplicate cell counts.

Table 4-6. Calculated cell concentration in the wet cell pellet.

'Wet pellet' denotes the centrifuge pellet including a small residual layer of supernatant associated with the pellet surface; this residual supernatant layer appeared to be of the order of pellet volume. Cell concentration in the wet pellet was calculated as the mean of all samples based on (1) number of cells recovered in cell concentrate; (2) number of cells initially fed to the centrifuge tube. (3) The cell concentration in the wet pellet was determined graphically (the inverse slope of figure 4-14). For (1-3) the cell volume fraction in the wet pellet was calculated from the numerical cell concentration via mean cell volume (determined previously, section 4.1.2.). Overall the calculated range of cell volume fraction in the wet pellet was 0.27 – 0.46.

| Concentration protocol | n | Cell volume fraction in the wet pellet (v/v ± 1 SD) | | |
|---|---|---|---|---|
| | | (1) | (2) | (3) |
| (A) | 15 | 0.27 ± 0.18 | 0.46 ± 0.26 | 0.37 |
| (B) | 15 | 0.30 ± 0.10 | 0.39 ± 0.14 | 0.31 |
| (A) + (B) | 30 | 0.28 ± 0.14 | 0.42 ± 0.21 | 0.33 |

uniform spheres ('loose' cuboidal packing, $\phi = 0.524$; 'close' rhombohedral packing $\phi = 0.74$ [Coulson and Richardson, 1991]). Considering the presence of the residual pellet-associated supernatant, it is likely that cell volume fraction in the pellet approaches the range $0.524 < \phi < 0.74$. There is no evidence that cell volume fraction exceeds the high end of this range, indicating that little or no deformation or dewatering of cells occurs under the centrifugation conditions examined. Qualitatively the cell pellet appeared solid or 'gel-like', supporting the earlier assertion (section 4.1.5.) that suspension rheology may include a transition to 'solid-like' or 'gel-like' behaviour at around $\phi = 0.4$.

4.4.6. Aggregate formation and break-up

While both protocols were consistently able to resuspend cell pellets, typically one or more 'stringy' aggregates (clearly visible to the naked eye) was found in the cell concentrate. Adherent rat aortic smooth muscle cell suspensions were generally observed to be aggregating suspensions; cell aggregation could be caused by electrostatic effects, cell surface proteins or flocculation process mediated via remnants of extracellular matrix proteins secreted by cells during culture. Images illustrating the typical appearance of aggregates in the harvested cell suspension and cell concentrate are presented in figure 4-15. Typically, many small and medium sized aggregates occur in the cell harvest, apparently consisting of cells and an associated matrix, probably a secreted basement matrix sheet which is formed by the cells in culture flasks. After concentration (protocol (B)), typically only medium and large aggregates are observed (usually only one or two large), with the rest of the resuspended concentrate appearing homogeneous to the naked eye. After concentration, the basement matrix sheet is rarely visible in aggregates; this may be explained by free cells attaching to exposed matrix surfaces during concentration. The large aggregates are probably formed by coalescence of small and medium aggregates present in the cell harvest. Visually dense areas within aggregates and resuspended cell concentrates may be areas of compacted cells and secreted matrix protein with little or no fluid voids. Additional cohesive forces between matrix and cells would account for the resistance of aggregates to resuspension during the concentration protocol. In addition cells could become trapped within a network of interconnected strands, fragments or sheets of matrix. The generation of such aggregates or flocs is likely to cause apparent loss of cells because large aggregates (and

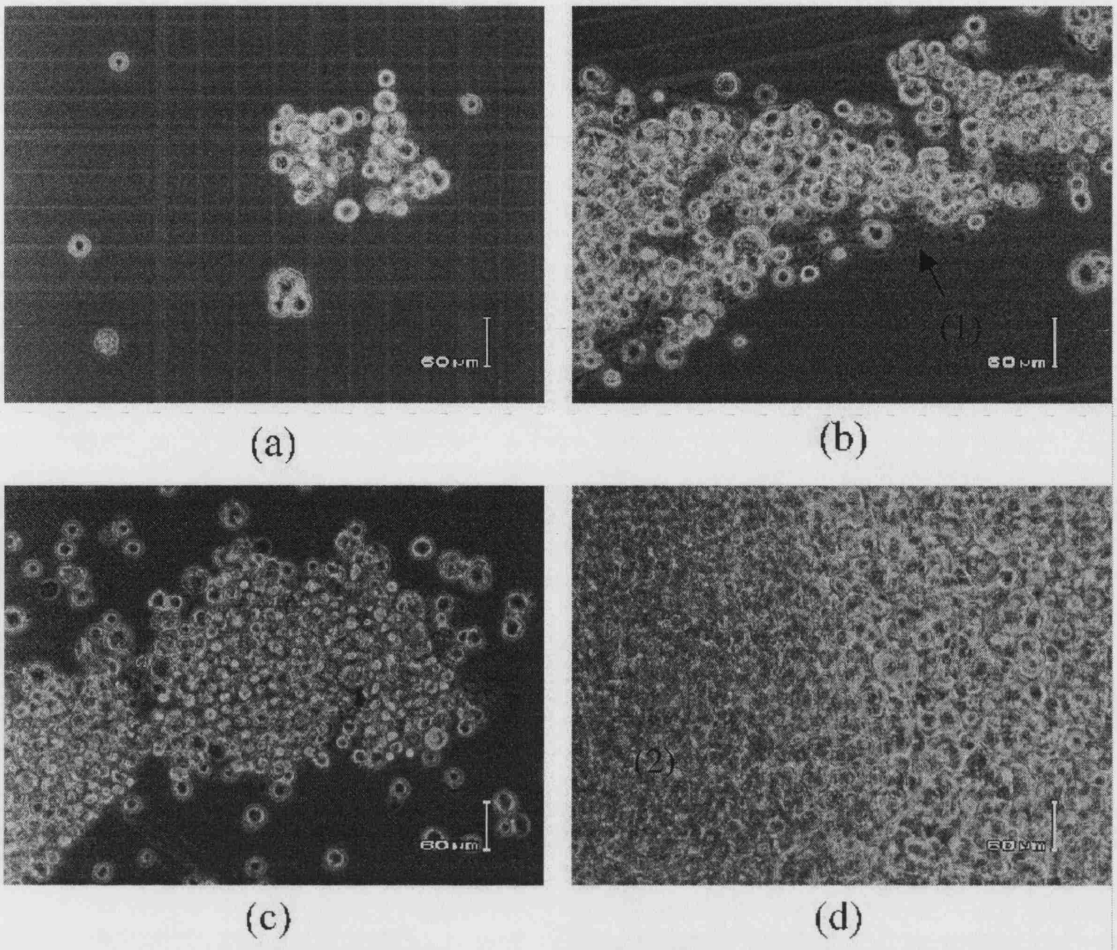


Figure 4-15. Images showing cell aggregates before and after cell concentration.

Undiluted aggregates were sampled from cell harvest suspension and cell suspension following concentration (protocol (B), table 4-4) and visualised on a standard haemocytometer slide (no stain). Photographs were taken with a digital camera and inverted phase contrast microscope, 100x magnification, scale bar 60µm. Photographs illustrate the typical appearance of cell aggregates following cell harvest (a), (b) and after subsequent concentration (c), (d). (a) Small aggregate in cell harvest, (b) medium aggregate in cell harvest with exposed basement matrix (1), (c) medium aggregate in concentrate, little or no exposed basement matrix, (d) large aggregate in cell concentrate with densely packed region (2).

associated cells) are excluded from manual cell counts due to sampling, counting and other experimental issues. Large aggregates are likely to interfere with subsequent tissue formation operations (e.g. viscosity-sensitive processes such as dynamic rod coating), causing defect formation in tissue products.

4.4.7. Discussion – cell concentration performance

Semi-automated protocols (A) and (B) are able to concentrate rat aortic smooth muscle cells to around $\phi$ = 0.3-0.4 in the wet cell pellet, which is of the same order as smooth muscle volume fraction in the rat aorta ($\phi$ = 0.41, [Olivetti et al., 1980]). Development of the concentration protocol (B) reduced process variability, damage to and apparent loss of cells. Increasing centrifuge force is thought to have improved both sedimentation of cells and firmness of the cell pellet, reducing cell loss in aspirated supernatant. The reduction in resuspend intensity can account for reduced cell damage (lower shear forces). While remaining apparent cell loss may be in part due to surface adhesion and assay error, a major mechanism of apparent loss is thought to be sequestration of free cells into large aggregates or flocs by adhesion and compaction during concentration, and/or high-affinity cell interactions with secreted matrix fragments.

Aggregate formation following cell concentration is observed to be highly variable in this study, indicating that control parameters are not well understood or regulated in this work and probably lie upstream of the cell concentration process. It is thought that a major controlling factor is the quantity of basement matrix secretion and carry-over from cell culture. Although no correlation in cell yield was found with cell density at harvest ($1/cm^2$), investigation and improved control of cell culture and harvest parameters might lead to a reduction in aggregation. Other potential strategies, such as aggregate removal by filtration or break-up by controlled shear, could also be explored for potential to improve concentrate homogeneity and cell yield. Cell aggregation during concentration is likely to be a generic issue, relevant for any cell or tissue-based therapy using cells which normally produce, or are stimulated to produce, extracellular matrix deposits. Given the stipulated mechanism of large aggregate formation, potential damage with aggregate break-up and anticipated losses associated with aggregate removal, it is thought that the preferred process development strategy would be to characterise the upstream control parameters responsible for aggregation (e.g. time in culture, time and temperature of exposure to enzymatic harvest solution) and thus clarify a preventative design basis.

## 4.5. Summary

Expansion of rat aortic smooth muscle cells (RSMC) may be carried out in standard 'single-deck' T-flasks or 'triple-deck' T-flasks. Cultures in triple-deck flasks behaved similarly to single-deck flasks and, although cell number after 4-day cultures was slightly lower for triple-deck flasks, they provided a substantial reduction (~50%) in cell culture labour and incubator space when growing large numbers of cells.

RSMC volume mean cell diameter was found to be 22.4μm and a simple conversion between numerical cell concentration and cell volume fraction has been presented. Expression of cell concentrations as 'cell volume fraction' may be used to standardise between cell lines exhibiting different sizes and is useful in visualising suspensions, correlating suspension rheology and may also be useful in other studies e.g. standardising oxygen consumption rates on a 'per cell volume' basis.

Concentrated RSMC suspensions exhibit shear thinning behaviour and may be described by Power law correlations. Following exposure to increased shear levels, apparent viscosity is reduced indicating time-dependent or irreversible changes in suspension micro-structure, suggesting that significant cell-cell and/or cell-matrix interactions exist in suspension, particularly at high concentration. Further work is required to establish a generalised equation including the effect of cell concentration and also characterise suspension time-dependent and possible shear thickening behaviour. Despite lack of standardisation between reports, RSMC suspension rheology was similar to plant and yeast cell concentrates, indicating that useful parallels may be drawn with the body of established literature on various cell concentrates.

Oxygen depletion during cell concentration and concentrate processing is likely to occur over the timescales required for manual processing operations. Depending on the cell type characteristics (oxygen uptake and hypoxia sensitivity) it may be necessary to take steps to attenuate hypoxia such as reducing process time or temperature, or providing controlled oxygen supply to concentrates. It is envisaged that implementation of full process automation would enable substantial reduction in processing times.

We have shown that, using a semi-automated protocol, it is possible to concentrate and recover RSMC with moderate losses (~25%). The high level of '% cell integrity' (~93%) following concentration suggests that, with further refinements, automated procedures causing little or no mechanical cell damage could be developed and applied in therapeutic processes. Semi-automated cell concentration achieved cell volume fraction of ~0.3-0.4 in the wet cell pellet, demonstrating the feasibility of developing

automated cell concentration procedures which can achieve cell volume fractions approximating those found *in vivo*. Apparent concentration process variability remains an issue, and is thought to be related both to the assays employed and to the variable formation of large aggregates which persist in the cell concentrate. It is proposed that aggregation or flocculation of cells during concentration is largely due to presence of small aggregates and secreted matrix deposits in the harvested cell suspension, carried over from cell culture and harvest processes. As the presence of large residual aggregates is likely to adversely affect subsequent tissue formation processes, further work is required to characterise the control factors governing aggregation and elucidate a design basis for prevention, or for the removal or break-up of aggregates.

These initial concentration studies have considered only obvious effects on cells (i.e. cell number and membrane integrity) at relatively low final cell volume fraction (~0.02). Further studies are required to increase the range of conditions (e.g. cell density in concentrate) and ascertain any more subtle effects of processing stress (e.g. shear, hypoxia) such as induction of apoptosis and other alterations to cell metabolism, growth potential, functional response and gene expression profiles.

# Chapter 5: Discussion

## 5.0. Introductory remarks

To date the field of tissue engineering has been largely research-oriented, focusing on invention and development of novel technologies [Pangarkar et al., 2003] and has brought few products to clinical trial or large-scale manufacture. The demise of the pioneering firms (Advanced Tissue Sciences and Organogenesis), partially attributed to poor manufacturing efficiency and a lack of process automation [Moore SK, 2002], has underlined the need for a realistic appraisal during early research and development of issues including scaleable manufacture and commercial viability of a product and the manufacturing process.

In order to apply a systematic approach to process characterisation and development of design bases for processing systems, properties of cellular materials including rheology and cell size were examined and the stability of cellular process materials assessed with respect to physical (mechanical) and biochemical conditions likely to occur in a model automated process. It was intended to demonstrate proof of principle for application of an automated procedure to the generic unit operation of cell concentration, assessing performance and moving towards a fundamental design basis for improvements. At an early stage in product/process development it is prudent to make a predictive appraisal of the practicality of scaleable product manufacture and commercial viability in order to assess risk associated with undertaking product/process development and the estimated feasibility of such a development project.

## 5.1. Predicted implications for manufacturing process feasibility and cost

Manufacturing process issues such as yield of healthy cells and cost of processing may have significant implications for product feasibility, in terms of practical and economic feasibility of the manufacturing process. In the case of autologous tissue manufacture, a major concern is the ability to generate sufficient cells for tissue formation from a limited biopsy size and at reasonable cost. Consideration of alternative process scenarios may provide some indication of research & design targets required to achieve practical and economic process (product) feasibility.

A preliminary analysis was constructed examining the feasibility of generating sufficient cells from a biopsy using currently available automated cell culture apparatus, taking account of cell loss during processing. A 'windows of operation' approach

(section 1.5.5.) was used to generate graphical output indicating feasible processing scenarios, using estimated process parameters for a stipulated autologous blood vessel manufacture process (section 1.3.9., table 2-3). Resulting feasible processing scenarios were extended with basic cell culture cost data to provide a preliminary indication of the balance and magnitude of associated processing costs (section 5.1.3.).

5.1.1. Description of the 'windows of operation' analysis

As the diagrams presented here are complex compound diagrams, the separate elements are first presented individually (see below, i.e. '**operating line**', figure 5-1a.i ; '**design line**', figure 5-1a.ii), then combined (e.g. figure 5-1a.iii), before adding further process constraints to generate a final compound diagram (figure 5-1a.iv).

This analysis examines the ability of an automated cell culture process to generate sufficient cells for tissue formation from a limited biopsy size. The automated cell culture processing system considered is 'SelecT' (The Automation Partnership, Cambridge, UK); process flowsheets for automated cell culture are presented in figures 2-2a-b, processing times given in tables 2-3a-b, and additional assumptions describing the cell culture process given in table 2-2a.

'**Operating line**': A brief algebraic representation of the analysis is provided in table 5-0a along with example data, and a verbal description is presented here. A specified number of cells are required in the formed tissue (see table 2-3a). As there are yield losses during 'harvested cell concentration', 'cell reformulation' and 'tissue formation' (denoted 'downstream' process i.e. downstream of cell culture), it is necessary to generate a larger number of cells during cell culture to account for these 'downstream' yield losses (see eq. 2-9, table 5-1). Having calculated this (increased) number of cells which must be produced at the end of cell culture (and equivalent cell culture area required), it is possible to construct cell culture passage trains backwards from the final required area, returning initial '**biopsy size**' (required to seed the first passage) as a function of '**number of passages**'; an example calculation is presented for clarification of this point (table 2-4). This calculation returns the '**operating line**' (describing the number of cells required for the process to operate according to specified tissue seeding cell density); the '**operating line**' is represented as 'initial **biopsy size** required (cm of vein)' as a function of '**number of passages**'. This 'line' essentially takes the form of a histogram plot with a single value of '**biopsy size**' for each value of '**number of passages**' (see figure 5-1a.i).

Table 5-0a. Example calculation for construction of windows diagrams. This example corresponds to the 'operating line' in figure 5-1a.

NB See also table 2-3a for data and 2-4 for a more detailed example calculation.

(*) The area for passage 5 was specified using a combination of 500, 175 and 25 $cm^2$ culture flasks, using larger flasks preferentially. Area for passage 5 was specified as being the minimum area with was greater than ($N_H$ / $C_H$). NB the same method was used when specifying area for each passage.

($) The cell culture train was constructed by repeating this loop 'backwards' from the final passage, considering passages (n, n-1, n-2 . . .) on successive iterations.

(#) Alternatively, cells extracted from a length of surface vein biopsy may be used to plant any given passage, rather than using cells harvested from an earlier passage.

| | Quantity | Formula | Units | Example value |
|---|---|---|---|---|
| | | | | |
| | Confluent cell density (at harvest) | $C_H$ | ($cell/cm^2$) | 18000 |
| | Seeding cell density in culture flasks | $C_S = (C_H / 3)$ | ($cell/cm^2$) | 6000 |
| | | | | |
| | Final no. cells required in the formed tissue | $N_T$ | (cell) | $6.1x10^7$ |
| | **Downstream process yield** factor | $Y_d$ | (-) | 0.5 |
| | No. cells required in final passage harvest (e.g. passage 5) | $N_H = (N_T / Y_d)$ | (cell) | $12.2x10^7$ |
| | Area of passage 5 (*) | $A_5 \geq (N_H / C_H)$ | ($cm^2$) | 6775 |
| ($) | No. cells required to seed passage 5 | $S_5 = A_5 / C_S$ | (cell) | $4.1x10^7$ |
| ($) | Area of passage 4 (*) | $A_4 \geq (S_5 / C_H)$ | ($cm^2$) | 2275 |
| ($) | OR (i.e.) Area of passage 4 (*) | $A_4 \geq (A_5 / 3)$ | ($cm^2$) | 2275 |
| | | | | |
| (#) | Cell density yielded from biopsy | $C_B$ | (cell/cm) | $1.5x10^5$ |
| (#) | No. cells required to seed passage 5 | $S_5 = A_5 / C_S$ | (cell) | $4.1x10^7$ |
| (#) | **Biopsy size** required to seed passage 5 | $B_5 = (S_5 / C_B)$ | (cm) | 271 |
| (#) | No. cells required to seed passage 4 | $S_4 = A_4 / C_S$ | (cell) | $1.4x10^7$ |
| (#) | **Biopsy size** required to seed passage 4 | $B_4 = (S_4 / C_B)$ | (cm) | 91 |

Table 5-0b. Example calculation for construction of windows diagrams. This example corresponds to the **'design line'** in figure 5-1a. See also tables 2-3b-c for source data, and table 2-4 for an example calculation showing cell culture train set up.

(#) It was assumed that the production facility produces the same number of product (patient) **units** on each day. Thus it follows that (for a rolling cell culture schedule) the cell culture robot performs the equivalent of all passaging operations in 'T' cell culture trains every day. e.g. passage p1→p2 for patient (A), p2→p3 for patient (B), and so on.

(*) The number of flasks which can be processed per patient unit must be rounded down to the nearest integer.

Once the maximum number of flasks per unit ($f_u$) had been calculated, multiple cell culture trains of various 'final cell culture area' (i.e. number of cells in final passage harvest) and various **'number of passages'** were constructed (see table 5-0a for method). Cell culture trains with highest achievable final passage area were selected, on the condition that the number of flasks used (in the entire passage train) was not greater than the maximum number of flasks [per **unit**], ($f_u$). These selected cell culture trains were then presented in the final windows diagrams (figure 5-1a-c) as the **'design line'**, i.e. taking **biopsy size** and **number of passages** as the output (presented) data (see tables 5-0a and 2-4 for example calculations).

| Quantity | Formula | Units | Example value |
|---|---|---|---|
| | | | |
| **Throughput** [of patient **units**, on a per robot per day basis] | T | **units** | 4 |
| Total time per day | $t_d$ | min | 1440 |
| Robot downtime factor for maintenance | $D_m$ | (-) | 0.25 |
| Robot downtime factor for changeover and cleaning | $D_c$ | (-) | 0.125 |
| Processing time required per flask | $t_f$ | min/flask | 7.6 |
| | | | |
| Total available processing time [on a per robot per day basis] | $t_p = t_d.(1-D_m-D_c)$ | min | 900 |
| (#) Total available processing time [per patient unit] | $t_u = t_p / T$ | min / **unit** | 225 |
| (*) Maximum number of flasks [per patient unit, i.e. per cell culture train] | $f_u = t_u / t_f$ | flask / **unit** | 29 |

'**Design line**': A brief algebraic representation of the analysis is given in table 5-0b along with example data, and a verbal description is presented here. In order to ensure that the cost of automated cell culture apparatus is controlled, process design engineers may specify a required process '**throughput**' for each automated cell culture module (robot). '**Throughput**' is specified on a per robot per day basis, and has units of '[patient] **units**'. Taking the example of case (A) below, this is specified as '4 **units**' i.e. every day each cell culture robot will harvest all of the flasks in the final passage for each of 4 patients (4 [patient] **units**, on a per robot per day basis). Given (1) the required '**throughput**' (4 **units** [per robot per day basis]), (2) the processing time available (900 minutes [per robot per day basis], table 2-3c), and (3) the time required to process each cell culture flask (7.6 minutes per flask, table 2-3b), we may calculate the maximum number of flasks per [patient] **unit** (eq. 2-10). In this case the maximum is 29 flasks per [patient] **unit** (table 2-3c), representing the maximum number of flasks which may be passaged in the entire cell culture train for each [patient] **unit**. The '**design line**' was then calculated by constructing many different cell culture passage trains of various final cell culture area (by the same method as the operating line (see above, table 2-4), and selecting the appropriate passage train providing the maximum final cell culture area BUT NOT exceeding the constraint on 'number of flasks per unit' i.e. 29 flasks in this case. Thus the output of calculations for the '**design line**' takes the same form as the '**operating line**' i.e. this 'line' is effectively a histogram plot with a single value for **biopsy size** for each value for **number of passages**.

Construction of compound windows diagrams: As the '**operating line**' is a *minimum* constraint (we must produce at least the *minimum* number of cells required in the formed tissue), the area *above* this line is shaded as a feasible region in the windows diagrams (see figure 5-1a.i). As the '**design line**' is a *maximum* constraint (calculated *maximum* number of flasks which can be processed per [patient] **unit**), the area *below* this line is shaded as a feasible region in the windows diagrams (see figure 5-1a.ii). The process is feasible only where the **design line** is either coincident with, or above, the **operating line**. This is illustrated in figure 5-1a.iii where the **operating line** (figure 5-1a.i) and the **design line** (figure 5-1a.ii) are superimposed; in this case there is no feasible region (see diagrams 5-1b-c for feasible regions).

Additional constraints: There are also a few further constraints on the process (see table 2-2b), briefly: (1) The *minimum* **biopsy size** must be sufficient to seed one small ($25cm^2$) culture flask; thus the process is only feasible with **biopsy size** $\geq$ 1cm. (2) The

**biopsy size** should not be so large as to cause distress or post-operative complications to the patient; *maximum* **biopsy size** is specified as 10cm. Thus the process is only feasible where:

$$10\text{cm} \geq \textbf{biopsy size} \geq 1\text{cm}$$

(3) It is well established that after many successive cell culture passages, primary cells tend to 'de-differentiate', reach 'replicative senescence' (stop growing), or otherwise become sufficiently altered so as to lose their functional characteristics. Thus there is a limit to the number of cell culture passages which can be performed while still producing usable cells. This limit was specified as 5 passages (table 2-2b). Thus the process is only feasible where: $5 \geq$ **number of passages**

These additional constraints are presented in the complete compound windows diagrams (e.g. figures 5-1a.iv) as dotted lines (- - -).

5.1.2. Process feasibility analysis

The graphical output of the analysis (figures 5-1a-c) essentially consists of an '**operating line**' and a '**design line**', respectively representing the 'number of cells required from cell culture' and 'specified process **throughput** [per robot per day]'. In these 'windows of operation' diagrams, process feasibility is indicated where the **design line** is above the **operating line**, signifying that (at the specified **throughput**) the cell culture robot is able to process sufficient flasks per patient unit to achieve the final cell culture area required.

The 'windows of operation' diagrams generated for the base case (Case A) are shown in figure 5-1a. For clarity all windows diagrams are built up successively. The total culture (flask) area required during a cell culture train is lowest near the origin and increases with **biopsy size** or **number of passages**; total culture area required increases towards ($x = \infty$, $y = \infty$). Figure 5-1a.i. illustrates the ***operating* line** (thick line), representing the number of cells required at the end of the cell culture process; this is the minimum number of cells (minimum final cell culture area) required for the downstream process to *operate*. As this is a minimum constraint, the area above is shaded as a feasible region.

Figure 5-1a.ii. illustrates the ***design* line** (thin line), which represents the maximum number of cells which can be produced for a fixed process **throughput** (number of patient **units** [per cell culture robot per day]); 'process **throughput**' is an imposed

*design* constraint. This constraint (limited by the maximum number of culture flasks which may be processed per patient unit) corresponds to the maximum achievable final cell culture area and so the area below the line is shaded as a feasible region. Wherever the design line is coincident with or above the operating line there exists a feasible operating space, or 'window of operation', which satisfies both the *operating* and *design* constraints.

Figure 5-1a.iii. superimposes the **operating line** and **design line** and we can see that for the base case (case (A)) feasibility could be achieved only at 7 passages, where the **design line** and **operating line** are coincident. Further constraints exist for both **number of passages** and **biopsy size** and are applied in figure 5-1a.iv.. In this instance the coincidence of the **operating line** and **design line** (at 7 passages) now falls outside the additional constraints and the process becomes infeasible. Encouragingly, however, both the operating line and the design line fall within the additional constraints (on **biopsy size** and **number of passages** (table 2-2b)), suggesting that a solution is possible.

The two major process engineering factors in the analysis are '**throughput** ([patient] **units** [per cell culture robot per day])' and '**downstream process yield**'. Windows diagrams were generated for two modifications to the base case (case (A)). Case B: From the base case, decreasing **throughput** from 4 to 2 **units** [per robot per day] i.e. doubling the maximum number of flasks which can be processed per patient unit (figure 5-1b.). One operating window has been created within the constraints on **biopsy size** and **number of passages**, at 5 passages. Case C: From the base case, increasing the **downstream process yield** from 50% to 95% (figure 5-1c.). Two operating windows have been created within the constraints. While a larger **biopsy size** with lower **number of passages** would be preferable to reduce the time in culture and hence minimise any changes in the cell population, a smaller biopsy would be better for patient and surgeon. In case C, the process is able to operate with a significantly smaller biopsy than case B.

The indicated process design objective is thus to achieve very high process yields, allowing the process to operate with high throughput per cell culture apparatus and at minimum **biopsy size** and/or **number of passages**. While maximisation of yields is very important, the risk of failing to achieve downstream process yield approaching 100% is mitigated by the ability to relax the constraint on process **throughput**, provided the patient/surgeon, biological and economic implications of increased **biopsy size**, **number of passages** and cell culture area are tolerable. In this analysis, larger

windows of operation correspond to greater excess of cell culture capacity over and above the requirement to generate sufficient cells, indicating a greater degree of available flexibility in specifying the final process; larger windows indicate that (modest) increases in the number of cells generated may be achieved at the specified **throughput**. Pursuing process development within a larger window may also yield a process with a higher level of robustness; e.g. a process generating more than the minimum number of cells required may be able to tolerate larger variations in process performance parameters (e.g. processing yields, cell culture productivity) without batch failure occurring.

Table 5-1. Estimation of approximate overall and downstream process yield. Data are either adapted from experimental results and observations or otherwise estimated. The product of process yield factors downstream of cell culture (*) was used in calculations determining the number of cells (cell culture area) required at the final cell culture passage (section 2.5.2.).

| Process operation | Estimated approx. yield factor | Rationale |
|---|---|---|
| | | |
| Cell isolation from biopsy | 1 | Value used for cell recovery (cells/cm biopsy ) already accounts for losses. |
| Cell transfer | 0.95 | Capillary shear studies (figure 3-12b.). |
| Cell culture | 0.9 | Harvested cells typically ~99% intact, estimate ~1% hold-up loss per passage. Estimated for 4 or 5 passages. |
| Cell transfer * | 0.95 | As above. |
| Concentration * | 0.8 | Observed intact cell yield ~75% (figure 4-11.). Assume further (minimal) process development achieves ~80%. |
| Cell transfer * | 0.95 | As above. |
| Formulation * | 0.85 | Estimated. Losses due to mixing stress and hold-up of viscous fluid. |
| Cell transfer * | 0.95 | As above. |
| Tissue formation * | 0.85 | Estimated. Losses due to flow stress and hold-up of viscous fluid. |
| | | |
| Overall process yield factor | 0.42 | Product of all estimated yield factors for individual process steps. |
| 'Downstream' process yield factor, $Y_d$ | 0.50 | Product of estimated yield factors for individual process steps downstream of cell culture (*). |

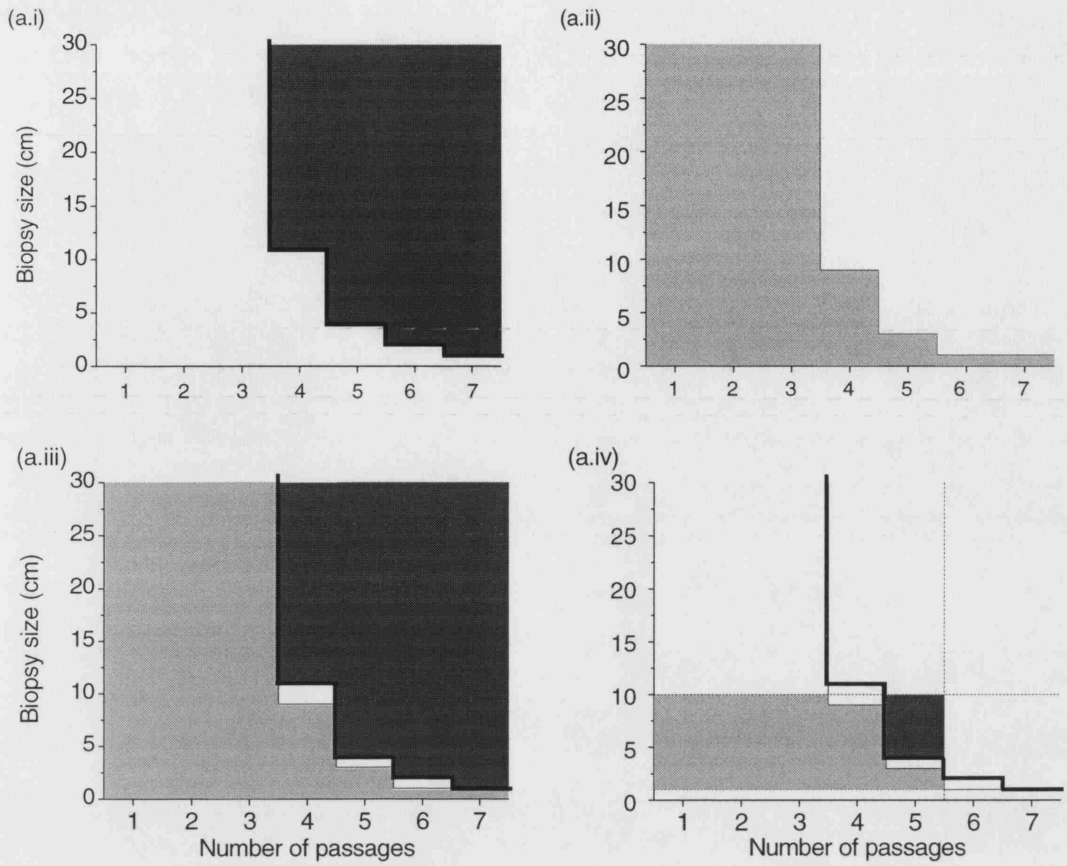


Figure 5-1a. Windows of operation case (A).

Predicted operating window diagrams for an autologous blood vessel production process, examining the effect of estimated '**downstream process yield**' (%) or specified 'process **throughput**' ( [patient] **units** [on a per cell culture robot per day basis] ).

Windows are built up successively for clarity; the complete compound diagram is presented in part (iv) of the sequence; see section 5.1.1. for an explanation of diagram setup. NB '**operating line**' and '**design line**' are effectively histogram plots.
(i) **Operating line** only (a *minimum* constraint). (ii) **Design line** only (a *maximum* constraint). (iii) **Operating** and **design line** constraints combined. (iv) Additional process constraints (table 2-2b) added: Maximum **number of passages** = 5 ; 1cm ≤ **biopsy size** (cm of vein) ≤ 10cm.

Shading: white = insufficient constraints satisfied, light grey = **design line** satisfied (a *maximum* constraint), dark grey = **operating line** satisfied (a *minimum* constraint), black = all constraints satisfied (NB no black region is present in figure 5-1a. See figures 5-1b-c for black (feasible) regions.

Case (A) (figure 5-1a): No operating window. '**Downstream process yield**' = 50%, 'process **throughput**' = 4 [patient] **units** [on a per cell culture robot per day basis].
Case (B) (figure 5-1b): Operating window created by decreasing **throughput** (design specification) from 4 to 2 **units** [per cell culture robot per day].
Case (C) (figure 5-1c): Operating windows created by increasing **downstream process yield** from 50% to 95%.

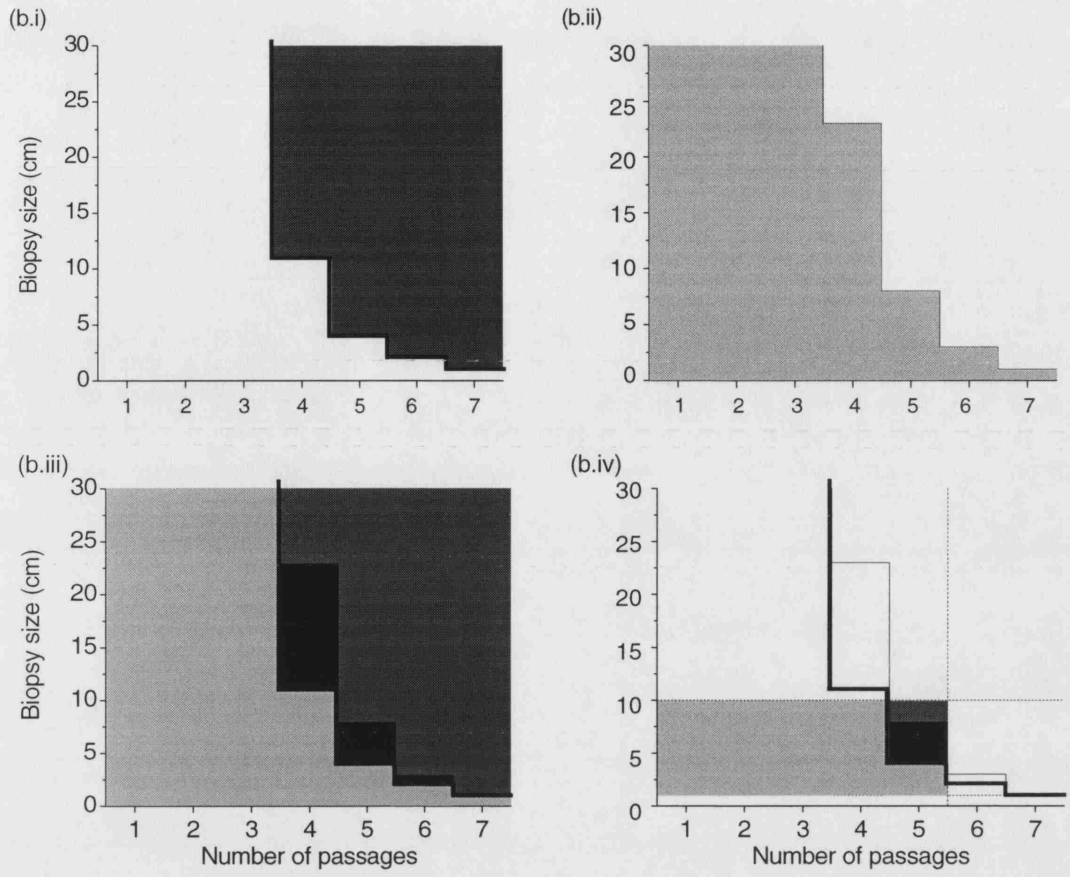


Figures 5-1b, 5-1c. Windows of operation case (B) and case (C). For legend see figure 5-1a.
Case (B): '**downstream process yield**' = 50%, '**throughput**' = 2 **units** [per robot per day].
Case (C): '**downstream process yield**' = 95%, '**throughput**' = 4 **units** [per robot per day].

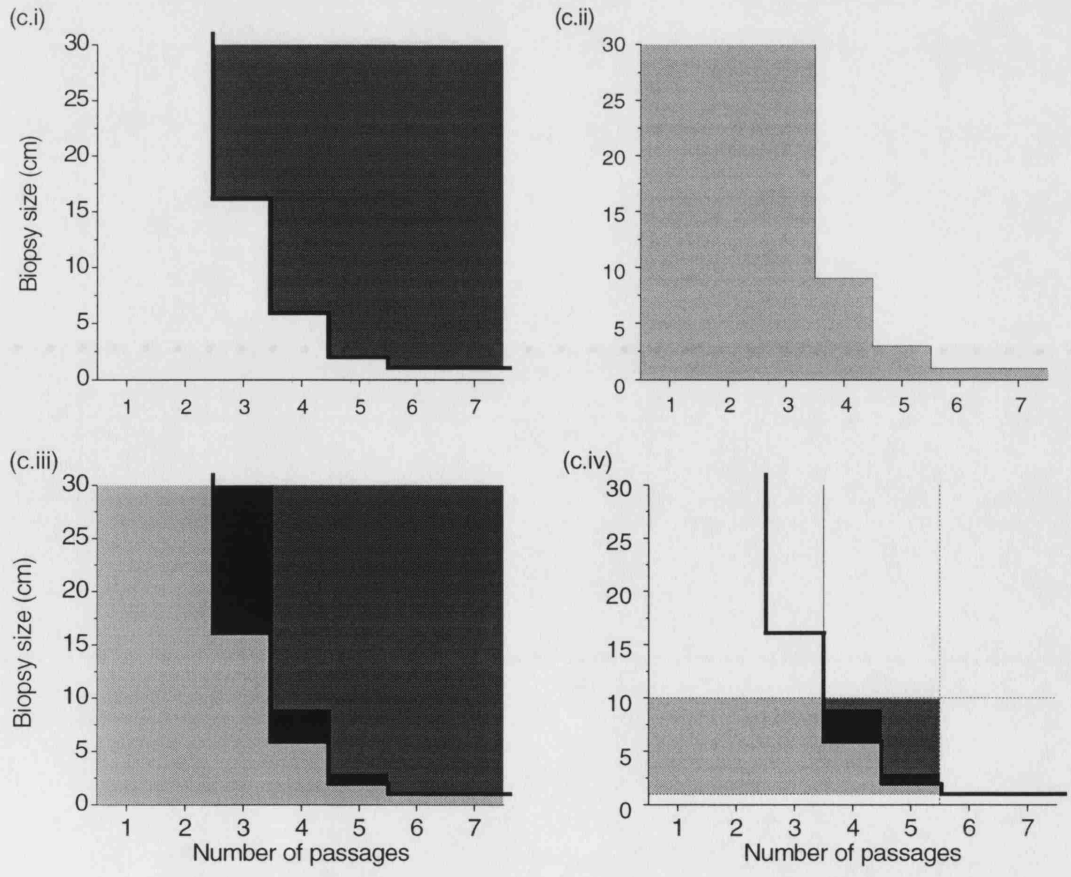

### 5.1.3. Estimated cell culture costs for feasible process scenarios

Feasible processing scenarios generated using the 'windows of operation' approach were subsequently evaluated in terms of basic cell culture costs to provide some indication of the approximate scale and balance of culture costs. Using the annual number of UK coronary artery bypass grafting procedures as a guide for market size, the cost of automated cell culture processing systems and cell culture consumables were estimated and are presented in table 5-2. Within the constraints applied in the 'windows of operation' analysis, there is little room for variation in either **number of passages** or **biopsy size** and the small variation in these parameters has little impact on cell culture costs. Process yields have a large economic impact because cell culture processing costs (both apparatus and consumables) rise in approximate proportion to the number of cells which must be generated during cell culture. It is thus vital to focus research and development efforts towards developing individual process operations with very high yield (>90%) of healthy cells, in order to achieve both practical and economic process feasibility. Elimination of step losses by combining process operations and also reducing the required number of cell suspension transfers is an attractive strategy for making substantial gains in overall yield. Achievable cell yield is likely to be a key consideration in selecting between alternative processing techniques.

Estimated cell culture costs are dominated by consumables costs, with automated apparatus cost being less than a quarter of the total. The total number of automated processing systems required (in the UK) and the associated capital cost suggests that it may be cost-effective to invest in development of an automated culture system optimised for the envisaged process, rather than using (adapting) the currently available SelecT system. It should be noted that cost of GMP-compliant serum supplements and complex media required for certain cell types (e.g. stem cells) may substantially increase media costs above those considered here. Development of a cost-effective culture medium suitable for autologous smooth muscle cells is very important to process economics, and examination of alternative culture flask and culture train configurations (e.g. roller bottles) may enable a reduction in consumables costs. Cell culture costs could also be significantly reduced by decreasing the number of cells in the formed tissue (reduce cell density, tissue volume); studies determining the minimum tissue volume/cell density required for product efficacy would be useful to ensure that the product is not 'over-engineered' resulting in high manufacturing costs.

Table 5-2. Estimated basic cell culture costs per patient unit. Cell culture consumables costs (flasks and process fluids) are based on standard commercially available supplies at 2005 prices (section 2.5.3.). Volumes of process fluids (media, trypsin, buffers) were as for standard cell culture protocol used in experimental studies. One 'unit' is a product batch for the treatment of a single patient. Cost data were generated based on cell culture trains for the 'operating line' in each case.

| Quantity | Case (1) | Case (2) | Case (3) | Rationale |
|---|---|---|---|---|
| | | | | |
| Windows case | (B) | (C) | (C) | See figure 5-1b,c. |
| **Downstream process yield** (%) | 50 | 95 | 95 | " |
| Process **throughput** (units) | 2 | 4 | 4 | " |
| **Biopsy size** (cm of vein) | 4 | 6 | 2 | " |
| **Number of passages** | 5 | 4 | 5 | " |
| Total cell culture area ($10^3$ $cm^2$) | 10.8 | 5.3 | 5.4 | Culture trains within windows analysis |
| No. cell culture robots required in UK | 39 | 20 | 20 | ~28,000 units/year in UK during 1997-2001 [Keogh and Kinsman, 2002]. |
| Capital cost of cell culture robots (£M) | 23.4 | 12 | 12 | SelecT culture systems cost ~ £0.6M each |
| Cost of cell culture robot (£/unit) | 89 | 45 | 45 | Cost annualised over ten years, plus £5k/yr service |
| Ratio of flask cost to media cost | 2.5 | 2.5 | 2.5 | Calculated from cost data and culture trains |
| Cost of cell culture consumables (£/unit) | 294 | 155 | 158 | Culture flasks and process fluids only |
| Total cost estimate for cell culture (£/unit) | 383 | 200 | 203 | Calculated |
| Ratio of consumables cost to robot cost | 3.3 | 3.4 | 3.5 | Calculated |

### 5.1.4. Summary

The 'windows of operation' analysis indicates that it is feasible to generate sufficient cells for the stipulated tissue formation process from a small biopsy, using an automated cell culture system. Substantial improvement in process yields (to >90% overall) is highly desirable as this enables choice between alternative processing schemes and significantly reduces cell culture apparatus (capital) and consumables (operating) costs. If large improvements in downstream process yield (above 50%) are impracticable, process feasibility may be maintained, although cell culture costs would be high. Reduction in cell culture costs could otherwise be achieved by optimising the design of process apparatus, cell culture trains and the tissue product itself.

This analysis has demonstrated the utility of a graphical 'windows of operation' approach to (1) examine feasibility of alternative manufacturing scenarios for a tissue engineering process, using predicted process parameters and design constraints; (2) visualise and rationalise the complex design problems associated with novel cell and tissue manufacturing processes (3) generate information (including design targets) which may be used to inform and direct further process and/or product development efforts early in the development cycle. An extended analysis examining all process steps from biopsy harvest to surgical use would be useful in clarifying major processing issues and the scale and balance of costs over the whole process. Such an analysis could help to ensure that process development efforts may be directed to the highest priority targets, in terms of achieving optimum product functionality, manufacturing efficiency and process economics.

## 5.2. Process design issues and strategy

This section aims to discuss key findings in the thesis in terms of major issues for consideration in the design of processes and processing systems and appropriate strategies for development of design heuristics.

### 5.2.1. Process yield

It has been shown that one of the most important factors in determining the overall feasibility and economy of cell processing is achieving very high yield of healthy cells across each process operation. The main factors encountered in this work which are expected to affect yield, health and uniformity of cell suspensions throughout the process are: hydrodynamic damage, biochemical stress, cell surface adhesion and aggregation. Once established, unit operation performance correlations may elucidate potential trade-offs between yield and other factors such as processing time, although given the importance of achieving very high cell yields terms of predicted process practical and economic feasibility, it is likely that only marginal avoidable losses would be acceptable. Process optimisation would more likely take the form of maximising yield where there is a trade-off between two or more competing loss effects (e.g. high flowrate = shear damage vs. low flowrate = loss by adhesion). Clarifying mechanisms of losses in cell yield and cell heath is very important for the development of robust design bases. Empirical studies simply determining apparent ranges of high yield and associated correlations may become inaccurate if unknown (unmeasured) control factors vary unexpectedly. Developing a good understanding of underlying mechanisms and critical control factors enables a clearer consideration of risks to process performance (e.g. due to variations in process feedstocks) and should enable apparatus and process designs to factor in such risks and thus have a higher level of robustness.

### 5.2.2. Shear stress

As some form of hydrodynamic stress is present in virtually all processing operations, consideration of the impact on cells is required throughout processing. Results indicate that laminar capillary flow can cause cell lysis and possibly cause sub-lytic cell damage resulting in delayed cell death, and that surviving cells are able to grow normally. While shear studies were limited to capillary geometry, the effects of shear stress (and magnitude of effects at a given shear stress) are likely to be reasonably consistent throughout processing; the correlation between prediction of approximate shear stresses

and damage levels during pellet resuspension supports this assertion. Thus information gained on appropriate shear stress levels in one environment (e.g. capillary flow) may be used as a guide to determining process conditions in other process operations (e.g. pellet resuspension, tissue formation). Development of suitable models or correlations for shear stress levels in various process operations and process regimes (e.g. very diluted and concentrated cell suspensions) and correlation of all results against a specific investigative situation (e.g. capillary flow) should enable development of quantitative design bases for conditions throughout the process requiring only a single assessment procedure for calibration.

The range of shear stresses associated with both capillary flow and cell concentration (i.e. pellet resuspension) investigations included conditions resulting in relatively low levels of mechanical cell damage. These results are very promising as they suggest that, generally speaking, smooth muscle cells are likely to be sufficiently robust to retain membrane integrity at processing stresses of the order of magnitude associated with desired process conditions (i.e. suspension transfer time and pellet resuspension intensity), although other cell types (e.g. stem cells) may be more sensitive to shear.

### 5.2.3. Cell surface adhesion

Results from shear studies indicate that, below a certain surface shear stress, cells may attach to apparatus surfaces. Calculations predicted that the number of cells which could be lost in a cell monolayer is of the order of fluid-surface contact area in experimental studies. Thus cell loss by surface adhesion is a potentially serious problem which must be addressed. An appropriate strategy would be to clarify the mechanistic basis of cell adhesion by characterising cell surface properties responsible for surface interactions, such as charge, hydrophobicity etc.. By understanding which cell properties may affect surface adhesion, it should be possible to target likely candidate low-adhesion materials or coatings for experimental trials. A related issue is indiscriminate loss of material due to hold-up (wetting), which could be minimised by surface materials selection, minimisation of surface contact area and contact area to volume ratio in fluid lines, and controlled positive displacement of materials from flow lines with a suitable fluid.

### 5.2.4. Cell aggregation

Cell aggregation has been observed as a recurrent phenomenon throughout experimental work; cells in suspension tended to aggregate if left undisturbed. Observations

suggested that secreted matrix deposits carried over from cell culture may be responsible for formation of large flocs during cell concentration. The primary strategy would be to prevent large floc formation by determining and optimising for cell culture and harvest parameters which may influence this process. Alternative strategies such as filtering out large flocs or shear-induced break-up may also be explored as necessary. Formation of aggregates in cell suspension might also be mediated by non-matrix related interactions. Cell pellets may largely be resuspended to single cell suspensions and as such any 'non-matrix related' aggregate formation is likely to be a reversible process. Examination of cell surface properties and the kinetics and energetics of such cell interactions should provide a fundamental understanding of this type of aggregation process, enabling generation of strategies for the prevention, control and/or reversal of such aggregate formation. The issues of cell aggregation, break-up in suspension and rheology of cell suspension are linked, particularly in concentrated cell suspensions where intercellular interactions will dominate these phenomena and may also influence mechanisms of flow-associated cell damage.

### 5.2.5. Rheology

Rheology of process materials (fluids) is an important engineering fundamental which has relevance in many areas of processing, such as transfer, mixing, dispersion (pellet resuspension) and various tissue formation or seeding techniques. Rheology also has a direct impact on the magnitude of hydrodynamic stress under given flow conditions. Experimental studies showed that adherent RSMC cell suspensions behave approximately as would be expected for other cell types. Further development of design heuristics for process operations where rheology is a major factor can thus utilise the established body of knowledge for cell, and other similar, suspensions. Investigating aspects of cell suspension rheology such as shear-thickening, time-dependence and viscoelasticity is also appropriate for process materials characterisation, which may lead to discovery of unusual or unexpected suspension behaviours. Examining time-dependence of rheology in particular may provide information on intercellular interactions controlling cell aggregation and aggregate break-up in suspension. A good understanding and detailed consideration of these aspects of rheology is likely to be important in the development of models enabling design and fine control of process operations such as dynamic tissue formation (e.g. rod coating with cell suspension to form a tube) and tortuous network flow through porous scaffolds during seeding.

### 5.2.6. Biochemical stress

Biochemical stress is a complex issue which may adversely affect cells at any stage of processing. Principal concerns are maintaining 'safe' and/or 'optimal' concentration ranges for important biochemical species (e.g. oxygen, glucose, amino acids, growth factors, lactate, ammonia) and other factors (e.g. pH, osmolarity). In traditional large-scale cell culture (i.e. bioreactors), many such parameters may be monitored with feedback control. In the case of scale-out of tissue engineering (e.g. autologous tissue maturation), monitoring and control may be more difficult to implement due to requirements for maintenance of closed sterile systems and the potentially high cost and complexity of multiple instrumentation systems. It is desirable to develop a very high level of knowledge and understanding of the behaviour of such systems, with the aim of developing processes with minimal monitoring and control requirements, and/or implementing non-invasive strategies. For example, if the cell source is reproducible and the nutrient requirement profile for cells in a developing tissue construct (or concentrated cell suspension) can be well characterised during development, this may provide the design basis enabling implementation of a defined feeding strategy or media formulation which can supply all requirements, eliminating the need for online control in the manufacturing process.

It has been shown that, without supply, oxygen depletion could potentially occur rapidly during processing of cell pellets or concentrates. As monitoring and control of oxygen levels within cell pellets and suspension transfer pipework would be difficult, this type of 'hands-free' strategy should be implemented to ensure oxygen levels are maintained within appropriate limits. Other factors modulating biochemical activity (e.g. temperature) may also be investigated for effect on cells and potential process utility.

### 5.2.7. Characterising cellular response

Shear sensitivity of cells and concentration process performance has been evaluated on the basis of the most palpable parameters such as cell yield, membrane integrity, and simple characteristics of growth and metabolism. While this represents a good starting point for engineering design studies, the regenerative capacity of cells relies on the preservation or induction of a variety of cellular functions not assessed thus far. In order to develop design bases which take account of more subtle cellular responses to stress, and which can be used to specify processes such that appropriate cell functions are maintained, more sophisticated analytical techniques are required which can identify and quantify non-lethal responses to various process conditions (including hydrodynamic and biochemical stress). Developing a clear understanding of more subtle cellular responses to a range of processing conditions may elucidate specific indicators of cell health and function which are more suitable for routine measurement in a process environment.

## 5.3. Process validation

The aim of this section is to discuss the status and future strategy for the model tissue process with respect to establishing a validated process and achieving regulatory approval. While the overall validation process for a novel product encompasses demonstration of reliable efficacy of product, apparatus and process, the scope of this discussion is mainly limited to the key validation issues at the current stage of process development as considered in this work.

### 5.3.1. General

Process validation is defined by the US Food and Drug Administration as "establishing by objective evidence that a process consistently produces a result or product meeting its predetermined specifications" [F.D.A. 21 CFR Part 1271, 2001]. Process validation generally entails exhaustive equipment and process qualification studies and generates large amounts of documentation as required evidence. While thorough process validation may be perceived as a burden, it is an important aspect of a 'total quality' process management approach whereby product quality is paramount. Regulatory guidelines may be viewed as welcome assistance for process development engineers aiming to ensure consistently high process performance and product quality with zero batch failure rate, providing associated benefits for process economics and business performance.

Validation of a new processing facility comprises three main phases. Apparatus installation qualification (IQ) and operational qualification (OQ) establish confidence and provide documented evidence that the process equipment and ancillary systems are capable of consistently operating within established limits and tolerances, performing as intended throughout anticipated operating ranges. Performance qualification (PQ) generates the documented evidence that the process, operated within established parameters, performs effectively and reproducibly to produce a product meeting its predetermined specifications. Typically for biopharmaceutical production this involves manufacturing three batches of product at full-scale and providing documented evidence of conformance throughout the process and final product.

However, the model process considered in this work is at an early stage of development and as such efforts must be focused towards establishing product/process specifications and quality attributes and a high level of reproducibility in process performance within suitable tolerances. Generally, in order for a processing operation to operate reliably

within the (relatively narrow) tolerances suitable for achieving regulatory approval, it is necessary to achieve a good understanding of process control mechanisms and parameters and process sensitivity to variation in these parameters. This will enable characterisation of allowable tolerances for both control parameters and performance of the various operations throughout the process. By planning for validation during development and application of design bases for various operations (i.e. 'design for validation') it is generally possible to design a robust process.

### 5.3.2. Automated systems

Validation of automated systems performance (hardware and software) will generally take place as part of the IQ/OQ procedures. However at the development stage it is appropriate to verify performance and lifespan of components and systems, typically including exhaustive repeat-cycle testing for standard process operations (e.g. aspirate, dispense, robotic arm movements) and monitoring any component wear or drift in performance characteristics such as accuracy, precision and speed. In addition it is prudent to design in and test system tolerances to potential failure modes, such as challenging systems with mains electricity failure and excessive process variations. Good manufacturing practice (GMP) rules require comprehensive process monitoring documentation and record-keeping. Fortunately, for automated systems computers can take over much of this work; this is done in so-called Manufacturing Execution Systems (MES). These dedicated computer systems can monitor and control all product and information flows, the production environment and production processes in the facility [Dorresteijn et al., 1997]. Such systems must comply with requirements such as F.D.A. regulations on electronic records and signatures [F.D.A. 21 CFR part 11, 2003].

### 5.3.3. Process feedstocks

Variability of process feedstocks is likely to have a direct impact on process performance as so is a critical issue for validation. It is envisaged that the majority of supplies such as media, flasks, scaffold etc. could be obtained from reputable sources which implement meticulous validation procedures and provide the attendant documentation. As autologous cellular feedstocks may be inherently variable, with biopsy collection procedures likely to take place in a clinical environment outside the control of the processing facility, understanding process sensitivity to variation in quality and size of biopsies is a high priority. While an approach has been demonstrated

in this work to perform predictive analysis of process feasibility in relation to biopsy size as a fixed parameter, the issue of variability on a patient-to-patient basis remains unresolved. Development, validation and implementation of responsive processes (e.g. increase culture time for small biopsy or slow growing cells) is unlikely to be straightforward in an automated GMP facility and may be prohibitively complex. Therefore it is necessary to examine the expected nature and extent of biopsy variability and compare this against studies of the sensitivity of the process to such variation. As biopsy variation could potentially cause compliance problems later in the process, it will be necessary to establish appropriate quality attributes and tolerances for incoming biopsies and implement a screening system to ensure 'early failure' of unsuitable specimens.

### 5.3.4. Cell aggregation and surface adhesion

Aggregation of cell suspensions as observed in experimental work is potentially quite a serious hurdle in terms of achieving process validation. As this phenomenon was observed to be highly variable during cell concentration and is neither well characterised nor well understood, either in terms of mechanisms or control variables, it represents a high risk to reproducible process development and regulatory approval. Investigating aggregation and achieving a good level of understanding of mechanisms and control is thus a high development priority to ensure validation can be achieved. While cell losses attributed to surface adhesion were observed qualitatively to be less variable than apparent cell loss due to aggregation, surface adhesion must also be investigated thoroughly to achieve the required level of understanding and control.

### 5.3.5. Rheology

As discussed above (section 5.2.5.), rheology of cell suspensions is likely to be an significant factor in a variety of process operations. In order to establish the importance of rheology as a control variable, and establish tolerances at various processing stages, it is necessary to investigate the impact of changes in rheology on process performance. Combining the results of such studies with suitable design models for various operations, it may be possible to specify process operations such that variations in rheology are tolerated (e.g. increase specified mixing time such that good mixing is achieved throughout the conceivable range of suspension rheology), thus removing the need for fine monitoring and control of rheology in such instances. Alternatively, if

rheology is found to be a critical control parameter, e.g. for tissue formation, it may be necessary to monitor rheology and/or the associated process to ensure tolerances are not exceeded. As cell suspension rheology is a strong function of cell concentration, measurement of rheology could potentially be used for in-process monitoring of cell concentration. In order to achieve validation of such a monitoring technique, it would be necessary to develop a clear understanding of the influence of cell aggregation and/or flocculation on rheology such that relatively simple rheology measurements could be proven to provide definitive information about the nature and composition of cell suspension.

### 5.3.6. Specific operations

In this work initial studies have been performed examining performance of cell suspension transfer (capillary aspirate-dispense) and cell concentration (centrifuge-resuspend). These studies have elucidated several potentially important design and performance control factors, i.e. shear damage, centrifugation parameters, cell loss by adhesion, cell aggregation, and oxygen depletion. Generally, characterisation of these factors has been empirical, predictive or qualitative, range-finding or elucidating important processing issues which must be addressed thoroughly for any specific process. More detailed studies will be required to achieve the level of mechanistic and/or empirical understanding and clarification of quality attributes, control factors and tolerances, as required to establish and prove sufficient reproducibility in processing.

### 5.3.7. Cell and tissue monitoring and quality assurance

Due to the inherent complexity of cells and cellular or tissue products and difficulties associated with maintaining sterility and invasiveness of testing, production monitoring systems and release tests are likely to be somewhat limited in their ability to characterise process materials or the final product. A lack of sophisticated monitoring in the production process may be mitigated by development and demonstration of a high level of process/product understanding and reproducibility and robustness in manufacture. In order to enable experimental studies establishing a suitable level of understanding of process performance in terms of process impact on cellular materials (e.g. effects of biochemical stress, shear stress) and allowable tolerances, it is necessary to develop definitive quality attributes for cell health and regenerative function. Lack of detailed characterisation of cellular materials or products in-process may be mitigated

by application of exhaustive analytical techniques during process research and development, followed by a reduction of the 'research analytical toolkit' to simpler indicators of process performance or product quality attributes. Final process specifications (for monitoring and validation) could then be based around the simplified indicators, along with associated procedures for assay calibration and validation. In order to establish practicable and economic monitoring systems for process monitoring and validation, a reasonable compromise between exhaustive and minimal characterisation of process materials and product must be established through dialogue with regulators. This process of dialogue is especially important in the field of cell and tissue therapies where both regulators and developers may be uncertain as to the appropriate level of characterisation required for validation in this new class of complex processes and products.

### 5.3.8. Final remarks

At this early stage of development of cell and tissue products, processes and regulation thereof, establishing sufficient, practicable, quality attributes is a key issue which must be addressed as a high priority. To ensure timely and efficient achievement of regulatory approval for products and processes, it will be essential to establish a dialogue and build a rapport with regulators, planning for validation accordingly from the early stages of process development. Where products are intended for manufacture and sale in multiple countries, it will be essential to consider diverse regulatory requirements and procedures for all target markets to avoid or minimise requirements for process redevelopment and revalidation, enabling rapid international 'roll-out' of product. Once quality attributes meeting with 'preliminary approval' with are in place and key process control mechanisms and parameters have been clarified, development work can proceed to sensitivity investigations determining process/product response to variation in control factors and thus establish suitable tolerances for quality attributes and control parameters throughout the process. Final process and product specifications may then be established and formulated along with the required documentary evidence of process performance. Overall achieving validation of novel cell and tissue processes is likely to be a complex and laborious process, but, if approached systematically from the early stages of development through setup and implementation of a 'validation master plan', 'design for validation' can be integrated as a natural part of process

development to achieve a 'right first time' process design with a high level of robustness, reproducibility and product quality.

## 5.4. Conclusions

The primary aims of this project were to work towards developing engineering design bases for automated cell and tissue therapy manufacturing processes and process systems, demonstrate proof of principle for an automated cell concentration protocol and illustrate the utility of predictive feasibility studies in aiding direction of research and development work.

Early capillary shear studies showed that repeated exposure to high laminar capillary shear stress (>100 Pa) caused substantial cell loss by catastrophic cell lysis, consistent with literature reports, and indicated that cell loss was occurring at very low shear stress (2 Pa). Surviving cells were able to grow normally, with no significant changes in growth rate or metabolism. The manual trypan blue dye exclusion test used (for cell membrane integrity) was found to be too variable for precise measurements, such that small changes in cell populations could not be detected with confidence. The flow cytometry assay developed yielded significant improvements over the trypan blue assay in terms of speed (2-fold), precision (4-fold), removal of operator subjectivity and increased resolution between intact and permeable cells.

Subsequent capillary shear studies (utilising the flow cytometry assay) confirmed that cell loss was occurring at low shear stress (<2 Pa) and was not associated with cell damage; low shear cell loss was attributed to cell adhesion to apparatus surfaces. Low-level cell damage occurred at moderate to high shear stress (35-75 Pa), with no significant cell damage or loss occurring at low to moderate shear (2-25 Pa). Reduction in the magnitude of cell damage in the second round of capillary shear studies was attributed to changes in experimental setup, principally the use of customised capillaries with polished entry and exits, leading to a reduction in end effects during capillary flow. Overall, results indicated that some background cell loss (≤10%) was occurring; this loss was attributed to cell adhesion to apparatus surfaces. The recommended range of shear stress for maximal yield of cells in capillary flow is 5-25 Pa and represents a good design basis for specification of pipe sizes and flowrate combinations for relatively dilute (volume fraction < 0.02) cell suspensions.

Rheological studies of adherent cell suspensions indicated that they may be described as Power law fluids i.e. they exhibit shear thinning behaviour. Coupled with a measured value for volume mean cell size (diameter 22.4 μm) enabling conversion from cell concentration to cell volume fraction, results indicated that rheological behaviour of

concentrated cell suspensions (volume fraction $\leq 0.34$) was similar to other cell suspensions previously examined in the literature. Reference to previous work indicated the possibility of unexpected shear thickening behaviour at high cell concentration, which may have implications for altered shear damage mechanisms in this regime. Observed reduction in concentrated suspension apparent viscosity following exposure to increased shear rates (in the rheometer) revealed that changes in suspension micro-structure can occur due to shear; these changes show that cell-cell interactions are a factor in controlling concentrated suspension rheology.

Predictive calculations showed that oxygen depletion is likely to occur in cell pellets and concentrated cell suspensions during processing unless preventative measures are taken. Quantification of cell characteristics (oxygen uptake, hypoxia sensitivity) will enable systematic evaluation of the severity of oxygen depletion and preventative strategies.

Development and performance characterisation of semi-automated cell concentration procedures demonstrated proof of principle for the application of process automation to this unit operation. The initial semi-automated cell concentration protocol was refined on the basis of a theoretical analysis of cell sedimentation, reduction in process time (to reduce oxygen depletion), reduction in resuspension intensity (to reduce shear damage) and reduced variation in process control parameters. The final semi-automated cell concentration protocol provided significantly improved intact cell yield and a reduction in process variability compared to the initial semi-automated method. Concentration procedures achieved cell volume fractions of ~0.3-0.4 in the wet pellet, indicating that tissues could be formed or seeded with cells at the approximate volume fraction found in native tissues. Substantial aggregation was often observed following cell concentration and was attributed to carry-over of secreted matrix deposits from cell culture. Due to the high variability observed in aggregate formation and the potential impact on (risk to) the downstream processes, developing understanding and control of this phenomenon is a high priority. Provided cell aggregation can be controlled, further development of cell concentration design bases and procedures is expected to enable design of fully automated apparatus and protocols exhibiting high intact cell yield and high reproducibility, suitable for application in therapeutic manufacture processes.

The 'windows of operation' analysis demonstrated that development of the stipulated autologous process is likely to be feasible with a reasonable biopsy size, and using currently available automated cell culture technology. Application of this type of

analysis or alternative feasibility studies has utility in terms of assessing process feasibility, visualising and rationalising design of complex cell and tissue processes, and generating process development targets early in the development cycle. In addition the analysis has highlighted the importance of developing process technology capable of achieving very high cell yield and associated practical and economic implications for the process considered.

Overall, the level of sophistication of experimental and design studies in this work has reflected the very early stage of development of application of established engineering design principles in the field of tissue engineering and cell therapy. In terms of process design the field is at the stage where the key quality attributes for process materials (including products), mechanisms governing process performance and key control parameters are, at best, under investigation. The general approach to systematic development of engineering design bases has been a recurring theme through this work and it is believed that both industry and academia must embrace this approach to engineering research and development of process technology in order to build the 'engineering toolkit' required to enable rapid, rational design of cost-effective and validatable cell and tissue processes.

## 5.5. Further work

It is desirable to develop shear damage correlations for various process operations (e.g. resuspension, tissue formation) and correlate them against a single investigative technique such that all shear-related design bases may be calibrated for any cell type with a single assessment of shear sensitivity. Ideally an ultra-scaledown technique would be developed such that only a small sample of cells is required, enabling characterisation of the sensitivity of a wide range of cell types relevant to cell and tissue therapies, rapidly and at low cost. The influence of shear exposure time on cell damage requires clarification as this may have important design implications in terms of geometrical design of process apparatus i.e. length of flow lines. The relationship between shear sensitivity and cell size should be investigated; as the largest cells in a population may be more susceptible to shear damage and account for a relatively large proportion of cell volume (mass), loss of relatively few large cells may have a substantial impact on cell yield on a volume (mass) basis. Such studies might be carried out using flow cytometry, FACS or light scatter particle sizing systems. Investigation of potential alternative mechanisms of shear damage at high concentration (where cell-cell interactions dominate) is vital due to the occurrence of highly concentrated cell suspensions during cell concentration and their potential application in tissue formation or seeding. At some stage it will be necessary to develop and apply a more sensitive assay toolkit than used in this work to detect subtle cellular responses to shear effects.

Further studies should be carried out to investigate cell suspension viscoelasticity due to potential relevance to various tissue formation techniques. Also time-dependant or irreversible changes in rheology should be examined with a view to characterising shear-induced changes in suspension micro-structure and relationship with cell-cell interactions. Such studies may also yield design information relating to control over aggregation and aggregate break-up in shear flow. It is necessary to investigate possibility of shear thickening properties of concentrated cell suspensions and any implications for alternative shear damage mechanisms in this regime. Due to the cost and practicality of growing large quantities of directly relevant cell types (i.e. adherent cells, stem cells), such studies will require development of either scale-up mimics (e.g. using suspension cells such as hybridoma cells) to allow use of conventional rheometry systems, and/or development of scale-down rheometry techniques to enable such studies to be carried out with very small quantities of cells.

Surface properties of cells should be characterised (e.g. charge, hydrophobicity, zeta potential) with a view to understanding mechanisms of aggregation and surface adhesion and developing control strategies for these phenomena. Definitive evidence is required to either confirm or deny the stipulated mechanism of cell loss by surface adhesion; this could include microscopic evidence of cell surface adhesion and/or development of parallel plate flow systems enabling video imaging of cell-surface interactions during flow. In addition investigation of the influence of various materials with different surface characteristics such as charge, hydrophobicity and roughness, may aid selection of materials appropriate for manufacturing systems. Development of a high-throughput experimental system (e.g. microwell based) to investigate the effect of various cell culture parameters on magnitude and variability of subsequent cell aggregation should lead to an empirical, or more detailed, understanding of culture parameters influencing this phenomenon and elucidate any suitable preventative measures. In addition alternative strategies for handling formation of large aggregates such as filtering out or shear-induced break-up may be considered and investigated in terms of implications for healthy cell yield and process variability.

Development of an engineering design basis for cell concentration requires characterisation of the influence of concentration process parameters (i.e. sedimentation force and time, resuspension intensity and time) on cell yield, health and process variability. As the coupled centrifuge/resuspend process is multivariate, it is a good candidate for application of statistical 'Design of Experiments' approaches initially to 'decoupled' centrifugation and resuspension operations and subsequently to the combined operation. Further investigation is required to determine mechanisms of deleterious effects on cells during concentration, e.g. relative magnitudes of hypoxia effects (in the pellet) vs. shear effects (during sedimentation and/or resuspension). Development of quantitative models or correlations for deleterious processes would enable optimisation of process conditions.

In order to generate definitive understanding of the magnitude and impact of potential oxygen depletion in cell pellets and concentrated suspensions, it is necessary to characterise the oxygen uptake rates of relevant cell types under various process conditions (e.g. while adherent, range of suspended cell concentration, range of temperature) and develop and apply analytical tools able to detect subtle cellular responses to such conditions, including hypoxia. Analytical methods should probe general cellular response and specific regenerative functional capacity of the cells;

potential candidates include genomic and proteomic techniques. Ultimately it is desirable to elucidate 'simpler' indicators of subtle cellular response and functional capacity such that quality attributes of cellular process materials can be monitored practicably in the manufacturing process environment.

Development of predictive design tools to the next level of sophistication, enabling detailed process performance sensitivity analyses based on changes in process control parameters, will require establishment of quantitative performance correlations for various operations in the process. More detailed studies of manufacturing costs throughout the process are required in order to enable (1) process design decisions to be made on the basis of cost-efficiency (2) accurate prediction of overall manufacturing costs for prediction of product economic feasibility and business planning purposes.

## Appendix A: Glossary of abbreviations

| | |
|---|---|
| 7AAD | 7-Aminoactinomycin D |
| ATCC | American tissue culture collection |
| BHK | Baby hamster kidney (cells) |
| CFR | Code of federal regulations (US F.D.A.) |
| cGMP | Current good tissue practice |
| cGTP | Current good manufacturing practice |
| CHO | Chinese hamster ovary (cells) |
| CV | Coefficient of variation (%) (Standard deviation as % of mean) |
| DMEM | Dulbecco's modified Eagle's medium |
| DNA | Deoxyribonucleic acid |
| EC | Endothelian cell(s) |
| EDTA | Ethylenediaminetetraacetic acid |
| ES | Embryonic stem (cells) |
| EU | European Union |
| FACS | Fluorescence-activated cell sorting |
| FB | Fibroblast(s) |
| FBS | Fetal bovine serum |
| F.D.A. | Food and Drug Administration (United States) |
| FDA | Fluorescein diacetate |
| FS | Forward angle light scatter (forward scatter) |
| GMP | Good manufacturing practice |
| GTP | Good tissue practice |
| HVAC | Heating ventilation air conditioning |
| ID | Internal (pipe) diameter |
| ISO | International standards organisation |
| IQ | Installation qualification |
| LDH | Lactate dehydrogenase |
| MES | Manufacturing execution system(s) |
| MSC | Mesenchymal stem cells |
| OQ | Operational qualification |
| OUR | Oxygen uptake rate |

| | |
|---|---|
| Pa | Pascals. Equivalent units to $N/m^2$ (Newtons per metre squared) |
| PBS | Phosphate buffered saline |
| PGA | Polyglycolic acid |
| PI | Propidium iodide |
| PLA | Polylactic acid |
| PLGA | unspecified copolymer of polylactic acid and polyglycolic acid |
| PQ | Performance qualification |
| RCF | Relative centrifugal force |
| $Re_f$ | Reynolds number for a shaking flask (no units) |
| $Re_p$ | Reynolds number for pipe flow (no units) |
| RPM | Revolutions per minute |
| RSMC | Rat aortic smooth muscle cells (as used in experimental studies) |
| SelecT | A commercially available robotic cell culture system (The Automation Partnership, Cambridge, UK) |
| SMC | Smooth muscle cells |
| SOP | Standard operating procedure |
| SS | Side angle light scatter (side scatter) |
| UK | United Kingdom |
| US or USA | United States of America |
| VAT | Value added tax (UK, 17.5%) |

## Appendix B: Nomenclature

Greek symbols

| | |
|---|---|
| $\rho$ | Fluid density ($kg/m^3$) |
| $\rho_f$ | Density of suspending fluid ($kg/m^3$) |
| $\rho_o$ | Density of particle, being cells in this case ($kg/m^3$) |
| $\mu$ | Fluid viscosity ($N.s/m^2$) or (Pa.s) |
| $\mu_b$ | 'Bingham viscosity' ($N.s/m^2$) or (Pa.s) |
| $\mu_o$ | Diluent (suspending fluid) viscosity where $\phi = 0$ ($N.s/m^2$) or (Pa.s) |
| $\mu_r$ | Relative suspension viscosity (relative to diluent viscosity) |
| $\mu_s$ | Suspension viscosity |
| $\phi$ | Solids (i.e. cell) volume fraction (v/v) |
| $\gamma$ | Shear rate ($s^{-1}$) |
| $\tau$ | Shear stress ($N/m^2$ or Pa) |
| $\tau_w$ | Wall shear stress ($N/m^2$ or Pa) |
| $\tau_y$ | Bingham yield stress ($N/m^2$ or Pa) |
| $\Delta P$ | Pressure drop in pipe flow ($N/m^2$ or Pa) |

Other

| | |
|---|---|
| A | Equivalent cell culture area required at final passage ($cm^2$) |
| $A_n$ | Total culture flask area of passage 'n' |
| $B_n$ | Biopsy size required to supply sufficient cells to seed passage 'n' |
| C | Correlation constant (shear stress in shaking flasks) |
| c | Cell concentration (cell/L) |
| $C_B$ | Cell density yielded from biopsy (cell/cm [of surface vein]) |
| $c_{f\ [or]}\ C_H$ | Cell density in culture flasks at harvest (cell/$cm^2$) (confluent cell density) |
| $C_H$ | Confluent cell density (at harvest) (cell/$cm^2$) |
| $c_{max}$ | Theoretical cell concentration at $\phi = 1.0$ ($1.71 \times 10^8$ cell/mL) |
| $C_S$ | Cell seeding density in culture flasks (cell/$cm^2$) |
| $c_t$ | Cell density in formed tissue (cell/mL) |
| d | Capillary internal diameter (m) |
| d | Maximum internal diameter of shaken vessel (m) |
| $D_c$ | Robot downtime factor for changeover and cleaning (no units) |
| $D_m$ | Robot downtime factor for maintenance (no units) |

| | |
|---|---|
| $f_u$ | Maximum number of culture flasks per patient unit (flasks/unit) |
| g | Force of gravity (9.81 $m/s^2$ or N/kg) |
| h | Height of fall (m) [sedimentation distance] |
| k | Consistency index (for fluid with power law characteristics) ($Pa.s^n$) |
| $k_c$ | Growth rate of cells (1/h) |
| n | Orbital shaking speed (1/s) |
| n | Power law index (for fluid with power law characteristics) (-) |
| $n_c$ | Cell number density ($cm^{-2}$) [surface attached cells] |
| $n_{c0}$ | Initial viable cell number density ($cm^{-2}$) [surface attached cells] |
| $N_H$ | No. cell required in the final passage harvest (cell) |
| $N_T$ | Number of cells required in the formed tissue (cell) |
| OUR | Oxygen uptake rate ($g.cell^{-1}.h^{-1}$) |
| r | Radius of gyration for a shaking system, i.e. orbital throw (m) |
| r | Radius of particle, in this case a cell (m) |
| RCF | Relative centrifugal force (no units) |
| $Re_f$ | Reynolds number for a shaking flask (no units) |
| $Re_p$ | Reynolds number for pipe flow (no units) |
| s | Oxygen solubility in suspending fluid ($g.L^{-1}$) |
| $S_n$ | Total number of cells required to seed passage 'n' |
| T | '**Throughput**' ([patient] **units** [on a per robot per day basis]) |
| t | Predicted time to oxygen depletion (h) |
| t | Sedimentation time (s) |
| t | Time in culture (h) |
| $t_d$ | Total time per day (min) |
| $t_f$ | Processing time required per flask (min/flask) |
| $t_p$ | Total available cell culture processing time [per robot per day basis] (min) |
| $t_u$ | Total available cell culture processing time [per patient unit] (min/**unit**) |
| u | Superficial fluid velocity (m/s) [mean fluid velocity in pipe flow] |
| v | Cell volume (L/cell) |
| V | Volume of particle ($m^3$) ; volume of a sphere = $4/3.\pi.r^3$ |
| $V_{pc}$ | Volume of wet cell pellet per cell (μL) |
| $V_t$ | Volume of formed tissue (mL) |
| $Y_d$ | 'Downstream' process yield factor |
| $\Delta P$ | Pressure drop in pipe flow (Pa) |

## Appendix C: Errors and statistics

Errors:

In many experimental studies, quantities reported were calculated by algebraic manipulation of raw data gathered. 'Source' or 'raw' errors were taken as standard deviations of assay replicates where available, but also included other estimates of measurement accuracy where unavailable (e.g. graduation spacing for fluid volume measurement by graduated pipette). Errors (or error bars) reported were generally propagated according to the formulae given in table 6-1, reproduced from 'Guide to Errors' handbook published by the Chemistry Department, University of Cambridge, UK. In some instances manual estimates of error were required (e.g. estimation of error in the slope of a linearised plot, based on error bars within the plot).

Table 6-1. Propagation of errors resulting from algebraic manipulations

A, B ... are variables with errors dA, dB ... ; c is a known constant.

| Relationship | Error in the result, dX |
|---|---|
| $X = A \pm B$ | $(dX)^2 = (dA)^2 + (dB)^2$ |
| $X = c.A$ | $(dX) = c(dA)$ |
| $X = c.(A.B.C...)$ or $X = c.((A/B).C...)$ | $(dX/X)^2 = (dA/A)^2 + (dB/B)^2 + (dC/C)^2 ...$ |
| $X = c.A^n$ | $(dX/X) = \lvert n \rvert.(dA/A)$ |
| $X = \ln(c.A)$ | $dX = (dA/A)$ |
| $X = \exp(A)$ | $(dX/X) = dA$ |

Statistics:

Quoted $R^2$ values were calculated using the charting 'Trendline' tool in the Microsoft Excel spreadsheet. Standard deviations were calculated using 'Standard Deviation' function within Microsoft Excel software. Student's t-tests (both paired and unpaired) were performed using a web-based t-test calculator, which can be found at

http://www.physics.csbsju.edu/stats/t-test.html

P-values are quoted as returned by the calculator and represent 'probability of the results occurring by chance'. Generally a difference in the mean (between the two data sets tested) is considered to be significant at either the 95% level ($P < 0.05$) or very significant at the 99% level ($P < 0.01$).

## Appendix D: References


Aebischer P, Wahlberg L, Tresco PA, Winn SR. 1991. Macroencapsulation of dopamine-secreting cells by coextrusion with an organic polymer solution. Biomaterials 12: 50-56.

Al-Rubeai M, Singh RP, Goldman MH, Emery AN. 1995. Death Mechanisms of animal cells in conditions of intensive agitation. Biotechnology and bioengineering 45: 463-472.

Al-Rubeai M, Welzenbach K, Lloyd DR, Emery AN. 1997. A rapid method for the evaluation of cell number and viability by flow cytometry. Cytotechnology 24: 161-168.

Altman SA, Randers L, Rao G. 1993. Comparison of trypan blue dye exclusion and fluorometric assays for mammalian cell viability determinations. Biotechnology progress 9: 671-674.

Archer R, Wood L. 1992. Production Tissue Culture by Robots. In: Spier RE, editor. Animal Cell Technology: Developments Processes and Products (11$^{th}$ ESACT Annual Meeting). Butterworth Heinemann. 403-408.

Armstrong RD, Maluta J, Roecker DW. 2001. Portable growth cassette for use in maintaining and growing biological cells. US patent number 6228635.

Armstrong RD, Ogier WC, Maluta J. 1995. Clinical systems for the production of human cells and tissues. Biotechnology 13 (5): 449-453.

Babensee JE, Anderson JM, McIntire LV, Mikos AG. 1998. Host response to tissue engineered devices. Advanced drug delivery reviews 33: 111-139.

Ballica R, Ryu DDY. 1993. Effects of rheological properties and mass transfer on plant cell bioreactor performance: production of tropane alkaloids. Biotechnology bioengineering 42: 1181-1189.

Bankiewicz KS, Bringas J, Pivirotto P, Kutzscher E, Nagy D, Emborg ME. 2000. Technique for bilateral intracranial implantation of cells in monkeys using an automated delivery system. Cell transplantation 9 (5): 595-607.

Barthelmes G, Pratsinis SE, Buggisch H. 2003. Particle size distributions and viscosity of suspensions undergoing shear-induced coagulation and fragmentation. Chemical engineering science 58: 2893-2902.

Bauer J. 1999. Advances in cell separation: recent developments in counterflow centrifugal elutriation and continuous flow separation. Journal of chromatography B 722: 55-69.

Bellamkonda R, Aebischer P. 1994. Review: Tissue engineering in the nervous system. Biotechnology and bioengineering 43: 543-554.

Berger TG, Feuerstein B, Strasser E, Hirsch U, Schreiner D, Schuler G, Schuler-Thurner B. 2002. Large-scale generation of mature monocyte-derived dendritic cells for clinical application in cell factories. Journal of immunological methods. 268:131-140.

Bergers G, Hanahan D. 2001. Cell factories for fighting cancer. Nature biotechnology 19: 20-21.

Biowhittaker UK Ltd. 2003. Biowhittaker cell biology products catalogue. Technical appendix, pp15.5.

Born C, Zhang Z, Al-Rubeai M, Thomas CR. 1992. Estimation of disruption of animal cells by laminar shear stress. Biotechnology bioengineering 40: 1004-1010.

Boyce ST. 2004. Fabrication, quality assurance and assessment of cultured skin substitutes for treatment of skin wounds. Biochemical engineering journal 20: 107-112.

Breuer C K, Shin'oka T, Tanel RE, Zund G, Mooney DJ, Ma PX, Miura T, Colan S, Langer R, Mayer JE, Vacanti JP. 1996. Tissue engineering lamb heart leaflet valves. Biotechnology bioengineering 50: 562-567.

Buchs J, Maier U, Milbradt C, Zoels B. 2000. Power consumption in shaking flasks on rotary shaking machines: 1. Power consumption measurement in unbaffled flasks at low liquid viscosity. Biotechnology bioengineering 68: 589-593.

Burger SR. 2003. GTP/GMP cell engineering for cell and gene therapies. Bioprocessing journal, Jan/Feb 2003: 66-69.

Button MCJ, Barden G, Fuller BJ, Hamilton G. 2002. Optimised extraction of smooth muscle cells from human vein for use in tissue engineered vascular graft. Cardiovascular pathology 11: 5-66.

Caleb BL, Hardenbrook M, Cherington V, Castellot JR. 1996. Isolation of vascular smooth muscle cell cultures with altered responsiveness to the antiproliferative effect of heparin. Journal of cellular physiology 167: 185-195.

Cartmell JS, Dunn MG. 2004. Development of cell-seeded patellar tendon allografts for anterior cruciate ligament reconstruction. Tissue engineering 10 (7/8): 1065-1075.

Carver SE, Heath CA. 1999. Semi-continuous perfusion system for delivering intermittent physiological pressure to regenerating cartilage. Tissue engineering 5 (1): 1-11.

Chisti Y, 1999. Shear sensitivity. In: Encyclopaedia of bioprocess technology. Edited by: Flickinger MC, Drew SW. Wiley and sons. 2379-2403.

Chisti Y. 2001. Hydrodynamic damage to animal cells. Critical reviews in biotechnology 21(2): 67-110.

Christenson L, Mikos AG, Gibbons DF, Picciolo GL. 1997. Biomaterials for tissue engineering: summary. Tissue engineering 3 (1): 71-76.

Cooke MN, Fisher JP, Dean D, Rimnac C, Mikos AG. 2003. Use of stereolithography to manufacture critical-sized 3D biodegradable scaffolds for bone ingrowth. Journal of biomedical materials research 15; 64B(2): 65-9.

Coulson JM and Richardson JF. 1991. Chemical engineering volume II: Particle technology & separation processes. pp700, fourth edition, Butterworth-Heinemann, UK.

Curtis W, Emery AH. 1993. Plant cell suspension culture rheology. Biotechnology bioengineering 42: 520-526.

Dar A, Shachar M, Leor J, Cohen S. 2002. Cardiac tissue engineering: Optimisation of cardiac cell seeding and distribution in 3D porous alginate scaffolds. Biotechnology bioengineering 80: 305-312.

Darzynkiewicz Z, Li X, Gong J. 1994. Assays of cell viability: discrimination of cells dying by apoptosis. Methods in cell biology 41: 15-38.

Devore-Carter D, Morway PF, Weiss EB. 1988. Isolation and characterisation of guinea-pig tracheal smooth muscle cells that retain differentiated function in long-term subculture. Cell and tissue research 251: 325-331.

Doran PM. 1995. Bioprocess engineering principles, Academic Press (London) p207.

Dorresteijn RC, Wieten G, van Santen PTE, Philippi MC, de Gooijer CD, Tramper J, Beuvery EC. 1997. Current good manufacturing practice in plant automation of biological production processes. Cytotechnology 23: 19-28.

du Moulin GC, Stack J, Pitkin Z, Chew-Darke J, Cyr C, White A, Ho L, Shen Y-J, Hamilton D, Davies B, Charles C, Conti E, Liu V. 1994. A 3-year experience of quality control and quality assurance in the multisite delivery of a lymphocyte-based cellular therapy for renal cell carcinoma. Biotechnology bioengineering 43: 693-699.

Ducommem P, Ruffieux P-A, Furter M-P, Marison I, von Stockar U. 2000. A new method for on-line measurement of the volumetric oxygen uptake rate in membrane aerated animal cell cultures. Journal of biotechnology 78: 139-147.

Edwards J. 1998. The Use of Robotics in Cell Culture. European Biopharmaceutical Review, Ballantyne Ross Ltd, London, UK.

Eiselt P, Kim BS, Chacko B, Isenberg B, Peters MC, Greene KG, Roland WD, Loebsack AB, Burg KJL, Culberson C, Halberstadt CR, Holder WD, Mooney DJ. 1998. Development of technologies aiding large-tissue engineering. Biotechnology progress. 14: 134-140.

Farid SA, 2002. A Decision-Support Tool for Simulating the Process and Business Perspectives of Biopharmaceutical Manufacture. PhD thesis, University of London.

Farid SS, Novais JL, Karri S, Washbrook J, Titchener-Hooker NJ. 2000. A Tool for Modeling Strategic Decisions in Cell Culture Manufacturing. Biotechnology progress 16: 829-836.

F.D.A. 21 Code of federal regulations (CFR) Part 11: Electronic Records; Electronic Signatures. 2003.

F.D.A. 21 Code of federal regulations (CFR) Part 1271: Current Good Manufacturing Practice for Manufacturers of Human Cellular and Tissue-Based Products; Inspection and Enforcement; Proposed Rule. 2001.

Feng Y, Yang J-H, Huang H, Kennedy SP, Turi TG, Thompson JF, Libby P, Lee RT.1999. Transcriptional profile of mechanically induced genes in human vascular smooth muscle cells. Circulation research 85: 1118-.

Fiala J, Lloyd DR, Rychtera M, Kent CA, Al-Rubeai M. 1999. Evaluation of cell numbers and viability of Saccharomyces cerevisiae by different counting methods. Biotechnology techniques 13: 787-795.

Foy BD, Rotem A, Toner M, Tompkins RG, Yarmush ML. 1994. A device to measure the OUR of attached cells: importance in bioartificial organ design. Cell transplantation 3 (6): 515-527.

Gooch KJ, Kwon JH, Blunk T, Langer R, Freed LE, Vunjak-Novakovic G. 2001. Effects of mixing intensity on tissue-engineered cartilage. Biotechnology bioengineering 72: 402-407.

Grenier G, Remy-Zolghadri M, Guignard R, Bergeron F, Labbe R, Auger FA, Germain L. 2003. Isolation and culture of three vascular cell types from a small vein biopsy sample. In vitro cell developmental biology – animal 39: 131-139.

Griffith LG, Naughton G. 2002. Tissue engineering – current challenges and expanding opportunities. Science 295: 1009-1014.

Halayko AJ, Solway J. 2001. Molecular mechanisms of phenotypic plasticity in smooth muscle cells. Journal of applied physiology 90 (1): 358-368.

Halberstadt CR, Hardin R, Bezverkov K, Snyder D, Allen L, Landeen L. 1994. The in vitro growth of a three-dimensional human dermal replacement using a single-pass perfusion system. Biotechnology bioengineering 43: 740-746.

Hauselmann HJ, Masuda K, Hunziker EB, Neidhart M, Mok SS, Michel BA, Thonar EJMA. 1996. Adult human chondrocytes cultured in alginate form a matrix similar to native human articular cartilage. American journal of physiology 271 (Cell physiology 40): C742-C752.

Hokugo A, Kubo Y, Takahashi Y, Fukuda A, Horiuchi K, Mushimoto K, Morita S, Tabata Y. 2004. Prefabrication of vascularized bone graft using guided bone regeneration. Tissue engineering 10 (7/8): 978-986.

Honiger J, Sarkis R, Baudrimont M, Delelo R, Chafai N, Benoist S, Sarkis K, Balladur P, Capeau J, Nordlinger B. 2000. Semiautomatic macroencapsulation of large numbers of porcine hepatocytes by coextrusion with a solution of AN69 polymer. Biomaterials 21: 1269-1274.

Jerney TD, 1999. Process Industries. In: Nof SY editor. Handbook of Industrial Robotics, Wiley. pp1185-1200.

Jorjani P, Ozturk SS. 1999. Effects of cell density and temperature on oxygen consumption rate for different mammalian cell lines. Biotechnology and bioengineering 64: 349-356.

Kamlot A, Rozga J, Watanabe FD, Demetriou AA. 1996. Review: artificial liver support systems. Biotechnology Bioengineering 50: 382-391.

Karlsson JOM, Toner M. 1996. Long-term storage of tissues by cryopreservation: critical issues. Biomaterials 17: 243-256.

Kempner ME, Felder RA. 2002. A review of cell culture automation. Journal of the association for laboratory automation 7(2):56-62.

Keogh B E, Kinsman R. 2002. [UK] National adult cardiac surgical database report 2000-2001. Published by: The society of cardiothoracic surgeons of Great Britain and Ireland.

Kim BS, Putnam AJ, Kulik TJ, Mooney DJ. 1998. Optimising seeding and culture methods to engineer smooth muscle tissue on biodegradable polymer matrices. Biotechnology bioengineering 57: 46-54.

Kobashi T, Matsuda T. 1999. Fabrication of branched hybrid vascular protheses. Tissue Engineering 5(6): 515-524.

Koh CJ, Atala A. 2004. Prospects for engineering the urinary tract. Nephron experimental nephrology 98: 65-70.

Kose GT, Korkusuz F, Korkusuz P, Hasirci V. 2004. In vivo tissue engineering of bone using poly (3-hydroxybutiric acid-co-3-hydroxyvaleric acid) and collagen scaffolds. Tissue engineering 10(7/8): 1234-1250.

Kretzmer G. 2000. Influence of stress on adherent cells. Advanced biochemical engineering / biotechnology 67: 123-137

L'Heureux N, Paquet S, Labbe R, Germain L, Auger FA. 1998. A completely biological tissue-engineered blood vessel. FASEB J. 12(1): 47-56.

L'Heureux N, Stoclet JC, Auger FA, Lagaud GJL, Germain L, Andriantsitohaina AR. 2001. A human tissue-engineered vascular media: a new model for pharmacological studies of contractile responses. FASEB J. 15: 515-524.

Lakey JRT, Warnock GL, Brierton M, Ao Z, Hering BJ, London NJM, Ricordio C, Corbin F, Rajotte RV. 1997. Development of an automated computer-controlled islet isolation system. Cell transplantation 6(1)::47-57.

Lau FY, Cheng G. 2001. To err is human nature. Can transfusion errors due to human factors ever be eliminated? Clinica chimica acta. 313(1-2): 59-67.

Lawry J. 1998. The use of flow cytometry to sort cells or particles. Proceedings RMS 33(1): 27-29.

Lee KY, Mooney DJ. 2001. Hydrogels in tissue engineering. Chem. Rev. 101:1869-79.

Li Y, Ma T, Kniss DA, Lasky LC, Yang ST. 2001. Effects of filtration seeding on cell density, spatial distribution and proliferation in nonwoven fibrous matrices. Biotechnology progress 17: 935-944.

Lindqvist A., Dreja K, Sward K, Hellstrand AP. 2002. Effects of oxygen tension on energetics of vascular smooth muscle. Am. J. Physiol. Heart Circ. Physiol. 283: H110-H117.

Linge C, Green MR, Brooks RF. 1989. A method for the removal of fibroblasts from human tissue culture systems. Experimental cell research 185: 519-528.

Lowel M. 2003. Manufacturing of autologous cell transplants. Screening trends in drug discovery 1: 34-36.

Luhm J, Brand J-M, Koritke P, Hoppner M, Kirchner H, Frohn C. 2002. Large-scale generation of natural killer lymphocytes for clinical application. Journal of hematotherapy and stem cell research 11: 651-657.

Lutkemeyer D, Poggendorf I, Scherer T, Zhang J, Knoll A, Lehmann J. 2000. First steps in robot automation of sampling and sample management during cultivation of mammalian cells in pilot scale. Biotechnology progress 16: 822-828.

Lysaght MJ, Hazlehurst AL, 2004. Tissue engineering: the end of the beginning. Tissue engineering 10(1/2): 309-321.

Lysaght MJ, Hazlehurst AL. 2003. Private sector development of stem cell technology and therapeutic cloning. Tissue engineering 9(3): 555-561.

Mardikar H, Niranjan K. 2000. Observations on the shear damage to different animal cells in a concentric cylinder viscometer. Biotechnology bioengineering 68: 697-704.

Markusen JF. 2005. Growth and characterization of cells used to design a tissue engineered blood vessel, PhD Thesis, University College London.

Marler JJ, Upton J, Langer R, Vacanti JP. 1998. Transplantation of cells in matrices for tissue regeneration. Advanced drug delivery reviews 33:165-182.

Mascotti K, McCullough J, Burger SR. 2000. HPC viability measurement: trypan blue versus acridine orange and propidium iodide. Transfusion 40(6): 693-6.

Matijasic G, Glasnovic A. 2002. Influence of dispersed phase characteristics on rheological behaviour of suspensions. Chem. Biochem. Eng. Q. 16(4): 165-172.

Mayhew TA, Williams GR, Senica MA, Kuniholm G, du Moulin GC. 1998. Validation of a quality assurance program for autologous cultured chondrocyte implantation. Tissue engineering 4(3): 325-334.

McQueen A, Meilhoc E, Bailey JE. 1987. Flow effects on the viability and lysis of suspended mammalian cells. Biotechnology letters 9(12): 831-836.

Meek MF, Varejao ASP, Geuna S. 2004. Use of skeletal muscle tissue in peripheral nerve repair: review of the literature. Tissue engineering 10(7/8): 1027-1036.

Menasche P, Hagege AA, Vilquin J-T, Desnos M, Abergel E, Pouzet B, Bel A, Sarateanu S, Scorsin M, Schwartz K, Bruneval P, Benbunan M, Marolleau J-P, Duboc D. 2003. Autologous skeletal myoblast transplantation for severe postinfarction left ventricular dysfunction. Journal of the American college of cardiology 41:(7) 1078-1083.

Mercille S, Massie B. 1994. Induction of apoptosis in oxygen deprived cultures of hybridoma cells. Cytotechnology 15: 117-128.

Moore SK. 2002. Tissue engineering pioneers fall to financial troubles. IEEE Spectrum online news, December 2002.

Murphy SJ, Watt DJ, Jones GE. 1992. An evaluation of cell separation techniques in a mixed cell population. Journal of cell science 102: 789-798.

Naughton G. 2001. Commentary: An industry imperilled by regulatory bottlenecks. Nature biotechnology 19: 709-710.

Naughton GK. 2002. From lab bench to market, critical issues in tissue engineering. Annals of the New York academy of sciences 961: 372-385

Niklason LE, Gao J, Abbott WM, Hirschi KK, Houser S, Marini S, Langer R. 1999. Functional arteries grown in vitro. Science 284: 489-493.

Oakes BW, Batty AC. 1982. The synthesis of elastin, collagen and glycosaminoglycans by high density primary cultures of neonatal rat aortic smooth muscle. An ultrastructural and biochemical study. European journal of cell biology 27: 34-46.

Oberpenning F, Meng J, Yoo JJ, Atala A. 1999. De novo reconstitution of a functional mammalian urinary bladder by tissue engineering. Nature biotechnology 17: 149-155.

Offin P. 1999. Automated cell culture processing - robotics alleviates bottleneck in assay development. Genetic engineering news 19: 11.

Olivetti G, Anversa P, Melissari M, Loud AV. 1980. Morphometry of medial hypertrophy in the rat thoracic aorta. Lab Invest 42: 559-565.

Olivier LA, Truskey GA. 1993. A numerical analysis of forces exerted by laminar flow on spreading cells in a parallel plate flow chamber assay. Biotechnology bioengineering 42: 963-973.

Omasa T, Ishimoto M, Higashiyama K, Shioya S, Suga K. 1992. The enhancement of specific antibody production rate in glucose- and glutamine-controlled fed-batch culture. Cytotechnology 8: 75-84.

Omstead DR, Baird LG, Christenson L, du Moulin G, Tubo R, Maxted DD, Davis J, Gentile FT. 1998. Voluntary guidance for the development of tissue-engineered Products. Tissue engineering 4(3): 239-266.

Ozturk SS, Palsson BO. 1991. Effect of medium osmolarity on hybridoma growth , metabolism and antibody production. Biotechnology bioengineering 37: 989-993.

Ozturk SS, Thrift JC, Blackie JD, Naveh D. 1997. Real-time monitoring and control of glucose and lactate concentrations in a mammalian cell perfusion reactor. Biotechnology bioengineering 53: 372-378.

Pandian RP, Kutala VK, Parinandi NL, Zweier JL, Kuppusamy P. 2003. Measurement of oxygen consumption in mouse aortic endothelial cells using a microparticulate oximetry probe. Archives of biochemistry and biophysics 420: 169-175.

Pangarkar N, Hutmacher DW. 2003. Invention and business performance in the tissue-engineering industry. Tissue engineering 9(6) 1313-1322.

Partington KM, Jenkinson EJ, Anderson G. 1999. A novel method of cell separation based on dual parameter immunomagnetic separation. Journal of immunological methods 23: 195-205.

Patel SD, Papoutsakis ET, Winter JN, Miller WM. 2000. The lactate issue revisited: Novel feeding protocols to examine inhibition of cell proliferation and glucose metabolism in haematopoietic cell cultures. Biotechnology progress, 16: 885-892.

Patzer JF. 2004. Oxygen consumption in a hollow fibre bioartificial liver – revisited. Artificial organs 28(1): 83-98.

Peng C, Palsson BO. 1996. Determination of specific OURs in Human Hematopoietic cultures & implications for bioreactor design. Annals of biomedical engineering 24: 373-381.

Persidis A. 1999. Tissue engineering. Nature biotechnology, 17: 508-510.

Petit-Zeman S. 2001. Regenerative medicine. Science 19: 201-206.

Pittenger MF, Mackay AM, Beck SC, Jaiswal RK, Douglas R, Mosca JD, Moorman MA, Simonetti DW, Craig S, Marshak DR. 1999. Multilineage potential of adult human mesenchymal stem cells. Science 284: 143-147.

Pouzet B, Vilquin JT, Hagege AA, Scorsin M, Messas E, Fiszman M, Schwartz K, Menasche P. 2000. Intramyocardial transplantation of autologous myoblasts. Circulation 102(19): 210-215 (Supplement S)

Prenosil JE, Kino-oka M. 1999. Computer Controlled bioreactor for large-scale production of cultured skin grafts. Annals of the New York academy of sciences 18(875): 386-97.

Rabkin JM, Olyaei AJ, Orloff SL, Geisler SM, Wahoff DC, Hering BJ, Sutherland DER. 1999. Distant processing of pancreas islets for autotransplantation following total pancreatectomy. The American journal of surgery 177(5):423-427.

Radisic M, Euloth M, Yang L, Langer R, Freed LE, Vunjak-Novakovic G. 2003. High-density seeding of myocyte cells for cardiac tissue engineering. Biotechnology bioengineering 82: 403-414.

Ratcliffe A. 2000. Tissue engineering of vascular grafts. Matrix biology 19: 353-357.

Read TA, Sorensen DR, Mahesparan R, Enger PO, Timpl R, Olsen BR, Hjelstuen MHB, Haraldseth O, Bjerkvig R. 2001. Local endostatin treatment of gliomas administered by microencapsulated producer cells. Nature biotechnology 19: 29-34.

Reuss M, Josic D, Popovic M, Bronn WK. 1979. Viscosity of yeast suspensions. European journal of applied microbiology biotechnology 8: 168

Reyes M, Dudek A, Jahagirdar, Koodie L, Marker PH, Verfaillie CM. 2002. Origin of endothelian progenitors in human postnatal bone marrow. Journal of clinical investigation 109: 337-346.

Rieseberg M, Kasper C, Reardon KF, Scheper T. 2001. Flow cytometry in biotechnology. Applied microbiology biotechnology 56: 350-360.

Rochon M-H, Auger FA, Gauthier M-J, Germain L. 2001. Simultaneous isolation of keratinocytes and fibroblasts from a human cutaneous biopsy for the production of autologous reconstructed skin. The Canadian journal of chemical engineering. 79: 663-667.

Rodriguez JM, Carmona M, Noguerol P, Ruiz M, Parody R, Vidal F, Perez-Hurtado JM, Espigado I. 1992. A fully automated method for mononuclear bone marrow cell concentration. Journal of clinical apheresis 7(3): 101-9.

Rogers JJ. 1993. Developing the budget for a pharmaceutical/biotechnology cleanroom project. Microcontamination, January 1993: 46-50.

Rotem A, Toner M, Bhatia S, Foy BD, Tompkins RG. 1994. Oxygen is a factor determining in vitro tissue assembly: effects of attachment and spreading of hepatocytes. Biotechnology bioengineering 43: 654-660.

Rowley JA, Madlambayan G, Mooney DJ. 1999. Alginate hydrogels as synthetic extracellular matrix materials. Biomaterials 20: 45-53.

Ruiz-Torres A, Gimeno A, Melon J, Mendez L, Munoz FJ, Macia M. 1999. Age-related loss of proliferative activity of human vascular smooth muscle cells in culture. Mechanisms of aging and development 110: 49-55.

Sachlos E, Reis N, Ainsley C, Derby B, Czernuska JT. 2003. Novel collagen scaffolds with predefined internal morphology made by solid freeform fabrication. Biomaterials 24(8): 1487-97.

Safarik I, Safaikova M. 1999. Use of magnetic techniques for the isolation of cells. Journal of chromatography B, 722: 33-53.

Schmid I, Krall WJ, Uittenbogaart CH, Braun J, Giorgio JV. 1992. Dead cell discrimination with 7AAD in combination with dual colour immunofluorescence in single laser flow cytometry. Cytometry 13: 204-208.

Sherman P. 1970. Industrial rheology. Academic Press, London. pp131-133.

Sherwood JK, Riley SL, Palazzolo R, Brown SC, Monkhouse DC, Coates M, Griffith LG, Landeen LK, Ratcliffe A. 2002. A three-dimensional osteochondral composite scaffold for articular cartilage repair. Biomaterials 23(24): 4739-4751.

Shin'oka T, Imai Y, Ikada Y. 2001. Transplantation of a tissue-engineered pulmonary ertery. New England journal of medicine 344: 532-533.

Shortkroff S, Spector M. 1999. Culture and identification of autologous human articular chondrocytes for implantation. In: Methods in molecular medicine, Vol. 18: Tissue engineering methods and protocols. Edited by Morgan JR, Yarmush ML. Humana Press, NJ, USA. pp205-215.

Shum-Tim D, Stock U, Hrkach J, Shinoka T, Lien J, Moses MA, Stamp A, Taylor G, Moran AM, Landis W, Langer R, Vacanti JP, Mayer JE. 1999. Tissue engineering of autologous aorta using a new biodegradable polymer. Annals of thoracic surgery 68: 2298-2305.

Singh RP, Finka G, Emery AN, Al-Rubeai M. 1997. Apoptosis and its control in animal cell culture systems. Cytotechnology 23:87-93.

Sittinger M, Bujia J, Rotter N, Reitzel D, Minuth WW, Burmester GR. 1996. Tissue engineering and autologous transplant formation: practical approaches with resorbable biomaterials and new cell culture techniques. Biomaterials 17: 237-242.

Snabre P, Mills P. 1999. Rheology of concentrated suspensions of viscoelastic particles. Colloids and surfaces A: Physiochemical and engineering aspects. 152: 79-88.

Solan A, Mitchell S, Moses M, Nicklason L. 2003. Effect of pulse rate on collagen deposition in the tissue-engineered blood vessel. Tissue engineering 9 (4): 579-586.

Stone A. 2003. F.D.A. issues felled Advanced Tissue Sciences. Genetic engineering news 23(11): 25-25.

Sundback C, Hadlock T, Cheney M, Vacanti J. 2003. Manufacture of porous polymer conduits by a novel low-pressure injection molding process. Biomaterials 24: 819-830.

Szabo SE. 2003. Automating the assessment of cell viability. Genetic engineering news 23: 10, 40.

Temenoff JS, Mikos AG. 2000. Review: tissue engineering for regeneration of articular cartilage. Biomaterials 21: 431-440.

Thomson RC, Shung AK, Yaszemski MJ, Mikos AG. 2000. Polymer scaffold processing. In: Principles of tissue engineering. Edited by: Lanza RP, Langer R, Vacanti J. Academic press. pp 251-261.

Tilles AW, Baskaran H, Roy P, Yarmush ML, Toner M. 2001. Effects of oxygenation and flow on the viability and function of rat hepatopcytes cocultured in a microchannel flat-plate bioreactor. Biotechnology bioengineering 73: 379-389.

Timoney CF, Felder RA. 2002. A collaborative approach to creating an automated cell culture system. Journal of the association for laboratory automation 7(1): 55-58.

Tubo R, Binette F. 1999. Culture and identification of autologous human articular chondrocytes for implantation. In: Methods in molecular medicine, Vol. 18: Tissue engineering methods and protocols. Edited by Morgan JR, Yarmush ML. Humana Press, NJ, USA. pp205-215.

Tuyaerts S, Noppe SM, Corthals J, Breckpot K, Heirman C, De Greef C, Riet IV, Thielemans K. 2002. Generation of large numbers of dendritic cells in a closed system using cell factories. Journal of immunological methods 264: 135-151.

Usui H, Kishimoto K, Suzuki H. 2001. Non-newtonian viscosity of dense slurries prepared by spherical particles. Chemical engineering science 56: 2979-2989.

Vacanti JP, Langer R. 1999. Tissue engineering: the design and fabrication of living tissue replacement devices for surgical reconstruction and transplantation. The lancet, 354: 32-34 (supplement 1)

Villaschi S, Nicosia RF, Smith MR. 1994. Isolation of a morphologically and functionally distinct smooth muscle cell type from the intimal aspect of the normal rat aorta. Evidence for smooth muscle cell heterogeneity. In vitro cell developmental biology 30A: 589-595.

Ward PN. The characterisation of biological suspensions with a view to selecting and optimising dewatering processes. [PhD Thesis]. 1989; University of London.

Weinberg CB, Bell E. 1986. A blood vessel model constructed from collagen and cultured vascular cells. Science 231: 397-400.

Wendt D, Marsano A, Jakob M, Heberer M, Martin I. 2003. Oscillating perfusion of cell suspensions through three-dimensional scaffolds enhances cell seeding efficiency and uniformity. Biotechnology bioengineering 84: 205-214.

Wilkins LM, Watson SR, Prosky SJ, Meunier SF, Parenteau NL. 1994. Development of a bilayered living skin construct for clinical applications. Biotechnology bioengineering 43: 747-756.

Woodley JM, Titchener-Hooker NJ. 1996. The use of windows of operation as a bioprocess design tool. Bioprocess engineering 14: 263-268.

Xui Z-L, Deckwer W-D, Zeng A-P. 1999. Estimation of rates of oxygen uptake and carbon dioxide evolution of animal cell culture using material and energy balances. Cytotechnology 29: 159-166.

Yang TH, Miyoshi H, Ohshima N. 2001. Novel cell immobilization methods utilizing centrifugal force to achieve high-density hepatocyte culture in porous scaffold. Journal of biomedical materials research 55: 379-386.

Zeilinger K, Holland G, Sauer I, Efimova E, Kardassis D, Obermayer N, Liu M, Neuhaus P, Gerlach JC. 2004. Time course of primary liver cell reorganisation in three-dimensional high-density bioreactors for extracorporeal liver support: an immunohistochemical and ultrastructural study. Tissue engineering 10(7/8): 1113-1124.

Zhang Z, Al-Rubeai M, Thomas CR. 1993. Estimation of disruption of animal cells by turbulent capillary flow. Biotechnology bioengineering 42: 987-993.

Zhou YH, Titchener-Hooker NJ. 1999. Visualising integrated bioprocess designs through "windows of operation". Biotechnology bioengineering 65: 550-557.

Zuk PA, Zhu M, Mizuno H, Huang J, Futrell W, Katz AJ, Benhaim P, Lorenz HP, Hendrick MH. 2001. Multilineage cells from human adipose tissue: Implications for cell-based therapies. Tissue engineering 7(2): 211-228.